UNIVERSIDADE DE LISBOA

INSTITUTO SUPERIOR TÉCNICO

Dissecting the Mechanisms of Notch Signalling in Human HSCs: Implications in Stem Cell Expansion

Joana Isabel Gonçalves Carmelo

Supervisor: Doctor Fernando dos Anjos Afonso

Co-Supervisor: Doctor Cláudia Alexandra Martins Lobato da Silva

Thesis approved in public session to obtain the PhD Degree in Bioengineering

Jury final classification: Pass

2020

UNIVERSIDADE DE LISBOA

INSTITUTO SUPERIOR TÉCNICO

Dissecting the Mechanisms of Notch Signalling in Human HSCs: Implications in Stem Cell Expansion

Joana Isabel Gonçalves Carmelo

Supervisor: Doctor Fernando dos Anjos Afonso

Co-Supervisor: Doctor Cláudia Alexandra Martins Lobato da Silva

Thesis approved in public session to obtain the PhD Degree in Bioengineering

Jury final classification: Pass

Jury

Chairperson: Doctor Joaquim Manuel Sampaio Cabral, Instituto Superior Técnico, Universidade de Lisboa

Members of the Committee:

Doctor Joaquim Manuel Sampaio Cabral, Instituto Superior Técnico, Universidade de Lisboa

Doctor Fernando dos Anjos Afonso, European Cancer Stem Cell Research Institute, Cardiff University, UK

Doctor Ricardo Neves Pires das Neves, Centro de Neurociências e Biologia Celular, Instituto de Investigação Interdisciplinar, Universidade de Coimbra

Doctor Raquel Madeira Gonçalves, Instituto de Engenharia Biomédica

Doctor Evguenia Pavlovna Bekman, Universidade de Lisboa

Funding Institution - **Fundação para a Ciência e Tecnologia**

2020

RESUMO

O sangue é um dos tecidos mais regenerativos do corpo humano, em que mais de 100 biliões de novas células sanguíneas são produzidas por dia num adulto saudável. Atualmente acredita-se que o sistema hematopoiético é organizado hierarquicamente, em que no topo se encontram as células com maior potencial de auto-renovação e diferenciação, as células estaminais hematopoiéticas (HSCs), que dão origem a células progenitoras mais comprometidas que se tornam progressivamente mais restritas em termos da sua capacidade de diferenciação, originando finalmente as células sanguíneas maduras. O sistema hematopoiético necessita, portanto, de ser rigorosamente regulado. A via de sinalização *Notch* foi já associada a decisões de destino celular em hematopoiese, mas o seu papel na regulação de HSCs humanas em condições homeostáticas ainda não é evidente.

A via de sinalização *Notch* também tem sido explorada em protocolos de expansão *ex vivo* de células hematopoiéticas estaminais e progenitoras (HSPCs) do sangue do cordão umbilical (UCB). Todavia, os mecanismos moleculares desencadeados pela interação com os diferentes ligandos *Notch* não são ainda compreendidos e são necessários estudos mais abrangentes.

Um dos objetivos deste trabalho foi realizar uma comparação lado a lado dos efeitos dos ligandos *Notch*, Delta-like1 (Dll1), Delta-like4 (Dll4) e Jagged1 (Jag1), quando apresentados a HSPCs *in vitro*. No estudo realizado foi observado que após cultura de curto-prazo, o Dll4 foi capaz de duplicar o número de células com potencial de repopulação, enquanto que o Jag1 promoveu a manutenção destas células. Mecanisticamente verificou-se que o Jag1 bloqueia a progressão no ciclo celular através da sobre-expressão de p57, ao passo que o Dll4 bloqueia a diferenciação através da sub-expressão de CEBPα.

Outro objetivo deste trabalho foi avaliar as funções dos recetores *Notch*, NOTCH1 (N1) e NOTCH2 (N2) através de silenciamento génico com shRNA por meio de vetores lentivirais em UCB HSPCs. Após uma extensa validação em linhas celulares, as eficiências de silenciamento obtidas em HSPCs foram em média de 72% e 89% para os recetores N1 e N2, respetivamente. Foi verificado

que ambos os recetores são fortemente expressos nas populações HSPC e HSC, com maior ativação em HSCs. No estudo de xenotransplante foi observado que, apesar de não ter afetado o enxerto total, o silenciamento dos recetores N1 e N2 em HSPCs transplantadas provoca diferentes efeitos *in vivo*. o silenciamento do recetor N1 favoreceu significativamente a diferenciação mieloide sobre a linfoide, aumentando também a frequência de progenitores hematopoiéticos, enquanto que o silenciamento do recetor N2 diminuiu significativamente a frequência de HSCs.

Neste trabalho foi também desenvolvido um vetor lentiviral com componentes de ponta para silenciamento e sobrexpressão génica induzível. Estes vetores otimizados *all-in-one Tet-on* com duas cores foram desenvolvidos integrando os melhores componentes disponíveis na literatura e apresentam um desempenho superior aos mesmo tipo de vetores atualmente disponíveis. Com estes vetores foi observado um controlo firme da expressão génica, alta indutibilidade e estabilidade ao longo do tempo, gerando silenciamento ou expressão de proteína robustos, que não se verificam na ausência de indução.

Palavras-chave: Células estaminais e progenitoras hematopoiéticas (HSPCs); via de sinalização *Notch*; regulação de HSPCs; silenciamento génico; vetores lentivirais induzíveis

ABSTRACT

The blood is one of the most highly regenerative tissues in the human body, with more than 100 billion new blood cells being produced every day in a healthy adult. It is currently believed that the haematopoietic system is hierarchically organised, where at the top reside the cells with higher self-renewal and differentiation capacity, the haematopoietic stem cells (HSCs), which give rise to more committed progenitors that become progressively more restricted in terms of their differentiation capacity, finally originating the mature blood cells. Thus, the haematopoietic system needs to be tightly regulated and the Notch signalling pathway has been linked to cell fate decisions in haematopoiesis, however its role in the regulation of steady-state human HSCs is still unclear.

Notch signalling has also been explored for *ex vivo* expansion of umbilical cord blood (UCB) haematopoietic stem and progenitor cells (HSPCs), however, there is a lack of understanding of the molecular mechanisms triggered by the different Notch ligands and a need for more comprehensive studies.

One of the aims of this work was to perform a side-by-side comparison of the effects of Notch ligands, Delta-like1 (Dll1), Delta-like4 (Dll4) and Jagged1 (Jag1), when presented to HSPCs *in vitro*. In the study performed it was observed that after a short-time culture, Dll4 was able to duplicate the number of cells with repopulating capacity, whereas Jag1 promoted maintenance of these cells. Mechanistically it was verified that Jag1 blocks cell cycle progression through upregulation of p57 while Dll4 blocks differentiation through downregulation of CEBPα.

Another aim of this work was to evaluate the roles of Notch receptors, NOTCH1 (N1) and NOTCH2 (N2) through lentiviral shRNA-mediated gene silencing in UCB HSPCs. After a thorough validation in cell lines, average knockdown efficiencies of 72% and 89% were achieved for N1 and N2 receptors in HSPCs, respectively. Both receptors were found to be highly expressed on HSPC and HSC populations, with higher activation in HSCs. In the xenotransplantation assay it was observed that, although the total human engraftment was not affected, N1 and N2 receptors silencing in the transplanted HSPCs promoted different phenotypic outcomes *in vivo*. N1 receptor silencing significantly favoured myeloid

over lymphoid differentiation, while increasing the frequency of haematopoietic progenitors but had no effect in HSCs, whereas N2 receptor silencing significantly decreased HSCs frequency.

In this work it was also developed state-of-art lentiviral vectors for inducible gene silencing and overexpression. These optimised all-in-one Tet-on dual colour vectors were developed by integrating the best features available in the literature, presenting a superior performance to the same type of vectors currently available. With these vectors it was observed a tight inducibility that led to potent knockdowns or protein overexpression which were stable overtime *in vitro* and virtually silent in the absence of induction.

Key-words: Haematopoietic stem and progenitor cells (HSPCs); Notch signalling pathway; HSPCs regulation*;* gene silencing; inducible lentiviral vectors

ACKNOWLEDGMENTS

I would like to start by deeply acknowledge my supervisor Doctor Fernando dos Anjos Afonso for taking me under his wing and guide me to become a better scientist. I am truly grateful for having a person with so much knowledge and experience mentoring me in a field that was mostly new to me and that can be so technically challenging. He was a true hands-on supervisor, teaching and helping with experiments and troubleshooting. I am also thankful to him for trusting in me, giving me the opportunity to continue working in his lab.

I would also like to express my sincere gratitude to my co-supervisor Professor Cláudia Lobato da Silva that was the steppingstone to my scientific journey. I am very thankful for her support and optimism that always made me believe in myself and persevere. I can say without a doubt that she was the reason I wanted to continue in the field of scientific research after graduation and expand my knowledge in stem cells biology.

I also want to acknowledge Professor Joaquim Sampaio Cabral, director of the PhD program in Bioengineering – Cell Therapies and Regenerative Medicine for the opportunity to pursue this exciting PhD project abroad which made me grow so much as a scientist.

I feel lucky I found such an amazing group of friends and co-workers in the new lab I joined for this project. I believe they really made a difference in turning this experience abroad much easier and for that I am truly grateful. So thank you Ana, Aleix, Carlotta, Fábio, Irina, Juan, Leigh-Anne, Pedro, Simone and, more recently Bea, for being my Cardiff family, for all the shared moments full of laughs and all the lunches where I learned so much about other cultures. Thanks for being my “shoulder to cry” and my “antidepression pill” when things did not go as planned. I feel blessed that from this experience I can take friends for life and I am looking forward to host you all when you visit Portugal.

Special thanks to Fábio, my “partner in crime” in the lab, for all the discussions, help and brainstorming, but also for all the funny and easy-going attitude that makes you great to work with.

I also want to acknowledge all the members of the European Cancer Stem Cell Research Institute for all the help and for making this institute a very friendly and supportive working place.

I would also like to thank my colleagues and friends from my early research lab in Portugal (Stem Cell Engineering Research Group) with whom I don't have everyday contact anymore, but they do occupy a special place in my heart from the times we did. Thank you António, Diogo, Francisco, Joana, João, Márcia, Marta, Sara and Raquel for the encouragement words and for all the jokes that made me laugh so much. Once again, I feel lucky to have met such great people in the workplace that I can consider good friends and with whom I passed moments I cherish.

A special thank you to my dear friends, Gui, Joana, João, Rita, Marta, Verde and Eduardo, that have been with me since University and shared with me the student life that now I really miss. Thank you for all your support and for meeting with me in the scarce time I am in Portugal. I truly cherish your friendship and I hope to get in touch much more often once I return.

I am deeply grateful to my parents for their never-ending support and encouragement, giving me the opportunity to have the education that I wished. Thank you for raising me to be an independent person and for remembering me to relax and appreciate life more often.

Finally, to the love of my life, Filipe, there are no words enough to thank you for all your unconditional support. For all the patience and comforting, for all the great moments, the great trips, for having faith in us, for all the love, thank you.

INDEX

LIST OF FIGURES

LIST OF TABLES

LIST OF ABBREVIATIONS

ANG-1	Angiopoietin-1
ANK	Ankyrin repeats
Ab	Antibody
AhR	Aryl hydrocarbon receptor
BFU-E	Blast forming unit-erythroid
BM	Bone marrow
BMP	Bone morphogenic protein
BSA	Bovine serum albumin
CAFC	Cobblestone area forming cell
CD	Cluster of differentiation
CFU	Colony forming unit
CFU-E	Colony forming unit-erythroid
CFU-G	Colony forming unit-granulocyte
CFU-GEMM	Colony forming unit-granulocyte-erythroid-macrophage-megakaryocyte
CFU-GM	Colony forming unit-granulocyte-macrophage
CFU-M	Colony forming unit-macrophage
CHO	Chinese hamster ovary
c-kit	Tyrosine-protein kinase kit
CLP	Common lymphoid progenitor
CMP	Common myeloid progenitor
CMV	Cytomegalovirus
CSL	CBF1/ RBPjκ, Su(H) and Lag-1
DAPI	4′,6-diamidino-2-phenylindole dihydrochloride
DAPT	N-[N-(3,5-Difluorophenacetyl)-L-alanyl]-S-phenylglycine t-butyl ester
DC	Dendritic cell
dH2O	Distilled H_2O
Dll1	Delta-like 1
Dll3	Delta-like 3
Dll4	Delta-like 4
DMSO	Dimethyl sulfoxide
dnMAML1	Dominant negative form of Mastermind-like 1
Dox	Doxycycline
DSL	Delta/Serrate/LAG-2
DMEM	Dulbecco's Modified Eagle's Medium
ECFC	Endothelial colony-forming cell
EDTA	Ethylenediaminetetraacetic acid
EF1α	Elongation factor 1-alpha
EGF	Epidermal growth factor
FACS	Fluorescence-activated cell sorting
FBS	Foetal bovine serum
FCM	Flow cytometry
Flt3	FMS-like tyrosine kinase 3
Flt3L	FMS-like tyrosine kinase 3-ligand
G-CSF	Granulocyte colony-stimulating factor
GFP	Green Fluorescent Protein
GM-CSF	Granulocyte-macrophage colony-stimulating factor
GMP	Granulocyte/macrophage progenitor
GvHD	Graft-versus-host disease

HBS	HEPES buffered saline
HD	Heterodimerisation domain
HEPES	4-(2-hydroxyethyl)piperazine-1-ethanesulfonic acid
HPC	Haematopoietic progenitor cell
HRP	Horseradish peroxidase
HSC	Haematopoietic stem cell
HSCT	Haematopoietic stem cell transplantation
HSPC	Haematopoietic stem and progenitor cell
ICC	Immunocytochemistry
IHC	Immunohistochemistry
IL	Interleukin
IMDM	Iscove's Modified Dulbecco's Medium
Jag1	Jagged1
Jag2	Jagged2
LB	Lennox broth
LBA	Long bone area
LDA	Limiting dilution assay
Lin$^-$	Lineage$^-$
LMPP	Lymphoid-primed multipotent progenitor
LNR	Lin12/Notch repeats
LSK	Lin$^-$Sca1$^+$c-kit$^+$
LTC	Long-term culture
LTC-IC	Long-term culture-initiating cell
LT-HSC	Long-term haematopoietic stem cell
MAML	Mastermind-like
MCS	Multiple cloning site
M-CSF	Macrophage colony stimulating factor
MEP	Megakaryocyte/erythrocyte progenitors
MFI	Mean fluorescence intensity
MHC	Major histocompatibility complex
Mib1	Mind bomb1
miRNA	MircroRNA
MLP	Multilymphoid progenitor
MNCs	Mononuclear cells
MNNL	Module at the N-terminus of Notch ligands
MPD	Myeloproliferative disease
MPP	Multipotent progenitor
mRNA	Messenger RNA
MSC	Mesenchymal stromal cells
N1-4	Notch1-4
NAM	Nicotinamide
NECD	Notch extracellular domain
NEXT	Notch extracellular truncation
NF- H_20	Nuclease-free H_20
NFL	Notch full length
NICD	Notch intracellular domain
NK	Natural killer
NLS	Nuclear localisation signal
NOD	Nonobese diabetic
NRR	Negative regulatory region
NSG	NOD/SCID/IL2Rγ-null
NTM	Notch transmembrane

OB	Osteoblast
P/S	Penicillin-Streptomycin
PB	Peripheral blood
PBS	Phosphate buffered saline
PCR	Polymerase chain reaction
PGE_2	Prostaglandin E_2
PGK	Phosphoglycerate kinase
Pofut1	O-fucosyl transferase 1
Pol	Polymerase
PVDF	Polyvinylidene difluoride
qPCR	Quantitative polymerase chain reaction
Rag	Recombination activating gene
RAM	RBPjκ-associated molecule
RBPjκ	Recombination binding protein jκ
RE	Restriction enzymes
RISC	RNA-induced silencing complex
RNAi	RNA interference
RPMI	Roswell Park Memorial Institute
RS	Restriction sites
RT	Room temperature
rtTA	Reverse tetracycline responsive transactivator
Sca-1	Stem cell antigen 1
SCF	Spleen focus-forming virus
SCID	Severe combined immunodeficient
SFFV	Spleen focus-forming virus
shRNA	Short hairpin RNA
siRNA	Short interfering RNA
SR1	StemRegenin 1
SRC	SCID-repopulating cell
ST-HSC	Short-term HSC
T_a	Annealing temperature
TAD	Transcriptional activation domain
TAE	Tris-acetate-EDTA
T-ALL	T-cell acute lymphoblastic leukaemia
TBA	Trabecular bone area
TBS	Tris-buffered saline
TetO	Tetracycline operator sequence
TNCs	Total nucleated cells
TNFα	Tumour necrosis factor α
TNR	Transgenic Notch reporter
TPO	Thrombopoietin
TPO-R	Thrombopoietin receptor
tTA	Tetracycline responsive transactivator
UBC	Ubiquitin C
UCB	Umbilical cord blood
VEGF-A	Vascular endothelial growth factor A
WB	Western blot
β2m	Beta2microglobulin

CHAPTER I

INTRODUCTION

I.1. HUMAN HAEMATOPOIESIS: CHARACTERISATION AND REGULATION

The haematopoietic system is composed by different types of blood cells believed to be hierarchically organised. Lying at the bottom of the hierarchy are the mature blood cells which are predominantly short lived, requiring a constant replenishment throughout adult life. Haematopoietic stem cells (HSCs) that sit at the top of the hierarchy are rare cells responsible for generating multipotent progenitors (MPPs) that in turn give rise to intermediate precursors that become progressively restricted in terms of their differentiation capacity [1]. Finally, these precursors differentiate into mature blood cells. The regulation of stem cells self-renewal and differentiation requires a specific microenvironment of surrounding cells, known as the stem cell niche, which for the adult HSCs is found in the bone marrow (BM) [2].

Due to their ability to self-renew and to maintain multilineage potential, HSCs have the capacity to reconstitute the entire blood system of a recipient following transplantation, thus sustaining lifelong blood formation [2]. Under homeostasis, HSCs persist mainly quiescent in the G0 or G1 cell cycle phases, while upon stress they actively divide and differentiate.

The first evidence of HSCs existence came during the atomic era, when it was discovered that lethally irradiated mice could be rescued following injection of spleen or marrow cells from unirradiated donors [3]. However, HSC multilineage potential was demonstrated later through clonal *in vivo* repopulation assays [4, 5]. Following these discoveries, research in the field evolved towards the establishment of haematopoietic stem and progenitor cells (HSPCs) hierarchical system and their phenotypic identification.

Given that the generation of blood cells is largely conserved throughout vertebrate evolution, studies in several model organisms like mouse and zebrafish have shed light on our understanding of the haematopoietic process in humans. Most of the knowledge on the haematopoietic system *in vivo* has been derived from mouse

studies. However, significant discoveries have been made in human haematopoiesis thanks to the emergence of the xenotransplantation assay, the development of more robust *in vitro* clonal assays and the refinement of sorting strategies based on cell surface antigens (reviewed in [6]).

I.1.1. THE HAEMATOPOIETIC HIERARCHY, A BRIEF NOTE

The high turnover of blood cells under homeostasis requires a thigh regulation of haematopoiesis in order to meet the demands without exhausting the HSC pool, also required for regenerative purposes. This tight control relies on the hierarchical structure of the haematopoietic system, where at the top lies a reservoir of long-term HSCs (LT-HSCs). The LT-HSCs are mainly quiescent and are responsible for the lifetime supply of blood cells. Downstream of these cells are the short-term HSCs (ST-HSCs) and the MPPs with decreasing self-renewal potential and increasing proliferative capacity than the LT-HSCs. MPPs give rise to the oligopotent and lineage restricted progenitor which are the real “workhorses” of the haematopoietic system, dividing rapidly and generating high numbers of mature blood cells.

Many studies have increased our understanding on this hierarchy organisation by focusing on the identification of HSC and progenitor subpopulations (**Figure I.1**), by relying on two core experimental settings: cell sorting and clonal assays. Ideally, to truly define a population, each cell within a purified subset should possess the same differentiation potential. The identification of pure haematopoietic populations is still an unresolved subject, with new studies suggesting a redefinition of the current hierarchy model.

I.1.1.1. HUMAN HSCS

HSCs can be phenotypically identified through the expression of specific surface antigens and by the functional ability to self-renew and reconstitute multiple blood lineages at the clonal level.

The murine model is still largely used to explore the haematopoietic system regulation especially in the context of disease. Very briefly, in the murine system functional HSCs are identified by the lack of expression of several cell surface antigens found in differentiated or mature cells (Lineage$^-$, Lin$^-$) and by the high expression of the stem cell antigen 1 (Sca-1) [7] and the tyrosine-protein kinase kit (c-kit; CD117) [8], being commonly referred to as the LSK population (Lin$^-$Sca1$^+$c-kit$^+$). This population, however, is heterogeneous in terms of self-renewal capacity, containing LT-HSCs, ST-HSCs and MPPs. LT-HSC population is defined by further selecting for negative expression of CD34 and Flt3 (FMS-like tyrosine kinase 3) antigens [9-11]. Alternatively, antigens of the Slam family (CD150 and CD48) can also be used to define a similar population of LT-HSCs (LSK CD150$^+$CD48$^-$, [12]).

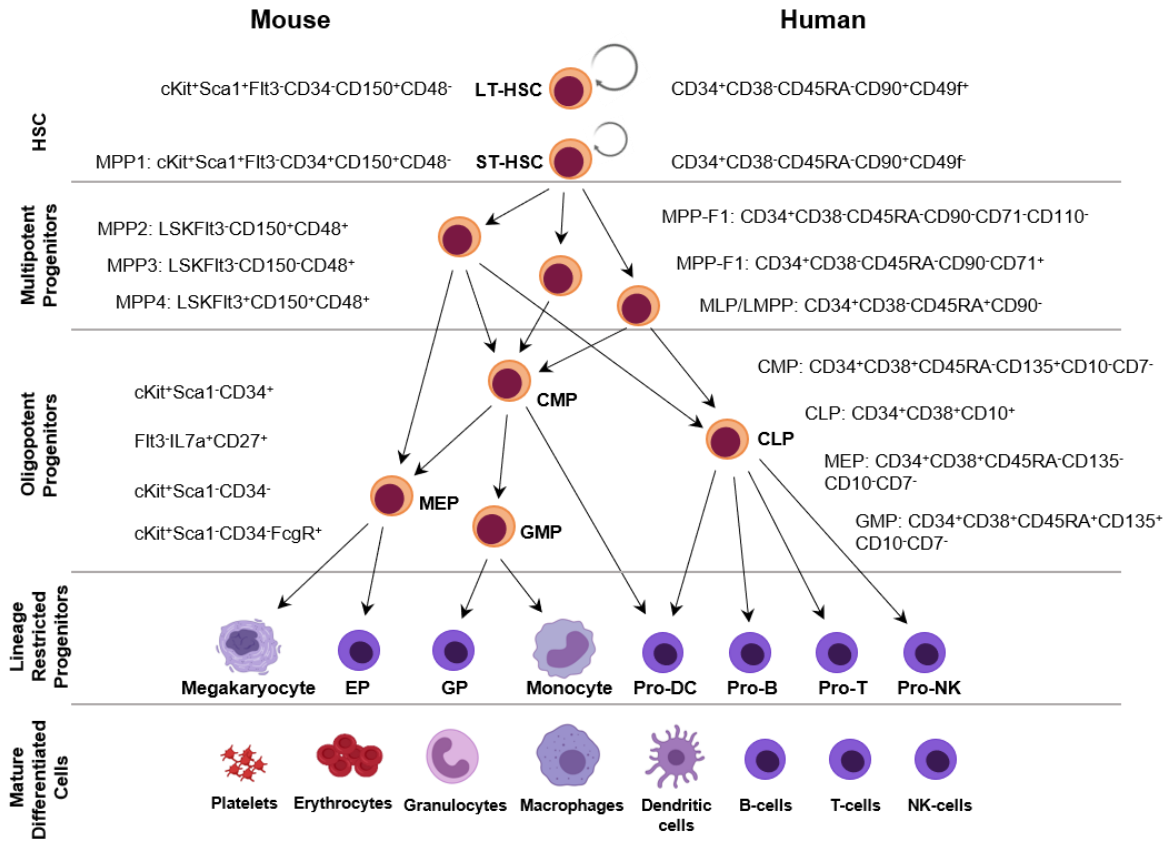

Figure I.1 – Haematopoietic hierarchy model and currently accepted phenotypes of different haematopoietic stem and progenitor cells populations from human and mice. Abbreviations: LT-HSC, long-term HSC; ST-HSC, short-term HSC; MPP, multipotent progenitor; MLP/LMPP, multilymphoid progenitor/lymphoid-primed MPP; CMP, common myeloid progenitor; CLP, common lymphoid progenitor; MEP, megakaryocyte/erythrocyte progenitor; GMP, granulocyte/macrophage progenitor; EP, erythroid progenitor; GP, granulocyte progenitor.

Regarding human HSCs, the identification of human LT-HSC and ST-HSC populations has relied on the xenotransplantation of human cells in limiting cell doses in order to assess multilineage repopulation ability. The selection of primitive human haematopoietic cells has been widely based on the expression of the CD34 antigen [13]. The CD34 antigen is a single-pass transmembrane glycoprotein which exact function is still unclear in HSPC biology, but that has been suggested to participate in cell-cell adhesion within the BM (reviewed in [14]). $CD34^+$ cells contain a mixture of HSPCs that make up 1-4% of the BM mononuclear cells (MNCs) [13], up to 6% of mobilised peripheral blood (PB) MNCs [15] and 1-2% of umbilical cord blood (UCB) MNCs [16]. To further purify a more primitive population, additional markers have been identified. The CD90 antigen was first shown to identify a subset of $CD34^+$ cells capable of repopulating SCID (severe combined immunodeficient) mice with multilineage engraftment [17]. Further HSC refinement was then achieved by depleting CD38 [18, 19] and CD45RA [20] positive cells.

Thus, it is now considered that the $Lin^-CD34^+CD38^-CD90^+CD45RA^-$ phenotype represents a highly enriched human HSC population, which comprises around 25% of the $Lin^-CD34^+CD38^-$ population from UCB and around 30% from BM. In fact, it was demonstrated successful long-term multilineage engraftment of these cells in most of NOD/SCID/IL2Rγ-null (NSG; nonobese diabetic/SCID, gamma chain null) mice after injection of 100 cells [21]. In the same study it was proposed that the expression of CD90 on $CD34^+CD38^-CD45RA^-$ cells might distinguish HSCs from the less primitive MPPs. However,$CD90^-$ MPPs were still able to be serially transplanted, although to a much lesser extent than the $CD90^+$ HSCs [21].

Thus, there was need for further characterisation to distinguish HSCs from the nearest progeny with less stemness property. In fact, the expression of integrin α2 (CD49b) was shown to distinguish mouse LT-HSCs from ST-HSCs [22]. By analogy, for human cells it was shown that cells enriched in HSCs ($Lin^-CD34^+CD38^-CD45RA^+Rho^{lo}$) but expressing CD49f (integrin α6) antigen were capable of long-term multilineage engraftment and successful secondary transplantation [23] thus, identifying a purer human LT-HSC population.

Furthermore, other studies demonstrated that, analogously to mouse HSCs, a more primitive $CD34^-$ HSC population with SCID-repopulating capacity exists at the top of

$CD34^+$ cells [24-26]. Indeed, an early report showed that the repopulation capacity of the $Lin^-CD34^-CD38^-$ UCB population was associated to the $CD93^{hi}$ sub-fraction [25]. Although, a much later study reported that $CD34^-$ cells purified from UCB could give rise to $CD34^+$ cells [26], still little was known about these rare $CD34^-$ cells and their relationship with $CD34^+$ populations. Only recently it was demonstrated that the $CD34^-$ population comprises HSCs residing at the top of the human haematopoietic hierarchy, capable of generating self-renewing $CD34^+CD38^-$ cells *in vivo* and more competent in serial transplantation than the $CD34^+CD38^-$ population and in particular the $Lin^-CD34^+CD38^-CD90^+CD45RA^-CD49f^+$ HSCs [27].

I.1.1.2. MULTIPOTENT PROGENITORS

When compared to HSCs, the MMPs right below in the hierarchy are characterised by limited self-renewal capacity but still with full differentiation potential.

As previously mentioned, Majeti and colleagues distinguished MPPs from HSCs by the lack of expression of CD90 [21]. They showed that when transplanting 500 of these cells into NSG mice, multipotent haematopoiesis was achieved although with low levels of BM chimerism and limited serial-transplantability. Later on, Dick's group further defined this MPP population as $Lin^-CD34^+CD38^-CD45RA^-CD90^-CD49f^-$ showing these cells were only capable of transient engraftment peaking at 4 weeks and undetectable by 16 weeks [23]. Recently, analogous to the murine system, MPPs subpopulations were identified based on expression of CD71 (transferrin receptor) and CD110 (thrombopoietin receptor) [28]. These subpopulations were shown to have early lineage bias, with MPP F1 ($CD34^+CD38^-CD90^-CD45RA^-CD71^-CD110^-$) giving rise predominantly to megakaryocytes and F2/F3 cells ($CD34^+CD38^-CD90^-CD45RA^-CD71^+$) being more biased towards erythroid lineages. The authors also carried a comparison in different development stages of haematopoiesis and showed that foetal liver cells had more oligopotent progenitors whereas the adult BM contained primarily unipotent progenitors that appeared to arise directly from MPPs. Based on these observations the authors proposed that adult haematopoiesis could be organised as a 'two-tier' system, defying the widely accepted hierarchical model with progressively differentiated populations.

I.1.1.3. LINEAGE COMMITTED PROGENITORS

According to the classical hierarchical system, progenitors with biased differentiation capacity can be found downstream of MPPs. These progenitors are known as common lymphoid progenitors (CLP) and common myeloid progenitors (CMP). The latter give rise to granulocyte/macrophage progenitors (GMPs) and megakaryocyte/erythrocyte progenitors (MEPs). GMPs differentiate to the granulocyte-monocyte fate while MEPs give rise to red blood cells and platelets.

Unlike their precedents, in the human system these progenitors are positive for CD38 expression. The myeloid populations can then be distinguished based on CD45RA and CD123 (alpha chain of the interleukin 3 receptor, IL-3Rα) expressions [29], or alternatively, by Flt3 and TPO-R (thrombopoietin receptor) expressions [30, 31]. As mentioned above, the classical model of haematopoiesis suggests that the first stage of lineage commitment occurs at the bifurcation between the CMP and CLP populations. However, this model was redefined in the mouse system with the discovery of LMPPs (lymphoid-primed MPPs) [32]. In human cord blood, it was later described a multilymphoid progenitor population (MLP) defined as $CD34^+CD38^-CD90^-CD45RA^+$, and positive for CD10, with the ability to originate all lymphoid lineages and some monocytic/macrophage, but without granulocytic, erythroid and megakaryocytic outputs [30]. Later on, another study demonstrated the presence of an LMPP-like population with granulocyte potential, within the $CD34^+CD38^-CD90^-CD45RA^+$ compartment, distinct from the one previously described by the lack of CD10 [31]. Moreover, another bone marrow population similar to cord blood MLPs, devoid of clonogenic myelo-erythroid potential, was isolated from $CD34^+CD38^+CD45RA^+CD10^-$ cells based on high expression of L-selectin (CD62L) [33].

Recently, an interesting study described functional and transcriptional differences between the $CD34^+CD38^-CD90^{-/lo}CD45RA^+CD10^-$ LMPP population, the $CD34^+CD38^-CD90^{-/lo}CD45RA^+CD10^+$ MLPs and the $CD34^+CD38^+CD123^+$ $CD45RA^+CD10^-$ GMPs [34]. It was also demonstrated that these populations were heterogeneous at the single cell level, containing not only the more abundant uni-lineage progenitors, but also bi- and rarer multi-lineage progenitors, particularly in the LMPP compartment. This, coupled with single cell expression analyses, suggests that a continuum of

progenitors execute lymphoid and myeloid differentiation rather than uni-lineage progenitors present downstream of stem cells.

Thus, it seems that the bifurcation between myeloid and lymphoid commitment is still not clear in the human system and is dependent on the development stage of haematopoiesis.

I.1.2. HSCs FUNCTIONAL CHARACTERISATION

I.1.2.1. IN VITRO ASSAYS

Under the proper conditions, *in vitro* assays allow a first line evaluation of HSPC self-renewal and differentiation capacity in response to given extrinsic stimuli (growth factors, niche cells interactions, etc) or genetic manipulation (overexpression or silencing of haematopoietic regulators. These assays can be divided into short-term and long-term assays.

Short-term assays: suspension culture and CFU assay

Suspension culture of HSPCs in serum-free medium supplemented with cytokine allows to maintain and expand these cells at some extent for further evaluation of the different subpopulations. The output cells are usually evaluated for phenotype, cell cycle, differentiation capacity and ability to reconstitute immunodeficient mice.

Cytokines cocktails usually include stem cell factor (SCF), FMS-like tyrosine kinase 3-ligand (Flt3L) and thrombopoietin (TPO). A high concentration cocktail of SCF and Flt3 at 300 ng/mL combined with TPO was shown to be able to maintain human repopulating cells up to 9 days in culture [35]. On the other hand, lower concentrations of SCF and Flt3L combined with interleukin (IL)-6, IL-3 and granulocyte colony-stimulating factor (G-CSF) have been shown to promote HSPCs proliferation but at the expense of self-renewal [36, 37].

The colony-forming unit (CFU) assay allows to assess the content of haematopoietic multipotent and lineage-restricted progenitors based on the number and morphology

of generated colonies. However, this assay only enables the generation of colonies from myeloid lineage and thus, not suitable to assess lymphoid output.

In this assay, low cell doses are plated in a semisolid medium supplemented with appropriate combinations of cytokines, enabling proliferation and differentiation of haematopoietic progenitors which give rise to discrete colonies. The semi-solid medium is usually provided by methylcellulose that provides viscosity, which supports the three-dimensional growth of the haematopoietic colonies and prevents migration of the cells so that they remain within a colony. A colony is derived from a single cell and can contain mature cells of different lineages depending on the growth factors used and the multipotentiality of the progenitor cell. The type of colony yielded can be assessed based on their morphology, being classified as CFU-M (macrophage), CFU-G (granulocyte), CFU-GM (granulocyte-macrophage), CFU-E (erythroid), BFU-E (blast forming unit-erythroid) and CFU-GEMM (granulocyte-erythroid-macrophage-megakaryocyte). The latter represents the more primitive multilineage colony, being an indicator of a more immature population. To further assess the most primitive progenitors it is possible to replate the colonies in a secondary colony assay [38]. Additionally, colonies can be harvested to check their numbers and phenotype using flow cytometry and morphologic evaluation by Giemsa-staining.

Liquid cultures can also be used to assess the lymphoid and myeloid differentiation potential of a population. For instance, to define the MLP population, a liquid culture of cells on MS5 stroma supplemented with SCF, IL-7, TPO, IL-2, granulocyte-macrophage colony stimulating factor (GM-CSF), G-CSF and macrophage colony stimulating factor (M-CSF) has been used [30]. Alternatively, a recent study has reported an optimised liquid culture for human progenitors on MS5 stroma supplemented with SCF, G-CSF, Flt3L, IL-2, IL-15 and the prostaglandin-synthesis inhibitor DUP-697 [34]. Both conditions were shown to support the production of neutrophils, monocytes, B cells and natural killer (NK) cells, although the former was less permissive for granulocytic output.

Long-term culture: LTC-IC assay

Long-term cultures (LTCs) are used to measure the frequency of HSCs or immature progenitors content in a population. A long-term assay enables to select for the more primitive cells with more longevity and thus, with higher self-renewal ability, which should retain their full differentiation capacity.

This type of assay was first implemented by Dexter and colleagues upon discovery that in a culture containing horse serum and corticosteroids, murine bone marrow cells naturally form an adherent layer that supports the generation of granulocytes and macrophages for several weeks without the need of exogenous growth factors [39, 40]. These culture conditions were shown to be required for the maintenance of both stroma and haematopoietic primitive cells [41, 42]. Based on these findings LTC systems were established using irradiated adherent feeder layers to allow the continuous *in vitro* generation of myeloid [39, 40] as well as lymphoid cells [43, 44] and the quantification of more primitive cells which can be identified as LTC-initiating cells (LTC-ICs) [45, 46] or cobblestone area forming cells (CAFCs) [47] depending on the type of assay.

Although originally performed with primary bone marrow stromal cells, feeder layers of stromal cell lines are preferred due to reproducibility and other practical considerations. Several stromal cell lines have been tested for their ability to support haematopoiesis in LTC systems, including M210B4, CFC034, AFT024 [48, 49] and MS5 [50, 51]. The murine stromal cell line MS5 secretes extracellular matrix proteins such as fibronectin, laminin, collagen type I, heparan and proteoglycans, making them ideal to create a niche to which HSPCs closely associate with, allowing the regulation of their differentiation or expansion [52, 53].

To perform an LTC assay, purified primitive haematopoietic cells are seeded onto irradiated stromal cell layers, where throughout 5 weeks the more committed progenitors will mature and be discarded through media changes. Meanwhile, the more primitive cells are kept in culture due to their ability to migrate underneath the feeder layer, thus continuing to expand and giving rise to new progenitors. In an LTC-IC assay, these progenitors with colony-forming ability are then quantified through a CFU assay. The LTC-IC frequency can be determined either through the total number of CFUs in culture divided by the average of CFUs produced per LTC-IC for the

standard conditions used, or through a limiting dilution assay (LDA) based on Poisson statistics and the method of maximum likelihood [54]. During the LTC assay wells can be microscopically screened for the presence of “cobblestone areas” which are defined as colonies of at least five small, non-refractile cells that grow underneath the stromal layer, creating a cluster of flattened, optically dense cells [55, 47]. The LTC-IC and CAFC represent similar but not identical primitive cells, which have been placed hierarchically above CFUs, but below the SCID-repopulating cell (SRC). Indeed, cells identified in these assays are functionally heterogeneous and are found in both $Lin^-CD34^+CD38^-$ (HSPCs) and $Lin^-CD34^+CD38^+$ (HPCs) populations [56], though higher proliferative activity appears to be in the $CD34^+CD38^-$ compartment [57, 58]

Nevertheless, these assays can only measure stem cell-like and progenitor cell-like activity, and they are usually used as a screening method before assessing the population ability to fully reconstitute all the blood cell lineages of a conditioned recipient.

I.1.2.2. *IN VIVO* XENOGRAFT ASSAY

The HSC repopulation capacity *in vivo* was first observed by Till and McCulloh upon discovery of colonies in the spleen of irradiated mice after bone marrow transplantation [4]. For human HSCs, the advent of xenotransplantation model introduced the gold standard assay to evaluate the long-term self-renewal and multipotential of these cells. In initial reports several groups demonstrated the engraftment of human BM cells in mice with severe combined immunodeficiency (SCID, *Prkdc*^{scid}) [59-62]. SCID mice have a disrupted protein kinase DNA-activated catalytic polypeptide (*Prkdc*) gene, which results in the lack of expression of rearranged antigen receptors, and therefore lack of functional B and T cells. However, this model has limitations due to the high level of innate immune function and spontaneous emergence of B and T cells with age, hampering human engraftment. Improvement of xenotransplantation was obtained when SCID mice were crossed with non-obese diabetic (NOD) mice, originating a more profound immunodeficient mouse model (NOD/SCID) [63], in which the injection of small numbers of human $CD34^+$ cells was demonstrated to reconstitute multilineage human haematopoiesis [63]. However, the NOD/SCID model has high incidence of thymic lymphoma and persistent activity of NK cells, precluding long-term

engraftment studies [63]. Further improvement of the xenograft model resulted in the NOD/SCID/β2m$^{-/-}$ mouse, with deletion of the beta2microglobulin (β2m) gene, which encodes an essential component of the major histocompatibility complex (MHC) class I thus, resulting in loss of MHC I expression and consequently lower NK cell activity. However, although more immunodeficient than the original NOD/SCID mouse, this model is still limited by susceptibility to thymic lymphoma. Thereafter, mice with deleted (NOG) or truncated (NSG) IL2R- common γ chain were generated. This receptor is a critical component of the IL-2, IL-4, IL-7, IL-9, IL-15 and IL-21 signalling [64, 65] and deficiency of this gene results in complete loss of B, T and NK cells. Alternatively, the mouse model BALB/c-Rag2$^{-/-}$ Il2rg$^{-/-}$, lacking recombination activating gene (Rag), also shows deficiency in B, T and NK cells, and has also been used as xenograft model [66]. Transplantation of human HSCs into either NSG or BALB/c-Rag2$^{-/-}$ Il2r$\gamma^{-/-}$ recipients leads to stable, long-term engraftment of HSCs in the recipient BM and generation of all human-blood lineage cells in the periphery [67, 66].

However, the multilineage differentiation of the xenograft is limited and biased: while human B cell reconstitution is robust and T cell is delayed, reconstitution of NK cells and myeloid cells is usually poor. This appears to be mainly due to lack of human cytokines that are required for the development and maintenance of the latter cell lineages [68]. Thus, efforts to further improve the xenograft models were directed into the development of humanised models with expression of human cytokines such as TPO, IL-3, GM-CSF, and other not cross-reactive cytokines [69, 70].

Nevertheless, despite all the improvements, there is currently no standard in the field regarding which mice, approaches and time-points for best measuring human HSC activity *in vivo*. In the case of mouse HSCs, engraftment endpoints are well established: LT-HSCs are defined as the ones with repopulation capacity beyond 12 weeks, whereas ST-HCs are the ones with multilineage potential at 6 weeks. For human HSC studies many investigators have adopted a 12-week period, however a longer period or secondary transplant might be needed to better distinguish between human transient and durable-reconstituting cells [6].

All things considered, the xenograft model is still the best assay available at present to assess the presence of human normal and leukaemic initiating cells, and much work is ongoing to improve the limitations of the xenograft model.

I.1.2.3. 3D SCAFFOLDS FOR HUMANISED NICHE MODELS

Many recent studies have established the essential role of the BM niche in the maintenance of HSCs by balancing quiescence, expansion and multipotency [71-73]. In the niche, HSCs closely associate with supporting niche cells including osteoblasts and mesenchymal stromal cells (MSCs) [74-76], further discussed in **section I.1.3.3**. Additional cues derive from the extracellular matrix and even the 3D structure of the niche was shown to influence HSCs [77, 78]. Artificial reconstruction of all these niche components is a current approach to better simulate the *in vivo* niche of HSCs. These 3D systems consist of co-culturing mesenchymal stromal cells and/or endothelial cells with HSCs in a tri-dimensional matrix to guarantee not only the fundamental components and molecules, but also the right structure and space for the long-term maintenance of the HSC multipotency [79, 80]. In fact, it was demonstrated that 3D cultures have superior supporting activity compared to the 2D systems [81, 82] and it might represent a bridge to fill the gap between the *in vitro* and *in vivo* systems.

As previously mentioned, the xenograft model is the most widely used and relevant readout system for studying normal and malignant haematopoiesis. However, the difficulties to genetically manipulate the BM niche in immunodeficient mice models as well as the unfeasibility to engraft BM stromal cells [83, 84] prompted the use of scaffolds of 3D bone-tissue-like models. Indeed, in the xenograft model, human HSCs engraft in a murine microenvironment that may not reflect the interactions between HSCs and the BM microenvironment in humans. Thus, in 2012 the group of Konopleva and Andreeff developed an extramedullary bone marrow model using human MSCs and endothelial colony-forming cells (ECFCs) with Matrigel scaffolds in NSG mice [85]. The authors showed that the extramedullary bones had similar structure and provided an environment functionally equivalent to the normal bones. Furthermore, MSCs and ECFCs were able to be genetically modified to identify genes critical for the maintenance of normal and leukaemic cells, such as *Hif1α* (Hypoxia-inducible factor 1 alpha) thus, allowing to downregulate or upregulate the expression of single proteins, activating or silencing specific molecular pathway in specific niche cells. The possibility to genetically modify components of the BM niche in different human or murine cell types enables the systematic investigation of their effect on the development and

progression of normal and malignant haematopoiesis, as well as the possibility to find new regulatory mechanisms and therapeutic targets.

I.1.3. HSC REGULATION

In order to meet the demand of cells in a highly regenerative tissue like the blood, not only under regenerative conditions after acute blood loss or infection, but also during normal homeostasis, haematopoiesis must be tightly regulated.

The HSPC regulation depends on both intrinsic and extrinsic elements, the former being a wide variety of regulatory molecules present within the cell, whereas the latter include the different cell types and soluble signals with which HSPCs interact in their niche. Thus, the fate of HSPCs is controlled by intrinsic cell regulators, which in turn, are modulated by external signals.

The intrinsic regulators of stem cell function include nuclear transcription factors, molecular regulators of cell cycle, molecules that act as mitotic clocks that set up the number of rounds of division (HSCs have shown to express high levels of telomerase [86]) and epigenetic regulators controlling the structure and organisation of DNA and chromatin [87].

In postnatal life, blood cell formation takes place primarily in the bone marrow, where HSCs are surrounded by different cell types, including MSCs, osteoblasts, fibroblasts, adipocytes, endothelial and accessory cells (e.g., macrophages, lymphocytes). All these different cell types are part of the HSC niche that is responsible for providing the right conditions for their functions (reviewed in [88, 89]). Recent evidences indicate that there are several haematopoietic niches within the marrow microenvironment including endosteal, vascular, and perivascular niches, which exert differential effects on HSCs [90].

As this work is focused on HSPC regulation through the Notch signalling pathway, some important regulators will be only briefly mentioned here, whereas the role of Notch signalling will be covered in more detail in the following subchapter.

I.1.3.1. HSC CELL CYCLE

Tissue homeostasis requires the presence of multipotent adult stem cells which have been shown to exist in a dormant, or quiescent cell cycle state. This quiescent state is considered a fundamental property of HSCs in the adult bone marrow, avoiding functional exhaustion and cellular insults to maintain lifelong haematopoietic cell production [91, 92]. The decision of whether or not to exit quiescence is considered to be stochastic and deterministic and both cell-intrinsic and -extrinsic signals induced in response to stress, like inflammation or blood loss that allow quiescent HSCs to re-enter the cell cycle, proliferate and differentiate [8, 93].

Dormant HSCs are believed to be the most immature LT-HSCs residing at the apex of the hierarchy and thus, the precise regulation of their cell cycle is required for the effective production of mature haematopoietic cells with minimal stem cell exhaustion [94] .

In mouse studies, highly dormant HSCs identified by label retention of H2B-GFP (Green Fluorescent Protein) have been showed to have higher repopulation ability compared to cycling HSCs [95, 71]. Consistently, most gene knockout mice models that lead to HSC defects with excessive proliferation and loss of quiescence result in defective HSC repopulation capacity [96] thus, implying the existence of cell-autonomous, intrinsic regulatory mechanisms that link quiescence to the repopulating potential of HSCs. However, other contradictory reports also showed that knockout of some genes such as *Cdkn2c* or *Myb* resulted in higher repopulation potential with higher proliferation of HSCs [97, 98]. In addition, the administration of a cell cycle inhibitor can inhibit the engraftment of human HSCs in NOD/SCID mice [99]. It was also suggested that there is no correlation between the duration of G0 phase and the repopulation potential of HSCs [100]. These contradictory effects may be due to functional heterogeneity within dormant HSCs or lack of discrimination between symmetric or asymmetric cell divisions. A combination of single cell paired-daughter assay with detailed genetic analysis could help to unravel the relationship between HSC quiescence, self-renewal capacity and repopulation potential [101]. It is also unclear whether a correlation exists between cell cycle status and the differentiation potential of HSCs, with several studies indicating that quiescent HSCs are a heterogenous group with varying lineage bias [102, 103].

Due to the limitations to study human HSCs, the delineation of quiescent properties of human HSCs ultimately relies on the repopulation capacity in immunocompromised mice. In the initial studies where BM $CD34^+$ cells were analysed using simultaneous DNA/RNA staining, approximately two-thirds of LTC-ICs were identified as quiescent [104]. More recently, highly purified HSCs with repopulating capacity were identified in a cord blood-derived $Lin^-CD34^-CD38^-CD93^{high}$ population, which were shown to be more quiescent compared to any of $CD34^+$ HSPC sub-populations studied [27].

Furthermore, there is still a lack of understanding on how division, self-renewal, and differentiation are integrated. A recent study established CDK6 levels as a master regulator of the duration of quiescence exit in human HSCs [105]. The authors of this study found CDK6 to be differentially regulated in HSCs subsets, and that the absence of CDK6 in LT-HSCs resulted in a 5–6 hr delay in G0 exit. The cumulative effect of this delay was illustrated to limit LT-HSC divisions and to ultimately preserve HSC pool integrity in the long term [105]. Also, a previous study demonstrated that the cytokine G-CSF produced a heterogenous response in cell cycling of human HSCs *in vitro* [106]. When human HSCs were subdivided according to G-CSF receptor (CD114) expression, it was uncovered that $CD114^{-/lo}$ HSCs exhibited significantly higher long-term repopulation potentials in NSG mice, suggesting that the exit from quiescence *in vitro* is regulated through the cell intrinsic expression of CD114.

Several molecular regulators of cell cycle progression and transcription factors have been identified as intrinsic regulators of HSC quiescence and some examples are given below, as well as components of the BM niche known to maintain HSC quiescence.

I.1.3.2. TRANSCRIPTION FACTORS AND MOLECULAR REGULATORS

A large but still not fully characterised list of molecules including cell surface receptors, signal transduction molecules and several transcription factors have been recognised for their regulatory roles in HSCs (reviewed in [107]). Transcription factors have attracted much attention given their essential roles in the initial development, expansion and maintenance of HSCs [2]. Their importance has been reinforced by the understanding that many of these key transcription factors such as mixed-lineage

leukaemia (MLL), Runt-related transcription factor (AML1), and stem cell leukaemia (SCL) are also major players in leukaemogenesis [6].

In human cells, many transcription factors, including ID genes, SOX8, SOX18, and NFIB have been associated with HSCs phenotype, while factors such as MYC and IKZF1 have been identified in differentiation into MPPs [23]. HOXB4 is one of the most extensively studied HSC transcription factor shown to be important in both mice and human HSCs. Overexpression of this factor in mouse HSCs was the first shown to lead to profound HSC expansion *in vitro* and *in vivo* [108]. However, HOXB4-transduced human $CD34^+$ cells have shown a limited (2- to 4-fold) expansion of HSCs [109]. The polycomb-group factor, BMI1 appears to maintain HSC self-renewal through the regulation of genes involved in cell cycle regulation and apoptosis [110] and to increase the multilineage potential of human HSCs, as well as their replating capacity [111]. Other genes in which the expression was shown to increase self-renewal and repopulation potential includes *Hes1* and *Hlf* [112] as well as *Notch1* [113]. In contrast, activation of certain genes and pathways like the mTOR pathway leads to loss of HSC self-renewal [114], similarly to BATF activation that limits HSC self-renewal in response to DNA damage, a feature that can contribute to cancer protection but may also promote tissue ageing [115].

In addition, HSC fate choices are greatly influenced and controlled by epigenetic changes. For example, it was revealed that increase in H4K16Ac levels led to inhibition of Cdc42 which resulted in functional restauration of aged HSCs [116]. Also, increased levels of H3K9me2 was shown to set HSC lineage commitment, whereas inhibition of G9 improved HSC maintenance [117].

Specifically acting on cell cycle, the transcription factor and chromatin remodeler SATB1 was shown to regulate various cell cycle regulators (including MYC) in HSCs [118]. The lack of this gene in mouse HSCs was revealed to lead to lower quiescence, lower repopulation potential and decreased symmetric self-renewal cell division frequencies at the single cell level. Similarly, the transcription factor PU.1 regulates the transcription of multiple cell cycle regulators in HSCs [119]. Accordingly, low levels of PU.1 in HSCs promote loss of HSC quiescence and increase in cell proliferation. Chromatin immunoprecipitation followed by sequencing (ChIP-seq) studies in LSK cells revealed that PU.1 binds to enhancers and promoters of multiple cell cycle

inhibitors and activators, including *Gfi1*, *E2f1*, *Cdc25a*, *Cdk1*, *Cdkn1a* and *Cdkn1c*, regulating their expression.

Recently, the application of next generation sequencing to genome-wide analysis of haematopoietic transcription factors has evidenced interactions in a complex combinatorial manner [120-122]. These multidimensional interaction studies provided new insights into the HSC regulatory machinery and also highlighted the importance of epigenetic regulation in the coordination of expression and activity of these transcription factors in both normal and leukaemic initiating cells.

I.1.3.3. THE HSC NICHE

The concept of stem cell niche was first introduced by Schofield as a region that can harbour stem cells and maintain the balance between self-renewal and differentiation [123]. Since then, much progress has been made in the identification of HSC niche components in the BM.

The osteoblastic niche was first demonstrated in 2003 by two research groups that showed that increase in the number of osteoblasts (OBs) *in vivo* was associated with increased number of HSCs [74, 75]. Zhang and colleagues demonstrated interactions via N-cadherin between label retaining haematopoietic cells and osteoblasts on the endosteal surface. Angiopoietin-1 (ANG-1) and TPO expressed by OBs which bind to Tie2 and MPL receptors respectively, can also contribute to HSC quiescence [124, 72]. The work demonstrating the Tie2/Ang-1 signalling pathway also confirmed the expression of N-cadherin in $Tie2^{+}$LSK cells, however none of the subsequent studies identified a functional role for N-cadherin in the HSC niche. Other two studies that followed have identified the expression of N-cadherin on LSK [125] and $Flk2^{-}$LSK cells [126] thus, proposing roles for N-cadherin in the HSC niche. However, in direct conflict with these observations, two other papers reported no evidence of N-cadherin expression on $Flk2^{-}$LSK cells or a further enriched population, SLAM-LSK HSCs [127, 128]. In addition, these authors found that N-cadherin conditional knockout mice had no observable phenotype in HSC frequency, long-term competitive repopulation, or serial transplantability [128]. This led to a heated debate between Linheng Li and Sean Morrison groups that upon mediation led to the conclusion that N-cadherin does not

play an essential functional role in HSCs [129]. In fact, although OBs have been shown to sustain the quiescence and retention of HSCs [130-132, 72], recent imaging studies did not reveal a significant association between osteoblasts and HSCs [133].

Meanwhile, in 2005, Kiel *et al* identified HSCs in close proximity to vascular sinusoids using SLAM family markers (CD150, CD244, CD48) thus, providing first evidence of the vascular niche [12]. Shortly after, perivascular stromal cells expressing CXCL12 (CAR cells) were identified in contact with HSCs near sinusoids and shown to regulate HSC self-renewal, proliferation and trafficking [134]. Chemokine CXCL12 is essential for migration, retention and mobilisation of HSCs [135]. Additionally, perivascular human MSCs ($CD146^+$) were shown to reconstitute bone marrow niche, suggesting their importance in regulating haematopoiesis [136]. Importantly, sinusoidal endothelial cells can balance the expansion and differentiation of LT-HSCs by preventing exhaustion of the repopulating LT-HSC pool through Notch signalling [137] and endothelial-specific Jagged1 appears to be required to maintain functional HSCs in steady state and to prevent premature exhaustion during BM regeneration [138].

In the last years the advanced imaging technologies helped in unveiling cellular location specificity, new cellular components and candidates involved in the HSC maintenance. In mice, $Nestin^+$ perivascular MSCs are spatially associated with HSCs, and *in vivo* $Nestin^+$ cell depletion was shown to rapidly reduce HSC content in the bone marrow and to reduce HSPC bone marrow homing [76]. In addition, sympathetic nerves that are associated to $Nestin^+$ cells regulate circadian expression of CXCL12 [139]. Conditional knockdown of *Scf* in endothelial and perivascular cells was shown to cause reduction in HSC frequency in BM [140], whereas deletion of *Cxcl12* in perivascular stromal cells ($LepR^+$) and CAR cells revealed no effect in HSC and progenitor numbers or reconstitution levels but increased mobilisation [141, 140]. In another interesting study, quiescent HSCs were illustrated to preferentially associate with arterioles, where high Nestin-expressing cells were observed, while proliferative HSCs were found to be away from this niche [133].

Other types of cells known to regulate HSCs are the mature blood cells found in BM. For instance, $CD169^+$ macrophages promote HSC retention by inducing CXCL12 production by $Nestin^+$ perivascular cells [142]. Also, megakaryocytes were shown to

localise with a subset of HSCs and promote their quiescence through production of CXCL4 and TGF-β1 [143].

Thus, several niche cells have been shown to be important regulators of HSPCs not only through direct contact but also through secreted signals. The diversity of these signals provides multiple targets for new agents for haematopoietic recovery and to increase stem cell yields for transplantation. Interactions between these signals must continue to be explored to unravel the complex nature of the HSC niche. Of note, alteration of the niche can also lead to a pathological microenvironment leading to abnormal haematopoiesis (reviewed in [144]). Studies on benign and malignant BM niche are crucial not only for the understanding of the basic biology of this system but also to ensure a safe translation to the treatment of malignancies. Therefore, the identification and characterisation of new niche components can not only elucidate HSPC regulation but may also be exploited for therapeutic ends.

I.2. NOTCH SIGNALLING IN HAEMATOPOIESIS

The canonical Notch signalling is an evolutionarily conserved pathway with a fundamental role in many cellular functions including cell fate determination in most developing tissues and organs, as well as cell differentiation, proliferation and survival in adult tissues [145, 146]. The essential role of Notch signalling during development is supported by the embryonic lethality that is associated with deficiencies in Notch signalling in various model organisms, including worms, flies and mice. Notch signals are used iteratively at different decision points to guide functional outcomes dependent on gene dose and signalling context [147]. Indeed, aberrant levels of Notch signalling are associated not only with human developmental anomalies but also with the progression of several malignancies, where it can either promote an oncogenic or tumour suppressive effect depending on the tissue and cellular context (reviewed in [148]). Particularly, in the haematopoietic system, although Notch is a well-recognised oncogene in several lymphoid malignancies (T-cell acute lymphoblastic leukaemia (T-ALL), B-cell chronic lymphocytic leukaemia, splenic marginal zone lymphoma), more recent studies are focusing on the role of Notch signalling as a tumour suppressor in myeloid malignancies [148].

Notch signalling differs from a conventional signalling pathway triggered by the interaction of soluble factors and their receptors. This pathway requires cell-to-cell contact for activation through the interaction of a ligand and a receptor as transmembrane proteins expressed on the cell surface, making it an ideal candidate for instructing communication between a cell and other closely associated cells like HSPCs and niche cells.

The importance of Notch signalling in haematopoiesis was firstly highlighted by its association with haematological malignancies [149], motivating further efforts to elucidate its role in HSC regulation and lineage determination. Moreover, Notch receptors and ligands are widely expressed in the haematopoietic system, further implying the importance of this signalling pathway in adult haematopoiesis.

However, although Notch signalling proved a well-established role in HSC emergence during development [150] and in T cell formation [151], its role in the maintenance of adult HSCs has been controversial due to conflicting reports. Many studies have been performed to elucidate the role of Notch signalling in HSPC regulation in a cell autonomous and non-autonomous manner. These studies will be reviewed in this sub-chapter to help understand the current stand on the role of Notch signalling in human haematopoiesis.

I.2.1. THE NOTCH SIGNALLING PATHWAY

After over a century of its discovery, many biochemical and biological studies have put together the details of the Notch signalling mechanism. This signalling pathway was first studied in *Drosophila* where it was shown that the *Notch* gene encodes a large transmembrane receptor that interacts extracellularly with membrane-bound ligands encoded by the *Delta* and *Serrate* genes [152].

In a simplistic way, cellular outcomes mediated by canonical Notch signalling are determined by a signal transduction mechanism in which proteolysis of a Notch receptor is enabled upon effective binding to a Notch ligand, releasing the Notch receptor intracellular domain (NICD) which translocates to the nucleus where it associates with DNA-binding factor RBPjκ and coactivators to enable the transcription of Notch target genes.

I.2.1.1. NOTCH RECEPTORS AND LIGANDS

Notch receptors are single-pass transmembrane heterodimer proteins composed by distinct protein modules (**Figure I.2**). The extracellular region consists of a series of N-terminal epidermal growth factor (EGF)-like repeats and it is followed by a juxtamembrane negative regulatory region (NRR) comprised of three Lin12/Notch repeats (LNR) and a heterodimerisation domain (HD). The intracellular region comprises a protein-binding RBPjκ-associated molecule (RAM) region, seven ankyrin repeats (ANK), nuclear localisation signals (NLS), a transcriptional activation domain (TAD), and a C-terminal degron domain rich in amino acids proline, glutamate, serine,

and threonine (PEST) [153]. In mammals, four different Notch receptors Notch1-4 (N1-4) have been identified, encoded by different genes. These receptors differ in the number of EGF repeats (from 29 to 36) and also in the structure of their C-terminal intracellular regions.

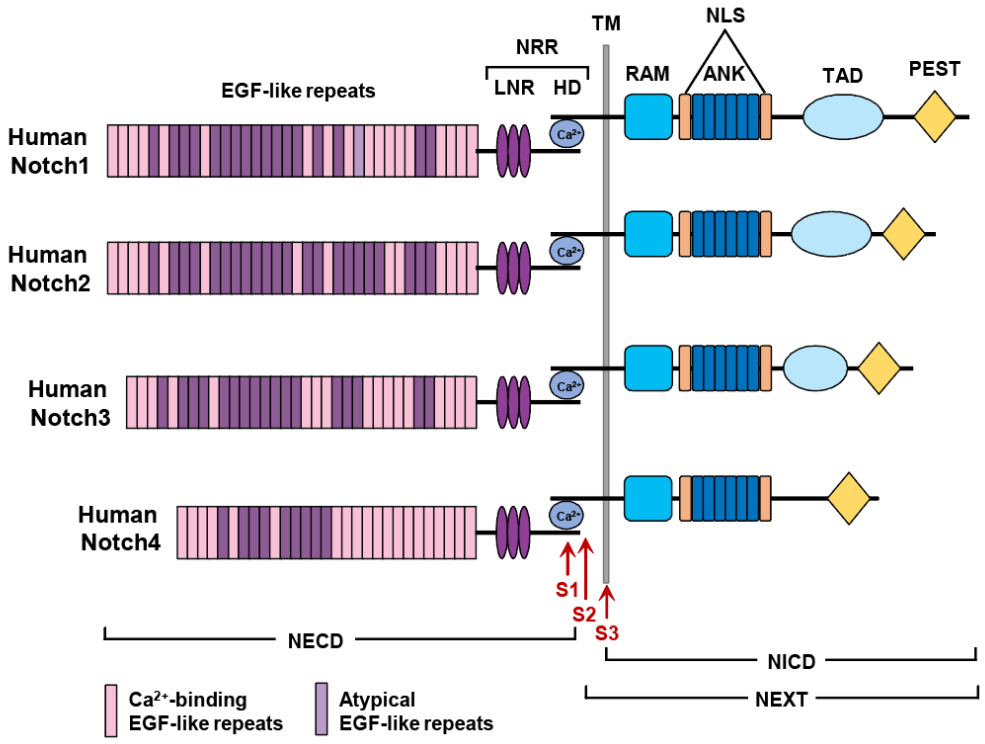

Figure I.2 - Structure of human Notch receptors. Abbreviations: ANK, ankyrin repeat domain; DSL, HD, heterodimerisation domain; LNR, Lin-12/Notch repeat; NECD, Notch extracellular domain; NEXT, Notch extracellular truncation; NICD, Notch intracellular domain; NLS, nuclear localisation signals; NRR, negative regulatory region; PEST, proline, glutamate, serine, and threonine; RAM, RPBjκ-associated molecule; TAD, transcriptional activation domain; TM, transmembrane domain. Adapted from [154].

In the extracellular domain (NECD), effective interactions with a ligand from neighbouring cells (trans interactions) are known to be mediated by EGF repeats 11–12, whereas inhibitory interactions with a ligand co-expressed in the same cell (cis interactions) are mediated by repeats 24–29 [155]. Calcium-binding EGF repeats play an important role in determining the structure and affinity of Notch to its ligands [156, 154]. The EGF repeats are followed by a NRR, identical between receptors, and are considered as the ‘activation switch’ of the receptor, responsible for keeping the receptor in an autoinhibited conformation and preventing ligand-independent activation [157]. Disruption of this autoinhibition is frequently observed in T-ALL with

mutations that affect the NRR from N1 receptor [158]. During trafficking to the cell surface, Notch receptors undergo a series of maturation steps in the trans-Golgi network that include glycosylation by enzymes like O-fucosyl transferase 1 (Pofut1) and Fringe proteins (Lunatic, Manic, and Radical Fringe) [159, 160]. Additionally, immature receptors are cleaved by a Furin-like protease at site S1 in an unstructured region of the HD [161], originating the mature Notch heterodimer in which a Notch extracellular subunit (NECD) and a transmembrane Notch subunit (NTM) are associated by a calcium-dependent non-covalent bond [162]. In this structure, the NRR stays enclosed between the ligand-binding and transmembrane domains, adopting a conformation in which an extensive interface between the LNR and HD domains buries a metalloprotease site (S2), the first cleavage site necessary for Notch activation.

Intracellularly, the RAM domain is a high affinity binding module with a conserved WxP (tryptophan-any amino acid-proline) motif, believed to be essential for co-repressors displacement from DNA binding factor RBPjκ by NICD [163]. An unstructured linker containing one NLS sequence connects RAM to the ANK domain, which is followed by an additional NLS and the TAD.

Unlike the RAM, ANK, and PEST domains, which are highly conserved, the TAD shows substantial evolutionary divergence among the four mammalian Notch receptors. N1 TAD is homologous to its Drosophila counterpart, while N2 contains a similar TAD with weaker activity. In contrast, N3 contains a TAD that shares minimal function and sequence conservation, while N4 does not possess one at all [164]. N1 TAD can directly interact with transcriptional coactivators [164] which can increase N1-induced transcription by recruiting additional coactivators or stabilising the association of acetyltransferase p300 with the Notch transcriptional complex [165]. Actually, N3 and N4 have a weaker transcription activation as compared to N1 and N2, and this strength appears to be dependent on promoter context and the cooperation of RAM-ANK and TAD domains within each Notch receptor [166]. Interestingly, N3 appears to be able to repress N1-mediated activation through HES promoters due to competition for RBPjκ access and for a common coactivator present in limiting amounts [167]. Also, in a more recent report, N4 was shown to be able to inhibit N1 activation by receptor cis-inhibition [168]. These reports indicate that under certain contexts N3 and N4 receptors can play a role in the regulation of N1 signalling strength.

Finally, the end part of the C-terminus of the Notch receptors contains a conserved PEST domain, containing degrons that regulate the stability of NICD. Phosphorylation of PEST domain is recognised by E3 ubiquitin ligases FBW7 that promote ubiquitin-mediated degradation of the NICD. In addition to mutations in HD, the main N1 active mutation in T-ALL affects the PEST domain, producing insensitivity to FBW7 [169]. Additionally, the levels of Notch receptors at the cell surface and therefore their availability for ligand binding can be regulated by E3 ligases - Deltex, Supressor of Deltex (Itch/AIP4) - that control Notch receptor trafficking either towards lysosomal degradation or recycling, impacting its half-life [170].

Regarding Notch ligands, there are also four functional ligands in mammals (**Figure I.3**), all of which are single-pass transmembrane proteins: Delta-like1 (Dll1) and Delta-like (Dll4) are members of the Delta family of ligands, and Jagged1 (Jag1) and Jagged2 (Jag2) that are members of the Serrate family of ligands. Delta-like 3 (Dll3) is incapable of activating Notch signalling and has been recognised as a decoy ligand, since phenotypes observed in *Dll3*-deficient mice are consistent with Notch gain of function [171]. Notch ligands are also composed by an extracellular domain with a variable number of EGF-like repeats but unlike the receptors, the ligands possess only a small intracellular portion without distinct protein modules.

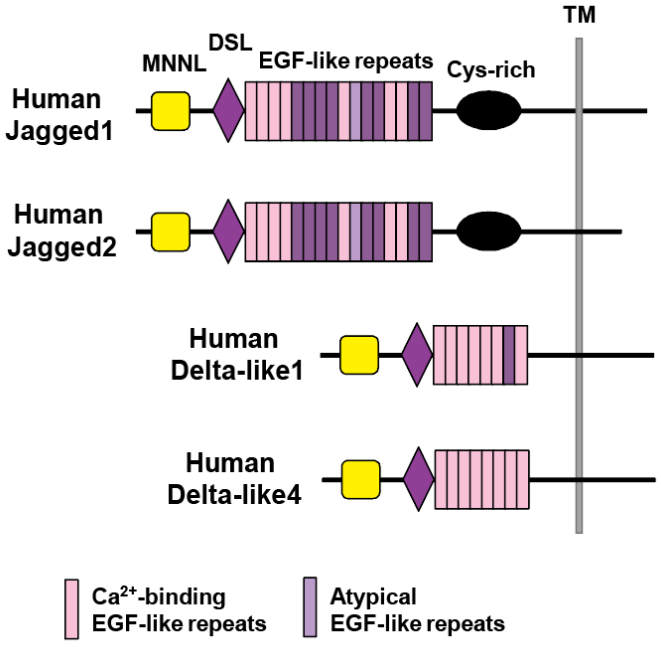

Figure I.3 – Structure of human Notch ligands. Abbreviations: DSL, Delta-Serrate-Lag2 domain; MNNL, N-terminal domain of Notch ligand; TM, transmembrane domain. Adapted from [154].

The extracellular domain of human Notch ligands is characterised by three related structural motifs: a conserved MNNL (module at the N-terminus of Notch ligands) domain, a distinct cysteine-rich DSL (Delta/Serrate/LAG-2) motif which is followed by a series of iterated EGF-like repeats (both calcium-binding and non-calcium binding) that precede the transmembrane segment. Jagged ligands also contain a cysteine-rich domain between the EGF-like repeats and the transmembrane domain that is not observed in Delta ligands [154]. Several mutagenesis and deletion studies previously showed that the DSL domain conferred specificity of binding to Notch receptors which is facilitated by the covalent linkage of EGF1 and 2 to the DSL [154].

Many studies have focused on investigating the secondary structure of Notch receptors and ligands, as well as the structure of receptor-ligands complexes to elucidate the extracellular regions that are involved in the binding interaction that leads to a signal (reviewed in [154, 172]). Initial studies indicated that the DSL domain within each ligand could interact with Notch EGF11-12, with possible involvement of additional domains [153]. Recently, two landmark studies solved the X-ray structures of N1-Dll4 [173] and N1-Jag1 complexes [174]. These comparison studies between receptor and ligand complexes revealed that the interface observed between N1 and Dll4 was larger than between N1 and Jag1. This data supports other experiments that demonstrated higher *in vitro* affinity of Dll4 for N1 compared to Jag1 [175]. Interestingly, while N1-Dll4 interactions involve only EGF10-13, in N1-Jag1 complex additional interactions seem to occur between EGF1-3 in Jag1 and EGF8-10 in N1. This was demonstrated by the existence of *catch bonds* in which the strength of interaction was shown to increase when greater forces or shear stress were applied. This finding suggests that when a low force is applied, the Jag1/N1 interaction may be unproductive, whereas for Dll4/N1 may result in receptor activation, and this difference may be important for the function of distinct ligands under different physiological settings.

The concept of Notch activation requiring a pulling force was first introduced nearly two decades ago when Parks *et al*. proposed that the mechanical strain generated by receptor trans-endocytosis upon ligand binding somehow exposed the S2 cleavage site [176]. However, only more recently, studies employed molecular force measurements which demonstrated that forces between 4 and 9 pN were sufficient to unfold the N1 NRR in response to Dll1, and that allosteric interactions mediated by

EGF repeats did not affect the force required [172]. The origin of this *in vivo* force remains poorly defined, with the prevailing hypothesis being ligand endocytosis mediated by ubiquitination of the ligand intracellular domain by E3 ligase Mind bomb1 (Mib1) [177]. Nevertheless, how the ubiquitination mechanistically contributes to endocytosis is still not understood, and alternative candidates for producing a “pulling force” have been proposed to be associated to cell migration and shear stress generated by blood flow [178].

Despite substantial advances there is still limited understanding on how much binding affinities vary for different ligand-receptor pairs, and how much do regions that flank the key interacting domains contribute to binding affinity and specificity.

As mentioned above, Notch receptors suffer post-translational glycosylation modifications which modulate their relative response to ligands of the Delta versus Jagged families. Indeed, modifications by Fringe potentiates interactions of N1 with Dll1 and reduces responsiveness to Jag1 [179], although it is still unknown how these modifications can inhibit Jag1-mediated activation. Nevertheless, these observations suggest that the presence of specific Fringe enzymes could help to fine-tune the response of Notch receptors to available ligands in different cellular environments. Certainly, it is well established that different Fringe homologs modulate Notch-mediated biologic processes in a specific manner, such is the case of Lunatic Fringe in the haematopoietic lineage commitment and differentiation [180].

I.2.1.2. NOTCH SIGNALLING MECHANISM

Notch signalling is initiated when a productive trans interaction between a Notch receptor and Notch ligand occurs, leading to the activation of the receptor through two sequential cleavages (**Figure I.4**).

Ligand binding produces a conformational change of the receptor releasing the autoinhibition imposed by the NRR thus, allowing ADAM metalloproteases to cleave at S2 site, which lies immediately externally to the transmembrane domain (**Figure I.2**) [181, 182]. Both ADAM10 and ADAM17 have been implicated in S2 cleavage, with reports suggesting that ADAM10 acts predominantly under physiologic conditions [183, 184], whereas ADAM17 appears to be associated to ligand-independent

pathophysiologic Notch activation [185]. S2 cleavage results in shedding of the NECD, creating a short-lived membrane-bound form of Notch, termed Notch extracellular truncation (NEXT) that is rapidly cleaved within its transmembrane segment at S3 site by the γ-secretase complex [186, 187] thus, releasing the NICD. Once released, the NICD translocates to the nucleus and integrates a ternary transcription complex by association to the DNA binding factor RBPjκ (also known as CSL [for CBF1/ RBPjκ (C-promoter Binding Factor1/ Recombination Binding Protein jκ), Su(H) (Suppressor of Hairless), and Lag-1]), and the coactivator Mastermind-like (MAML) [188], to activate transcription of Notch target genes.

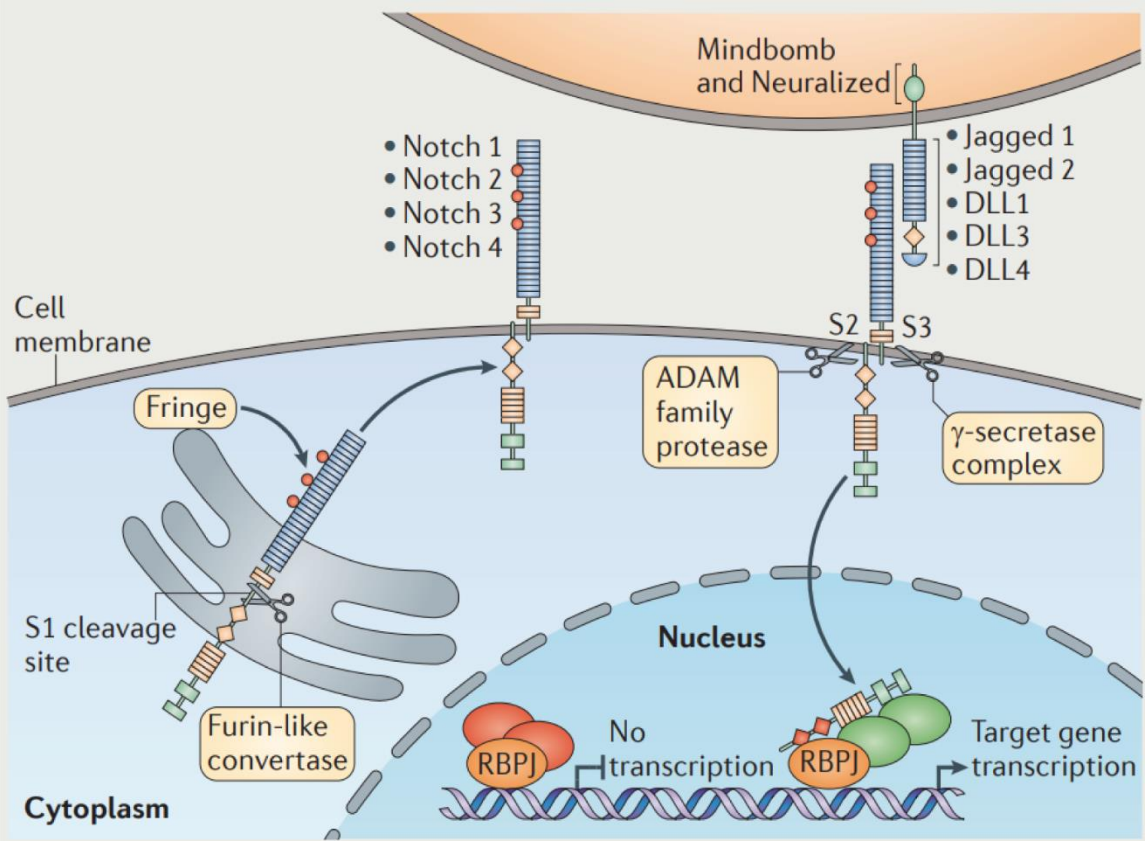

Figure I.4 – Notch signalling pathway. Immature Notch receptors are subjected to cleavage by furin-like proteases (S1), glycosylation by Pofut1 (not shown) and Fringe glycosylases in the Golgi apparatus before presentation of the functional form at the cell surface. Productive binding of the receptors with ligands on neighbouring cells induces successive cleavages by ADAM proteases (S2) and γ-secretase (S3), releasing the intracellular domain of Notch that translocates to the nucleus and integrates a transcription activation complex by association to the DNA binding factor RBPjκ. Proteins shown in red and green are co-repressors and co-activators of RBPjκ, respectively [189].

Despite the number of ligands and receptors, the DNA-binding protein CSL is the centrepiece of transcriptional regulation in the canonical Notch pathway, acting as a molecular hub for interactions with either corepressors or coactivators to repress or activate transcription respectively [190]. In the absence of an active Notch signal CSL acts as a transcriptional repressor through association with corepressor complexes that keep the target enhancers silenced by recruiting histone deacetylases or other modifying enzymes (reviewed in [191]). Although it was originally proposed that the presence of the NICD could displace the co-repressors from CSL, recent studies have challenged this model, suggesting that an exchange of entire complexes (rather than co-activators substituting for co-repressors on DNA-resident CSL) is more likely [191]. Binding of the Notch transcription complex CSL-NICD-MAML recruits histone modifying coactivators, like CBP/EP300 (CREB Binding Protein/ E1A Binding Protein P300) or PCAF (P300/CBP-associated factor). This leads to rapid increases in the deposition of chromatin marks on nucleosomes, including H3K4 trimethylation and H2B ubiquitinylation in the promoters of Notch regulated genes, and H3K27 and H3K56 acetylation in Notch-regulated enhancer elements, enabling transcription of the target genes [191, 172].

Given the fact that all cell types use this common core complex (CSL/NICD) to mediate Notch transcriptional responses, many studies have been focusing on how this complex can regulate distinct sets of target genes within different cell types. In fact, CSL DNA binding sites architecture, affinity, and combinatorial cis-regulatory logic appear to differ between enhancers and are likely to contribute to target gene specificity. Additionally, expression of cooperating factors and repressors differ within different cell contexts enabling different Notch responses [191].

The best-characterised Notch targets belong to the *Hes/Hey* families, which codify for bHLH (basic helix-loop-helix) proteins that in general, function as DNA-binding transcriptional repressors. Expression of several members of the family (including *Hes1*, *Hes5*, *Hes7*, *Hey1*, and *Hey2*) depends mostly on Notch activity and are known to participate in many of the Notch-assigned functions, including proliferation, differentiation, apoptosis, self-renewal, and asymmetric cell division regulation, by repressing key cell fate determinants and cell cycle regulators [192]. *Hes* genes are generally responsible for Notch functions that require the inhibition of one specific cell fate to allow the determination of an alternative fate (lateral inhibition). In addition,

many components of the Notch pathway are themselves direct targets. For instance, *Deltex1* encodes a ubiquitin ligase that regulates Notch trafficking and was first shown to be positively regulated by Notch thus, acting as a negative feedback regulator [193]. Other common targets include components of other signalling pathways, like positive and negative regulators of Ras [194] and EGF receptor [195] pathways. The precise nature of the Notch targets and the consequences for the cross-regulation of signalling pathways are likely to differ depending on cell context. Importantly, Notch also directly regulates expression of genes encoding proteins that actually implement cell functions. For example, in T-ALL cells many of the direct targets are involved in metabolism [196], while in several developmental contexts direct targets include cytoskeletal regulators [197].

Although Notch mediates a number of biological processes through the canonical pathway, a ligand- or CSL-independent (non-canonical) function of Notch has also been reported. The most well-studied and conserved effect of non-canonical Notch function is the regulation of Wnt/β-catenin signalling, in which Notch titrates levels of active β-catenin (reviewed in [198]).

I.2.1.3. NOTCH EXPRESSION AND FUNCTIONS

Given that each Notch molecule undergoes proteolysis to generate a signal and thus, can only signal once, regulation of either ligand or receptor availability at the cell surface are key to control Notch activation. A simple way of regulating availability is to restrict ligand and/or receptor expression spatially and temporally. Indeed, different ligands and receptors can have overlapping as well as distinct expression patterns during development and are subject to regulation by other signalling pathways (reviewed in [199]).

N1 and N2 receptors are widely expressed in many tissues during development and also in adult mammals. N3 expression is particularly found in vascular smooth muscle and pericytes, while N4 is most highly expressed in endothelium. Accordingly, *Notch1* [200] and *Notch2* [201] knockout mice result in embryonic lethality associated with developmental defects in many organs, whereas *Notch3* [202] and *Notch4* [200] knockout mice are viable displaying multiple blood vessels defects.

The presence of four mammalian Notch receptors and many ligands led to the suggestion that each Notch protein may target a discrete set of downstream genes. However, it has been reported that Notch receptors can display both unique [203, 150] and redundant functions [204, 205] during development of different tissues. Interestingly, it has been shown that Notch paralogs can have contrasting roles in the same tissue, as observed in different stages of human breast cancer where N1 may act as an oncogene and N2 may play a tumour-suppressor role [206].

Although expression patterns of ligands are less well defined than for receptors, some knockout mice studies and congenital human disorders have revealed specific ligand functions and preferred ligand-receptor pairs. For instance, knockout mice show that expression of Dll4 on thymic epithelial cells [207] and Notch1 on haematopoietic progenitors [151] are required to induce T cell development, in accordance with biochemical studies showing that N1 has a higher affinity for Dll4 than for Dll1 [175]. On the other hand, the Dll1-Notch2 interaction is required for marginal zone B-cell development [208, 209] and mast cell adhesion at inflammatory sites [210]. Additionally, Dll1 and Dll4 appear to play distinct roles in vascular signalling [211] and were even shown to have opposing effects on muscle differentiation [212, 213]. In fact, Dll4 is unable to replace Dll1 function in many tissues, leading to embryonic lethality in mice when knocked into the *Dll1* locus [214]. Moreover, ligand specification has been associated to N1 indispensable role in arterial specification and HSCs emergence, given that *Dll4* deletion results in strong arterial defects [215], whereas *Jag1* deletion impairs definitive haematopoiesis [216]. Accordingly, arterial endothelial cells and HSCs originate from distinct endothelial precursors characterised by different N1 signal strengths triggered by different ligands: Jag1 was shown to produce low Notch strength thus, inhibiting the endothelial programme and allowing HSC specification, while Dll4 was demonstrated to induce high Notch activation by selecting the endothelial fate [217]. However, it remains unclear whether these effects were merely due to the spatial and temporal differences in expression patterns or if there were underlying intrinsic differences in affinity among various ligand-receptor complexes.

An interesting new study has started to shed some light on this subject, showing that ligand identity can control Notch activity dynamics. In this study it was revealed that Dll1 induced a pulsatile N1 activation, whereas Dll4 triggered a sustained activation,

which preferentially upregulated *Hes1* and *Hey1/HeyL*, respectively, producing opposite cell fates in embryonic myogenesis [218].

Regarding the adult haematopoietic system, *Notch1 and Notch2* were first shown to be expressed in human BM haematopoietic progenitors [219]. More recently, expression of N1, N2 and N4 was also demonstrated at the protein level in UCB and BM HSPCs, including in the more primitive $CD34^-$ HSC population, which was revealed to have higher Notch activation [27]. Accordingly, the expression of Notch ligands in haematopoietic niche cells has been extensively reported [220]. So far, a great number of studies have tried to understand the effects of Notch signalling in adult haematopoiesis and in particular, the distinct roles of each receptor and ligand in the niche context, which will be discussed in the following sections.

I.2.2. NOTCH SIGNALLING IN HSPC REGULATION

As previously mentioned, although it has been established an essential role for Notch signalling during development of the haematopoietic system [150] and in T cell specification [151], its role in the regulation of adult HSCs in physiological conditions remains controversial due to conflicting reports.

Initial studies suggested that activation of Notch signalling in HSPCs was associated with increased stemness, given that HSPCs expressing a constitutively active form of N1ICD [221] or the Notch target Hes1 [222] presented increased self-renewal capacity. Further to this, activation of Notch signalling through exposure of haematopoietic precursors to Notch ligands *in vivo* and *in vitro*, such as Jag1 [75], Dll1 [223] and soluble Jag1 [224] also promoted stem cell self-renewal while inhibiting differentiation.

Although these early reports suggested that Notch signalling could be a regulator of haematopoiesis, it might be contested that this effect could likely to be due to super-physiological levels of Notch signalling *in vitro*. Nevertheless, in an interesting study, loss of *Itch* (an E3 ubiquitin ligase that controls Notch receptor degradation) in HSPCs led to sustained levels of Notch1 activation thus, functioning as an indirect Notch gain-of-function approach [225]. Mice that were transplanted with Itch-deficient LSK cells

had an expanded stem cell pool with enhanced haematopoietic contribution up to 24 weeks as compared to control LSK cells.

Despite these positive results that paved the way for approaches that allowed the development of *in vitro* HSPCs expansion protocols [226, 227], the understanding of the functional role of Notch signalling remains unclear as loss of function approaches have led to the proposal that the Notch pathway is not required in steady-state haematopoiesis.

I.2.2.1. NOTCH LOSS-OF-FUNCTION EFFECTS IN HSPCS

A summary of the Notch loss-of-function studies and their effects on haematopoiesis is presented in **Table I.1**.

In early reports, loss of *Notch1* [151] and *Rbpj* [228] have established the Notch1-RBPjκ-Hes1 axis as a major regulator of T cell differentiation, while no myeloid and B-cell lineage defects were observed. Although these studies did not focus on HSCs, LSK cells from a transgenic Notch reporter (TNR-GFP) mouse have been shown in a subsequent study to harbour high Notch activity. In this study, the authors observed co-localisation of c-kit$^+$ and GFP$^+$ cells in bone marrow sections and GFP expression in primitive LSK cells by flow cytometry. Additionally, transplantation of murine Lin$^-$ cells transduced with dominant-negative *Rbpj* resulted in the depletion of HSCs population after long-term reconstitution [229].

Moreover, as in other contexts, it is still largely unknown which Notch ligand/receptor pairing is preferentially used by HSPCs or if the different receptor-ligand interactions trigger different responses. Jag1 was shown to be expressed on bone marrow osteoblasts from mouse and human [75, 230]. However, both loss of *Jagged1* and *Notch1* in the bone marrow had no effect either on HSCs homeostasis, on haematopoietic reconstitution after genotoxic insult or in cell numbers of stem and progenitor subsets after bone marrow transplant [231]. Thus, this study excluded an essential role for Jag1-mediated N1 signalling on HSCs self-renewal or differentiation. However, these studies did not rule out the possible redundant effects from other Notch receptors or ligands. Indeed, Varnum-Finney and colleagues demonstrated that N2 specifically inhibited myeloid differentiation *in vitro* and promoted LSK cell self-

renewal and repopulation following transplantation. However, under steady-state conditions, neither loss of N1 nor N2 had any effect on the number of HSCs [232]. It was also recently reported that activation of N2 mediated by EC-derived Jag2 was essential for HSPCs recovery after myelosuppression, regulating HSPC cell cycle and quiescence during regeneration [233]. Another recent study on the role of N2 found that N2 blockade, but not N1, and N2 deficiency (*Vav-Cre*/*Notch2*$^{fl/fl}$) led to increase in HSPC egress from BM [234]. Interestingly, N2-blocked LSK and N2-deficient LSK showed less cells in G0 and more in G1, suggesting that N2 helps maintain HSPCs quiescence. Nevertheless, BM HSPC homeostasis remained unaffected either in N2-deficient mice or recipients of N2-deficient HSPCs. Although a mild decrease in HSPCS subpopulations (MPPs, CMPs, MEPs and CLPs) was observed after N2 blockade, no effect in reconstitution capacity was observed after BM transplantation. Accordingly, another study evaluated a pan-inhibition of canonical Notch signalling, where LSK cells expressing a dominant negative form of MAML1 (dnMAML1) showed comparable repopulation capacities to control LSK cells [235]. In contrast to the observations of Duncan *et al.* [229], it is now generally viewed that mouse HSPCs cells are in fact exposed to very low levels of Notch signalling *in vivo* (due to low Notch receptors expression on mouse HSPCs). This could explain why loss of the canonical Notch signalling reported in few studies failed to result in dramatic effects, whereas exposing cells to super-physiological levels of ligands or NICD *in vitro* resulted in stem cell self-renewal.

Despite this divergent data in mice, only more recently it was explored the role of Notch pathway in human HSCs *in vivo*. Benveniste *et al*. directly compared the effects of blocking canonical Notch signalling by overexpressing dnMAML1 in human purified HSCs *in vitro* and *in vivo* [236]. In this study the authors claimed that, similar to the mice system [235], excluding the blockage of T-lineage development from dnMAML1-HSCs, there was comparable contribution to all haematopoietic lineages in a transplantation competition assay between control- and dnMAML1-HSCs. On the other hand, *in vitro* dnMAML1-HSCs showed both blocked T-cell differentiation and impaired HSCs maintenance/expansion. Nevertheless, a more cautious evaluation of the engraftment assay in this study could infer a different interpretation. Firstly, it should be noted that the frequency of the engrafted human dnMAML1-HSCs population was half as compared to controls and secondly, the total number of

dnMAML1 engrafted cells ($CD45^+$) was more than double than in control mice. Thus, the authors claim that the total number of engrafted dnMAML1-HSCs was comparable to control HSCs might not be correct, as the frequency of dnMAML1-HSCs was reduced, likely due to increase in differentiation leading to expansion of total human $CD45^+$ cells.

Table I.1 – Studies of Notch signalling in HSPCs regulation

Study	Method	Species	Effect on general haematopoiesis	Effect on HSCs/HSPCs	Ref.
Notch1 **deletion**	*Mx1-Cre*	Mouse	Impaired T cell development; Myeloid and B cell development is normal	ND	[151]
Rbpj **deletion**	*Mx1-Cre*	Mouse	Impaired T cell development; Myeloid and B cell development is normal	ND	[228]
dnRBPjκ LSK cells	Overexpression of dnMAML1 or dnRBPjκ	Mouse	Accelerated differentiation towards B and myeloid cell lineages	Depletion of LT-HSC	[229]
Jagged1 **and** ***Jagged1/ Notch1*** **deletion**	*Mx1-Cre*	Mouse	No effect on progenitor nor mature lymphoid, myeloid and erythroid lineages	Normal LSK	[231]
dnMAML1 LSK cells ***Rbpj*** **deletion**	Overexpression of dnMAML1 *Mx1-Cre*	Mouse	Impaired T cell development but normal myeloid and B cell development	Normal HSCs	[235]
Notch1 **and** ***Notch2*** **deletion**	*Mx1-Cre*	Mouse	Myeloid and B cell development normal in steady state	Normal HSCs	[232]
dnMAML1 HSCs	Overexpression of dnMAML1 in UCB cells	Human	Impaired T cell development but normal myeloid and B cell development	Reduced frequency but higher HSCs numbers	[236]
γ-secretase inhibitor (DAPT)	DAPT administration *in vivo*	Human	Early differentiation of HSPCs	Higher engraftment (increased generation of $CD34^+CD38^-$ from $CD34^-$ HSCs)	[27]

ND: not determined

Furthermore, it is important to consider possible non-canonical functions of the Notch receptors as a compensatory mechanism. In fact, it has been described that exposure to Dll1 can rewire IL-6 mediated signal in human $CD34^+$ cells through non-canonical mechanisms that reduce membrane-bound IL-6 receptor expression, converting progenitors from being directly IL-6 responsive, reducing myeloid differentiation [237].

Importantly, it should be noted that the more primitive population, defined as $Lin^-CD34^-CD38^-CD93^{hi}$ (-/-/+), has higher Notch activity than the more mature but still enriched $CD34^+$ HSCs population ($Lin^-CD34^+CD45RA^-CD90^+CD49f^+$). Indeed, the engraftment potential of the -/-/+ HSCs was demonstrated to increase after several administrations of the γ-secretase inhibitor DAPT in a xenograft model [27]. Although a more prolonged DAPT administration was shown to further increase human engraftment, this occurred at the expense of $CD34^+$ cells that are normally derived from the transplanted -/-/+ HSCs. These results suggest that the activation of the Notch pathway is important for the maintenance of the human HSCs repopulation capacity. However, the potential effects induced by the microenvironment was not determined in this study since DAPT treatment may have also affected the niche cells.

Therefore, although these discrepancies suggest possible differences of Notch signalling effects on murine and human systems, this uncertainty underlies the need for having more stringent and well-described methods to disrupt Notch signalling.

I.2.2.2. NOTCH LOSS-OF-FUNCTION EFFECTS IN MYELOPOIESIS

While the previous studies focused on the performance of Notch defective HSPCs, several other studies have evaluated mouse models in which different members of the Notch pathway were deleted in the BM microenvironment, considering non-cell autonomous effects. **Table I.2** summarises some of these studies which have determined that Notch loss-of-function in the BM compartment frequently leads to the development of a myeloproliferative disease (MPD) phenotype.

In an early report, deletion of γ-secretase members Presenilin1 and 2 resulted in an expanded granulocytic compartment in mice with signs of MPD, although no effects were observed in a side population (primitive population identified by a subset of $Sca\text{-}1^+$ cells capable of excluding dyes such as Hoechst33342) [238].

As previously mentioned, Notch receptors are subjected to post-translational modifications. FX (homolog of human GDP-L-fucose synthase) enzyme mediates the addition of N-acetylglucasamine residues [239], which are essential for proper interaction with ligands [240]. *Fx*$^{-/-}$ mice developed a fucosylation-dependent myeloproliferative phenotype, with expanded Gr1^{+} granulocytes and Ter119^{+} erythrocytes [241] . Additionally, these mutant mice showed increased CMP, GMP and MEP compartments, while CLPs were significantly reduced. Similar to FX-deficient cells, Pofut-deficient marrow progenitors have defective O-fucosylation of Notch receptors disabling their ability to bind to Delta-like ligands. Mice with pan-haematopoietic (*Mx1-Cre*) deletion of *Pofut* had increased numbers of myeloid cells and progenitors and reduced lymphocytes. In fact, overexpression of N1ICD in Pofut-deficient cells was able to rescue T cell development and myeloid hyperplasia, suggesting a role for O-fucose-dependent N1 activation [242]. Interestingly, these observations suggest that Notch must be important at the multipotent progenitor stage, where the fine-tuning of the pathway regulates the lymphoid *versus* myeloid cell fate decisions.

In addition, using two Cre lines, *MMTV-Cre* and *Mx1-Cre*, Kim and colleagues showed that the loss of *Mib1*, an essential component for Notch ligands endocytosis, led to MPD originated from the LSK population [243]. Interestingly, transplantation of BM cells from TNR-GFP mice showed that LSKs from reconstituted *Mib1*-mutant mice had the same level of Notch activation as wild-type cells, meaning that the MPD was not being caused by defective Notch receptor cleavage in HSPCs. In fact, the constitutive expression of N1ICD in *Mib1*-null microenvironment significantly delayed the development of MPD, suggesting that defective Notch signalling between the niche cells caused the MPD phenotype. Nevertheless, this data suggests that appropriate Notch signalling among the BM niche is required for LSK cells. In another study, the metalloprotease *Adam10* was deleted in the bone marrow compartment, which led to both cell-autonomous and non-cell-autonomous MPD characterised by increased granulopoiesis and HSCs pool [244]. This suggests once again that proper Notch signalling must be maintained not only in HSPCs but also in the BM microenvironment.

Table I.2 – Studies of Notch signalling in myelopoiesis

Mouse model	Phenotype	Effect on stem cells	Ref.
***Psen1*$^{+/-}$*/Psen2*$^{-/-}$**	MPD (expanded granulocytes)	Normal side population	[238]
***Fx*$^{-/-}$**	MPD	Normal LSK	[241]
MMTV-Cre/*Mib1*$^{f/f}$ ***Mx1-Cre/Mib1*$^{f/f}$**	MPD (expanded granulocytes)	Expanded LSK	[243]
***Mx1-Cre/Pofut*$^{f/f}$**	Increased neutrophils	ND	[242]
***Mx1-Cre/Adam10*$^{f/f}$**	MPD (expanded granulocytes)	Expanded LSK	[244]
***Mx1-Cre/Ncstn*$^{f/f}$**	CMML-like	Expanded LSK	[245]
***Mx1-Cre/Rbpj*$^{f/f}$** ***Tie2-Cre/Rbpj*$^{f/f}$**	MPD	Expanded LSK	[246]
***Vav-iCre*/dn*MAML1*$^{f/-}$**	Increased GMP but no myeloid neoplasm	Normal LSK and LT-HSC Decreased myeloid potential	[247]
***Mx1-Cre/Rbpj*$^{f/f}$** ***Vav-Cre/Rbpj*$^{f/f}$**	Normal	No effect	[248]

ND: not determined

Importantly, a subsequent work from Aifantis' group revealed that mice transplanted with Nicastrin (γ-secretase component)-deficient HSCs developed a human chronic myelomonocytic leukaemia-like disease with an expanded LSK compartment. This is one of the few studies that attempted to understand the mechanisms behind this effect, showing that Nicastrin-deficient LSK cells had a de-repressed myeloid program, which is thought to be carried out by Hes1-mediated inhibition of *Cepba* and *Spi1* expression [245].

In another interesting study, Carlesso's group showed that conditional deletion of *Rbpj* using *Mx1-Cre* led to MPD [246]. When performing reciprocal transplantation experiments, the authors observed that the mutant-LSK pool was significantly increased but the GMP, CMP and MEP subsets were unaffected in wild-type mice, showing similar survival compared to the control cohort. In contrast, when transplanting wild-type HSPCs into mutant mice, CMPs and GMPs in BM and spleen were significantly increased similarly to the parental *Rbpj*$^{-/-}$ mice, resulting in lethal

MPD. Interestingly, the disease evolved faster after BM transplant. Additionally, the wild-type LSK pool in mutant recipients was less affected than in parental *Rbpj*$^{-/-}$ mice or when mutant cells were transplanted into wild-type mice, demonstrating a cell-autonomous contribution of RBPjκ in HSCs regulation. However, this also suggests that cell autonomous loss of Notch activation is not sufficient to develop a myeloid disease, while loss of Notch signalling in the microenvironment induces lethal MPD in a non-cell-autonomous manner. Mechanistically, deletion of RBPjκ led to increase in miR-155 expression in BM niche cells where interestingly the NICD/RBPjκ complex acts as a transcription repressor of miR-155. miR-155 up-regulates NF-κB activation by targeting one if its inhibitors κB-Ras1, leading to increased expression of G-CSF and TNFα (tumour necrosis factor α) thus, inducing a persistent inflammatory state in the BM.

Contrasting to these results however, two different reports recently published indicated that loss of Notch signalling *in vivo* was insufficient for the development of MPD [247, 248]. In one study, the authors used a mouse model with dnMAML1 expression under the inducible Vav promoter, arguing this model should yield a more specific disruption of canonical Notch signalling than deleting Nicastrin (which has other substrates besides Notch) and that *Mx1-Cre* requires an interferon response for induction which can alter stem cell function and induce proliferation of myeloid cells [247]. Although there was a significant increase in GMPs, associated to a decrease in CMPs, there was no effect on the LSK and LT-HSC populations. This phenotype was not sufficient to generate myeloid neoplasms though this study does not discard a role for Notch signalling in myelopoiesis. In another recent study, the authors evaluated the deletion of *Rbpj* using the constitutive *Vav-Cre* and the inducible *Mx1-Cre*. In direct contrast to the results from Carlesso's group [246], no distinct defects were observed at any progenitor stage of myeloid lineages in RBPjκ -deficient mice under steady-state or regenerative conditions. Although these results are in in agreement with early reports of unaffected myeloid potential in RBPjκ-deficient mice [228], the authors did not provide any explanation for the discrepancy between the studies using the same genetic approach.

Overall, inhibition of Notch through the loss of different regulators of the pathway seems to lead to expansion of haematopoietic progenitors. This can probably result from early differentiation induced by the loss of a quiescent state imposed by Notch

signalling. It would be relevant to clarify whether this effect leads to stem cell pool exhaustion or if in some cases, stem cells can divide seemingly indefinitely as has been previously described [225]. But most importantly, these studies demonstrate that Notch activation *via* Notch ligand-receptor interactions between niche cells is also required for normal haematopoiesis. Altogether these studies highlight the importance of Notch signalling in the BM microenvironment for the proper regulation of haematopoiesis.

I.2.2.3. NOTCH SIGNALLING IN THE HAEMATOPOIETIC NICHE

Due to the close contact required for Notch signalling communication, several studies have evaluated the presence and functions of Notch ligands in the different bone marrow niche cells (endothelial cells, osteoblasts, and mesenchymal stromal cells) that are able to support HSPCs *in vitro* or appear closely associated to them *in vivo*.

Indeed, bone marrow endothelial cells express Notch ligands and its expression can be regulated by pro-inflammatory stimuli *in vitro* and *in vivo* [249]. In a study by Fernandez and colleagues, Jagged ligands expression was observed in the human BM endothelial cell line BMEC and primary human BM endothelial cells. In addition, their ability to expand haematopoietic progenitors in an *in vitro* co-culture system was shown to be dependent on Notch signalling. The authors have also demonstrated that the ligand density and Notch signal intensity could result in different degrees of HSPCs expansion. Furthermore, *in vivo* pro-inflammatory cues (TNFα, LPS) caused an increase in Jag2 expression on endothelial cells and in N1 and N2 receptors on haematopoietic progenitors, which led to increase in Notch activation [249].

Later on, a comprehensive study by Butler and colleagues showed that endothelial cells are able to support long-term expansion of Notch activated (TNR-GFP^{+}) LSK HSPCs, but not Notch1 and Notch2 defective HSCs (*Notch1*$^{-/-}$*Notch2*$^{-/-}$CD34^{-}Flt-3^{-} LSK) [137]. The authors also demonstrated in their experimental settings that when exposed to soluble SCF *in vitro*, HSCs were shown to secrete vascular endothelial growth factor A (VEGF-A) thus, stimulating the translocation of Jag2 ligand on the endothelial cells surface, which then supported the expansion of the HSCs by interacting with N1 and N2 receptors. Furthermore, *in vivo* inhibition of both VEGFR2

and VE-cadherin, essential for endothelial angiocrine signalling, led to a profound decrease in the instructive capacity of endothelial cells. This caused impaired reconstitution of TNR-GFP$^+$ haematopoietic cells after sub-lethal irradiation due to a significant decrease in the regeneration capacity of TNR-GFP$^+$ HSCs. These results highlight the importance of Notch communication in the vascular niche, revealing that during haematopoietic recovery angiocrine expression of Notch ligands is essential to balance the expansion and differentiation of HSCs.

Consequently, *in vivo* conditional deletion of *Jag1* in endothelial cells (*VE-cadherin-Cre*) caused a decrease in the number of phenotypically and functional HSCs in steady state, which was associated with a significant reduction in Notch activation in LSK HSPCs [138]. In fact, mutant mice showed deficient haematopoietic recovery after sub-lethal irradiation leading to reduced survival rate. Moreover, *in vitro* co-cultures with endothelial cells from mutant mice resulted in greater haematopoietic expansion exclusively from differentiated cells with a significant increase in myeloid cells [138]. These data emphasise the importance of niche Jagged ligands in balancing expansion and differentiation of HSPCs, demonstrating that Notch signalling activation by BM endothelial cells through Jag1 ligand is essential to maintain homeostatic and regenerative haematopoiesis.

Of note, this data contradicts the observations of Mancini *et al*., in which conditional deletion of *Jag1* driven by the *Mx1* promoter had no effect on haematopoietic regulation at steady-state or regenerative conditions [231]. The authors of the latter study verified that while the *VE-cadherin-Cre* efficiently deleted the floxed *Jag1* in BM endothelial cells whereas the inducible *Mx1-Cre* system did not. These data indicate that the observations of Mancini *et al*. could be associated with the lack of deletion of endothelial-specific *Jag1*.

Apart from endothelial cells, other bone marrow stromal cells have also been shown to be associated to HSPCs regulation via Notch signalling. A subset of human CD146$^+$ perivascular MSCs was found to support long-term culture of functional human HSPCs partially through Notch activation [250]. Indeed, CD146$^+$ perivascular cells express high levels of Jag1 and Notch activation was observed to be significantly higher in HSPCs co-cultured with CD146$^+$ cells than in co-cultures with total MSCs or CD146$^-$ cells [250]. Moreover, Notch inhibition with DAPT resulted in decreased HSPCs

number and CFUs and increased B-cell differentiation. These results suggest that $CD146^+$ perivascular cells can also regulate self-renewal and lineage commitment of HSPCs through Notch signalling [250].

Interestingly, a recent study shed some light on the human BM niche *in vivo* by analysing human bone biopsy specimens and human-mouse xenografts. This study revealed that HSCs with superior regenerative and self-renewal capacity tend to localise in the endosteal regions of the trabecular bone area (TBA) [230]. These HSCs were described to have distinct molecular activation enriched with Notch signalling signature compared to HSCs from the long bone area (LBA). Particularly within the TBA, phenotypic human HSCs and HPCs preferentially locate in the endosteal over vascular regions [230]. The authors also showed that osteoblasts from the TBA were found to have increased expression of Notch ligands Jag1, Jag2 and Dll4 compared to osteoblasts from the LBA, consistent with the HSCs activation profile. In particular, a 3-fold higher proportion of Jag1-expressing osteoblasts was detected in the TBA compared to LBA and Jag1-binding HSPCs were found to have higher CFU capacity and repopulating capacity. Upon Notch inhibition with DAPT treatment *in vivo*, total human engraftment and HSPCs numbers were not affected in the LBA, whereas a significant reduction in the TBA was observed, suggesting that only this region is sensitive to Notch inhibition leading to an overall reduction in human engraftment in a region-specific manner. These observations support a critical role of Notch signalling in HSCs regulation through interactions with specific BM niche cells.

In a subsequent study, further investigation on the role of endosteal osteoblasts in HSCs regulation showed that osteoblast ablation (*Col2.3*Δtk) led to reduced quiescence, long-term engraftment and self-renewal capacity of HSCs [251]. Moreover, osteoblast ablation in a transgenic chronic myeloid leukaemia mouse model showed accelerated leukaemia progression with reduced survival compared to control mice. In this mouse model, osteoblasts were found to express high levels of Jag1 and co-culture of leukemic or normal HSCs with stromal cells expressing Jag1 resulted in reduced cell cycling and total cell numbers. These data suggest that Jag1 signalling in the osteogenic niche is essential for maintaining HSCs quiescence and long-term self-renewal capacity.

Finally, to further evidence the importance of Notch ligands in the osteogenic niche, in humanised mice with human Jag1-expressing osteoblasts, human HSPCs repopulation was higher than in control mice [252]. In addition, mice with human Dll1-expressing osteoblasts developed severe osteoclerosis, which suppressed the generation of human B lymphocytes and retention of human HSPCs in the bone marrow [253].

Altogether, these studies highlight the importance of Notch signalling in the osteogenic niche for regulation of HSCs self-renewal and quiescence, particularly through Jag1 in the trabecular bone area, where interactions and Notch activation seem to be higher. However, the activated Notch receptors and the molecular mechanisms behind this regulation are still not understood and a more comprehensive study is necessary to clearly identify the functions of the different ligands on HSPCs regulation both *in vitro* and *in vivo*.

I.3. NOTCH SIGNALLING IN HAEMATOPOIETIC STEM CELL EXPANSION

In clinical settings, haematopoietic stem cell transplantation (HSCT) is used to treat high-risk haematological malignant disorders and other life-threatening haematological and genetic diseases (reviewed in [254]).

HSPCs for HSCT can be harvested from BM, which requires an invasive procedure for BM aspiration from the posterior iliac crests. Alternatively, these cells can be obtained from G-CSF mobilised PB which is non-invasive and produces more rapid haematopoietic reconstitution as compared to BM cells. However, in allogeneic settings, PB transplant is associated with increased incidence and prolonged treatment of chronic graft-versus-host disease (GvHD) [255, 256], due to the higher T cells content.

GvHD is one of the major complications of allogeneic HSCT consisting in an aggressive immune response of the donor T cells believed to be stimulated by tissue injury resulting from prior conditioning regimen [257]. Although mortality is considerably lower with autologous transplantation than with allogenic transplantation, the absence of graft-versus-tumour activity in autotransplantation reduces its effectiveness. Moreover, autologous grafts can be contaminated with tumour cells which contributes to relapse in haematological malignancies.

UCB emerged as an attractive alternative source of HSPCs for allogeneic transplant, considering that in contrast with the two other sources, is non-evasive and easily accessible. Additionally, due to immunological immaturity of the immune cells, CB-derived cells require less stringent HLA matching being less likely to cause GVHD, without losing the graft-versus-leukaemia effect [258]. The first successful UCB transplantation was performed in 1988 to treat a paediatric patient with Fanconi´s anaemia [259].

Nevertheless, UCB transplant is limited by the blood volume that can be collected from the cord and placenta and the number of total nucleated cells (TNCs) which can vary

widely ($9.8\times10^8 \pm 4.7\times10^8$ [260]). Therefore, given the therapeutic numbers recommended – $>3\times10^7$ TNCs/kg or $\geq2\times10^5$ $CD34^+$ cells/kg – UCB transplantation is usually only a viable option for paediatric patients, being associated with graft failure in adults [261]. Alternatively, the use of two partially HLA-matched UCB units may overcome the cell-dose barrier that limits UCB transplant in many adults and adolescents [262]. However, a randomised clinical trial comparing one-unit versus two-unit UCB transplantation did not observe any survival benefit using the double unit and was actually associated with higher incidence of severe GvHD [263]. Moreover, due to their more primitive nature, haematologic and immunologic reconstitution is slower with UCB grafts and delayed neutrophil engraftment has been associated with early transplantation-related mortality mainly due to infection [264].

In order to overcome these limitations of UCB transplantation, the *ex vivo* expansion of UCB HSPCs has gained significant interest in the experimental haematology field. Indeed, compared to adult BM-derived HSPCs, UCB progenitors have higher proliferative potential, reportedly up to eightfold and four times more $CD34^+$ cells. Furthermore, UCB contains higher frequency of transplantable HSCs, higher output of progenitor cells, more CFUs, higher cell-cycle rate and a relatively long telomere length [265-267].

However, it has been constantly debated that expanded HSCs have less potency for engraftment and haematogenesis compared to unexpanded HSCs thus, preclinical studies have continuously been focusing on increasing the potency of expanded HSCs. The major hurdle to tackle in HSPCs *ex vivo* expansion protocols is the balance between HSCs self-renewal and differentiation, which has been stalled by the uncomplete understanding of HSPCs hierarchy and regulation. The following sections review some of the main work towards HSPCs expansion, with focus on the use of Notch ligands which have shown to promote stem cell self-renewal while inhibiting differentiation [75, 223, 224].

I.3.1. *EX VIVO* EXPANSION OF UCB HSPCS

As previously explained, the therapeutic potential of an UCB unit could be maximised through *ex* vivo expansion methods that allow not only the increase in stem cells with

haematopoietic reconstitution potential, but also the selective expansion of short-term engrafting HSPCs that will allow rapid recovery from pancytopenia thus, decreasing early morbidity and mortality. Also, the combination of an *ex vivo* expanded unit with an unmanipulated UCB unit might prove to be a beneficial strategy since it would provide more rapid initial haematopoietic reconstitution (expanded cells) and long-term sustainable haematopoiesis (unmanipulated cells). In fact, this approach has been implemented in some clinical trials as it improves safety (back-up in case expansion fails or interferes with engraftment) and offers the possibility to track each unit engraftment contribution overtime based on the genetic differences between grafts [268, 269].

Current expansion protocols for UCB HSPCs are still in development and evolving continually with the increase in understanding of cell-intrinsic and cell-extrinsic (BM niches) regulators of HSC self-renewal, fostered by the advances in cell and molecular technologies. Early studies focused on the optimisation of cocktails of cytokines and growth factors such as SCF, TPO, and Flt3L that are still widely used. However, these cocktails generally fail to promote efficient HSCs self-renewal by themselves and are known to induce differentiation, suggesting that additional factors are required. In recent years, several developmental factors and chemical compounds, have been reported to affect HSC self-renewal and are being explored in combination with cytokine-based expansion cultures.

I.3.1.1. CYTOKINES AND GROWTH FACTORS

In early studies, the effects of single cytokines and growth factors and their combination have been investigated on murine and human HSPCs *in vitro* cultures (reviewed in [270]).

SCF is one of the first identified cytokines used in HSC expansion and remained an essential component in many cocktails. However, much like TPO and Flt3L, although able to stimulate proliferation of progenitor cells, their individual potential to induce HSC expansion is insufficient [271, 272]. SCF and Flt3L have been considered key cytokines for HSC expansion, since c-Kit and Flt3, the tyrosine kinase receptors for SCF and Flt3L, respectively, were shown to transduce signals crucial for HSC

development [273, 274]. TPO, a ligand for c-Mpl, was originally identified as a primary regulator for megakaryopoiesis, but was also shown to promote the expansion of primitive haematopoietic cells [275, 276]. Additionally, c-Kit and Flt3 signals can synergise with glycoprotein (gp)130 signal mediated by a complex of IL-6 and soluble IL-6 receptor (IL-6/sIL-6R) to stimulate the expansion of HPCs [277, 278]. On the other hand, the effect of IL-3 is controversial, showing a negative impact on HSC expansion in some studies [279] but not in others [280, 56].

Therefore, several combinations of cytokines and growth factors were explored with SCID transplantation assays demonstrating that SCF, Flt3L and TPO are crucial for the expansion of SRC [56, 18, 281]. Indeed, this was first demonstrated by two independent studies from Dick's and Eaves' groups which achieved 2–4-fold increases in UCB SRCs after 4 days [280] or 5–8 days [56] of culture in complex growth factor cocktails of Flt3L, SCF, G-CSF, IL-3 and IL-6. Later on, another study reported a 4.2-fold expansion of SRCs in a 7-day culture with a novel cocktail combination of Flt3L, SCF, TPO and IL-6 and the soluble IL-6 receptor, in which the latter was included to maximise the IL-6 signalling in cells where receptor density might be limiting [279].

However, despite examining a wide range of single and complex growth factor cocktails, HSC expansion obtained with these protocols was still modest and dramatically less than the readily achievable multilog expansion of progenitors. Work of Conneally *et al*, demonstrated a robust 100-fold CFU expansion compared to a 2-fold SRC expansion [56]. However, these conditions were not able to sustain the output of rigorously defined repopulating HSC beyond a very limited time of culture. For example, Bhatia and colleagues observed that the reconstitution ability of the expanded HSPCs was lost after 9 days of culture despite further increase in the total number of CD34+ cells, which suggests an exhaustion of the HSC pool [280]. In fact, a recent study by Knapp *et al*. indicated that the Flt3L, SCF, G-CSF, IL-3 and IL-6 cocktail might only regulate short-term (4 days) survival and proliferation of human HSCs, rather than maintenance of functional long-term HSC *in vitro* [282].

Furthermore, cytokine-based expansion protocols were translated into clinical trials where no significant differences in haematopoietic recovery were obtained [283]. Thus, these poor outcomes using cytokine only *ex vivo* expansion protocols clearly

suggest the need for additional factors to support *in vitro* HSC maintenance and expansion.

Clues to extrinsic mediators of HSC self-renewal emerged from a broader understanding of the key receptor signalling pathways involved in the development and maintenance of the haematopoietic system. For instance, several bone morphogenic proteins (BMPs), which have critical roles in haematopoietic specification, were tested in cultures of UCB $Lin^{-}CD34^{+}CD38^{-}$ cells together with multiple haematopoietic cytokines, revealing that BMP4 exclusively was able to extend the period in which cells with repopulating potential could be recovered from culture, suggesting a role in HSC survival that could be useful for achieving enhanced stem cell expansion *in vitro* [284]. Nevertheless, some of the most compelling evidences of early developmental growth factors impacting HSC self-renewal came from *in vitro* studies of Notch signalling which will be explored in more detailed further ahead.

I.3.1.2. SMALL MOLECULES

Identification of small molecules has significant interest since they are capable of penetrating into the cell and target cytoplasmic components of an intrinsic pathway unlike growth factors or cytokines. Moreover, they can be easily produced and are cost efficient. High-throughput screenings of thousands of molecules have been used to find new compounds by testing their potential for HSCs *ex vivo* expansion (reviewed in [285]).

A major break-through in the field was achieved by Cooke's group that used high-throughput technology for an unbiased screen of factors that could expand human HSCs [286]. They screened a library of 100,000 small molecules in serum-free medium containing TPO, SCF, Flt3L and IL-6 and successfully found a purine derivative, StemRegenin 1 (SR1), shown to be able to promote a 50-fold expansion of UCB-derived $CD34^{+}$ cells and a 17-fold increase in long-term SRCs. SR1 is an antagonist of the aryl hydrocarbon receptor (AhR), which was shown to express in human HSCs and associated to pathways regulating haematopoiesis, including HES-1, c-Myc, C/EBP, PU.1, β-catenin, CXCR4, and Stat5 [287] dependent processes. However, the exact mechanism by which SR1 induces HSC expansion is not known yet. Recently, a clinical study evaluated double-unit UCB transplantation where one

unit was expanded for 15 days with SR1 [269]. This study successfully demonstrated early neutrophil and platelet recovery and better engraftment in patients that received expanded $CD34^+$ cells as compared to patients that received equal numbers of $CD34^+$ cells from unmanipulated UCB. In addition, the marked expansion of CD34+ cells with SR-1 can ameliorate the limitation of cell dose in recipients of UCB and allow the use of UCB units with less cells.

A later preclinical study from Sauvageau's group found a pyrimidoindole derivative (UM171) that promoted human HSC self-renewal and *ex vivo* expansion in an AhR-independent manner given that the expression of AhR targets (AhRR and CYP1B1) were not altered upon UM171 treatment [288]. In this work, a library of 5280 low-molecular weight compounds was screened for their ability to expand human PB $CD34^+CD45RA^-$ cells (population enriched in LT-HSCs). A further screen of 300 analogs of a promising AhR-independent compound led to the discovery of UM171 with superior ability to stimulate the expansion of HSC-enriched population. In fact, the authors showed that UM171 resulted in higher expansion of $CD34^+CD45RA^-$ cells than SR1, although $CD34^+$ cell frequencies were similar, suggesting that UM171 targets phenotypically more primitive cells than those targeted by SR1. Also, simultaneous addition of SR1 to UM171 showed that there was a cooperation to enhance *ex vivo* expansion of progenitor cells and to suppress differentiation, since SR1 alone induced $CD45RA^+$ cell proliferation that was inhibited upon addition of UM171. A very recent small clinical study just proved the safety and efficacy of UM171 expanded UCB, achieving fast neutrophil recover (median of 10 days) [289]. Therefore, UM171 and SR1 may represent promising chemical compounds for clinical *ex vivo* expansion of human HSCs. However, the mechanisms of SR-1 or UM171-mediated HSC self-renewal and differentiation block are unknown.

Another promising compound, the small lipid mediator prostaglandin E_2 (PGE_2), was identified as a regulator of HSC self-renewal using library screens in zebrafish. Hoggatt *et al.* reported an improved engraftment of mouse HSPCs cultured with PGE_2 which remained upon serial transplantation, suggesting an effect on LT-HSCs [290]. It was later shown in UCB HSPCs that PGE_2 was able to both activate general cell survival and proliferation pathways but also to lead to a specific cytokine response [291, 292]. In a preclinical study, treatment with PGE_2 improved engraftment of UCB HSCs into NOD/SCID mice and autologous transplantation of treated PB

HSCs in non-human primates showed stable long-term engraftment [291]. This was followed by a two-year clinical trial for double-unit UCB transplantation with one unmanipulated unit and one with a 2-hour *ex vivo* pulse of PGE_2. This study demonstrated clinical safety of PGE_2 treatment and improvements in neutrophil recovery and overall engraftment, giving grounds for phase II clinical trial [292].

Another group of molecules that has been considered for HSCs expansion are pan-inhibitors of DNA methylation, based on the observation that DNA hypermethylation occurs during culture expansion of HSCs and is correlated to loss of proliferation and engraftment capacity [293]. Among various genes that were shown to be methylated during *ex vivo* expansion were genes that play a central role in the haematopoietic development and immune response, suggesting their relevance for the rapid loss of stemness during *in vitro* manipulation, although the mechanistic pathways still need to be elucidated [293]. Nonetheless, DNA methyltransferase inhibitors including histone deacetylase inhibitors like valproic acid (VPA) [294], 5-aza-2'-deoxycytidine (aza-D) [295] and nicotinamide (NAM) [296], were tested for their efficacy in reducing hypermethylation of the regulatory or marker genes during UCB HSPCs *ex vivo* expansion, showing promising results in xenotransplantation assays. In particular, NAM, an inhibitor of SIRT1 (class III NAD(+)-dependent-histone-deacetylase) promoted an 80-fold increase in $CD34^+$ cells, by delaying differentiation and increasing homing and engraftment efficacy of UCB $CD34^+$ cells when cultured with cytokines [296]. In fact, recent results of a phase I/II clinical study using only one expanded UCB unit, revealed reduction in neutrophil recovery by 9.5 days (median time of 11.5 days) and platelet recovery by 12 days compared to standard UCB transplant [297]. While in a first clinical study a second unmanipulated UCB unit was co-infused with the NAM expanded unit to maintain patient safety [268], long-term follow-up revealed stable haematopoiesis derived from the expanded unit. Thus, unlike in other clinical studies, transplant of a single expanded UCB unit was evaluated, establishing feasibility, safety, and efficacy of a NAM-based expansion protocol for the use one expanded UCB unit as stand-alone graft [297].

I.3.1.3. STROMAL FEEDER LAYERS

As previously mentioned, stromal cells are well-established supportive niche cells that play a key role in supporting both maintenance and differentiation of the stem cell pool *in vivo*. Thus, co-culture of HSCPs with human stromal cells, like MSCs, supplemented with growth factors has been explored in an attempt to mimic these interactions *ex vivo* to expand functional HSCs [298].

However, over the last years, several studies with MSCs have demonstrated different degrees of efficacy to expand HSPCs *in vitro* (reviewed in [299, 300]) and the precise cellular and molecular mechanisms involved in these interactions are still not clear. It appears that cell-to-cell contact is crucial and that the HSPCs fraction adherent to the MSCs layer after expansion is enriched in more primitive cells with higher migratory potential [301-304]. On the other hand, it was also reported that soluble factors released by MSCs were sufficient to promote HSPCs expansion [298]. In particular, it was demonstrated that activation of the CXCL12/CXCR4 axis in co-cultures promoted HSPCs proliferation and was essential for LTC-IC potential [305]. However, when HSPC were separated from MSCs by a semipermeable membrane, LTC-IC activity became CXCR4 independent [305].

Different studies have attempted to establish the optimal cytokine cocktail to expand HSPCs in co-culture with BM derived-MSCs but with divergent results (reviewed in [299, 300]). Furthermore, other MSCs sources have been evaluated given the higher availability and ease and non-invasive collection, such as adipose tissue (AT)-MSCs and umbilical cord matrix (UCM)-MSCs. However, the supportive potential of these cells has shown contradictory results, which may be due to the different isolation methods and culture media used in the studies [306-308].

Besides different cytokines cocktails, alternative strategies to improve HSPCs expansion in MSC co-culture have been explored. For instance, the addition of two epigenetic regulators, aza-D and trichostatin A (TSA) to the culture medium was found to increase the number of total HSCs and this was associated to a synergistic effect that increased stemness and survival [309]. Another strategy to strengthen the BM-MSCs function as feeder layers is their genetic manipulation in order to induce the secretion of crucial factors for HSPCs growth such as angiopoietin-like 5 [310]. As previously mentioned, a more recent approach focused on mimicking the BM niche

structure by seeding the MSCs on 3D systems like collagen or fibrin scaffolds together with HSPCs [78, 311]. 3D-cultures of HSPCs have been shown to be superior to conventional 2D cultures, promoting increased migration of HPSCs toward MSCs associated to higher levels of molecules involved in the maintenance of HSCs quiescence. Moreover, the synergic action between 3D scaffolds and MSCs was shown to increase the proliferation of HSPCs which retained a more primitive phenotype [79, 312].

The initial studies of UCB HSPCs co-cultures with MSCs demonstrated modest progenitors expansion [313] but led to higher haematopoietic engraftment [314, 315], hence paving the way to clinical translation. In a clinical study, De Lima and colleagues transplanted two UCB units, one un-manipulated and one expanded for 14 days on BM-MSCs layers supplemented with cytokines (SCF, Flt3L, G-CSF, and TPO), which significantly improved engraftment compared to un-manipulated double UCB units as a graft. They also reported a median 30-fold expansion of $CD34^+$ cells and a median time to neutrophil and platelet engraftment of 15 and 40 days, respectively. However, long-term follow-up showed that only the cells derived from the un-manipulated UCB unit ultimately contributed to long-term donor-derived haematopoiesis. The authors attributed the positive engraftment results to the increased numbers of committed progenitors in the expanded cells that accelerated the haematopoietic recovery [316].

Although BM-MSCs are considered the gold standard for HSPCs *ex vivo* expansion, the extended time required to expand sufficient numbers to be used as feeder layers represents a logistical problem for clinical applications, since the progression of some haematological diseases has a fast clinical course. For this reason, MSCs derived from UCM are considered an attractive alternative for their prompt availability and great proliferation capacity with most studies demonstrating haematopoietic supportive function [317].

Nevertheless, the use of MSCs feeder layers for HSPCs *ex vivo* expansion remains a controversial issue since extended characterisation of MSCs intrinsic properties are required to better understand their supportive mechanisms. Furthermore, there is a need for systematic and comprehensive comparison between the different MSCs sources in order to finally establish their potential for HSCs *ex vivo* expansion and maintenance.

I.3.2. NOTCH LIGANDS IN HSPCS EXPANSION

As previously described, the role of Notch signalling in human HSCs regulation in physiological conditions is still unclear.

Nevertheless, initial studies demonstrated that activation of Notch signalling in HSPCs *in vitro* was associated to increased stemness, given that HSPCs expressing a constitutively active form of N1 [221, 113] or the Notch target Hes1 [222] delayed differentiation and preserved long-term multilineage reconstituting capacity. Furthermore, exposure of haematopoietic precursors to Notch ligands, such as Jag1 expressed by osteoblasts *in vivo* [75], or *in vitro* immobilised Dll1 [223] and soluble Jag1 [224] also promoted stem cell self-renewal while inhibiting differentiation. Although mouse models of Notch loss-of-function failed to show an effect in HSCs, this early work proved the usefulness of Notch ligands for activation of Notch signalling *ex vivo* as a novel approach for expanding HSPCs, of which the main studies are described here and summarised in Table I.3.

Initially, the *in vitro* effects of Notch ligands on HSPCs were studied by adding soluble forms to the cytokine supplemented-media. For instance, the addition of soluble Jag1 to $CD34^{+}CD38^{-}$ HSPCs cultures resulted in modest effects in terms of cell proliferation, but induced survival of HSCs with repopulating capacity [224]. The addition of soluble Dll1 and Dll4 was initially shown to promote the expansion of primitive and multilineage progenitors, but only Dll1 led to increase in numbers of HSCs with repopulating ability [318]. However, subsequent work from Bernstein's group demonstrated that immobilisation of Dll1 ligand was crucial for Notch signalling activation, and the soluble form of Dll1 not only failed to activate but actually inhibited Notch signalling [319]. Shortly after, it was reported for the first time the effects of membrane-bound Dll1 and Jag1 (S17 stromal cells overexpressing Dll1 and Jag1) in UCB HSPCs differentiation [320]. Importantly, later work by Lauret and colleagues first reported that membrane-bound Dll4 (S17 cells overexpressing Dll4) actually inhibited HSPCs proliferation while maintaining long-term repopulating cells [227]. Furthermore, in a direct comparison study, the soluble form of Dll4 was shown to enhance proliferation of HSPCs associated with the loss of stemness as opposed to the membrane-bound form [321].

Table I.3 – Studies of Notch signalling in UCB HSPCs *ex vivo* expansion

Notch ligand	Study	Outcome	Ref
Dll1	Culture with soluble Dll1	Increased expansion of HSPC and SRC	[318]
	Culture with immobilised Dll1	100-fold increase in $CD34^+$ cells with increased SRC and myeloid and B cell engraftment	[226]
	Dose-dependent effects of Dll1	Lower densities increased $CD34^+$ cells and SRC Higher densities induced apoptosis of $CD34^+$ cells and reduced SRC and myeloid engraftment	[322]
	Culture with immobilised Dll1 for UCB HSCT phase I clinical trial	>150-fold increase in $CD34^+$ and 15.6 fold-increase in SRC frequency Faster myeloid engraftment in transplanted patients	[323]
	Fed-batch culture with immobilised Dll1	6-fold increase in long-term SRC Increased long-term engraftment compared to standard Dll1 culture	[237]
	Culture with immobilised Dll1 and SR1	3-fold higher rapid myeloid repopulating cells than in cultures with each component alone	[324]
Dll4	Co-culture on mbD4/S17	Inhibition of HSPCs proliferation but maintenance of LTC-IC and engraftment potential	[227]
	Co-culture on solD4/S17 vs mbD4/S17	solD4/S17 increased HSPCs with loss of LTC-IC	[321]
Jag1	Co-culture on $CD146^+$ BM stromal cells	Maintenance of HSPCs with short-term and long-term repopulating capacity	[250]
	Co-culture on OP9	Increased expansion of HSPCs	[325]
Jag2	Co-culture on BM endothelial cells	Expansion of CFUs, increased with higher Jag2 density	[249]

Based on these results, it is now generally viewed that soluble forms of Notch ligands have an antagonistic effect of Notch signalling in haematopoietic cells and thus, ligands are either presented immobilised on a plastic surface [226] or by stromal cells

overexpressing a membrane-bound ligand [321, 325] or by a specific fraction of niche cells that naturally express high levels of Notch ligands [250, 249].

Work by Bernstein's group on HSPCs culture with immobilised Dll1 ligand resulted in 100-fold increase in $CD34^+$ cell numbers and this was associated with reduced myeloid differentiation which led to increase in myeloid and B cell engraftment in immunodeficient mice [226]. Further work from this group revealed that *in vitro* Notch activation with Dll1 at specific doses promoted different outcomes. While lower densities increased numbers of $CD34^+$ HSPCs and SRCs, higher densities induced apoptosis of $CD34^+$ cells and reduced the generation of SRCs and human myeloid engraftment [322]. Indeed, work from this group was translated to a phase I clinical trial of double unit UCB transplantation, using one unmanipulated unit and one Dll1-expanded unit [323]. In this study, $CD34^+$ cells were expanded for 17-21 days in the presence of fibronectin fragments and immobilised Dll1 in serum free conditions supplemented with five cytokines (SCF 300 ng/mL, Flt3L 300 ng/mL, TPO 100 ng/mL, IL–6 10 ng/mL, and IL–3 10 ng/mL), which resulted in >150-fold increase in $CD34^+$ cells and 15.6 fold-increase in SRC frequency. Preliminary results from the clinical study suggested faster myeloid engraftment and shortened neutrophil recovery by a median of 10 days compared to patients receiving two unmanipulated units. Although the long-term engraftment was derived from the co-transplanted unmanipulated unit, it was the first demonstration of rapid haematopoietic engraftment supported by *ex vivo* expanded UCB-HSPCs [323].

Mechanistic insight on the effects of Dll1 on HSPCs *in vitro* was obtained in a collaborative work between Bernstein and Zandstra groups [237]. The authors demonstrated that Dll1 reduced myeloid cell production by reducing expression of IL-6R on myeloid-restricted progenitors thus, preventing the accumulation of monocytes and granulocytes in their experimental settings. These culture conditions provided a more supportive environment for HSC expansion and self-renewal. However, in the absence of membrane IL-6R, myeloid cells can respond to IL-6 via trans-signalling in the presence of soluble IL-6R. Using a fed-batch culture system, IL-6R was continuously depleted from the culture, resulting in enhanced production of LT-HSCs [237]. Hence, the environmental regulation from the combination of Dll1 in a fed-batch culture system allowed an output of HSPCs with both rapid and sustained engraftment capacity.

In another study, it was demonstrated that HSPCs cultured on Dll1 along with AhR antagonist SR1 led to enhanced rapid myeloid reconstitution associated with an increase in rapid repopulating cells by 3-fold in comparison to treatment with either component alone. However, no significant differences were obtained in the generation of LT-HSCs [324].

Focusing on Dll4, although previous studies have suggested a weak potential for HSPCs *ex vivo* expansion, Dll4 was shown to support the maintenance of short-term repopulating capacity [227, 321]. More recently Lauret's group reported that mouse BM HSPCs maintained a higher proportion of cells in the G0 phase when co-cultured with Dll4, limiting the loss of HSPCs with repopulating capacity during *ex vivo* expansion. This effect was correlated to a downregulation of cell cycle genes like *Ccnd1*, *Ccnd2*, and *Ccnd3*, and upregulation of stemness related genes such as *Bmi1*, *Gata2*, *Hoxb4* and *Myc* [326].

Regarding Notch ligands Jag1 and Jag2, not many studies have explored their effect on human HSPCs *ex vivo* expansion. One study co-cultured HSPCs on OP9 stroma cell line that naturally expresses Jag1 with OP9 overexpressing Dll1 and BM-MSCs [325]. After 7 days of culture both OP9 conditions promoted expansion of $CD34^{+}CD38^{-}$ cells while inhibiting total cell proliferation, particularly in the OP9 control condition (Jag1), which was not observed in MSC co-cultures. Also, other study showed that co-culture with human $CD146^{+}$ perivascular MSCs, which express high levels of Jag1, supported maintenance of ST- and LT-HSPCs while inhibiting differentiation, whereas unfractionated MSCs and $CD146^{-}$ cells induced differentiation and compromised *ex vivo* maintenance of HSPCs [250]. In another work, BM ECs were found to express Jag2 and co-culture with $CD34^{+}$ cells promoted expansion of haematopoietic progenitors (CFUs), which was enhanced by increased Jag2 density from an overexpressing BMEC cell line. Furthermore, expression of Jag2 was shown to be upregulated on BM ECs by proinflammatory cytokine TNFα, which was associated with increased N1 activation in HSPCs, suggesting that under conditions of inflammatory stress *in vivo*, Jag2-mediated Notch signalling plays a role in HSPCs activation and expansion [249].

Thus, currently, Notch signalling-based protocols for HSPCs *ex vivo* expansion have mostly focused on activation through Dll1 ligand and further studies are necessary to

better understand the effect of other Notch ligands, particularly on the expansion of human HSCs with reconstitution capacity [327].

I.4. REFERENCES

1. Orkin SH. Diversification of haematopoietic stem cells to specific lineages. Nat Rev Genet. 2000;1(1):57-64.

2. Orkin SH, Zon LI. SnapShot: hematopoiesis. Cell. 2008;132(4):712.

3. Lorenz E, Uphoff D, Reid TR, Shelton E. Modification of irradiation injury in mice and guinea pigs by bone marrow injections. J Natl Cancer Inst. 1951;12(1):197-201.

4. Till JE, Mc CE. A direct measurement of the radiation sensitivity of normal mouse bone marrow cells. Radiat Res. 1961;14:213-22.

5. Becker AJ, Mc CE, Till JE. Cytological demonstration of the clonal nature of spleen colonies derived from transplanted mouse marrow cells. Nature. 1963;197:452-4.

6. Doulatov S, Notta F, Laurenti E, Dick JE. Hematopoiesis: a human perspective. Cell Stem Cell. 2012;10(2):120-36.

7. Spangrude GJ, Aihara Y, Weissman IL, Klein J. The stem cell antigens Sca-1 and Sca-2 subdivide thymic and peripheral T lymphocytes into unique subsets. J Immunol. 1988;141(11):3697-707.

8. Morrison SJ, Weissman IL. The long-term repopulating subset of hematopoietic stem cells is deterministic and isolatable by phenotype. Immunity. 1994;1(8):661-73.

9. Osawa M, Hanada K, Hamada H, Nakauchi H. Long-term lymphohematopoietic reconstitution by a single CD34-low/negative hematopoietic stem cell. Science. 1996;273(5272):242-5.

10. Yang L, Bryder D, Adolfsson J, Nygren J, Mansson R, Sigvardsson M et al. Identification of Lin(-)Sca1(+)kit(+)CD34(+)Flt3- short-term hematopoietic stem cells capable of rapidly reconstituting and rescuing myeloablated transplant recipients. Blood. 2005;105(7):2717-23.

11. Adolfsson J, Borge OJ, Bryder D, Theilgaard-Monch K, Astrand-Grundstrom I, Sitnicka E et al. Upregulation of Flt3 expression within the bone marrow Lin(-)Sca1(+)c-kit(+) stem cell compartment is accompanied by loss of self-renewal capacity. Immunity. 2001;15(4):659-69.

12. Kiel MJ, Yilmaz OH, Iwashita T, Yilmaz OH, Terhorst C, Morrison SJ. SLAM family receptors distinguish hematopoietic stem and progenitor cells and reveal endothelial niches for stem cells. Cell. 2005;121(7):1109-21.

13. Civin CI, Strauss LC, Brovall C, Fackler MJ, Schwartz JF, Shaper JH. Antigenic analysis of hematopoiesis. III. A hematopoietic progenitor cell surface antigen defined by a monoclonal antibody raised against KG-1a cells. J Immunol. 1984;133(1):157-65.

14. Nielsen JS, McNagny KM. CD34 is a key regulator of hematopoietic stem cell trafficking to bone marrow and mast cell progenitor trafficking in the periphery. Microcirculation. 2009;16(6):487-96.

15. Weaver CH, Schwartzberg L, Zhen B, Mangum M, Leff R, Tauer K et al. High-dose chemotherapy and peripheral blood stem cell infusion in patients with non-Hodgkin's lymphoma: results of outpatient treatment in community cancer centers. Bone Marrow Transplant. 1997;20(9):753-60.

16. Fritsch G, Stimpfl M, Kurz M, Printz D, Buchinger P, Fischmeister G et al. The composition of CD34 subpopulations differs between bone marrow, blood and cord blood. Bone Marrow Transplant. 1996;17(2):169-78.

17. Baum CM, Weissman IL, Tsukamoto AS, Buckle AM, Peault B. Isolation of a candidate human hematopoietic stem-cell population. Proc Natl Acad Sci U S A. 1992;89(7):2804-8.

18. Bhatia M, Wang JC, Kapp U, Bonnet D, Dick JE. Purification of primitive human hematopoietic cells capable of repopulating immune-deficient mice. Proc Natl Acad Sci U S A. 1997;94(10):5320-5.

19. Cashman J, Bockhold K, Hogge DE, Eaves AC, Eaves CJ. Sustained proliferation, multi-lineage differentiation and maintenance of primitive human haemopoietic cells in NOD/SCID mice transplanted with human cord blood. Br J Haematol. 1997;98(4):1026-36.

20. Lansdorp PM, Sutherland HJ, Eaves CJ. Selective expression of CD45 isoforms on functional subpopulations of CD34+ hemopoietic cells from human bone marrow. J Exp Med. 1990;172(1):363-6.

21. Majeti R, Park CY, Weissman IL. Identification of a hierarchy of multipotent hematopoietic progenitors in human cord blood. Cell Stem Cell. 2007;1(6):635-45.

22. Benveniste P, Frelin C, Janmohamed S, Barbara M, Herrington R, Hyam D et al. Intermediate-term hematopoietic stem cells with extended but time-limited reconstitution potential. Cell Stem Cell. 2010;6(1):48-58.

23. Notta F, Doulatov S, Laurenti E, Poeppl A, Jurisica I, Dick JE. Isolation of single human hematopoietic stem cells capable of long-term multilineage engraftment. Science. 2011;333(6039):218-21.

24. Goodell MA, Rosenzweig M, Kim H, Marks DF, DeMaria M, Paradis G et al. Dye efflux studies suggest that hematopoietic stem cells expressing low or undetectable levels of CD34 antigen exist in multiple species. Nature medicine. 1997;3(12):1337-45.

25. Danet GH, Luongo JL, Butler G, Lu MM, Tenner AJ, Simon MC et al. C1qRp defines a new human stem cell population with hematopoietic and hepatic potential. Proc Natl Acad Sci U S A. 2002;99(16):10441-5.

26. Ishii M, Matsuoka Y, Sasaki Y, Nakatsuka R, Takahashi M, Nakamoto T et al. Development of a high-resolution purification method for precise functional characterization of primitive human cord blood-derived CD34-negative SCID-repopulating cells. Exp Hematol. 2011;39(2):203-13 e1.

27. Anjos-Afonso F, Currie E, Palmer HG, Foster KE, Taussig DC, Bonnet D. CD34(-) cells at the apex of the human hematopoietic stem cell hierarchy have distinctive cellular and molecular signatures. Cell Stem Cell. 2013;13(2):161-74.

28. Notta F, Zandi S, Takayama N, Dobson S, Gan OI, Wilson G et al. Distinct routes of lineage development reshape the human blood hierarchy across ontogeny. Science. 2016;351(6269):aab2116.

29. Manz MG, Miyamoto T, Akashi K, Weissman IL. Prospective isolation of human clonogenic common myeloid progenitors. Proc Natl Acad Sci U S A. 2002;99(18):11872-7.

30. Doulatov S, Notta F, Eppert K, Nguyen LT, Ohashi PS, Dick JE. Revised map of the human progenitor hierarchy shows the origin of macrophages and dendritic cells in early lymphoid development. Nat Immunol. 2010;11(7):585-93.

31. Goardon N, Marchi E, Atzberger A, Quek L, Schuh A, Soneji S et al. Coexistence of LMPP-like and GMP-like leukemia stem cells in acute myeloid leukemia. Cancer Cell. 2011;19(1):138-52.

32. Adolfsson J, Mansson R, Buza-Vidas N, Hultquist A, Liuba K, Jensen CT et al. Identification of Flt3+ lympho-myeloid stem cells lacking erythro-megakaryocytic potential a revised road map for adult blood lineage commitment. Cell. 2005;121(2):295-306.

33. Kohn LA, Hao QL, Sasidharan R, Parekh C, Ge S, Zhu Y et al. Lymphoid priming in human bone marrow begins before expression of CD10 with upregulation of L-selectin. Nat Immunol. 2012;13(10):963-71.

34. Karamitros D, Stoilova B, Aboukhalil Z, Hamey F, Reinisch A, Samitsch M et al. Single-cell analysis reveals the continuum of human lympho-myeloid progenitor cells. Nat Immunol. 2018;19(1):85-97.

35. Levac K, Karanu F, Bhatia M. Identification of growth factor conditions that reduce ex vivo cord blood progenitor expansion but do not alter human repopulating cell function in vivo. Haematologica. 2005;90(2):166-72.

36. Nitsche A, Junghahn I, Thulke S, Aumann J, Radonic A, Fichtner I et al. Interleukin-3 promotes proliferation and differentiation of human hematopoietic stem cells but reduces their repopulation potential in NOD/SCID mice. Stem cells. 2003;21(2):236-44.

37. Bowie MB, Kent DG, Copley MR, Eaves CJ. Steel factor responsiveness regulates the high self-renewal phenotype of fetal hematopoietic stem cells. Blood. 2007;109(11):5043-8.

38. Broxmeyer HE. Colony assays of hematopoietic progenitor cells and correlations to clinical situations. Critical reviews in oncology/hematology. 1984;1(3):227-57.

39. Dexter TM, Wright EG, Krizsa F, Lajtha LG. Regulation of haemopoietic stem cell proliferation in long term bone marrow cultures. Biomedicine / [publiee pour l'AAICIG]. 1977;27(9-10):344-9.

40. Dexter TM, Garland J, Scott D, Scolnick E, Metcalf D. Growth of factor-dependent hemopoietic precursor cell lines. J Exp Med. 1980;152(4):1036-47.

41. Greenberger JS, Sakakeeny M, Parker LM. In vitro proliferation of hemopoietic stem cells in long-term marrow cultures: principles in mouse applied to man. Exp Hematol. 1979;7 Suppl 5:135-48.

42. Gartner S, Kaplan HS. Long-term culture of human bone marrow cells. Proc Natl Acad Sci U S A. 1980;77(8):4756-9.

43. Whitlock CA, Witte ON. Long-term culture of B lymphocytes and their precursors from murine bone marrow. Proc Natl Acad Sci U S A. 1982;79(11):3608-12.

44. Miller JS, Verfaillie C, McGlave P. The generation of human natural killer cells from CD34+/DR- primitive progenitors in long-term bone marrow culture. Blood. 1992;80(9):2182-7.

45. Sutherland HJ, Eaves CJ, Eaves AC, Dragowska W, Lansdorp PM. Characterization and partial purification of human marrow cells capable of initiating long-term hematopoiesis in vitro. Blood. 1989;74(5):1563-70.

46. Lemieux ME, Rebel VI, Lansdorp PM, Eaves CJ. Characterization and purification of a primitive hematopoietic cell type in adult mouse marrow capable of lymphomyeloid differentiation in long-term marrow "switch" cultures. Blood. 1995;86(4):1339-47.

47. Ploemacher RE, van der Sluijs JP, Voerman JS, Brons NH. An in vitro limiting-dilution assay of long-term repopulating hematopoietic stem cells in the mouse. Blood. 1989;74(8):2755-63.

48. Moore KA, Ema H, Lemischka IR. In vitro maintenance of highly purified, transplantable hematopoietic stem cells. Blood. 1997;89(12):4337-47.

49. Wineman J, Moore K, Lemischka I, Muller-Sieburg C. Functional heterogeneity of the hematopoietic microenvironment: rare stromal elements maintain long-term repopulating stem cells. Blood. 1996;87(10):4082-90.

50. Issaad C, Croisille L, Katz A, Vainchenker W, Coulombel L. A murine stromal cell line allows the proliferation of very primitive human CD34++/CD38- progenitor cells in long-term cultures and semisolid assays. Blood. 1993;81(11):2916-24.

51. Croisille L, Auffray I, Katz A, Izac B, Vainchenker W, Coulombel L. Hydrocortisone differentially affects the ability of murine stromal cells and human marrow-derived adherent cells to promote the differentiation of CD34++/CD38- long-term culture-initiating cells. Blood. 1994;84(12):4116-24.

52. Itoh K, Tezuka H, Sakoda H, Konno M, Nagata K, Uchiyama T et al. Reproducible establishment of hemopoietic supportive stromal cell lines from murine bone marrow. Exp Hematol. 1989;17(2):145-53.

53. Drzeniek Z, Siebertz B, Stocker G, Just U, Ostertag W, Greiling H et al. Proteoglycan synthesis in haematopoietic cells: isolation and characterization of heparan sulphate proteoglycans expressed by the bone-marrow stromal cell line MS-5. The Biochemical journal. 1997;327 (Pt 2):473-80.

54. De St. Groth SF. The evaluation of limiting dilution assays. Journal of Immunological Methods. 1982;49(2):R11-R23.

55. Breems DA, Blokland EA, Neben S, Ploemacher RE. Frequency analysis of human primitive haematopoietic stem cell subsets using a cobblestone area forming cell assay. Leukemia. 1994;8(7):1095-104.

56. Conneally E, Cashman J, Petzer A, Eaves C. Expansion in vitro of transplantable human cord blood stem cells demonstrated using a quantitative assay of their lympho-myeloid repopulating activity in nonobese diabetic-scid/scid mice. Proc Natl Acad Sci U S A. 1997;94(18):9836-41.

57. Hao QL, Shah AJ, Thiemann FT, Smogorzewska EM, Crooks GM. A functional comparison of CD34 + CD38- cells in cord blood and bone marrow. Blood. 1995;86(10):3745-53.

58. Civin CI, Almeida-Porada G, Lee MJ, Olweus J, Terstappen LW, Zanjani ED. Sustained, retransplantable, multilineage engraftment of highly purified adult human bone marrow stem cells in vivo. Blood. 1996;88(11):4102-9.

59. Kamel-Reid S, Dick JE. Engraftment of immune-deficient mice with human hematopoietic stem cells. Science. 1988;242(4886):1706-9.

60. Mosier DE, Gulizia RJ, Baird SM, Wilson DB. Transfer of a functional human immune system to mice with severe combined immunodeficiency. Nature. 1988;335(6187):256-9.

61. Vormoor J, Lapidot T, Pflumio F, Risdon G, Patterson B, Broxmeyer HE et al. Immature human cord blood progenitors engraft and proliferate to high levels in severe combined immunodeficient mice. Blood. 1994;83(9):2489-97.

62. Fraser CC, Kaneshima H, Hansteen G, Kilpatrick M, Hoffman R, Chen BP. Human allogeneic stem cell maintenance and differentiation in a long-term multilineage SCID-hu graft. Blood. 1995;86(5):1680-93.

63. Shultz LD, Schweitzer PA, Christianson SW, Gott B, Schweitzer IB, Tennent B et al. Multiple defects in innate and adaptive immunologic function in NOD/LtSz-scid mice. J Immunol. 1995;154(1):180-91.

64. Ito M, Hiramatsu H, Kobayashi K, Suzue K, Kawahata M, Hioki K et al. NOD/SCID/gamma(c)(null) mouse: an excellent recipient mouse model for engraftment of human cells. Blood. 2002;100(9):3175.

65. Shultz LD, Lyons BL, Burzenski LM, Gott B, Chen X, Chaleff S et al. Human lymphoid and myeloid cell development in NOD/LtSz-scid IL2R gamma null mice engrafted with mobilized human hemopoietic stem cells. J Immunol. 2005;174(10):6477-89.

66. Traggiai E, Chicha L, Mazzucchelli L, Bronz L, Piffaretti JC, Lanzavecchia A et al. Development of a human adaptive immune system in cord blood cell-transplanted mice. Science. 2004;304(5667):104-7.

67. Hiramatsu H, Nishikomori R, Heike T, Ito M, Kobayashi K, Katamura K et al. Complete reconstitution of human lymphocytes from cord blood CD34+ cells using the NOD/SCID/gammacnull mice model. Blood. 2003;102(3):873-80.

68. Chen Q, Khoury M, Chen J. Expression of human cytokines dramatically improves reconstitution of specific human-blood lineage cells in humanized mice. Proc Natl Acad Sci U S A. 2009;106(51):21783-8.

69. Rongvaux A, Willinger T, Takizawa H, Rathinam C, Auerbach W, Murphy AJ et al. Human thrombopoietin knockin mice efficiently support human hematopoiesis in vivo. Proc Natl Acad Sci U S A. 2011;108(6):2378-83.

70. Willinger T, Rongvaux A, Takizawa H, Yancopoulos GD, Valenzuela DM, Murphy AJ et al. Human IL-3/GM-CSF knock-in mice support human alveolar macrophage development and human immune responses in the lung. Proc Natl Acad Sci U S A. 2011;108(6):2390-5.

71. Wilson A, Laurenti E, Oser G, van der Wath RC, Blanco-Bose W, Jaworski M et al. Hematopoietic stem cells reversibly switch from dormancy to self-renewal during homeostasis and repair. Cell. 2008;135(6):1118-29.

72. Yoshihara H, Arai F, Hosokawa K, Hagiwara T, Takubo K, Nakamura Y et al. Thrombopoietin/MPL signaling regulates hematopoietic stem cell quiescence and interaction with the osteoblastic niche. Cell Stem Cell. 2007;1(6):685-97.

73. Martinez-Agosto JA, Mikkola HK, Hartenstein V, Banerjee U. The hematopoietic stem cell and its niche: a comparative view. Genes & development. 2007;21(23):3044-60.

74. Zhang J, Niu C, Ye L, Huang H, He X, Tong WG et al. Identification of the haematopoietic stem cell niche and control of the niche size. Nature. 2003;425(6960):836-41.

75. Calvi LM, Adams GB, Weibrecht KW, Weber JM, Olson DP, Knight MC et al. Osteoblastic cells regulate the haematopoietic stem cell niche. Nature. 2003;425(6960):841-6.

76. Mendez-Ferrer S, Michurina TV, Ferraro F, Mazloom AR, Macarthur BD, Lira SA et al. Mesenchymal and haematopoietic stem cells form a unique bone marrow niche. Nature. 2010;466(7308):829-34.

77. Gattazzo F, Urciuolo A, Bonaldo P. Extracellular matrix: a dynamic microenvironment for stem cell niche. Biochimica et biophysica acta. 2014;1840(8):2506-19.

78. Leisten I, Kramann R, Ventura Ferreira MS, Bovi M, Neuss S, Ziegler P et al. 3D co-culture of hematopoietic stem and progenitor cells and mesenchymal stem cells in collagen scaffolds as a model of the hematopoietic niche. Biomaterials. 2012;33(6):1736-47.

79. Di Maggio N, Piccinini E, Jaworski M, Trumpp A, Wendt DJ, Martin I. Toward modeling the bone marrow niche using scaffold-based 3D culture systems. Biomaterials. 2011;32(2):321-9.

80. Tan J, Liu T, Hou L, Meng W, Wang Y, Zhi W et al. Maintenance and expansion of hematopoietic stem/progenitor cells in biomimetic osteoblast niche. Cytotechnology. 2010;62(5):439-48.

81. Bagley J, Rosenzweig M, Marks DF, Pykett MJ. Extended culture of multipotent hematopoietic progenitors without cytokine augmentation in a novel three-dimensional device. Exp Hematol. 1999;27(3):496-504.

82. Banu N, Rosenzweig M, Kim H, Bagley J, Pykett M. Cytokine-augmented culture of haematopoietic progenitor cells in a novel three-dimensional cell growth matrix. Cytokine. 2001;13(6):349-58.

83. Bartsch K, Al-Ali H, Reinhardt A, Franke C, Hudecek M, Kamprad M et al. Mesenchymal stem cells remain host-derived independent of the source of the stem-cell graft and conditioning regimen used. Transplantation. 2009;87(2):217-21.

84. Rieger K, Marinets O, Fietz T, Korper S, Sommer D, Mucke C et al. Mesenchymal stem cells remain of host origin even a long time after allogeneic peripheral blood stem cell or bone marrow transplantation. Exp Hematol. 2005;33(5):605-11.

85. Chen Y, Jacamo R, Shi YX, Wang RY, Battula VL, Konoplev S et al. Human extramedullary bone marrow in mice: a novel in vivo model of genetically controlled hematopoietic microenvironment. Blood. 2012;119(21):4971-80.

86. Yui J, Chiu CP, Lansdorp PM. Telomerase activity in candidate stem cells from fetal liver and adult bone marrow. Blood. 1998;91(9):3255-62.

87. Mahmud N, Petro B, Baluchamy S, Li X, Taioli S, Lavelle D et al. Differential effects of epigenetic modifiers on the expansion and maintenance of human cord blood stem/progenitor cells. Biology of blood and marrow transplantation : journal of the American Society for Blood and Marrow Transplantation. 2014;20(4):480-9.

88. Boulais PE, Frenette PS. Making sense of hematopoietic stem cell niches. Blood. 2015;125(17):2621-9.

89. Reagan MR, Rosen CJ. Navigating the bone marrow niche: translational insights and cancer-driven dysfunction. Nature reviews Rheumatology. 2016;12(3):154-68.

90. Morrison SJ, Scadden DT. The bone marrow niche for haematopoietic stem cells. Nature. 2014;505(7483):327-34.

91. Till JE, McCulloch EA, Siminovitch L. A Stochastic Model of Stem Cell Proliferation, Based on the Growth of Spleen Colony-Forming Cells. Proc Natl Acad Sci U S A. 1964;51:29-36.

92. Bell DR, Van Zant G. Stem cells, aging, and cancer: inevitabilities and outcomes. Oncogene. 2004;23(43):7290-6.

93. Suda T, Suda J, Ogawa M. Single-cell origin of mouse hemopoietic colonies expressing multiple lineages in variable combinations. Proc Natl Acad Sci U S A. 1983;80(21):6689-93.

94. Orford KW, Scadden DT. Deconstructing stem cell self-renewal: genetic insights into cell-cycle regulation. Nat Rev Genet. 2008;9(2):115-28.

95. Foudi A, Hochedlinger K, Van Buren D, Schindler JW, Jaenisch R, Carey V et al. Analysis of histone 2B-GFP retention reveals slowly cycling hematopoietic stem cells. Nature biotechnology. 2009;27(1):84-90.

96. Rossi L, Lin KK, Boles NC, Yang L, King KY, Jeong M et al. Less is more: unveiling the functional core of hematopoietic stem cells through knockout mice. Cell Stem Cell. 2012;11(3):302-17.

97. Yuan Y, Shen H, Franklin DS, Scadden DT, Cheng T. In vivo self-renewing divisions of haematopoietic stem cells are increased in the absence of the early G1-phase inhibitor, p18INK4C. Nature cell biology. 2004;6(5):436-42.

98. Lieu YK, Reddy EP. Conditional c-myb knockout in adult hematopoietic stem cells leads to loss of self-renewal due to impaired proliferation and accelerated differentiation. Proc Natl Acad Sci U S A. 2009;106(51):21689-94.

99. Cashman J, Dykstra B, Clark-Lewis I, Eaves A, Eaves C. Changes in the proliferative activity of human hematopoietic stem cells in NOD/SCID mice and enhancement of their transplantability after in vivo treatment with cell cycle inhibitors. J Exp Med. 2002;196(9):1141-9.

100. Takizawa H, Regoes RR, Boddupalli CS, Bonhoeffer S, Manz MG. Dynamic variation in cycling of hematopoietic stem cells in steady state and inflammation. J Exp Med. 2011;208(2):273-84.

101. Schroeder T. Heterogeneity of sister cell fates. Nature reviews Molecular cell biology. 2013;14(6):327.

102. Sanjuan-Pla A, Macaulay IC, Jensen CT, Woll PS, Luis TC, Mead A et al. Platelet-biased stem cells reside at the apex of the haematopoietic stem-cell hierarchy. Nature. 2013;502(7470):232-6.

103. Oguro H, Ding L, Morrison SJ. SLAM family markers resolve functionally distinct subpopulations of hematopoietic stem cells and multipotent progenitors. Cell Stem Cell. 2013;13(1):102-16.

104. Gothot A, Pyatt R, McMahel J, Rice S, Srour EF. Functional heterogeneity of human CD34(+) cells isolated in subcompartments of the G0 /G1 phase of the cell cycle. Blood. 1997;90(11):4384-93.

105. Laurenti E, Frelin C, Xie S, Ferrari R, Dunant CF, Zandi S et al. CDK6 levels regulate quiescence exit in human hematopoietic stem cells. Cell Stem Cell. 2015;16(3):302-13.

106. Gibbs KD, Jr., Gilbert PM, Sachs K, Zhao F, Blau HM, Weissman IL et al. Single-cell phospho-specific flow cytometric analysis demonstrates biochemical and functional heterogeneity in human hematopoietic stem and progenitor compartments. Blood. 2011;117(16):4226-33.

107. Stein MI, Zhu J, Emerson SG. Molecular pathways regulating the self-renewal of hematopoietic stem cells. Exp Hematol. 2004;32(12):1129-36.

108. Antonchuk J, Sauvageau G, Humphries RK. HOXB4-induced expansion of adult hematopoietic stem cells ex vivo. Cell. 2002;109(1):39-45.

109. Amsellem S, Pflumio F, Bardinet D, Izac B, Charneau P, Romeo PH et al. Ex vivo expansion of human hematopoietic stem cells by direct delivery of the HOXB4 homeoprotein. Nature medicine. 2003;9(11):1423-7.

110. Park IK, Qian D, Kiel M, Becker MW, Pihalja M, Weissman IL et al. Bmi-1 is required for maintenance of adult self-renewing haematopoietic stem cells. Nature. 2003;423(6937):302-5.

111. Rizo A, Olthof S, Han L, Vellenga E, de Haan G, Schuringa JJ. Repression of BMI1 in normal and leukemic human CD34(+) cells impairs self-renewal and induces apoptosis. Blood. 2009;114(8):1498-505.

112. Shojaei F, Trowbridge J, Gallacher L, Yuefei L, Goodale D, Karanu F et al. Hierarchical and ontogenic positions serve to define the molecular basis of human hematopoietic stem cell behavior. Developmental cell. 2005;8(5):651-63.

113. Varnum-Finney B, Xu L, Brashem-Stein C, Nourigat C, Flowers D, Bakkour S et al. Pluripotent, cytokine-dependent, hematopoietic stem cells are immortalized by constitutive Notch1 signaling. Nature medicine. 2000;6(11):1278-81.

114. Huang J, Nguyen-McCarty M, Hexner EO, Danet-Desnoyers G, Klein PS. Maintenance of hematopoietic stem cells through regulation of Wnt and mTOR pathways. Nature medicine. 2012;18(12):1778-85.

115. Wang J, Sun Q, Morita Y, Jiang H, Gross A, Lechel A et al. A differentiation checkpoint limits hematopoietic stem cell self-renewal in response to DNA damage. Cell. 2012;148(5):1001-14.

116. Florian MC, Dorr K, Niebel A, Daria D, Schrezenmeier H, Rojewski M et al. Cdc42 activity regulates hematopoietic stem cell aging and rejuvenation. Cell Stem Cell. 2012;10(5):520-30.

117. Chen X, Skutt-Kakaria K, Davison J, Ou YL, Choi E, Malik P et al. G9a/GLP-dependent histone H3K9me2 patterning during human hematopoietic stem cell lineage commitment. Genes & development. 2012;26(22):2499-511.

118. Will B, Vogler TO, Bartholdy B, Garrett-Bakelman F, Mayer J, Barreyro L et al. Satb1 regulates the self-renewal of hematopoietic stem cells by promoting quiescence and repressing differentiation commitment. Nat Immunol. 2013;14(5):437-45.

119. Staber PB, Zhang P, Ye M, Welner RS, Nombela-Arrieta C, Bach C et al. Sustained PU.1 levels balance cell-cycle regulators to prevent exhaustion of adult hematopoietic stem cells. Molecular cell. 2013;49(5):934-46.

120. Wilson NK, Foster SD, Wang X, Knezevic K, Schutte J, Kaimakis P et al. Combinatorial transcriptional control in blood stem/progenitor cells: genome-wide analysis of ten major transcriptional regulators. Cell Stem Cell. 2010;7(4):532-44.

121. Novershtern N, Subramanian A, Lawton LN, Mak RH, Haining WN, McConkey ME et al. Densely interconnected transcriptional circuits control cell states in human hematopoiesis. Cell. 2011;144(2):296-309.

122. Moignard V, Macaulay IC, Swiers G, Buettner F, Schutte J, Calero-Nieto FJ et al. Characterization of transcriptional networks in blood stem and progenitor cells using high-throughput single-cell gene expression analysis. Nature cell biology. 2013;15(4):363-72.

123. Schofield R. The relationship between the spleen colony-forming cell and the haemopoietic stem cell. Blood cells. 1978;4(1-2):7-25.

124. Arai F, Hirao A, Ohmura M, Sato H, Matsuoka S, Takubo K et al. Tie2/angiopoietin-1 signaling regulates hematopoietic stem cell quiescence in the bone marrow niche. Cell. 2004;118(2):149-61.

125. Hosokawa K, Arai F, Yoshihara H, Nakamura Y, Gomei Y, Iwasaki H et al. Function of oxidative stress in the regulation of hematopoietic stem cell-niche interaction. Biochemical and biophysical research communications. 2007;363(3):578-83.

126. Haug JS, He XC, Grindley JC, Wunderlich JP, Gaudenz K, Ross JT et al. N-cadherin expression level distinguishes reserved versus primed states of hematopoietic stem cells. Cell Stem Cell. 2008;2(4):367-79.

127. Kiel MJ, Radice GL, Morrison SJ. Lack of evidence that hematopoietic stem cells depend on N-cadherin-mediated adhesion to osteoblasts for their maintenance. Cell Stem Cell. 2007;1(2):204-17.

128. Kiel MJ, Acar M, Radice GL, Morrison SJ. Hematopoietic stem cells do not depend on N-cadherin to regulate their maintenance. Cell Stem Cell. 2009;4(2):170-9.

129. Li P, Zon LI. Resolving the controversy about N-cadherin and hematopoietic stem cells. Cell Stem Cell. 2010;6(3):199-202.

130. Adams GB, Chabner KT, Alley IR, Olson DP, Szczepiorkowski ZM, Poznansky MC et al. Stem cell engraftment at the endosteal niche is specified by the calcium-sensing receptor. Nature. 2006;439(7076):599-603.

131. Lo Celso C, Fleming HE, Wu JW, Zhao CX, Miake-Lye S, Fujisaki J et al. Live-animal tracking of individual haematopoietic stem/progenitor cells in their niche. Nature. 2009;457(7225):92-6.

132. Xie Y, Yin T, Wiegraebe W, He XC, Miller D, Stark D et al. Detection of functional haematopoietic stem cell niche using real-time imaging. Nature. 2009;457(7225):97-101.

133. Kunisaki Y, Bruns I, Scheiermann C, Ahmed J, Pinho S, Zhang D et al. Arteriolar niches maintain haematopoietic stem cell quiescence. Nature. 2013;502(7473):637-43.

134. Sugiyama T, Kohara H, Noda M, Nagasawa T. Maintenance of the hematopoietic stem cell pool by CXCL12-CXCR4 chemokine signaling in bone marrow stromal cell niches. Immunity. 2006;25(6):977-88.

135. Ara T, Tokoyoda K, Sugiyama T, Egawa T, Kawabata K, Nagasawa T. Long-term hematopoietic stem cells require stromal cell-derived factor-1 for colonizing bone marrow during ontogeny. Immunity. 2003;19(2):257-67.

136. Sacchetti B, Funari A, Michienzi S, Di Cesare S, Piersanti S, Saggio I et al. Self-renewing osteoprogenitors in bone marrow sinusoids can organize a hematopoietic microenvironment. Cell. 2007;131(2):324-36.

137. Butler JM, Nolan DJ, Vertes EL, Varnum-Finney B, Kobayashi H, Hooper AT et al. Endothelial cells are essential for the self-renewal and repopulation of Notch-dependent hematopoietic stem cells. Cell Stem Cell. 2010;6(3):251-64.

138. Poulos MG, Guo P, Kofler NM, Pinho S, Gutkin MC, Tikhonova A et al. Endothelial Jagged-1 is necessary for homeostatic and regenerative hematopoiesis. Cell reports. 2013;4(5):1022-34.

139. Mendez-Ferrer S, Lucas D, Battista M, Frenette PS. Haematopoietic stem cell release is regulated by circadian oscillations. Nature. 2008;452(7186):442-7.

140. Ding L, Morrison SJ. Haematopoietic stem cells and early lymphoid progenitors occupy distinct bone marrow niches. Nature. 2013;495(7440):231-5.

141. Greenbaum A, Hsu YM, Day RB, Schuettpelz LG, Christopher MJ, Borgerding JN et al. CXCL12 in early mesenchymal progenitors is required for haematopoietic stem-cell maintenance. Nature. 2013;495(7440):227-30.

142. Chow A, Lucas D, Hidalgo A, Mendez-Ferrer S, Hashimoto D, Scheiermann C et al. Bone marrow CD169+ macrophages promote the retention of hematopoietic stem and progenitor cells in the mesenchymal stem cell niche. J Exp Med. 2011;208(2):261-71.

143. Bruns I, Lucas D, Pinho S, Ahmed J, Lambert MP, Kunisaki Y et al. Megakaryocytes regulate hematopoietic stem cell quiescence through CXCL4 secretion. Nature medicine. 2014;20(11):1315-20.

144. Schepers K, Campbell TB, Passegue E. Normal and leukemic stem cell niches: insights and therapeutic opportunities. Cell Stem Cell. 2015;16(3):254-67.

145. Artavanis-Tsakonas S, Rand MD, Lake RJ. Notch signaling: cell fate control and signal integration in development. Science. 1999;284(5415):770-6.

146. Milner LA, Bigas A. Notch as a mediator of cell fate determination in hematopoiesis: evidence and speculation. Blood. 1999;93(8):2431-48.

147. Bray SJ. Notch signalling: a simple pathway becomes complex. Nature reviews Molecular cell biology. 2006;7(9):678-89.

148. Lobry C, Oh P, Mansour MR, Look AT, Aifantis I. Notch signaling: switching an oncogene to a tumor suppressor. Blood. 2014;123(16):2451-9.

149. Ellisen LW, Bird J, West DC, Soreng AL, Reynolds TC, Smith SD et al. TAN-1, the human homolog of the Drosophila notch gene, is broken by chromosomal translocations in T lymphoblastic neoplasms. Cell. 1991;66(4):649-61.

150. Kumano K, Chiba S, Kunisato A, Sata M, Saito T, Nakagami-Yamaguchi E et al. Notch1 but not Notch2 is essential for generating hematopoietic stem cells from endothelial cells. Immunity. 2003;18(5):699-711.

151. Radtke F, Wilson A, Stark G, Bauer M, van Meerwijk J, MacDonald HR et al. Deficient T cell fate specification in mice with an induced inactivation of Notch1. Immunity. 1999;10(5):547-58.

152. Johansen KM, Fehon RG, Artavanis-Tsakonas S. The notch gene product is a glycoprotein expressed on the cell surface of both epidermal and neuronal precursor cells during Drosophila development. J Cell Biol. 1989;109(5):2427-40.

153. Kopan R, Ilagan MX. The canonical Notch signaling pathway: unfolding the activation mechanism. Cell. 2009;137(2):216-33.

154. Gordon WR, Arnett KL, Blacklow SC. The molecular logic of Notch signaling--a structural and biochemical perspective. J Cell Sci. 2008;121(Pt 19):3109-19.

155. de Celis JF, Bray SJ. The Abruptex domain of Notch regulates negative interactions between Notch, its ligands and Fringe. Development. 2000;127(6):1291-302.

156. Cordle J, Redfieldz C, Stacey M, van der Merwe PA, Willis AC, Champion BR et al. Localization of the delta-like-1-binding site in human Notch-1 and its modulation by calcium affinity. J Biol Chem. 2008;283(17):11785-93.

157. Gordon WR, Vardar-Ulu D, Histen G, Sanchez-Irizarry C, Aster JC, Blacklow SC. Structural basis for autoinhibition of Notch. Nat Struct Mol Biol. 2007;14(4):295-300.

158. Weng AP, Ferrando AA, Lee W, Morris JPt, Silverman LB, Sanchez-Irizarry C et al. Activating mutations of NOTCH1 in human T cell acute lymphoblastic leukemia. Science. 2004;306(5694):269-71.

159. Okajima T, Xu A, Lei L, Irvine KD. Chaperone activity of protein O-fucosyltransferase 1 promotes notch receptor folding. Science. 2005;307(5715):1599-603.

160. Bruckner K, Perez L, Clausen H, Cohen S. Glycosyltransferase activity of Fringe modulates Notch-Delta interactions. Nature. 2000;406(6794):411-5.

161. Logeat F, Bessia C, Brou C, LeBail O, Jarriault S, Seidah NG et al. The Notch1 receptor is cleaved constitutively by a furin-like convertase. Proc Natl Acad Sci U S A. 1998;95(14):8108-12.

162. Rand MD, Grimm LM, Artavanis-Tsakonas S, Patriub V, Blacklow SC, Sklar J et al. Calcium depletion dissociates and activates heterodimeric notch receptors. Mol Cell Biol. 2000;20(5):1825-35.

163. Lubman OY, Ilagan MX, Kopan R, Barrick D. Quantitative dissection of the Notch:CSL interaction: insights into the Notch-mediated transcriptional switch. J Mol Biol. 2007;365(3):577-89.

164. Kurooka H, Kuroda K, Honjo T. Roles of the ankyrin repeats and C-terminal region of the mouse notch1 intracellular region. Nucleic Acids Res. 1998;26(23):5448-55.

165. Wallberg AE, Pedersen K, Lendahl U, Roeder RG. p300 and PCAF act cooperatively to mediate transcriptional activation from chromatin templates by notch intracellular domains in vitro. Mol Cell Biol. 2002;22(22):7812-9.

166. Ong CT, Cheng HT, Chang LW, Ohtsuka T, Kageyama R, Stormo GD et al. Target selectivity of vertebrate notch proteins. Collaboration between discrete domains and CSL-binding site architecture determines activation probability. J Biol Chem. 2006;281(8):5106-19.

167. Beatus P, Lundkvist J, Oberg C, Lendahl U. The notch 3 intracellular domain represses notch 1-mediated activation through Hairy/Enhancer of split (HES) promoters. Development. 1999;126(17):3925-35.

168. James AC, Szot JO, Iyer K, Major JA, Pursglove SE, Chapman G et al. Notch4 reveals a novel mechanism regulating Notch signal transduction. Biochimica et biophysica acta. 2014;1843(7):1272-84.

169. Grabher C, von Boehmer H, Look AT. Notch 1 activation in the molecular pathogenesis of T-cell acute lymphoblastic leukaemia. Nat Rev Cancer. 2006;6(5):347-59.

170. Moretti J, Brou C. Ubiquitinations in the notch signaling pathway. International journal of molecular sciences. 2013;14(3):6359-81.

171. Chapman G, Sparrow DB, Kremmer E, Dunwoodie SL. Notch inhibition by the ligand DELTA-LIKE 3 defines the mechanism of abnormal vertebral segmentation in spondylocostal dysostosis. Hum Mol Genet. 2011;20(5):905-16.

172. Kovall RA, Gebelein B, Sprinzak D, Kopan R. The Canonical Notch Signaling Pathway: Structural and Biochemical Insights into Shape, Sugar, and Force. Developmental cell. 2017;41(3):228-41.

173. Luca VC, Jude KM, Pierce NW, Nachury MV, Fischer S, Garcia KC. Structural biology. Structural basis for Notch1 engagement of Delta-like 4. Science. 2015;347(6224):847-53.

174. Luca VC, Kim BC, Ge C, Kakuda S, Wu D, Roein-Peikar M et al. Notch-Jagged complex structure implicates a catch bond in tuning ligand sensitivity. Science. 2017;355(6331):1320-4.

175. Andrawes MB, Xu X, Liu H, Ficarro SB, Marto JA, Aster JC et al. Intrinsic selectivity of Notch 1 for Delta-like 4 over Delta-like 1. J Biol Chem. 2013;288(35):25477-89.

176. Parks AL, Klueg KM, Stout JR, Muskavitch MA. Ligand endocytosis drives receptor dissociation and activation in the Notch pathway. Development. 2000;127(7):1373-85.

177. Guo B, McMillan BJ, Blacklow SC. Structure and function of the Mind bomb E3 ligase in the context of Notch signal transduction. Current opinion in structural biology. 2016;41:38-45.

178. Theodoris CV, Li M, White MP, Liu L, He D, Pollard KS et al. Human disease modeling reveals integrated transcriptional and epigenetic mechanisms of NOTCH1 haploinsufficiency. Cell. 2015;160(6):1072-86.

179. Yang LT, Nichols JT, Yao C, Manilay JO, Robey EA, Weinmaster G. Fringe glycosyltransferases differentially modulate Notch1 proteolysis induced by Delta1 and Jagged1. Mol Biol Cell. 2005;16(2):927-42.

180. Visan I, Tan JB, Yuan JS, Harper JA, Koch U, Guidos CJ. Regulation of T lymphopoiesis by Notch1 and Lunatic fringe-mediated competition for intrathymic niches. Nat Immunol. 2006;7(6):634-43.

181. Brou C, Logeat F, Gupta N, Bessia C, LeBail O, Doedens JR et al. A novel proteolytic cleavage involved in Notch signaling: the role of the disintegrin-metalloprotease TACE. Molecular cell. 2000;5(2):207-16.

182. Mumm JS, Schroeter EH, Saxena MT, Griesemer A, Tian X, Pan DJ et al. A ligand-induced extracellular cleavage regulates gamma-secretase-like proteolytic activation of Notch1. Molecular cell. 2000;5(2):197-206.

183. van Tetering G, van Diest P, Verlaan I, van der Wall E, Kopan R, Vooijs M. Metalloprotease ADAM10 is required for Notch1 site 2 cleavage. J Biol Chem. 2009;284(45):31018-27.

184. Gibb DR, El Shikh M, Kang DJ, Rowe WJ, El Sayed R, Cichy J et al. ADAM10 is essential for Notch2-dependent marginal zone B cell development and CD23 cleavage in vivo. J Exp Med. 2010;207(3):623-35.

185. Bozkulak EC, Weinmaster G. Selective use of ADAM10 and ADAM17 in activation of Notch1 signaling. Mol Cell Biol. 2009;29(21):5679-95.

186. Schroeter EH, Kisslinger JA, Kopan R. Notch-1 signalling requires ligand-induced proteolytic release of intracellular domain. Nature. 1998;393(6683):382-6.

187. Struhl G, Greenwald I. Presenilin is required for activity and nuclear access of Notch in Drosophila. Nature. 1999;398(6727):522-5.

188. Wu L, Aster JC, Blacklow SC, Lake R, Artavanis-Tsakonas S, Griffin JD. MAML1, a human homologue of Drosophila mastermind, is a transcriptional co-activator for NOTCH receptors. Nat Genet. 2000;26(4):484-9.

189. Radtke F, MacDonald HR, Tacchini-Cottier F. Regulation of innate and adaptive immunity by Notch. Nature Reviews Immunology. 2013;13:427.

190. Nam Y, Weng AP, Aster JC, Blacklow SC. Structural requirements for assembly of the CSL.intracellular Notch1.Mastermind-like 1 transcriptional activation complex. J Biol Chem. 2003;278(23):21232-9.

191. Bray SJ. Notch signalling in context. Nature reviews Molecular cell biology. 2016;17(11):722-35.

192. Kageyama R, Ohtsuka T, Kobayashi T. The Hes gene family: repressors and oscillators that orchestrate embryogenesis. Development. 2007;134(7):1243-51.

193. Kishi N, Tang Z, Maeda Y, Hirai A, Mo R, Ito M et al. Murine homologs of deltex define a novel gene family involved in vertebrate Notch signaling and neurogenesis. Int J Dev Neurosci. 2001;19(1):21-35.

194. Sundaram MV. The love-hate relationship between Ras and Notch. Genes & development. 2005;19(16):1825-39.

195. Krejci A, Bernard F, Housden BE, Collins S, Bray SJ. Direct response to Notch activation: signaling crosstalk and incoherent logic. Sci Signal. 2009;2(55):ra1.

196. Palomero T, Lim WK, Odom DT, Sulis ML, Real PJ, Margolin A et al. NOTCH1 directly regulates c-MYC and activates a feed-forward-loop transcriptional network promoting leukemic cell growth. Proc Natl Acad Sci U S A. 2006;103(48):18261-6.

197. Pines MK, Housden BE, Bernard F, Bray SJ, Roper K. The cytolinker Pigs is a direct target and a negative regulator of Notch signalling. Development. 2010;137(6):913-22.

198. Andersen P, Uosaki H, Shenje LT, Kwon C. Non-canonical Notch signaling: emerging role and mechanism. Trends Cell Biol. 2012;22(5):257-65.

199. Wu J, Bresnick EH. Bare rudiments of notch signaling: how receptor levels are regulated. Trends Biochem Sci. 2007;32(10):477-85.

200. Krebs LT, Xue Y, Norton CR, Shutter JR, Maguire M, Sundberg JP et al. Notch signaling is essential for vascular morphogenesis in mice. Genes & development. 2000;14(11):1343-52.

201. Hamada Y, Kadokawa Y, Okabe M, Ikawa M, Coleman JR, Tsujimoto Y. Mutation in ankyrin repeats of the mouse Notch2 gene induces early embryonic lethality. Development. 1999;126(15):3415-24.

202. Domenga V, Fardoux P, Lacombe P, Monet M, Maciazek J, Krebs LT et al. Notch3 is required for arterial identity and maturation of vascular smooth muscle cells. Genes & development. 2004;18(22):2730-5.

203. Cheng HT, Kim M, Valerius MT, Surendran K, Schuster-Gossler K, Gossler A et al. Notch2, but not Notch1, is required for proximal fate acquisition in the mammalian nephron. Development. 2007;134(4):801-11.

204. Krebs LT, Iwai N, Nonaka S, Welsh IC, Lan Y, Jiang R et al. Notch signaling regulates left-right asymmetry determination by inducing Nodal expression. Genes & development. 2003;17(10):1207-12.

205. Kitamoto T, Takahashi K, Takimoto H, Tomizuka K, Hayasaka M, Tabira T et al. Functional redundancy of the Notch gene family during mouse embryogenesis: analysis of Notch gene expression in Notch3-deficient mice. Biochemical and biophysical research communications. 2005;331(4):1154-62.

206. Parr C, Watkins G, Jiang WG. The possible correlation of Notch-1 and Notch-2 with clinical outcome and tumour clinicopathological parameters in human breast cancer. International journal of molecular medicine. 2004;14(5):779-86.

207. Hozumi K, Mailhos C, Negishi N, Hirano K, Yahata T, Ando K et al. Delta-like 4 is indispensable in thymic environment specific for T cell development. J Exp Med. 2008;205(11):2507-13.

208. Saito T, Chiba S, Ichikawa M, Kunisato A, Asai T, Shimizu K et al. Notch2 is preferentially expressed in mature B cells and indispensable for marginal zone B lineage development. Immunity. 2003;18(5):675-85.

209. Hozumi K, Negishi N, Suzuki D, Abe N, Sotomaru Y, Tamaoki N et al. Delta-like 1 is necessary for the generation of marginal zone B cells but not T cells in vivo. Nat Immunol. 2004;5(6):638-44.

210. Murata A, Okuyama K, Sakano S, Kajiki M, Hirata T, Yagita H et al. A Notch ligand, Delta-like 1 functions as an adhesion molecule for mast cells. J Immunol. 2010;185(7):3905-12.

211. Sorensen I, Adams RH, Gossler A. DLL1-mediated Notch activation regulates endothelial identity in mouse fetal arteries. Blood. 2009;113(22):5680-8.

212. Rios AC, Serralbo O, Salgado D, Marcelle C. Neural crest regulates myogenesis through the transient activation of NOTCH. Nature. 2011;473(7348):532-5.

213. Cappellari O, Benedetti S, Innocenzi A, Tedesco FS, Moreno-Fortuny A, Ugarte G et al. Dll4 and PDGF-BB convert committed skeletal myoblasts to pericytes without erasing their myogenic memory. Developmental cell. 2013;24(6):586-99.

214. Preuße K, Tveriakhina L, Schuster-Gossler K, Gaspar C, Rosa AI, Henrique D et al. Context-Dependent Functional Divergence of the Notch Ligands DLL1 and DLL4 In Vivo. PLoS Genet. 2015;11(6):e1005328.

215. Duarte A, Hirashima M, Benedito R, Trindade A, Diniz P, Bekman E et al. Dosage-sensitive requirement for mouse Dll4 in artery development. Genes & development. 2004;18(20):2474-8.

216. Robert-Moreno A, Guiu J, Ruiz-Herguido C, Lopez ME, Ingles-Esteve J, Riera L et al. Impaired embryonic haematopoiesis yet normal arterial development in the absence of the Notch ligand Jagged1. EMBO J. 2008;27(13):1886-95.

217. Gama-Norton L, Ferrando E, Ruiz-Herguido C, Liu Z, Guiu J, Islam AB et al. Notch signal strength controls cell fate in the haemogenic endothelium. Nat Commun. 2015;6:8510.

218. Nandagopal N, Santat LA, LeBon L, Sprinzak D, Bronner ME, Elowitz MB. Dynamic Ligand Discrimination in the Notch Signaling Pathway. Cell. 2018;172(4):869-80 e19.

219. Milner LA, Kopan R, Martin DI, Bernstein ID. A human homologue of the Drosophila developmental gene, Notch, is expressed in CD34+ hematopoietic precursors. Blood. 1994;83(8):2057-62.

220. Weber JM, Calvi LM. Notch signaling and the bone marrow hematopoietic stem cell niche. Bone. 2010;46(2):281-5.

221. Carlesso N, Aster JC, Sklar J, Scadden DT. Notch1-induced delay of human hematopoietic progenitor cell differentiation is associated with altered cell cycle kinetics. Blood. 1999;93(3):838-48.

222. Kunisato A, Chiba S, Nakagami-Yamaguchi E, Kumano K, Saito T, Masuda S et al. HES-1 preserves purified hematopoietic stem cells ex vivo and accumulates side population cells in vivo. Blood. 2003;101(5):1777-83.

223. Varnum-Finney B, Brashem-Stein C, Bernstein ID. Combined effects of Notch signaling and cytokines induce a multiple log increase in precursors with lymphoid and myeloid reconstituting ability. Blood. 2003;101(5):1784-9.

224. Karanu FN, Murdoch B, Gallacher L, Wu DM, Koremoto M, Sakano S et al. The notch ligand jagged-1 represents a novel growth factor of human hematopoietic stem cells. J Exp Med. 2000;192(9):1365-72.

225. Rathinam C, Matesic LE, Flavell RA. The E3 ligase Itch is a negative regulator of the homeostasis and function of hematopoietic stem cells. Nat Immunol. 2011;12(5):399-407.

226. Ohishi K, Varnum-Finney B, Bernstein ID. Delta-1 enhances marrow and thymus repopulating ability of human CD34(+)CD38(-) cord blood cells. J Clin Invest. 2002;110(8):1165-74.

227. Lauret E, Catelain C, Titeux M, Poirault S, Dando JS, Dorsch M et al. Membrane-bound delta-4 notch ligand reduces the proliferative activity of primitive human hematopoietic CD34+CD38low cells while maintaining their LTC-IC potential. Leukemia. 2004;18(4):788-97.

228. Han H, Tanigaki K, Yamamoto N, Kuroda K, Yoshimoto M, Nakahata T et al. Inducible gene knockout of transcription factor recombination signal binding protein-J reveals its essential role in T versus B lineage decision. Int Immunol. 2002;14(6):637-45.

229. Duncan AW, Rattis FM, DiMascio LN, Congdon KL, Pazianos G, Zhao C et al. Integration of Notch and Wnt signaling in hematopoietic stem cell maintenance. Nat Immunol. 2005;6(3):314-22.

230. Guezguez B, Campbell CJ, Boyd AL, Karanu F, Casado FL, Di Cresce C et al. Regional localization within the bone marrow influences the functional capacity of human HSCs. Cell Stem Cell. 2013;13(2):175-89.

231. Mancini SJ, Mantei N, Dumortier A, Suter U, MacDonald HR, Radtke F. Jagged1-dependent Notch signaling is dispensable for hematopoietic stem cell self-renewal and differentiation. Blood. 2005;105(6):2340-2.

232. Varnum-Finney B, Halasz LM, Sun M, Gridley T, Radtke F, Bernstein ID. Notch2 governs the rate of generation of mouse long- and short-term repopulating stem cells. J Clin Invest. 2011;121(3):1207-16.

233. Guo P, Poulos MG, Palikuqi B, Badwe CR, Lis R, Kunar B et al. Endothelial jagged-2 sustains hematopoietic stem and progenitor reconstitution after myelosuppression. J Clin Invest. 2017;127(12):4242-56.

234. Wang W, Yu S, Myers J, Wang Y, Xin WW, Albakri M et al. Notch2 blockade enhances hematopoietic stem cell mobilization and homing. Haematologica. 2017;102(10):1785-95.

235. Maillard I, Koch U, Dumortier A, Shestova O, Xu L, Sai H et al. Canonical notch signaling is dispensable for the maintenance of adult hematopoietic stem cells. Cell Stem Cell. 2008;2(4):356-66.

236. Benveniste P, Serra P, Dervovic D, Herer E, Knowles G, Mohtashami M et al. Notch signals are required for in vitro but not in vivo maintenance of human hematopoietic stem cells and delay the appearance of multipotent progenitors. Blood. 2014;123(8):1167-77.

237. Csaszar E, Wang W, Usenko T, Qiao W, Delaney C, Bernstein ID et al. Blood stem cell fate regulation by Delta-1-mediated rewiring of IL-6 paracrine signaling. Blood. 2014;123(5):650-8.

238. Qyang Y, Chambers SM, Wang P, Xia X, Chen X, Goodell MA et al. Myeloproliferative disease in mice with reduced presenilin gene dosage: effect of gamma-secretase blockage. Biochemistry. 2004;43(18):5352-9.

239. Becker DJ, Lowe JB. Fucose: biosynthesis and biological function in mammals. Glycobiology. 2003;13(7):41R-53R.

240. Okajima T, Xu A, Irvine KD. Modulation of notch-ligand binding by protein O-fucosyltransferase 1 and fringe. J Biol Chem. 2003;278(43):42340-5.

241. Zhou L, Li LW, Yan Q, Petryniak B, Man Y, Su C et al. Notch-dependent control of myelopoiesis is regulated by fucosylation. Blood. 2008;112(2):308-19.

242. Yao D, Huang Y, Huang X, Wang W, Yan Q, Wei L et al. Protein O-fucosyltransferase 1 (Pofut1) regulates lymphoid and myeloid homeostasis through modulation of Notch receptor ligand interactions. Blood. 2011;117(21):5652-62.

243. Kim YW, Koo BK, Jeong HW, Yoon MJ, Song R, Shin J et al. Defective Notch activation in microenvironment leads to myeloproliferative disease. Blood. 2008;112(12):4628-38.

244. Yoda M, Kimura T, Tohmonda T, Uchikawa S, Koba T, Takito J et al. Dual functions of cell-autonomous and non-cell-autonomous ADAM10 activity in granulopoiesis. Blood. 2011;118(26):6939-42.

245. Klinakis A, Lobry C, Abdel-Wahab O, Oh P, Haeno H, Buonamici S et al. A novel tumour-suppressor function for the Notch pathway in myeloid leukaemia. Nature. 2011;473(7346):230-3.

246. Wang L, Zhang H, Rodriguez S, Cao L, Parish J, Mumaw C et al. Notch-dependent repression of miR-155 in the bone marrow niche regulates hematopoiesis in an NF-kappaB-dependent manner. Cell Stem Cell. 2014;15(1):51-65.

247. Francis OL, Chaudhry KK, Lamprecht T, Klco JM. Impact of Notch disruption on myeloid development. Blood cancer journal. 2017;7(8):e598.

248. Duarte S, Woll PS, Buza-Vidas N, Chin DWL, Boukarabila H, Luis TC et al. Canonical Notch signaling is dispensable for adult steady-state and stress myelo-erythropoiesis. Blood. 2018;131(15):1712-9.

249. Fernandez L, Rodriguez S, Huang H, Chora A, Fernandes J, Mumaw C et al. Tumor necrosis factor-alpha and endothelial cells modulate Notch signaling in the bone marrow microenvironment during inflammation. Exp Hematol. 2008;36(5):545-58.

250. Corselli M, Chin CJ, Parekh C, Sahaghian A, Wang W, Ge S et al. Perivascular support of human hematopoietic stem/progenitor cells. Blood. 2013;121(15):2891-901.

251. Bowers M, Zhang B, Ho Y, Agarwal P, Chen CC, Bhatia R. Osteoblast ablation reduces normal long-term hematopoietic stem cell self-renewal but accelerates leukemia development. Blood. 2015;125(17):2678-88.

252. Negishi N, Suzuki D, Ito R, Irie N, Matsuo K, Yahata T et al. Effective expansion of engrafted human hematopoietic stem cells in bone marrow of mice expressing human Jagged1. Exp Hematol. 2014;42(6):487-94 e1.

253. Ito R, Negishi N, Irie N, Matsuo K, Suzuki D, Katano I et al. Osteosclerosis and inhibition of human hematopoiesis in NOG mice expressing human Delta-like 1 in osteoblasts. Exp Hematol. 2012;40(11):953-63 e3.

254. Copelan EA. Hematopoietic stem-cell transplantation. The New England journal of medicine. 2006;354(17):1813-26.

255. Ravinet A, Cabrespine A, Socie G, Milpied N, Yakoub-Agha I, Nguyen S et al. Peripheral Blood Stem Cells Vs Bone Marrow: Stem Cell Source Comparison for Patients Acute Myeloid Leukemia and Myelodysplastic Syndrome Receiving an Allogeneic Stem Cell Transplantation from a 10/10 Matched Donor. Study from the French Society of Bone Marrow Transplantation and Cell Therapies (SFGM-TC). Blood. 2014;124(21):2552-.

256. Stewart BL, Storer B, Storek J, Deeg HJ, Storb R, Hansen JA et al. Duration of immunosuppressive treatment for chronic graft-versus-host disease. Blood. 2004;104(12):3501-6.

257. Ferrara JLM, Levine JE, Reddy P, Holler E. Graft-versus-host disease. The Lancet. 2009;373(9674):1550-61.

258. Wagner JE, Barker JN, DeFor TE, Baker KS, Blazar BR, Eide C et al. Transplantation of unrelated donor umbilical cord blood in 102 patients with malignant and nonmalignant diseases: influence of CD34 cell dose and HLA disparity on treatment-related mortality and survival. Blood. 2002;100(5):1611-8.

259. Gluckman E, Broxmeyer HA, Auerbach AD, Friedman HS, Douglas GW, Devergie A et al. Hematopoietic reconstitution in a patient with Fanconi's anemia by means of umbilical-cord blood from an HLA-identical sibling. The New England journal of medicine. 1989;321(17):1174-8.

260. Mazzoccoli G, Miscio G, Fontana A, Copetti M, Francavilla M, Bosi A et al. Time related variations in stem cell harvesting of umbilical cord blood. Scientific Reports. 2016;6:21404.

261. Gluckman E. History of cord blood transplantation. Bone Marrow Transplantation. 2009;44:621.

262. Barker JN, Weisdorf DJ, DeFor TE, Blazar BR, McGlave PB, Miller JS et al. Transplantation of 2 partially HLA-matched umbilical cord blood units to enhance engraftment in adults with hematologic malignancy. Blood. 2005;105(3):1343-7.

263. Wagner JE, Jr., Eapen M, Carter S, Wang Y, Schultz KR, Wall DA et al. One-unit versus two-unit cord-blood transplantation for hematologic cancers. The New England journal of medicine. 2014;371(18):1685-94.

264. Brunstein CG, Gutman JA, Weisdorf DJ, Woolfrey AE, DeFor TE, Gooley TA et al. Allogeneic hematopoietic cell transplantation for hematologic malignancy: relative risks and benefits of double umbilical cord blood. Blood. 2010;116(22):4693-9.

265. Broxmeyer HE, Douglas GW, Hangoc G, Cooper S, Bard J, English D et al. Human umbilical cord blood as a potential source of transplantable hematopoietic stem/progenitor cells. Proc Natl Acad Sci U S A. 1989;86(10):3828-32.

266. Cardoso AA, Li ML, Batard P, Hatzfeld A, Brown EL, Levesque JP et al. Release from quiescence of CD34+ CD38- human umbilical cord blood cells reveals their potentiality to engraft adults. Proceedings of the National Academy of Sciences. 1993;90(18):8707-11.

267. Rosler ES, Brandt JE, Chute J, Hoffman R. An in vivo competitive repopulation assay for various sources of human hematopoietic stem cells. Blood. 2000;96(10):3414-21.

268. Horwitz ME, Chao NJ, Rizzieri DA, Long GD, Sullivan KM, Gasparetto C et al. Umbilical cord blood expansion with nicotinamide provides long-term multilineage engraftment. The Journal of clinical investigation. 2014;124(7):3121-8.

269. Wagner John E, Jr., Brunstein Claudio G, Boitano Anthony E, DeFor Todd E, McKenna D, Sumstad D et al. Phase I/II Trial of StemRegenin-1 Expanded Umbilical Cord Blood Hematopoietic Stem Cells Supports Testing as a Stand-Alone Graft. Cell Stem Cell. 2016;18(1):144-55.

270. Sauvageau G, Iscove NN, Humphries RK. In vitro and in vivo expansion of hematopoietic stem cells. Oncogene. 2004;23(43):7223-32.

271. Cicuttini FM, Begley CG, Boyd AW. The effect of recombinant stem cell factor (SCF) on purified CD34-positive human umbilical cord blood progenitor cells. Growth factors. 1992;6(1):31-9.

272. Murray LJ, Young JC, Osborne LJ, Luens KM, Scollay R, Hill BL. Thrombopoietin, flt3, and kit ligands together suppress apoptosis of human mobilized CD34+ cells and recruit primitive CD34+ Thy-1+ cells into rapid division. Exp Hematol. 1999;27(6):1019-28.

273. Williams DE, de Vries P, Namen AE, Widmer MB, Lyman SD. The Steel factor. Developmental biology. 1992;151(2):368-76.

274. Matthews W, Jordan CT, Wiegand GW, Pardoll D, Lemischka IR. A receptor tyrosine kinase specific to hematopoietic stem and progenitor cell-enriched populations. Cell. 1991;65(7):1143-52.

275. Young JC, Bruno E, Luens KM, Wu S, Backer M, Murray LJ. Thrombopoietin stimulates megakaryocytopoiesis, myelopoiesis, and expansion of CD34+ progenitor cells from single CD34+Thy-1+Lin- primitive progenitor cells. Blood. 1996;88(5):1619-31.

276. Kobayashi M, Laver JH, Kato T, Miyazaki H, Ogawa M. Thrombopoietin supports proliferation of human primitive hematopoietic cells in synergy with steel factor and/or interleukin-3. Blood. 1996;88(2):429-36.

277. Ebihara Y, Tsuji K, Lyman SD, Sui X, Yoshida M, Muraoka K et al. Synergistic action of Flt3 and gp130 signalings in human hematopoiesis. Blood. 1997;90(11):4363-8.

278. Sui X, Tsuji K, Tanaka R, Tajima S, Muraoka K, Ebihara Y et al. gp130 and c-Kit signalings synergize for ex vivo expansion of human primitive hemopoietic progenitor cells. Proc Natl Acad Sci U S A. 1995;92(7):2859-63.

279. Ueda T, Tsuji K, Yoshino H, Ebihara Y, Yagasaki H, Hisakawa H et al. Expansion of human NOD/SCID-repopulating cells by stem cell factor, Flk2/Flt3 ligand, thrombopoietin, IL-6, and soluble IL-6 receptor. The Journal of clinical investigation. 2000;105(7):1013-21.

280. Bhatia M, Bonnet D, Kapp U, Wang JC, Murdoch B, Dick JE. Quantitative analysis reveals expansion of human hematopoietic repopulating cells after short-term ex vivo culture. The Journal of experimental medicine. 1997;186(4):619-24.

281. Piacibello W, Sanavio F, Severino A, Dane A, Gammaitoni L, Fagioli F et al. Engraftment in nonobese diabetic severe combined immunodeficient mice of human CD34(+) cord blood cells after ex vivo expansion: evidence for the amplification and self-renewal of repopulating stem cells. Blood. 1999;93(11):3736-49.

282. Knapp DJ, Hammond CA, Miller PH, Rabu GM, Beer PA, Ricicova M et al. Dissociation of Survival, Proliferation, and State Control in Human Hematopoietic Stem Cells. Stem cell reports. 2017;8(1):152-62.

283. Shpall EJ, Quinones R, Giller R, Zeng C, Baron AE, Jones RB et al. Transplantation of ex vivo expanded cord blood. Biology of blood and marrow transplantation : journal of the American Society for Blood and Marrow Transplantation. 2002;8(7):368-76.

284. Bhatia M, Bonnet D, Wu D, Murdoch B, Wrana J, Gallacher L et al. Bone morphogenetic proteins regulate the developmental program of human hematopoietic stem cells. The Journal of experimental medicine. 1999;189(7):1139-48.

285. Zhang Y, Gao Y. Novel chemical attempts at ex vivo hematopoietic stem cell expansion. International Journal of Hematology. 2016;103(5):519-29.

286. Boitano AE, Wang J, Romeo R, Bouchez LC, Parker AE, Sutton SE et al. Aryl hydrocarbon receptor antagonists promote the expansion of human hematopoietic stem cells. Science (New York, NY). 2010;329(5997):1345-8.

287. Singh KP, Casado FL, Opanashuk LA, Gasiewicz TA. The aryl hydrocarbon receptor has a normal function in the regulation of hematopoietic and other stem/progenitor cell populations. Biochemical pharmacology. 2009;77(4):577-87.

288. Fares I, Chagraoui J, Gareau Y, Gingras S, Ruel R, Mayotte N et al. Cord blood expansion. Pyrimidoindole derivatives are agonists of human hematopoietic stem cell self-renewal. Science (New York, NY). 2014;345(6203):1509-12.

289. Cohen S, Roy J, Lachance S, Marinier A, Barabé F, Delisle J-S et al. Single UM171 Expanded Cord Blood Transplant is Feasible, Safe, and Permits Transplantation of Better HLA Matched Cords with Very Low Transplant Related Mortality. Biology of Blood and Marrow Transplantation. 2018;24(3):S190-S1.

290. Hoggatt J, Singh P, Sampath J, Pelus LM. Prostaglandin E2 enhances hematopoietic stem cell homing, survival, and proliferation. Blood. 2009;113(22):5444-55.

291. Goessling W, Allen RS, Guan X, Jin P, Uchida N, Dovey M et al. Prostaglandin E2 enhances human cord blood stem cell xenotransplants and shows long-term safety in preclinical nonhuman primate transplant models. Cell Stem Cell. 2011;8(4):445-58.

292. Cutler C, Multani P, Robbins D, Kim HT, Le T, Hoggatt J et al. Prostaglandin-modulated umbilical cord blood hematopoietic stem cell transplantation. Blood. 2013;122(17):3074-81.

293. Weidner CI, Walenda T, Lin Q, Wölfler MM, Denecke B, Costa IG et al. Hematopoietic stem and progenitor cells acquire distinct DNA-hypermethylation during in vitro culture. Scientific reports. 2013;3:3372-.

294. Chaurasia P, Gajzer DC, Schaniel C, D'Souza S, Hoffman R. Epigenetic reprogramming induces the expansion of cord blood stem cells. The Journal of clinical investigation. 2014;124(6):2378-95.

295. Araki H, Yoshinaga K, Boccuni P, Zhao Y, Hoffman R, Mahmud N. Chromatin-modifying agents permit human hematopoietic stem cells to undergo multiple cell divisions while retaining their repopulating potential. Blood. 2007;109(8):3570-8.

296. Peled T, Shoham H, Aschengrau D, Yackoubov D, Frei G, Rosenheimer GN et al. Nicotinamide, a SIRT1 inhibitor, inhibits differentiation and facilitates expansion of hematopoietic progenitor cells with enhanced bone marrow homing and engraftment. Exp Hematol. 2012;40(4):342-55 e1.

297. Horwitz ME, Wease S, Blackwell B, Valcarcel D, Frassoni F, Boelens JJ et al. Phase I/II Study of Stem-Cell Transplantation Using a Single Cord Blood Unit Expanded Ex Vivo With Nicotinamide. Journal of clinical oncology : official journal of the American Society of Clinical Oncology. 2019;37(5):367-74.

298. Wagner W, Roderburg C, Wein F, Diehlmann A, Frankhauser M, Schubert R et al. Molecular and secretory profiles of human mesenchymal stromal cells and their abilities to maintain primitive hematopoietic progenitors. Stem cells. 2007;25(10):2638-47.

299. Andrade PZ, Santos Fd, Cabral JMS, da Silva CL. Stem cell bioengineering strategies to widen the therapeutic applications of haematopoietic stem/progenitor cells from umbilical cord blood. Journal of Tissue Engineering and Regenerative Medicine. 2015;9(9):988-1003.

300. Pineault N, Abu-Khader A. Advances in umbilical cord blood stem cell expansion and clinical translation. Exp Hematol. 2015;43(7):498-513.

301. Wagner W, Wein F, Roderburg C, Saffrich R, Faber A, Krause U et al. Adhesion of hematopoietic progenitor cells to human mesenchymal stem cells as a model for cell−cell interaction. Experimental Hematology. 2007;35(2):314-25.

302. Alakel N, Jing D, Muller K, Bornhauser M, Ehninger G, Ordemann R. Direct contact with mesenchymal stromal cells affects migratory behavior and gene expression profile of CD133+ hematopoietic stem cells during ex vivo expansion. Exp Hematol. 2009;37(4):504-13.

303. Alakel N, Jing D, Bornhaeuser M, Ehninger G, Ordemann R. CD133⁺ Purified Hematopoietic Stem Cells in Co-Culture with Mesenchymal Stromal Cells - The Cell to Cell Contact Matters. Blood. 2007;110(11):1421.

304. da Silva CL, Goncalves R, dos Santos F, Andrade PZ, Almeida-Porada G, Cabral JM. Dynamic cell-cell interactions between cord blood haematopoietic progenitors and the cellular niche are essential for the expansion of CD34+, CD34+CD38- and early lymphoid CD7+ cells. J Tissue Eng Regen Med. 2010;4(2):149-58.

305. Van Overstraeten-Schlogel N, Beguin Y, Gothot A. Role of stromal-derived factor-1 in the hematopoietic-supporting activity of human mesenchymal stem cells. European journal of haematology. 2006;76(6):488-93.

306. Lu LL, Liu YJ, Yang SG, Zhao QJ, Wang X, Gong W et al. Isolation and characterization of human umbilical cord mesenchymal stem cells with hematopoiesis-supportive function and other potentials. Haematologica. 2006;91(8):1017.

307. Corre J, Barreau C, Cousin B, Chavoin JP, Caton D, Fournial G et al. Human subcutaneous adipose cells support complete differentiation but not self-renewal of hematopoietic progenitors. Journal of cellular physiology. 2006;208(2):282-8.

308. Magin AS, Korfer NR, Partenheimer H, Lange C, Zander A, Noll T. Primary cells as feeder cells for coculture expansion of human hematopoietic stem cells from umbilical cord blood--a comparative study. Stem Cells Dev. 2009;18(1):173-86.

309. Koh SH, Choi HS, Park ES, Kang HJ, Ahn HS, Shin HY. Co-culture of human CD34+ cells with mesenchymal stem cells increases the survival of CD34+ cells against the 5-aza-deoxycytidine- or trichostatin A-induced cell death. Biochemical and biophysical research communications. 2005;329(3):1039-45.

310. Khoury M, Drake A, Chen Q, Dong D, Leskov I, Fragoso MF et al. Mesenchymal stem cells secreting angiopoietin-like-5 support efficient expansion of human hematopoietic stem cells without compromising their repopulating potential. Stem Cells Dev. 2011;20(8):1371-81.

311. Ferreira MS, Jahnen-Dechent W, Labude N, Bovi M, Hieronymus T, Zenke M et al. Cord blood-hematopoietic stem cell expansion in 3D fibrin scaffolds with stromal support. Biomaterials. 2012;33(29):6987-97.

312. Raic A, Rödling L, Kalbacher H, Lee-Thedieck C. Biomimetic macroporous PEG hydrogels as 3D scaffolds for the multiplication of human hematopoietic stem and progenitor cells. Biomaterials. 2014;35(3):929-40.

313. McNiece I, Harrington J, Turney J, Kellner J, Shpall EJ. Ex vivo expansion of cord blood mononuclear cells on mesenchymal stem cells. Cytotherapy. 2004;6(4):311-7.

314. Delalat B, Pourfathollah AA, Soleimani M, Mozdarani H, Ghaemi SR, Movassaghpour AA et al. Isolation and ex vivo expansion of human umbilical cord blood-derived CD34+ stem cells and their cotransplantation with or without mesenchymal stem cells. Hematology. 2009;14(3):125-32.

315. Han JY, Goh RY, Seo SY, Hwang TH, Kwon HC, Kim SH et al. Cotransplantation of cord blood hematopoietic stem cells and culture-expanded and GM-CSF-/SCF-transfected mesenchymal stem cells in SCID mice. Journal of Korean medical science. 2007;22(2):242-7.

316. de Lima M, McNiece I, Robinson SN, Munsell M, Eapen M, Horowitz M et al. Cord-blood engraftment with ex vivo mesenchymal-cell coculture. The New England journal of medicine. 2012;367(24):2305-15.

317. Lo Iacono M, Anzalone R, La Rocca G, Baiamonte E, Maggio A, Acuto S. Wharton's Jelly Mesenchymal Stromal Cells as a Feeder Layer for the Ex Vivo Expansion of Hematopoietic Stem and Progenitor Cells: a Review. Stem Cell Reviews and Reports. 2017;13(1):35-49.

318. Karanu FN, Murdoch B, Miyabayashi T, Ohno M, Koremoto M, Gallacher L et al. Human homologues of Delta-1 and Delta-4 function as mitogenic regulators of primitive human hematopoietic cells. Blood. 2001;97(7):1960-7.

319. Varnum-Finney B, Wu L, Yu M, Brashem-Stein C, Staats S, Flowers D et al. Immobilization of Notch ligand, Delta-1, is required for induction of notch signaling. J Cell Sci. 2000;113 Pt 23:4313-8.

320. Jaleco AC, Neves H, Hooijberg E, Gameiro P, Clode N, Haury M et al. Differential effects of Notch ligands Delta-1 and Jagged-1 in human lymphoid differentiation. J Exp Med. 2001;194(7):991-1002.

321. Lahmar M, Catelain C, Poirault S, Dorsch M, Villeval JL, Vainchenker W et al. Distinct effects of the soluble versus membrane-bound forms of the notch ligand delta-4 on human CD34+CD38low cell expansion and differentiation. Stem cells. 2008;26(3):621-9.

322. Delaney C, Varnum-Finney B, Aoyama K, Brashem-Stein C, Bernstein ID. Dose-dependent effects of the Notch ligand Delta1 on ex vivo differentiation and in vivo marrow repopulating ability of cord blood cells. Blood. 2005;106(8):2693-9.

323. Delaney C, Heimfeld S, Brashem-Stein C, Voorhies H, Manger RL, Bernstein ID. Notch-mediated expansion of human cord blood progenitor cells capable of rapid myeloid reconstitution. Nature medicine. 2010;16(2):232-6.

324. Dahlberg A, Brashem-Stein C, Delaney C, Bernstein ID. Enhanced generation of cord blood hematopoietic stem and progenitor cells by culture with StemRegenin1 and Delta1(Ext-IgG.). Leukemia. 2014;28(10):2097-101.

325. Fernandez-Sanchez V, Pelayo R, Flores-Guzman P, Flores-Figueroa E, Villanueva-Toledo J, Garrido E et al. In vitro effects of stromal cells expressing different levels of Jagged-1 and Delta-1 on the growth of primitive and intermediate CD34(+) cell subsets from human cord blood. Blood cells, molecules & diseases. 2011;47(4):205-13.

326. Catelain C, Michelet F, Hattabi A, Poirault-Chassac S, Kortulewski T, Tronik-Le Roux D et al. The Notch Delta-4 ligand helps to maintain the quiescence and the short-term reconstitutive potential of haematopoietic progenitor cells through activation of a key gene network. Stem cell research. 2014;13(3 Pt A):431-41.

327. Lampreia FP, Carmelo JG, Anjos-Afonso F. Notch Signaling in the Regulation of Hematopoietic Stem Cell. Current stem cell reports. 2017;3(3):202-9.

CHAPTER II

MATERIALS AND METHODS

II.1. CELL CULTURE

All cell culture work was performed under aseptic conditions in a Safe 2020 Class II Biological Safety Cabinet (Thermo Fisher Scientific, Waltham, MA, USA) with sterile materials. All cells were incubated at 37ºC, 5% CO_2 and under normoxia in a humidified incubator HeraCell 150 (Thermo Fisher Scientific). Centrifugation of cell suspensions were performed in a Beckman Allegra 6R (Beckman Coulter, Brea, CA, USA). All plasticware and tissue culture vessels were purchased from Greiner Bio-One (Stonehouse, UK) and VWR International (Radnor, PA, USA).

II.1.1. CELL LINES

Adherent cells

HEK293T, Lenti-X 293T, HeLa and Saos-2 cell lines were cultured in high glucose Dulbecco's Modified Eagle's Medium (DMEM; Merck KGaA, Darmstadt, Germany) supplemented with 10% inactivated foetal bovine serum (FBS, Life Science Group Ltd., UK), 1% GlutaMAX™ (Thermo Fisher Scientific) and 1% Penicillin-Streptomycin (P/S, 10000 U/mL, Thermo Fisher Scientific), herein termed as "complete DMEM". CHO and MS-5 cell lines were cultured in Iscove's Modified Dulbecco's Medium (IMDM, Thermo Fisher Scientific) supplemented with 10% FBS and 1% P/S – "complete IMDM". S17 stromal lines were cultured in αMEM with nucleosides and GlutaMAX™ (Thermo Fisher Scientific) supplemented with 10% FBS and 1% P/S – "complete αMEM". All the S17 stromal cell lines were kindly provided by Dr. Evelyne Lauret (University of Paris). Briefly, S17-Dll1, S17-Dll4 and S17-Jag1 cells were retrovirally transduced to overexpress the full length of human Delta1, Delta4 and Jagged1 respectively and vectors carry puromycin resistant gene for selection. All the other cell lines were provided by the cell services of Cancer Research UK – London Research Institute.

All adherent cells were split every 3-4 days (or when reaching 70-80% confluence) by trypsinisation. All cell lines, except HEK293T, were rinsed first with phosphate buffered

saline (PBS, Merck). For enzymatic cell detachment, 0.05% Trypsin-EDTA (Thermo Fisher Scientific) was added to cover the cell culture surface, incubating at 37ºC untill all cells were detached (for 3-7 min). Trypsin was inactivated by adding complete medium (twice the volume of trypsin) and cell suspension was transferred to Falcon tubes. Cells were centrifuged at 300× *g* for 5 min, resuspended in complete medium and replated at aproprate dilution. HEK293T and HeLa cells were generally split 1:8-1:10, Saos-2 cells were split 1:3-1:4 and CHO and MS-5 cells were split 1:4-1:6. All S17 cell lines were split 1:4 every 3 days.

All cell lines, with exception of MS-5 and S17 cells, were used for experiments 3 passages after thawing and kept in culture for a maximum of 6 weeks. MS-5 and S17 cells were used between 3 to 6 passages after thawing.

Suspension cells

K562, Molt4, Jurkat, Raji and U266 cell lines were cultured in RPMI (Roswell Park Memorial Institute) -1640 Medium (Merck) supplemented with 10% FBS and 1% P/S – “complete RPMI”. OCI-AML3 cells were cultured in IMDM supplemented with 20% FBS and 1% P/S – “IMDM20%”. Suspension cells were generally split to an initial cell density of 2.5-3×10^5 cells/mL every 3-4 days. All cell lines were provided by the cell services of Cancer Research UK – London Research Institute.

I.1.1. THAWING AND CRYOPRESERVATION

Cells were thawed in a 37ºC water bath and transferred dropwise to a 15 mL tube with the respective culture medium. Cell suspensions were centrifuged at 300× *g* for 5 min, resuspended in the respective culture medium as described and plated at apropriate density. Cells were counted using a hemocytometer and trypan blue exclusion method. Adherent cells were plated on tissue culture-treated surfaces at densities around 1.5-2.5 × 10^4 cells/cm^2 and split upon reaching 70-80% confluence as described. Suspension cells were plated on tissue culture-treated wells or flasks in vertical position at densities around 1-2×10^6 cells/mL and split after 2 days.

For cell cryopreservation, cells were frozen in the respective culture medium with 10% DMSO (dimethyl sulfoxide, Thermo Fisher Scientific) by adding an equal part of cold medium with 20% DMSO to the resuspended cells and transferring 1 mL per cryovial. Adherent cells were frozen at cell densities between 2-5×10^6 cells/mL and suspension cells at 8-10×10^6 cells/mL. Cryovials were placed at -80ºC in a CoolCell™ Container (Corning Inc., Corning, NYS, USA) or a Cryo Cooler® (VWR International) to allow freezing at -1ºC/min. In the following days cryovials were trasferred to liquid nitrogen storage.

I.1.2. CELL TREATMENTS

I.1.2.1. EDTA TREATMENT – NOTCH ACTIVATION

Molt4, Raji and Jurkat cells from ongoing cultures were plated at 1×10^6 cells/mL in fresh culture medium supplemented with EDTA (ethylenediaminetetraacetic acid, Merck) to 5 mM and incubated at 37ºC for 15 min. Cells were centrifuged as described and resuspended again in fresh medium at 1×10^6 cells/mL and incubated at 37ºC for further 45 min. After this period, cells were collected and proceeded to intracellular staining or protein extraction.

I.1.2.2. COMPOUND E TREATMENT – NOTCH BLOCKAGE

HeLa and Saos-2 cell lines were plated to 50-60% cell confluence and in the following day the culture medium was replaced by fresh medium supplemented with Compound E (Gamma Secretase Inhibitor XXI, Merck) to 2 µM. Cells were incubated at 37ºC for 36-48h and then collected by trypsinisation with 0.5% trypsin without EDTA (Thermo Fisher Scientific) to proceed to intracellular staining or protein extraction.

II.2. MOLECULAR BIOLOGY

All cell suspensions or protein samples were centrifuged in a Heraeus™ Fresco™ 21 Microcentrifuge (Thermo Fisher Scientific) or in a Beckman Allegra 6R (Beckman Coulter).

II.2.1. CLONING OF LENTIVIRAL VECTORS

All plasmids and primers used in the following cloning methods are listed in **Table II.1** and **Table II.2** (**Appendix I**), respectively. A list of the primers used for DNA sequencing can be found in **Table II.3**. All primers were purchased from Merck as lyophilised custom DNA oligos with desalt purification and were subsequently resuspended in nuclease-free (NF)-H_2O (Thermo Fisher Scientific) to a concentration of 100 µM. Primers design was based on melting temperatures and other properties (secondary structure, primer dimer) estimated by Sigma-Aldrich® OligoEvaluator™.

Please refer to **Table II.4** for the list of reagents/kits used in the referred cloning techniques; unless otherwise stated, all procedures were carried out according to manufacturer's instructions.

All centrifugations were performed in a Heraeus™ Fresco™ 21 Microcentrifuge (Thermo Fisher Scientific) or a Heraeus™ Megafuge™ 40R (Thermo Fisher Scientific). Gel electrophoresis was performed with PowerPac™ Basic (Biorad Laboratories, Hercules, CA, USA) power supply, Green Range horizontal tanks (Scie-Plas Lda., Cambridge, UK) and homemade TAE (tris-acetate-EDTA) buffer (**Appendix IV**).

II.2.1.1. CONSTITUTIVE MIR30SHRNA LENTIVECTOR

The lentiviral vector pLV.EF1α-miR30shRNA-GFP for constitutive expression of miR30shRNA with a GFP reporter was generated based on the vector pLV.EF1α-

premiRNA30a-rPuro. This vector contains an EF1α promoter and intron with the mir30a precursor sequence inside the intron, followed by the gene for red fluorescent puromycin-N-acetyl-transferase.

To obtain the GFP reporter, an EGFP (enhanced GFP) gene was amplified by polymerase chain reaction (PCR) from an in-house vector (pSIN.Tet-HPGK-rtTA2-hDKK-Ires-GFP) using the "GFP" primers to insert the restriction sites (RS) *XbaI* and *SalI*. PCR amplification was performed with HotstarTaq (Qiagen, Germantown, MD, USA) with an annealing temperature (T_a) of 70°C and the final product was cleaned up by gel electrophoresis in a 1% UltraPure Agarose (Thermo Fisher Scientific) gel, from which the product with the expected size was excised from the gel on an UV transilluminator. DNA was extracted from the gel and then digested with *XbaI* and *SalI* restriction enzymes (RE) followed by heat inactivation (all RE were from New England Biolabs, Ipswich, MA, USA). The pLV vector was also digested with *XbaI* and *SalI* RE, followed by dephosphorylation. The linearised vector was then separated by gel electrophoresis after which the respective product was excised, and the DNA extracted from the gel. Quantification of DNA and quality check were performed in a NanoDrop™ 2000 spectrophotometer (Thermo Fisher Scientific). The GFP insert was then ligated to the linear pLV vector with compatible cohesive ends at a ratio of 3:1. The ligation product and a negative control (with NF-H_2O as insert) were transformed in NEB® Stable (New England Biolabs) competent bacteria which were then plated in Lennox broth (LB) agar (Thermo Fisher Scientific) plates with ampicillin (100 µg/L, Merck). Several colonies were picked for screening according to the number of colonies in the negative control. Colonies were grown overnight in 5 mL of LB medium (Merck) for plasmid minipreps. Analytic digestions with *XbaI* and *SalI* RE were performed to confirm if a DNA fragment with the size of the GFP insert was detected after gel electrophoresis. Positive vectors were sent for sequencing at Eurofins Genomics (Ebersberg, Germany) with the primer "Seq gfp fwd" to confirm the presence of correct GFP sequence without any mutations.

Once the GFP sequence was confirmed, the next step consisted in replacing the miR30 precursor sequence by a mir30shRNA sequence. The mir30 backbone used for shRNA integration was obtained from a Dharmacon™ pGIPZ™ vector. The design of shRNA oligos and cloning inside the backbone is described below in section **II.2.1.3**.

II.2.1.2. INDUCIBLE TET-ON miR30shRNA LENTIVECTOR

The inducible vector pLV.TetSyntP-miR30shRNA-GFP was generated by adding and substituting the necessary components to the constitutive vector pLV.EF1α-miR30shRNA-GFP.

Firstly, the mCherry reporter was amplified from the pmCherry vector with the primers "mCherry" (T_a of 66°C) adding the cloning sites *ApaI* and *SalI*. The PCR product was cleaned up as previously described and digested with enzymes *ApaI* and *SalI* in a sequential digestion as recommended in NEBcloner® since these enzymes are incompatible; enzymes were heat inactivated also as recommended. The mCherry gene was inserted into the vector pRRL.SFFV-d20GFP-T2A-mBFP containing the spleen focus-forming virus (SFFV) promoter driving the expression of two sequences separated by the sequence that encodes for the self-cleaving peptide T2A. This vector was digested likewise with *ApaI* and *SalI* RE, dephosphorylated and purified for ligation to generate the vector pRRL.SFFV-d20GFP-T2A-mCherry. After transformation, several colonies were picked for colony PCR with the "mCherry" primers to confirm the presence of the mCherry gene. Colony PCR was performed by picking a colony and mix it in 10 µL of NF-H_2O from which 1 µL was used as template in the PCR reaction. Colonies that showed a PCR product with the size of the mCherry insert were used for minipreps of the vector pRRL.SFFV-d20GFP-T2A-mCherry.

The rtTA3 (reverse tetracycline responsive transactivator 3) gene was amplified from the pINDUCER21 (ORF-EG) vector with the primers "rtTA3" (Ta of 62°C) adding the cloning sites *XhoI* and *BmgBI* and part of the T2A sequence in the 3' end. The PCR product was cleaned up and digested with enzymes *XhoI* and *BmgBI* followed by heat inactivation. The rtTA3 gene was inserted into the intermediate vector pRRL.SFFV-d20GFP-T2A-mCherry which was digested likewise with *XhoI* and *BmgBI* RE, dephosphorylated and purified for ligation to generate the vector pRRL.SFFV-rtTA3-T2A-mCherry. After transformation, several colonies were picked for minipreps and the rtTA3 insert was confirmed by analytic digestion with *NdeI* (cuts inside rtTA3) and *XhoI* RE. The sequence of the SFFV-rtTA3-T2-mCherry cassette was confirmed by sequencing using the four primers listed in **Table II.3**.

After sequence confirmation, the cassette was amplified by PCR using the High Fidelity PCR Master (Roche, Basel, Switzerland) with the primers "Cassette" (T_a of

56°C) to insert the cloning sites *MluI* and *SalI*. The PCR product was cleaned up and digested with enzymes *MluI* and *SalI* followed by heat inactivation. The constitutive vector pLV.EF1α-miR30shRNA-GFP was then digested with *MluI* and *SalI* RE, dephosphorylated and purified for ligation to generate the vector pLV.EF1α-miR30shRNA-GFP-SFFV-rtTA3-(T2A)-mCherry. After transformation, several colonies were picked for minipreps and the cassette insert was confirmed by analytic digestion with *NdeI* (cuts inside rtTA3) and *BamHI* (cuts inside miR30) RE. In the positive minipreps the cassette sequence was again confirmed by sequencing using the four primers listed in **Table II.3**.

The last step was to replace the EF1α promoter by the inducible promoter TetSyntP (commercially known as TRE3G promoter) but maintaining the EF1α intron. The inducible promoter was obtained from the vector pTRE3G-mCherry first by cloning part of the intron in front of the TRE3G promoter in this vector to originate the vector pTRE3G-EF1intron. For this, a portion of the EF1α intron sequence from the vector pLV.EF1α-miR30shRNA-GFP was amplified by PCR using the primers "EF1intron" (T_a of 52°C) to insert a *SalI* RS in 5' end and maintaining the *BamHI* RS in the 3' end. The pTRE3G-mCherry vector and the PCR product were digested with *SalI* and *BamHI* RE and processed for ligation. The ligation product was transformed in One Shot™ TOP10 (Thermo Fisher Scientific) bacteria and several colonies were picked for minipreps. Successful ligation was verified by digestion with *SalI* and *BamHI* RS. The following step was to amplify the inducible promoter from the pTRE3G-EF1intron vector by introducing a *ClaI* RS in the 5' end using the primers "TRE3G" (T_a of 47°C) in order to be able to clone into the vector pLV.EF1α-miR30shRNA-GFP-SFFV-rtTA3-mCherry. Because the forward primer has multiple annealing sites that could not be avoided in primer design, the PCR product was purified in a 1.2% agarose gel and ran for longer time to excise the higher size PCR product. The purified DNA was then single digested with *ClaI* RE since the 3' end also contains a *ClaI* RS from the original sequence. The pLV vector was linearised also by single digestion with *ClaI* RE (cuts just upstream the EF1α promoter) and the ligation product was transformed in NEB® Stable bacteria. Because only one cloning site was used, ligation of the insert can occur in two orientations. Thus, analytic digestion with *ClaI* and *BamHI* was used to identify the minipreps with the correct sequence, since the *ClaI* site in the 5' end of the promoter becomes methylated. Then, the initial sequence of the intron in the pTRE3G-

EF1intron vector was cloned in the pLV vector downstream of the inducible promoter using the cloning sites *ClaI* and *BamHI*. Both vectors were digested with these enzymes and the fragments of interest were extracted after gel electrophoresis. The ligation product was transformed in NEB® Stable bacteria originating the final inducible vector pLV.TetSyntP-miR30shRNA-GFP-SFFV-rtTA3-mCherry. The inducible promoter and EF1α intron sequences were confirmed by sequencing with the primers "Seq fwd Teto", "Seq fwd SyntP" and "Seq rev SHMIR30 EF1".

For final quality control of the selected clone, all the elements cloned were verified by sequencing using all the sequencing primers mentioned above. The final vector and all the intermediate vectors were stored in bacterial glycerol stocks.

II.2.1.3. CLONING OF *NOTCH1* AND *NOTCH2* MIR30SHRNAS

Sequence Selection and Design

Several shRNA sequences were selected for human *NOTCH1* (*N1*) and *NOTCH2* (*N2*) receptors and cloned into the constitutive pLV vector for knockdown validation.

Initially, four target sequences were selected for each receptor from the options commercially available from Dharmacon™ pGIPZ lentivectors (Horizon Discovery Group plc, Cambridge, UK) and by selecting the sequences with less to no complementarity to other potential targets. These shRNA sequences were designed based on algorithms taking in consideration rules for efficient processing of miR30 backbone.

The selected target sequences with 19 nucleotides were then used to design oligos following the rules for miR30shRNA structure. First, nucleotides -1 upstream and +1 downstream the target mRNA sequence were added to the sense sequence and the complementary bases were added to the antisense sequence. For example, as can be seen in the sequence blast shown in **Figure II.1**, the sense sequence becomes 5'-**G**GAGCACCTGTGAGAGGAAT**A**-3' and the antisense sequences is 5'-**T**ATTCCTCTCACAGGTGCTC**C**-3'. Then, the nucleotide at position -2 the sense sequence is used to create a mismatch nucleotide C or A in the position +21 of the antisense sequence. In the given example the position -2 of the target sequence is a G which means the position +21 of the antisense sequence needs to be a C (5'-

TATTCCTCTCACAGGTGCTC**CC**-3') and the position -2 of the sense is an A (5'-**AG**GAGCACCTGTGAGAGGAAT**A**-3'). These sense and antisense sequences were integrated in the miR30 backbone including a loop sequence in between (5'mir30-sense-loop-antisense-3'mir30) based on the pGIPZ™ sequence design. Forward and reverse oligos are shown in **Table II.5** (**Appendix I**), synthesised ready to ligate with the cloning sites *XhoI* and *EcoRI* as described bellow.

Upon the initial testing of four shRNA sequences for each Notch receptor it was necessary to select more sequences to achieve more potent knockdowns. Additional sequences were chosen from Dharmacon™ pGIPZ selection, MISSION® shRNA Library (Merck) and published data. In total, ten shRNA sequences were tested for *N1* and six for *N2* to identify at least two shRNAs for each receptor that allowed consistent knockdowns above 60% in cell lines. The best shRNA sequences identified for *N1* (N1.1, N1.2 and N1.3) and *N2* (N2.2 and N2.2) can be found in **Table II.5**, as well as the *Luciferase* shRNA used as non-target control.

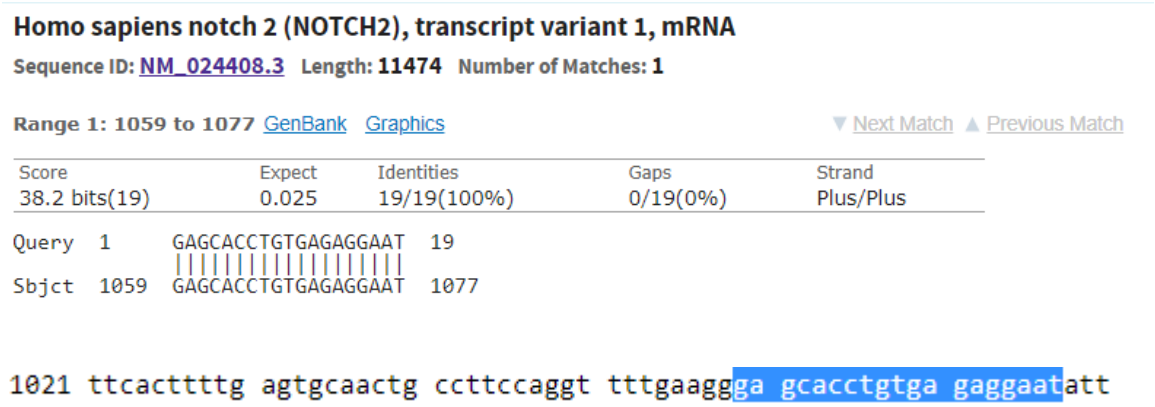

Figure II.1 – Standard Nucleotide BLAST® (National Center for Biotechnology Information database) of a *NOTCH2* shRNA sense sequence and localisation in the target sequence.

Cloning into mir30 backbone

Phosphorylated oligos with *XhoI* 5' overhang and *EcoRI* 3' overhang were purchased from Merck and resuspended in NF-H_2O to 1 mM. For the annealing reaction, 2 µL of each oligo were added to 48 µL of annealing buffer (**Appendix IV**) and incubated at 95°C for 4 min followed by 70°C for 10 min and allowed to cool down at room temperature (RT) for 30min. Annealed oligos were diluted 1:10 in NF-H_2O prior to

ligation. Because the cloning sites *XhoI* and *EcoRI* inside the miR30 backbone are not single restrictions sites in the pGIPZ vector or in the developed pLV vectors, the mir30shRNA sequence from the pGIPZ vector was first cloned into an intermediate vector (pECFP-C1) that does not contain *XhoI* and *EcoRI* RS that can interfere with the cloning strategy. For this, the miR30shRNA sequence was amplified by PCR with HotstarTaq using the primers "miR30shrRNA" (T_a of 56°C) to insert the *BamHI* and *NheI* cloning sites. The PCR product was cleaned up and digested with the *BamHI* and *NheI* RE which were then inactivated by ethanol precipitation of the DNA overnight. The pECFP-C1 vector was digested with *BamHI* and *NheI* RE, dephosphorylated and purified. Transformation of the ligation product was performed in One Shot™ TOP10 bacteria with kanamycin (Merck) selection plates (50 µg/L). Several colonies were picked for minipreps which were verified by sequencing with the primer "Seq fwd SHMIR30 pECFP". Once confirmed, the miR30shRNA sequence in the pECFP-miR30shRNA, the vector was digested with *XhoI* and *EcoRI* RE to insert the desired shRNA oligo. Transformation of the ligation product was performed in One Shot™ TOP10 bacteria with kanamycin selection plates and several colonies were verified by sequencing with the primer "Seq fwd SHMIR30 pECFP".

Upon sequence confirmation, the whole miR30shRNA sequence was cloned in the pLV vector using the *BamHI* and *NheI* cloning sites to replace the original miR30 precursor. Both the pECFP-miR30shRNA and the pLV vector were digested with *BamHI* and *NheI* and the fragments of interest were extracted after gel electrophoresis. The ligation product was transformed in NEB® Stable bacteria as previously described. The miR30shRNA sequence in the pLV vector was confirmed by sequencing with the primer "Seq rev SHMIR30 EF1". A positive clone for each shRNA was stored in a bacterial glycerol stock and used for endotoxin-free maxiprep for lentivirus production.

II.2.1.4. CLONING OF *NOTCH1* AND *NOTCH2* SHRNAS INTO A CONSTITUTIVE H1-SHRNA LENTIVECTOR

The lentiviral vector CS-RfA-EF from Riken (Wako, Saitama, Japan) was used for the expression of *N1* and *N2* shRNAs under an H1 promoter. This vector also contains a GFP reporter that is driven by an EF1α promoter. Company's instructions were

followed to design the shRNA oligos for cloning in the pEntr4-H1 vector that allows cloning into the CS-RfA-EF vector through Gateway® recombination.

Sequence Selection and Design

shRNA sequences used in this vector were first selected based on the sequences previously validated with the mir30shRNA system, adjusting the sequence according to Riken recommendations. Sense sequences starting with a C or T were altered to start with an A or G (preferably A) by shifting the target sequence one or two nucleotides. The oligos were designed with a *BglII* 5' overhang and a *XbaI* 3' overhang and with the loop sequence 5'-TTCAAGAGA-3' between the sense and anti-sense sequences. Phosphorylated oligos were purchased from Merck and annealed as previously described. An additional *N1* shRNA (N1.4) had to be selected to achieve higher knockdown than the ones obtained with sequences N1.1 and N1.3. The final shRNA sequences that promoted very efficient knockdowns can be found in the oligos listed in **Table II.6**.

Cloning into H1 Lentivector

The pEntr4-H1 vector was linearised by digestion with *BglII* and *XbaI* RE, dephosphorylated and purified after gel electrophoresis. Ligation to the shRNA oligo was performed followed by transformation in One Shot™ TOP10 bacteria with kanamycin selection plates. Several colonies were picked for minipreps and successful ligation was verified by digestion with *EcoRI* and *PstI* RE. The shRNA sequence in the positive clones was then verified by sequencing with the primer "pH1up2seq".

Once cloned, the pEntr4-H1-shRNA vectors, the H1-shRNA sequences were transferred to the destination vector CS-RfA-EG trough a Gateway® LR reaction. Reactions were incubated for at least 6 h due to the large size of the destination vector and transformed in One Shot™ TOP10 bacteria with ampicillin selection plates. Several colonies were picked for minipreps and shRNA sequences were confirmed once more by sequencing with the primer "pH1up2seq".

A positive clone for each shRNA was stored in a bacterial glycerol stock and used for endotoxin-free maxiprep for lentivirus production.

II.2.1.5. INDUCIBLE TET-ON miR30shRNA LENTIVECTORS – PGK AND UBC PROMOTERS

Two additional lentivectors for inducible expression of miR30shRNA were developed to replace the constitutive SFFV promoter in the pLV.TetSyntP-miR30shRNA-GFP-SFFV-rtTA3-mCherry vector. These were the human PGK (phosphoglycerate kinase) and the human UBC (ubiquitin C) promoters, generating the vectors pLV.TetSyntP-miR30shRNA-GFP-PGK-rtTA3-mCherry and pLV.TetSyntP-miR30shRNA-GFP-UBC-rtTA3-mCherry.

The two new promoters had to be first cloned in the intermediate vector pRRL.SFFV-rtTA3-T2A-mCherry, replacing the SFFV promoter with the cloning sites *NheI* and *XhoI*. The PGK promoter sequence was amplified by PCR from the in-house vector pSIN.Tet-HPGK-rtTA2-hDKK-Ires-GFP with the primers “PGK” (T_a of 65°C), adding the *NheI* and *MluI* RS in the 5’ end and *XhoI* in the 3’ end. The UBC promoter was PCR amplified from the pLVUT-tTR-KRAB vector using the High Fidelity PCR Master and the primers “UBC” (T_a of 67°C), adding the same restriction sites. Purified PCR products were digested with *NheI* and *XhoI* RE, as well as the vector pRRL.SFFV-rtTA3-T2A-mCherry and prepared for ligation as previously described. Ligation products were transformed in NEB® Stable bacteria and several colonies were picked for minipreps. Correct ligation was verified by the size of the fragments generated upon digestion with *NheI* and *XhoI* RE. The new promoters were inserted in the inducible pLV vector using the cloning sites *MluI* (upstream the promoter) and *NdeI* (inside the rtTA3). Both vectors were digested with these enzymes, the pLV vector was dephosphorylated and the fragments of interest were isolated for ligation as previously described. Ligation products were transformed in NEB® Stable bacteria and several colonies were picked for minipreps. Correct ligation was verified by the size of the fragments generated upon digestion with *MluI* and *NdeI* RE. The promoters sequences in the final vectors were confirmed by sequencing with the primer “Seq GFPend Fwd” which binds to the end of the GFP sequence just before the constitutive promoter in the inducible pLV vector.

Like for the constitutive promoter, the miR30shRNAs tested were cloned using the cloning sites *BamHI* and *NheI* (section **II.2.1.3**).

II.2.1.6. CONVERSION OF MIR30SHRNA TO MIRESHRNA

To generate miREshRNA lentivectors, the miR30 backbone of a desired miR30shRNA (sh*Luc,* sh*N1.1* and sh*N1.2*) was modified by PCR amplification with the primers "miRE" (T_a of 77°C) to obtain the exact miR sequence described in [1]. As described before for miR30shRNA cloning, the purified PCR product was cloned in the pLV vector using *BamHI* and *NheI* cloning sites. The miREshRNA sequence in the pLV vector was confirmed by sequencing with the primer "Seq rev SHMIR30 EF1".

After sequence confirmation, miREshRNA inserts were cloned in the inducible vector pLV.TetSyntP-miR30shRNA-GFP-UBC-rtTA3-mCherry replacing the miR30shRNA between *BamHI* and *NheI* RS.

The miREsh*Luc* (abbreviated to sh*LucE*) insert was also cloned in the intermediate vector pECFP-C1 using *BamHI* and *NheI* RS to allow more convenient cloning in the future of custom made shRNA oligos with *XhoI* and *EcoRI* RS. Note that, when using the mirE backbone, because the *EcoRI* RS position was moved, custom oligos must be 125 bp, instead of 110 bp as the ones used for miR30shRNA cloning presented in **Table II.5.** As an example, the forward and reverse oligos for sh*LucE* cloning into pECFP-C1 should be as follow:

Fwd: 5'pho- TCGAGAAGGTATATTGCTGTTGACAGTGAGCG**C**TACGCTGAGTACTTCGAA
ATGTAGTGAAGCCACAGATGTACATTTCGAAGTACTCAGCGTA**A**TGCCTACTGCCTCGG
ACTTCAAGGGGCTAG-3';
Rev: 5'pho- AATTCTAGCCCCTTGAAGTCCGAGGCAGTAGGCA**T**TACGCTGAGTACTTCG
AAATGTACATCTGTGGCTTCACTACATTTCGAAGTACTCAGCGTA**G**CGCTCACTGTCAA
CAGCAATATACCTTC-3'.

II.2.1.7. INDUCIBLE TET-ON OVEREXPRESSION LENTIVECTORS

The lentivectors for inducible gene overexpression were generated from the previous miR30shRNA vectors by replacing the whole EF1α intron for a multiple cloning site (MCS) followed by a sequence that encodes for the P2A self-cleaving peptide, originating the vectors pLV.TetSyntP-MCS-(P2A)-GFP-PGK-rtTA3-mCherry and pLV.TetSyntP-MCS-(P2A)-GFP-UBC-rtTA3-mCherry.

An additional vector was also developed with a constitutive EF1α promoter – pLV.TetSyntP-MCS-(P2A)-GFP-EF1α-rtTA3-mCherry. To generate this vector, first the EF1α promoter was cloned in the miR30shRNA vector using the same strategy as for PGK and UBC cloning. The EF1α promoter was amplified by PCR from the in-house vector pLV.EF1α-MCS-GFP with a high fidelity polymerase and the primers "EF1" (T_a of 62°C), adding the *NheI* and *MluI* RS in the 5' end and *XhoI* in the 3' end. Because the digested PCR product failed to ligate to the pRRL vector in multiple attempts, an additional cloning step for TA cloning was performed. The TA cloning kit allowed to directly ligate the purified PCR vector to an intermediate vector (pCR2.1) without need of any digestion. Once in the pCR2.1, the EF1α promoter was isolated by digestion with *NheI* and *XhoI* RE that allowed the successful ligation to the pRRL vector and subsequent ligation to the pLV vector as previously described.

For the PGK and UBC vectors, to replace the intron for the MCS-P2A, the EF1α intron-GFP sequence was replaced for the MCS-P2A-GFP sequence using the *ClaI* and *MluI* cloning sites. The MCS-P2A-GFP sequence was obtained from the in-house vector pLV.EF1α-MCS-GFP by PCR amplification with the primers "MCSforpLV" Fwd and Rev1 (T_a of 58°C). The purified PCR product and the PGK and UBC vectors were digested with *ClaI* and *MluI*-HF® RE and prepared for ligation and transformation according to the standard steps. Positive minipreps were verified by digestion with *ClaI* and *MluI*-HF® RE and the insert sequence was confirmed by sequencing with the primer "Seq fwd SyntP".

For the EF1α vector, because there are two *ClaI* RS (one before the intron and one before the constitutive EF1α promoter), the MCS-P2A-GFP sequence was amplified by PCR and added *ClaI* RS in both ends with the primers "MCSforpLV" Fwd and Rev2 (T_a of 60°C). The purified PCR product and the EF1α vector were digested with *ClaI* RE and prepared for ligation and transformation. After minipreps, the correct

orientation of the insert was verified by digestion with *BamHI* and *XbaI* RE and the insert sequence was confirmed by sequencing with the primer “Seq fwd SyntP”.

Negative control vectors were created by replacing the MCS-P2A-GFP sequence by the GFP sequence alone using the *BamHI* and *MluI* RS. The GFP sequence was amplified by PCR from the in-house vector pLV.EF1α-MCS-GFP with the primers “GFPkozak” (T_a of 60°C) introducing a *BamHI* RS and a consensus kozak sequence in the 5’ end and maintaining the *MluI* RS in the 3’ end. The purified PCR product and the three overexpression vectors were digested with *BamHI* and *MluI*-HF RE and prepared for ligation and transformation (digestion of the PCR DNA was inactivated with precipitation overnight). Positive minipreps were verified by digestion with *BsmBI* RE (that cuts inside the P2A sequence) and the insert sequence was confirmed by sequencing with the primer “Seq fwd SyntP”.

Luciferase overexpression vectors were generated by cloning the *Luc* sequence with the cloning sites *NheI* and *BamHI*. The *Luc* sequence was amplified by PCR from a pGL2 vector (Luciferase reporter vector) with a high fidelity polymerase and the primers “Luciferase” (T_a of 62°C), introducing an *NheI* RS and a consensus kozak sequence in the 5’ end and eliminating the stop codon in the 3’ end and adding a *BamHI* RS. The purified PCR product and the three overexpression vectors were digested with *NheI* and *BamHI* RE and prepared for ligation and transformation (digested PCR DNA was precipitated overnight). Positive minipreps were verified by digestion with the cloning enzymes and the *Luc* sequence was confirmed by sequencing with the primers “Seq fwd SyntP” and “Seq P2A Rev”.

II.2.2. WESTERN BLOT (WB)

II.2.2.1. WHOLE-CELL LYSATES

Suspension cells were counted, centrifuged and washed twice in PBS to remove traces of serum. Cell pellets were then resuspended in the appropriate volume of lysis buffer - RIPA buffer (Merck) supplemented with proteinase inhibitor cocktail (1:100, P8340, Merck). Cell lysates were incubated on ice for 15-20 min with vortexing every 5 min. Loosely attached cells like HEK293T were collected by pipetting up and down

with PBS then transferred to tubes and proceeded like for suspension cells. For adherent cells like HeLa, culture wells were washed twice with PBS and the lysis buffer was added directly to wells, with plates on ice. Cells were scraped with a cell scraper and the cell lysates were transferred to tubes, incubated on ice for 15-20 min with vortexing every 5 min. Cell lysates were cleared by centrifuging for 10 min at 16000× *g* at 4°C then the supernatants were harvested.

Protein concentration was quantified using the DC™ Protein Assay (Biorad Laboratories) according to manufacturer's instructions by measuring absorbances in a CLARIOstar® Plus microplate reader (BGM Labtech, Ortenberg, Germany). Protein concentration of the samples was extrapolated using a calibration curve generated with BSA (bovine serum albumin) standards prepared from a BSA stock (Merck).

II.2.2.2. SDS-PAGE

The desired protein quantities were mixed with water and 6× Laemmli buffer (**Appendix IV**) for a total volume of 24 µL. Samples were incubated for 5 min at 95°C and let to cool down at RT for 10 min followed by a quick spin.

Each NuPAGE™ 4-12% Bis-Tris Gel (Thermo Fisher Scientific) was prepared according to manufacturer's instructions to run with the NuPAGE™ MOPS SDS Running Buffer (Thermo Fisher Scientific) in a XCell SureLock® system (Thermo Fisher Scientific). After assembling and adding the running buffer, 20 µL of sample were loaded into each well and gel was run for 3-4 h at 90 V with a PowerPac™ Basic (Biorad Laboratories).

II.2.2.3. MEMBRANE TRANSFER (WET ELECTROBLOTTING)

A piece of PVDF (polyvinylidene difluoride) membrane (Maine Manufacturing LLC, Sanford, ME, EUA) with the same size of the gel was cut and activated by incubating in methanol (Merck) for 3 min. Membrane, two pads, filter paper and the protein gel were soaked in NuPAGE™ Transfer Buffer (Thermo Fisher Scientific) with 10% methanol to equilibrate. The gel-membrane sandwich was assembled on the open cassette with the black side down in the following order: pad, filter paper, gel,

membrane, filter paper and pad. Before closing the cassette, the sandwich was pressed with a roller to remove air bubbles. The cassette was placed in the transfer tank with the black side facing the black cathode. The tank was filled with transfer buffer and run overnight at 30 V at 4°C. After the transfer, the membrane was rinsed in tris-buffered saline (TBS, **Appendix IV**) with 0.05% Tween®20 (Merck) – "TBS-T" – and blocked for 2-3 h in blocking solution (**Appendix IV**) at RT shaking on a Stuart™ Gyro-Rocker (Staffordshire, UK).

II.2.2.4. PROBING AND SIGNAL DETECTION

After the blocking step, the membrane was probed with a primary antibody (ab) by placing inside a tube with the desired primary ab diluted in blocking solution, rotating overnight at 4°C. The list of the abs used and the respective dilutions can be found in **Table II.7** (**Appendix II**). The next day, the membrane was washed three times with TBS-T shaking for 5 min and then placed in a tube with the respective horseradish peroxidase (HRP) secondary abs (**Table II.9**) diluted in blocking solution. The membrane was then incubated with rotation for 1 h at RT and then washed again three times for 5 min with TBS-T. For chemiluminescence detection, the membrane was incubated with Immobilion® HRP Substrate (Merck) solution for 3-5 min (for β-actin detection membrane was incubated with used substrate). The light-producing reaction was captured either in a ChemiDoc™ XRS System (Biorad Laboratories) or with X-ray film (Hyperfilm™ ECL™, Merck) developed in an EcoMax X-ray Processor (PROTEC GmbH & Co. KG, Oberstenfeld, Germany).

II.2.2.5. WB QUANTIFICATION

WB signal was quantified either using the acquisition software ImageLab (Biorad Laboratories) when was acquired with the ChemiDoc system or using the ImageJ1 software [2] when detected with X-ray film.

II.2.3. IMMUNOHISTOCHEMISTRY (IHC)

Paraffin sections (4 µm thick) were first de-paraffinised by immersing in Xylene (Merck) twice for 5 min, followed by sequential hydrating steps in three decreasing grades of ethanol: twice for 3 min in 100% ethanol, once for 2 min in 90% ethanol and once for 2 min in 70% ethanol. Tissue sections were then immersed in water before submitting to antigen retrieval if necessary.

Antigen retrieval was achieved by microwaving the tissue sections in Antigen Unmasking Solution (citrate-based, Vector Laboratories, Peterborough, UK) diluted 1:100 in distilled H_2O (dH2O) and allowed to boil for 10 min (total 16 min in 700W microwave). Tissue sections were then washed twice with dH2O. When peroxidase-based systems were used for staining detection, endogenous peroxidase was quenched by incubating the tissue sections for 10 min in a 2% solution of hydrogen peroxide (Thermo Fisher Scientific) made in PBS followed by a washing step in PBS for 5 min. Non-specific staining was blocked by covering the tissue sections with PBS 10% serum (donkey or goat, Merck) for 30 minutes at RT. Incubation with primary abs (**Table II.8** in **Appendix II**) was performed overnight in a humidified chamber at 4°C. On the following day, tissue sections were washed twice with PBS for 5 min, incubated with appropriate secondary abs (**Table II.9**) for 1 h at RT in a humidified chamber followed by washing steps as described. For immunofluorescent detection, tissue sections were mounted with Dako Fluorescence Mounting Medium (Agilent Technologies, Santa Clara, CA, USA) containing DAPI (4′,6-diamidino-2-phenylindole dihydrochloride, Merck) diluted 1:3000 from a 2 mg/mL stock. When using DAB as a substrate, this was performed with the Dako Liquid DAB + Substrate Chromogen System (Agilent Technologies). Staining development was monitored under an inverted microscope which was stopped by placing the sections in dH_2O. Alternatively, VECTOR® NovaRed Substrate Kit (Vector Laboratories) was also used according to the manufacturer's instructions. After the substrate development, sections were washed three times in water for 3 min. At the end, sections were counterstained with Mayer's Haemalum solution (Atom Scientific, Cheshire, UK) by incubating for 2 min and rinsing thoroughly with water afterwards. Tissue sections were dehydrated by immersing in increasing ethanol grades for 1 min and twice in xylene for 5 min and finally mounted with DPX mounting medium (Thermo Fisher Scientific). Sections were

then visualised using an inverted microscope Olympus BX43 (Olympus, Tokyo, Japan) or a fluorescent microscope Leica DM2000 LED (Leica Camera, Wetzlar, Germany).

II.2.4. IMMUNOCYTOCHEMISTRY (ICC)

Adherent cell lines were grown on Nunc™ Lab-Tek™ Permanox chamber slides (Thermo Fisher Scientific) until 50% confluent. Suspension cell lines were allowed to attach to poly-L-lysine coated slides for 15 min. All cells were fixed with 4% methanol-free formaldehyde (16% solution (Taab Laboratory Equipment Ltd, Berks, UK) diluted in PBS) at RT for 10 min, permeabilised with PSB + 0.1% Triton™ X-100 (Merck) for 10 min, blocked with 10% serum (donkey or goat) for 30 min at RT, incubated with primary abs (**Table II.8**) at 4°C overnight and then with appropriate secondary abs (**Table II.9**) for 1 h at RT. Slides were mounted with Fluorescence Mounting Medium containing DAPI (1:3000 from a 2 mg/mL stock). Sections were then visualised with a fluorescent microscope.

II.2.5. LUCIFERASE ASSAY

The Luciferase Assay System E1500 (Promega, Madison, WI, USA) was used to quantify the expression of firefly luciferase. Based on manufacturer instructions, 2×10^5 cells were collected and washed twice in PBS. Pelleted cells were resuspended in 100 µL of Cell Culture Lysis Reagent and incubated on ice for 5 min with vortexing for 15 sec. The lysate was cleared by centrifuging at 12000× *g* for 1 min and collecting the supernatant to a new tube which was stored at -80°C. For the detection of luciferase activity, 20 µL of cell lysate were placed per well in an opaque 96-well plate and 100 µL of the Luciferase Assay Reagent were added. The plate was immediately placed in a CLARIOstar® Plus microplate reader programmed to mix the plate for 10 sec and perform a 2 sec measurement delay followed by a 10 sec measurement read for firefly luciferase luminescence. Values obtained were normalised by subtracting the background value obtained with the lysate of non-transduced cells.

II.2.6. QUANTITATIVE POLYMERASE CHAIN REACTION (QPCR)

RNA extraction was performed using the Direct-Zol RNA MicroPrep kit (Zymo Research, Irvine, CA, USA) according to manufacturer's instructions. cDNA was generated by reverse transcription of the mRNA using the SensiScript Kit (Qiagen) based on manufacturer's instructions. Briefly, 20 µL reactions containing 1 µL of reverse transcriptase enzyme, 2 µL of 2x reverse transcriptase buffer, 1 µL of Oligo-dT 14-mer (10 µM, Merck), 2 µL of dNTPs and varying amounts of RNA (up to 120 ng/reaction) and molecular grade water were incubated at 37°C for 1 h. The reaction was stopped by incubating at 93°C for 5 min. The cDNA solution was then placed on ice for a few minutes.

For qPCR, between 2-6 ng of the original equivalent mRNA were used per reaction (10 µL) using the PowerSYBR™ (Thermo Fisher Scientific) kit according to manufacturer's instructions. All the primers used are listed in **Table II.11** (**Appendix III**), which were added at a final concentration of 600 nM. The PCR reactions were amplified using QuantStudio 7 Flex Real-Time PCR system (Thermo Fisher Scientific). The targets were amplified using the following protocol: Hold stage – 2 min at 50°C, 10 min at 95°C; PCR stage (40 times) – 15 sec at 95°C, 1 min at 60°C; Melt curve stage – 15 sec at 95°C, 1 min at 60°C, 15 sec at 95°C.

The analysis was performed by using the ΔΔCt method [3-5], where Ct represents the number of cycles it takes to detect a real signal from the sample. The ΔCt for a certain gene is the difference between the Ct for the gene of interest and for the housekeeping gene:

$$\Delta Ct = Ct_{gene\ of\ interest} - Ct_{housekeeping\ gene} \quad \textbf{(II.1)}$$

The ΔΔCt value represents the difference between ΔCt values for the gene of interest and the housekeeping gene in the tested condition and in the control condition:

$$\Delta\Delta Ct = \Delta Ct_{condition\ X} - Ct_{control} \quad \textbf{(II.2)}$$

Lastly, the fold-change in the expression of the gene of interest in relation to a control condition is quantified based on the following equation:

$$relative\ mRNA\ expression = 2^{-\Delta\Delta Ct} \quad \textbf{(II.3)}$$

II.3. FLOW CYTOMETRY AND IMMUNOSTAINING

All the antibodies and the respective dilutions used for flow cytometry (FCM) analysis or FACS are listed in **Table II.10** (**Appendix II**).

II.3.1. EXTRACELLULAR STAINING

In general, for extracellular Notch receptors staining, 50 µL of PBS 2% FBS with HAG (Human γ-globulins from Cohn fraction II, III; Merck) at 1:5 final dilution (from a 20 mg/mL stock) containing 1.5-2.5×10^5 cells were used per staining in a 5 mL polystyrene tube. Two microliters of each ab were then added: isotype abs were added from the crude stock and Notch abs from a 1:2 dilution. Cells were incubated for 30 min at 4°C in the dark and then washed with PBS 2%. Pelleted cells were resuspended in 0.5 mL of PBS 2% + DAPI (1:2000) and immediately analysed in a BD LSRFortessa™ (BD Biosciences, San Jose, CA, USA). When less cells were available (e.g. to evaluate N1 and N2 knockdown on HSPCs), ~5×10^4 cells were resuspended in 25 µL of PBS 2% + HAG for each staining. Then, 2 µL of ab were added to each tube: isotype abs from a 1:2 dilution and N1 and N2 abs from a 1:4 dilution.

For haematopoietic cells multicolour staining, cells were resuspended in PBS 2% + HAG according to the general rule per staining: <1×10^6 cells in 25-30 µL, 1-2×10^6 cells in 50-80 µL. A master mix of abs was made first containing 5 µL of each ab per 1×10^6 cells, except for N1 and N2 abs which were added by half (2.5 µL/1×10^6 cells). The master mix of antibodies was added to the cells and incubated for 30 min at 4°C in the dark. If stainings were immediately analysed, then cells were washed in PBS 2% and resuspended in PBS 2% + P/S + DAPI. If was to proceed to intracellular staining, cells were washed and resuspended with PBS only. When multicolour FCM was performed, single stain controls were used for manual compensation. Analysis of FCM data was performed with the FlowJoV10 software (FlowJo LLC, Ashland, OR, USA).

II.3.2. INTRACELLULAR STAINING – NICD

For the validation of NICD abs in cell lines, the required number of cells was resuspended in PBS at 2×10^6 cells/mL in a 15 mL tube and the same volume of 4% methanol-free formaldehyde (16% solution diluted in PBS) was added and incubated for 10 min at 37°C (incubation at RT was also tested) to fix the cells. Cells were then washed by toping up the tube with PBS and centrifuging at 450× *g* for 10 min. Cells were resuspend in 1 mL of PBS and the same volume of 0.2% Triton™ X-100 made in PBS was added and incubated for 10 minutes at RT to permeabilise the cells. Then, 1 mL of FBS was added, tubes were topped up with PBS and centrifuged as before. Pelleted cells were resuspended in enough volume of PBS 2% to distribute 2.5×10^5 cells per 25 µL per staining. Two microliters of abs at different dilutions were added to each tube to define the best ab dilution. No ab was added to the control tube. Cells were incubated at 4°C for 50 min and washed with PBS 2% as before. An anti-rabbit secondary ab was prepared in a master mix by diluting the ab 1:100 in PBS 2% and 25 µL were added to each tube. Cells were incubated at 4°C in the dark for 45-50 min and washed as before. Cells were resuspended in 0.5 mL of PBS 2% with DAPI (1:100) and incubated for 5 min on ice before FCM analysis. During analysis, DAPI was acquired in linear mode and pulse-processing mode (DAPI-A vs DAPI-W) was used to exclude any unstained, apoptotic and clumped cells.

After the validation, to detect the expression of NICD, the testing cells were fixed and permeabilised as described. To detect N1ICD and N2ICD expressions, cells were stained with the respective abs diluted 1:16. To detect N4ICD expression, anti-Notch4 ab was diluted 1:50 and after staining, cells were resuspended in 25 µL of PBS 2% and DAPI was added to a final concentration of 2.0 ng/mL and samples were acquired in an Amnis® ImageStream® (Luminex, Austin, TX, USA) image flow cytometer and analysed using the IDEAS® software. This work was previously performed in the lab by António de Soure.

II.3.3. INTRACELLULAR STAINING – KI67 (CELL CYCLE)

For cell cycle analysis, following extracellular staining, cells were fixed at RT and permeabilised as previously described. Cells were resuspended in 50 µL of PBS 2% and divided into two tubes, one for the isotype control (mouse IgG1 κ) and other for the Ki67 stain. Then, 10 µL of the respective ab were added to each tube and cells were incubated at 4°C in the dark for 1 h. Cells were then washed in PBS 2% and resuspended in PBS2% with DAPI (1:100) and proceeded for FCM analysis as described.

II.3.4. FLUORESCENCE-ACTIVATED CELL SORTING (FACS)

All cell sorting was performed in a BD FACSAria™ Fusion (BD Biosciences) and using the BD FACSDiva™ software (BD Biosciences). Extracellular staining was performed in PBS2 % + P/S as described. If no staining was necessary, harvested cells were directly resuspended in PBS 2% + P/S + DAPI. Sorting was performed with a 16-16-0 precision mode and dead cells and debris were excluded by gating DAPI negative cells. All cells were sorted into PBS 2% + P/S.

II.4. LENTIVIRAL PRODUCTION AND CELL LINES TRANSDUCTION

II.4.1. PRODUCTION OF SECOND GENERATION LENTIVIRUSES

The Lenti-X 293T cell line (HEK293T subclone highly transfectable and that supports high levels of viral protein expression [6]) was used as packaging cells with a calcium phosphate transfection protocol.

II.4.1.1. CALCIUM PHOSPHATE TRANSFECTION

Lenti-X 293T cells were seeded in tissue culture dishes 16-18h before transfection. Around 5×10^4 cells/cm^2 were seeded in 100 mm (D100) or 150 mm (D150) dishes with 7 mL or 18 mL of complete DMEM, respectively, and incubated at 37ºC overnight. In the following morning, culture medium was carefully changed 2 h before transfection to Opti-MEM™ (Thermo Fisher Scientific) with 2% FBS, adding enough medium to cover the cells monolayer (5 mL on D100 or 15mL on D150).

For the calcium phosphate transfection method, homemade $CaCl_2$ (2.5 M) and 2× concentrate HEPES (4-(2-hydroxyethyl)piperazine-1-ethanesulfonic acid) buffered saline (HBS, Merck) was used. All reagents were warmed to RT before use. First, the plasmid DNA mix was prepared according to the following quantities per 150 mm dish:

	Per dish (D150 ~ 45-50 µg total DNA)
pMD2.G (1 µg/µL)	7.9 µL (7.9 µg)
pCMVdR8.74 (1 µg/µL)	16.1 µL (16.1 µg)
Transfer Vector	x µL
NF-H_2O (sterile)	x µL (up to 1128 µL)
2× HBS	1250 µL
$CaCl_2$ (2.5M)	122 µL
Total	2500 µL

Where the amount of transfer vector is calculated based on a molar ratio 2:1:1 for the transfer:packaging (pCMVdR8.74):envelope (pMD2.G) vectors, considering that:

$$M_{vector}\ (\mathrm{nM}) = \frac{[\mathrm{vector}]\ (\mu g/\mu L) \times 2{\times}10^{9}}{\mathrm{size\ (bp)} \times 650\ \mathrm{Da}} \quad \textbf{(II.4)}$$

After mixing all the plasmids with the required volume of NF-H_2O, the $CaCl_2$ was added dropwise and mixed gently by flicking. Then, 2× HBS was added dropwise while vortexing in mild speed. The mixture was incubated for 10 min at RT and then added to the cells drop by drop while gently swirling the dish. Cells were incubated at 37ºC and after 7-8 h the culture medium was carefully replaced with pre-warmed collection media (Opti-MEM with 2% FBS, 1% P/S and 25 mM of HEPES [OptiMEM comes with 12.5 mM of HEPES]), using 5 mL on D100 or 15mL on D150. On the following day cells were checked under a fluorescent microscope to assess quality of the transfection through the fluorescent reporter expression which should be over 70% for a good virus production.

The supernatant containing the virus was collected ~48 h after the medium change, centrifuged for 5 min at 1000× *g* to pellet detached cells and debris, and filtered through a 0.45 µm filter (Millex®-HV, Merck). When not concentrating the virus, the whole virus supernatant was aliquoted in 1 mL aliquots and immediately stored at -80ºC.

II.4.1.2. ULTRACENTRIFUGATION OF LENTIVIRAL SUPERNATANT

The virus supernatant was loaded into thinwall polypropylene konical tubes (Beckman Coulter) and balanced with a maximum of 0.2 g of difference. A sample of 0.5 mL was stored at -80ºC for virus titration. Ultracentrifugation was performed in a SW32Ti rotor (Optima XPN-80 Ultracentrifuge, Beckman Coulter), at 4ºC and 90000× *g* for 2.5 h. The centrifuged media was carefully discarded by pouring into an appropriate container for decontamination. Empty tubes were placed inverted on a paper towel to remove excess liquid and the walls of the tube were carefully wiped with a sterilised cotton swab without touching the pellet.

An appropriate amount of medium was added to each tube to resuspend the viral pellet very gently pipetting up and down several times. When using in cell lines, 100 µL of complete RPMI was added to each tube, whereas for use in HSPCs 40 µL of StemSpan™SFEM II (STEMCELL Technologies) was added to each tube. Tubes were left sealed with parafilm for 2 h on ice with occasional flicking of the tubes. All resuspended virus media were then transferred to a 0.5 mL tube and centrifuged for 1 min at 1000× *g* to pellet any major debris. The concentrated virus was aliquoted in 0.5 mL tubes, making aliquots of 20-30 µL for cell lines and 7-10 µL for HSPCs which were immediately put on dry ice and stored at -80°C.

II.4.1.3. LENTIVIRUS TITRATION

HeLa cells were plated in 24-well plates at 2.5×10^4 cells in 0.5 mL of complete DMEM 12-16 h before adding the virus suspensions. Serial dilutions of the virus media were prepared in 2 mL tubes with complete DMEM. When titrating unconcentrated virus, dilutions of 1 in 64, 128 and 256 were generally used. When titrating concentrated virus, dilutions of 1 in 2×10^4 and 4×10^4 were used. These dilutions were selected to achieve transduction efficiencies below to around 20%, which guarantees a more accurate virus titration. Diluted virus media (0.5 mL) was added to the cells (making a total volume of 1 mL) and plates were incubated at 37°C for 2-3 days, after which cells were detached as previously described. Cells were collected and centrifuged in 5 mL tubes and resuspended in 300 µL of PBS 2% + P/S + DAPI.

Transduction efficiencies were analysed by FCM in a BD LSRFortessa™, measuring the percentage of GFP or mCherry positive cells depending on the transfer vector being used. Virus titres were calculated based on the following equation and the average from two dilutions.

$$Virus\ titre\ (TU/mL) = \frac{\%\ reporter}{100} \times dilution\ factor \times 2.5 \times 10^4 cells \qquad \textbf{(II.5)}$$

II.4.2. TRANSDUCTION AND GENERATION OF STABLE CELL LINES

For the transduction of HEK293T cells, 1.25×10^4 cells/cm^2 were plated in culture wells with complete DMEM 12-16 h before adding the virus. Cells were transduced with an MOI of 10 by adding the required volume of virus suspension. When using unconcentrated virus, culture medium was carefully changed in the following day. Cells were split every 3 days.

For the transduction of suspension cells like K562 and OCI-AML3, cells were plated at 5×10^5 cells/mL in culture wells with complete RPMI and IMDM 20%, respectively, immediately before adding the virus. Cells were transduced with an MOI of 5 or 10 by adding the required volume of virus suspension. Culture medium was changed 16 h after transduction maintaining a concentration of 5×10^5 cells/mL and cells were split every 3 days.

In the knockdown validation assays with the constitutive shRNA and miR30shRNA vectors, transduced K562 and HEK293T cells were cultured for 6 days before analysis of N1 and N2 knockdown, respectively, by FCM (staining of extracellular N1 and N2 described in section **II.3.1**). These cells were cultured for an additional 3 days and then harvested for protein extraction as described in section **II.2.2.1**. In the inducible vectors validation study (**Chapter V**), transduced K562 and OCI-AML3 cells were sorted for mCherry$^+$ cells 3-6 days after transduction. When an appropriate number of cells was available ($2\text{-}5\times10^5$), mCherry$^+$ cells were purified by FACS until a minimum of $5\text{-}10\times10^4$ cells were collected into 2 mL tubes with PBS 2% + P/S. The collection tubes were centrifuged and cells were resuspended in the respective culture media to a concentration of 5×10^5 cells/mL. Cells were initially plated in wells of a 96-well plate, splitting 1:4 after 2-3 days to a 24-well plate, after which cells were split as previously described and maintained in a 12-well plate. Cells were collected in the referred time points for FCM analysis and luciferase quantification assay (described in section **II.2.5**).

II.5. HAEMATOPOIETIC ASSAYS

II.5.1. ISOLATION OF MNCS FROM UCB

UCB/UCB-MNCs were obtained from different sources (Anthony Nolan Cord Blood Bank, STEMCELL Technologies; Vancouver, Canada and The Royal London Hospitals) after informed consent approved by their respective local ethical committees and the Declaration of Helsinki.

MNCs were obtained by density centrifugation using Ficoll-Paque (STEMCELL Technologies). Briefly, blood was diluted three times in PBS and gently added to a layer of Ficoll (with 1 part Ficoll to ~2 parts blood) and tubes were centrifuged at 550× *g* for 30 min at RT without brake. The middle layer of cells was collected, diluted 1:2 with PBS and centrifuged. The pelleted cells were resuspended with PBS and ammonium chloride (STEMCELL Technologies) was added 3-4 times to the initial volume and put at 4°C for 7-10 min to lyse the red blood cells. Then, 1-2 mL of FBS was added to balance the osmolarity and tubes were topped up with PBS and centrifuged. Cells were resuspended in 1-5 mL of PBS 2% FBS + P/S depending on the cell pellet size. Cells were counted and immediately cryopreserved at 0.5-1.5×10^8 cells/mL in FBS with 10% DMSO as described.

II.5.2. HSPCS SELECTION

II.5.2.1. CD34+ CELLS ENRICHMENT

Frozen vials of MNCs (0.5-1.5×10^8 cells) were thawed in PBS 2% + P/S and resuspended in 0.5 mL of PBS 2% + P/S. Cells were counted and the resuspension volume was adjusted according to instructions of EasySep™ Human CD34 Positive Selection Kit II (STEMCELL Technologies). The kit protocol was followed, performing four rounds of selection. $CD34^+$ enriched cells were centrifuged, resuspended in 50 µL of PBS 2% + P/S and counted.

II.5.2.2. **CD34$^+$CD38$^-$ FACS**

CD34$^+$ enriched cells were stained with anti-CD34-APC and CD38-PECy7 abs as described in section **II.3.1**. Single stains were also prepared by staining 50 µL of discarded CD34$^-$ MNCs with anti-CD45-APC and CD38-PECy7 abs in separate tubes. After staining, cells were resuspended in 0.5 mL of PBS 2% + P/S + DAPI and filtered through a 70 µm nylon mesh. CD34$^+$CD38$^-$ HSPCs were isolated by FACS (section **II.3.4**) after compensation with single stains. CD34$^+$CD38$^-$ cells were selected by gating a CD38$^-$ population around 12-13% of the CD34$^+$ population.

II.5.3. **CO-CULTURE OF HSPCS WITH S17 STROMAL CELLS**

To prepare the stromal layers, the different S17 cell lines were plated 2-3 days before initiating co-culture, at 2×10^4 cells/cm^2 in a 24-well plate with complete αMEM. Co-cultures of CD34$^+$CD38$^-$ HSPCs were initiated by seeding 5×10^3 cells/well in 0.5 mL of αMEM with 5% FBS and 1% P/S supplemented with SCF (100 ng/mL), Flt3L (100 ng/mL) and TPO (40 ng/mL, all cytokines from PeproTech, Inc, London, UK). Cells were cultured for 5-6 days and then collected by harvesting all cells. Supernatant was collected into a 15 mL tube then, wells were washed once with PBS and the wash-out was also collected. The adherent fraction was harvested by trypsinisation for 7 min with 2 subsequent washes with PBS 2% and the whole content was transferred to the tube containing the non-adherent cells. Cells were centrifuged, resuspended in PBS 2%. The collected cells were either used for extracellular and intracellular staining (as described in sections **II.3.1** and **II.3.3**) for analysis of cell cycle and differentiation, sorting of CD45$^+$CD34$^+$ cells for RNA extraction (section **II.2.5**) or sorting of CD45$^+$ cells for mice transplantation (section **II.5.6**). The panel of abs used are listed in section **II.5.7**.

II.5.4. HSPCs TRANSDUCTION, SORTING AND CULTURE

FACS purified $CD34^+CD38^-$ HSPCs were resuspended in StemSpan™SFEM II containing SCF (100 ng/mL), Flt3L (100 ng/mL), IL-6 (10 ng/mL), IL-3 (10 ng/mL), G-CSF (25 ng/mL; all cytokines from PeproTech), 1% P/S and HEPES (10 mM). Cells were counted, the volume was adjusted to a concentration of 1-1.5×10^5 cells/mL and 100 µL of cell suspension (10000-15000 cells) were plated per well of a 96-well plate. Cells were incubated overnight (~16 h) for pre-stimulation before adding highly concentrated virus (titres > 10^8). Pre-stimulated HSPCs were transduced with MOI of 40-50. After 8-12 h, a drop of FBS was added to the wells to inactivate the viral particles and then cells were collected into 2 mL tubes by washing the wells with PBS several times. Collection tubes were centrifuged, and cells were resuspended in 100 µL of StemSpan™SFEM with SCF (300 ng/mL), Flt3L (300 ng/mL), TPO (20 ng/mL), 1% P/S and HEPES (10 mM) – "StemSpan 300/300/20". Cells were plated into new wells of a 96-well plate and incubated for 4 days. After this period, cells were collected into sterile 5 mL tubes by washing the wells with PBS 2% several times, centrifuged and resuspended in 0.5-1 mL of PBS 2% + DAPI + P/S. Next, GFP^+ cells were purified in a BD FACSAria™ Fusion cell sorter into 2 mL tubes with 1 mL of PBS 2% +P/S. After sorting, PBS was added to fill the collection tubes and cells were centrifuged, resuspended in the appropriate medium and counted.

For the *in vitro* studies, cells were resuspended in StemSpan 300/300/20 and the required number of cells were used for the LTC-IC assay (section **II.5.5**). The remaining cells were plated at a concentration of 2-3×10^5 cells/mL. After 3-4 days of culture, cells were split 1:2 or 1:3 and cultured for additional 4 days and then collected for N1 and N2 knockdown analysis by FCM. Cells were stained for N1 and N2 as described in section **II.5.3.1**. For *in vivo studies*, GFP^+ HSPCs were resuspended in PBS 2% for adoptive transfer into NSG mice (section **II.5.6**).

In vitro cell growth from the sorting day (day 4) to collection day for knockdown analysis (day 11) was quantified as population doublings, according to equation II.5, where N is the number of cells.

$$\text{Population doublings} = \frac{ln(N_{day\ 11}/N_{day\ 4})}{ln2} \quad \textbf{(II.6)}$$

II.5.5. LTC-IC ASSAY

To prepare the stromal feeder layers for the LTC-IC assay, early passage of MS-5 cells were thawed at least 12 days before the assay. Cells were cultured for 3-5 passages as previously described before being used as feeder layer. Before seeding the MS-5 cells, 96-well and 24-well plates were coated with collagen (STEMCELL Technologies) diluted 1:10 in PBS (0.3 mg/mL). To coat the wells, 35 µL or 200 µL of the diluted solution was added to each well of 96-well and 24-well plates, respectively. The solution was left for 1 min after which it was recovered and could re-used three more times. The plates were left open inside the hood to allow the wells to dry for ~1 h. After this, the plates were either used immediately or sealed with parafilm and stored at 4°C until use (for up to 2 weeks).

Before use, the collagen coated wells were washed two times with PBS to neutralise the collagen pH and then 3000 cells/well or 18000 cells/well were plated in 96-well or 24-well plates, respectively (~60-70% confluency) with complete IMDM. Cells were cultured for 2 days until 80-90% confluence was reached. On the day before HSPC seeding, plates were irradiated at 6.8 Gy to arrest cell growth and culture medium was changed 5-6 h after irradiation to 100 µL/well of MyeloCult™ H5100 (STEMCELL Technologies) with 1% P/S. Following sorting, GFP^+ HSPCs were seeded at different cell doses per well of 96-well plate – 2.5, 5, 10 and 15 cells/well, with 5-15 wells for each dose in one independent experiment. The required number of cells was determined and resuspended in complete IMDM in order to dispense 10-20 µL into each well. For 24-well plates, 60 cells/well were seeded, which is an equivalent dose of 10 cells/well in the 96-well plate. LTC-IC cultures were incubated for 5 weeks and half media change was performed once a week by removing 50 µL of the medium and non-adherent cells and replacing gently with 50 µL of fresh Myelocult H5100 + P/S. After 4 weeks, CAFCs were counted in each condition considering only large colonies of >50 packed haematopoietic cells, as exemplified in **Figure II.2**.

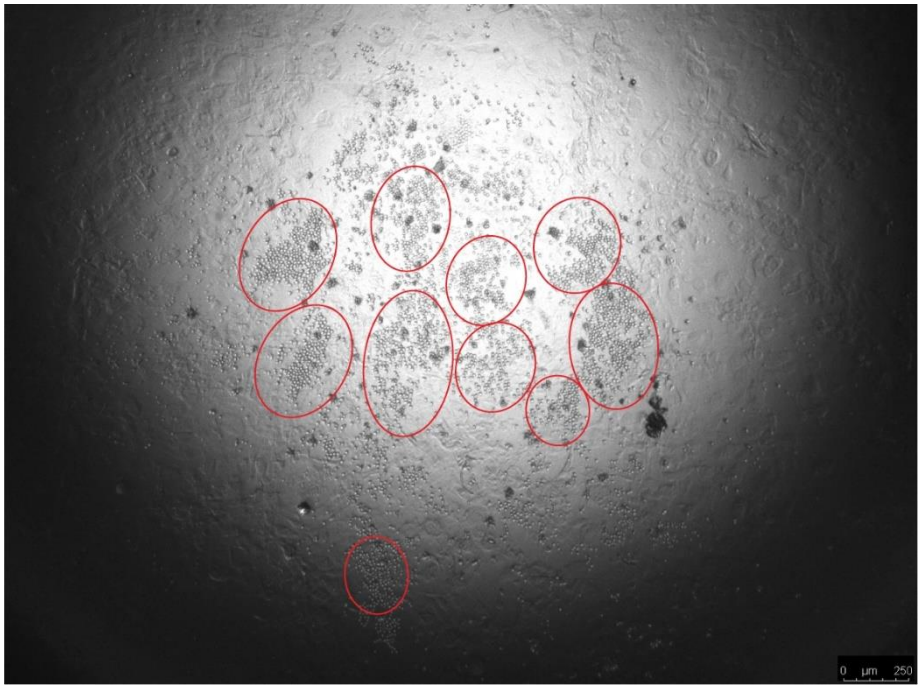

Figure II.2 – Example of a cobblestone-area at week 4 of the LTC-IC assay. In red circles are identified the large colonies counted in this area.

II.5.5.1. IMMUNOPHENOTYPIC CHARACTERISATION OF LTC CELLS

At the end of 5 weeks, all cells from each dose were harvested including the non-adherent cells similarly as described in section **II.5.3**. Collected cells were resuspended in an equivalent volume of 100 µL/well of complete IMDM/well and 100 µL were used for the CFU assay as described below. The remaining cells from cell doses of 5, 10 and 15 were pooled together, centrifuged and resuspended for immunophenotypic analysis. Cells collected from 24-well plates were frozen down. The panel of abs used in this assay can be found in section **II.5.7**.

II.5.5.2. CFU ASSAY (LTC-IC DERIVED)

To assess CFUs formation from the different LTC-IC doses used, 100 µL of the LTC-IC cell suspension, which corresponds to one well of a 96-well plate, were transferred into a 1.2 mL aliquot of enriched methylcellulose (MethoCult™ H4435, STEMCELL Technologies) with 1% P/S. Cells were then mixed by vigorously inverting and plated into 2 wells of a 12-well plate by loading 550 µL into each well using a blunt needle

and a 1 mL syringe. The remaining unused surrounding wells and space between the wells were filled with sterile water with 1% P/S. Plates were incubated at 37°C for 14 days, after which the total number of colonies were counted under an inverted microscope. The number of LTC-IC derived CFUs per input cell was calculated from the mean of the duplicate wells.

II.5.6. IN VIVO ASSAY

Due to the lack of an appropriate animal facility at Cardiff University to breed the number of pathogen-free immunodeficient mice required for this project, both the animal adoptive transfer and the schedule-1 sacrifice procedures were performed by Dr. Fernando dos Anjos Afonso at The Francis Crick Institute in London. All the animal procedures were performed in accordance with the UK Home Office regulations after The Francis Crick Institute ethics committee approval.

II.5.6.1. XENOTRANSPLANTATION OF HSPCS

For the Notch ligands study, NOD/SCID/β2m$^{-/-}$ aged 8 to 12 weeks were sub-lethally irradiated at 3.75 Gy (^{137}Cs) up to 24 hours before tail vein injection of sorted cells. Mice were either injected with total CD45^{+} derived from the different S17 co-cultures (section **II.5.3**) or with 5×10^{3} fresh CD34^{+}CD38^{-} cells (Day 0). For limiting dilution analysis (LDA) mice were injected with different cell doses ranging from 625 to 40000 CD45^{+} derived cells from the different S17 co-cultures. For each cell dose 4-6 mice were used. For the Notch receptors knockdown study, NSG mice aged 8 to 12 weeks were irradiated at 3.75 Gy (^{137}Cs) up to 24 hours before mice transplantation. For this study, 5000 FACS purified GFP^{+} HSPCs (section **II.5.4**) were injected into the tail vein.

II.5.6.2. IMMUNOPHENOTYPIC CHARACTERISATION OF ENGRAFTED CELLS

Mice were sacrificed by cervical dislocation 12 weeks after adoptive transfer and the tibiae, femurs and ileum were collected. Bone marrows were harvested by flushing the

bones with PBS 2% using an insulin syringe (25 gauge). Bones were flushed several times until they had a white appearance, indicating removal of most cellular content. Red blood cells were lysed by adding to the cells suspension three times its volume of ammonium chloride (STEMCELL Technologies) and incubating for 3-5 min at RT. At the end, few drops of FBS were added to balance the osmolarity, then cells were centrifuged, resuspended in 200 µL of PBS 2% and counted.

In the Notch ligands study, a fraction of the cell suspension (containing 5×10^5 to 1×10^6 cells) was stained with anti-CD45, -CD19 and -CD33 abs (panel in section **II.5.7**) to quantify the level of human myelo-lymphoid engraftment. Human engraftment was quantified as the proportion of live cells that were $CD45^+CD33^+$ and $CD45^+CD19^+$. Dead cells and debris were excluded from the analysis and the maximum number of lived effects were acquired. In the Notch receptors knockdown study, half of the cell suspension was cryopreserved, and the other half was used for extracellular staining dividing 20 µL to characterise human engraftment and differentiation phenotype and 80 µL to characterise engrafted HSPC sub-populations. The panels of abs used can be found in section **II.5.7**.

II.5.7. ANTIBODIES PANELS

Notch ligands study – *in vitro*

Cell cycle and differentiation: CD45-xx, CD34-xx, CD45RA-xx, Ki67-FITC

HSPCs sorting: CD45-xx, CD34-xx

Notch ligands study – *in vivo*

Human engraftment: CD45-xx, CD19-xx, CD33-xx

Notch receptors knockdown study – *in vitro*

HSPCs subpopulation: CD34-APC, CD38-PECy7, CD45RA-APCe789, CD90-BV605, CD135-BV711

Differentiation and knockdown: CD11c-APC, CD14-PECy7, CD19-APCe780, CD33-BV711, CD34-PerCP, CD56-BV605, IgG1/Notch1/Notch2-PE

Notch receptors knockdown study – *in vivo*

HSPCs subpopulation: CD10-APC, CD34-PerCP, CD38-AF780, CD45RA-PECy7, CD62L-PE, CD90-BV605, CD135-BV711, Lin-eFluor450, CD19-eFluor450

Human engraftment and differentiation: CD11c-PE, CD14-PECy7, CD19-APCe780, CD33-APC

“xx” denotes that different fluorochromes were used in different experiments.

II.6. DATA ANALYSIS

All statistical analysis was performed using the Prism8 software (GraphPad Software, San Diego, CA, USA).

When size of the sample was sufficient and passed the Shapiro-Wilk normality test, statistical analysis was performed with unpaired t-test. When these requirements were not satisfied, the nonparametric Mann-Whitney test was used. The p-value scale used was: *$p<0.03$, **$p<0.003$ and ***$p<0.0003$.

For the LDA experiments, the L-Calc software (STEMCELL Technologies) was used to calculate SRC frequency.

APPENDIX I – MOLECULAR CLONING

Table II.1 – Plasmids used for molecular cloning as templates, intermediate vectors and for shRNA expression.

Plasmid name	Source
pLV.EF1α-premiRNA30-RFP	Biossettia (San Diego, CA, USA)
pSIN.Tet-HPGK-rtTA2-hDKK-Ires-GFP	In-house vector
pGIPZ	Dharmacon – Horizon Discovery Group
pmCherry	Takara Bio (Mountain View, CA, USA)
pINDUCER 21 (ORF-EG)	Addgene (Watertown, MA, USA) This vector was gift from Stephen Elledge & Thomas Westbrook (Addgene plasmid #46948; http://n2t.net/addgene:46948; RRID: Addgene_46948) [7]
pRRL.SFFV-d20GFP-T2A-mTagBFP	Addgene This vector was a gift from Andrew Scharenberg (Addgene plasmid #31485; http://n2t.net/addgene:31485; RRID: Addgene_31485) [8]
pTRE3G-mCherry	Takara Bio
pECFP-C1	Takara Bio
pEntr4-H1	Riken
CS-RfA-EG	Riken
pLVUT-tTR-KRAB	Addgene This vector was a gift from Patrick Aebischer & Didier Trono (Addgene plasmid # 11651; http://n2t.net/addgene:11651; RRID: Addgene 11651) [9]
pLV.EF1α-MCS-GFP	In-house vector (EF1α promoter derived from the vector CSII-EF-MCS from Riken)
pGL2	Promega

Table II.2 – Forward (fwd) and reverse (rev) primers used for molecular cloning.

GFP	Fwd	5'-TACCCCTCTAGAGTCGAGCTACCGGTCGCCACCATGGTGAGCAAGGGCGAGG-3'
	Rev	5'-TTGGAACCTAAGTCGACACGCGTTTACTTGTACAGCTCGTCCATGCC-3'
miR30 shrna	Fwd	5'-TCTCGAGGATCCACAGAATCGTTGCCTGCAC-3'
	Rev	5'-GCTCGAGCTAGCTTCAGCTTTGTAAAAATGTATCAAAG-3'
rtTA3	Fwd	5'-GGATCGATCCTCGAGCGCCACCATGTCTAGACTGGACAAGAGCAAAGTC-3'
	Rev	5'-CTCCTCCACGTCACCGCATGTTAGAAGACTTCCTCTGCCCTCACCGGAACCCCCGGGGAGCATGTCAA-3'
mCherry	Fwd	5'-GAATCCGGGCCCCATGGTGAGCAAGGGCGAGG-3'
	Rev	5'-TTGTCGACCTACTACTTGTACAGCTCGTCCATGCCG-3'
Cassette	Fwd	5'-GGAACCTTACGCGTAGCTAGGTGCAGTAACGCCATT-3'
	Rev	5'-TTGATTGTCGACCTACTACTTGTACAG-3'
*EF1*intron	Fwd	5'-ACGTAAAGTCGACGGTATCGATAAGCTTGATATCGAATTCCTGCAGCCCGGGGGGTCCACGTTCTTTTTCGCAAC-3'
	Rev	5'- ATCAGCGTGGATCCTCGAGAACTAATC-3'
TRE3G	Fwd	5'-TAATCTTATCGATCACGAGACTAGCCTCGAGGTCGAGTTTACTCCCTATC-3'
	Rev	5'-CAGGAATTCGATATCAAG-3'
PGK	Fwd	5'-ACGTTCGCTAGCACGCGTAGCTGGAAGCTCAGCTCGAATTCCCACGGGGTTG-3'
	Rev	5'-TCGAACCTCGAGCTGGGGAGAGAGGTCGGTGATT-3'
UBC	Fwd	5'-ATCGTAGCTAGCACGCGTCGAATCCTAGCGCAGAGATCCAGTTTGGTTAATTAACCCGTG-3'
	Rev	5'-CAGTATCTCGAGGTCTAACAAAAAAGCCAAAAACGGCCAG-3'
EF1	Fwd	5'-ACTGTATGCTAGCACGCGTAAGCGGCCGCACTAGAGATATCGAATATCGATGCCTCCCCGTCA-3'
	Rev	5'-ATTGCTCTCGAGTTCACGACACCTGAAATGGAAG-3'
MCS for pLV	Fwd	5'-ACTGACATCGATGGCCGGCCATGCATGCTAGCACCGGTTCCGGTCTCGAGAATTC-3'
	Rev1	5'-AACTATACGCGTGGTAAGCGGCCGCACTAGAGATACGAATACCGATTACTTGTACAGCTCGTCCATG-3'
	Rev2	5'-AACTATATCGATGGTAAGCGGCCGCACTAGAGATATCGAATATCGGATTGTCGACACGCGTTTATTAC-3'
GFP kozak	Fwd	5'-CTGAACGGATCCGGCCACCATGGTGAGCAAGG-3'
	Rev	5'-CGATGTTAACTCTAGAACGCGTTTATTAC-3'
Luciferase	Fwd	5'-GCTACTGAGCTAGCGCCACCATGGAAGACGCCAAAAACATAAAG-3'
	Rev	5'-TCTAAGCTGGATCCCAATTTGGACTTTCCGCCCTTC-3'
mirE	Fwd	5'-AGTCTTGGATCCACAGAATCGTTGCCTGCACATCTTGGAAACACTTGCTGGGATTACTTCGACTTCTTAACCCAAC-3'
	Rev	5'-AATGCCGCTAGCTTCAGCTTTGTAAAAATGTATCAAAGAGATAGCAAGGTATTCAGTTTTAGTAAACAAGATAATTGCTC GAATTCTAGCCCCTTGAAGTCCGAGGCAG-3'

Table II.3 – Sequencing primers used to confirm DNA sequences

Seq fwd GFP	5'-CCTCTAGAGTCGAGCTACC-3'
Seq fwd1 cassette	5'-GCCACCATGTCTAGACTG-3'
Seq rev1 cassette	5'-CTTCACGTGCCAGTACAG-3'
Seq fwd2 cassette	5'-AAGCTGAAGGTGACCAAG-3'
Seq rev2 cassette	5'-TTCACGTAGGCCTTGGAG-3'
Seq fwd Teto	5'-TCGATTAGTGAACGGATCTC-3'
Seq fwd SyntP	5'-CTACCCTCGTAAAGTCGAC-3'
Seq rev SHMIR30 EF1	5'-TTACATCAAGTGCCAAGCTG-3'
Seq fwd SHMIR30 pECFP	5'-CCAAAATGTCGTAACAACTCC-3'
pH1up2seq	5'-CAGGAAGATGGCTGTGAGG-3'
Seq GFPend Fwd	5'-GACGAGCTGTACAAGTAAAC-3'
Seq P2A Rev	5'-TTCTCCTCCACGTCTCCAG-3'

Table II.4 – Reagents and kits used for the standard cloning techniques.

Techniques	**Reagent/Kit name**	**Brand**
PCR	HotStarTaq	Qiagen
	High Fidelity PCR Master	Roche
Gel extraction	PureLink™ Quick Gel Extraction Kit	Thermo Fisher Scientific
Enzymatic Restriction	*ApaI*, *BamHI*, *BglII*, *BmgBI*, *BsmBI*, *ClaI*, *EcoRI*, *NdeI*, *NheI*, *MluI*, *MluI*-HF®, *PstI*, *SalI*-HF®, *XbaI*, *XhoI*	New England Biolabs
Dephosphorylation	Shrimp Alkaline Phosphatase (rSAP)	New England Biolabs
Ligation	Quick Ligation™ Kit	New England Biolabs
Transformation	NEB® Stable Competent E. coli	New England Biolabs
	One Shot™ TOP10 Chemically Competent E. coli	Thermo Fisher Scientific
Miniprep	PureLink™ HiPure Plasmid Miniprep Kit	Thermo Fisher Scientific
Maxiprep	PureLink™ HiPure Plasmid Maxiprep Kit	Thermo Fisher Scientific
Gateway LR reaction	Gateway™ LR Clonase™ Enzyme mix	Thermo Fisher Scientific
TA cloning	The Original TA Cloning® Kit pCR®2.1 vector	Thermo Fisher Scientific

Table II.5 – Forward and reverse miR30shRNA oligos for cloning into the miR30 backbone. Sense and anti-sense sequences identified in red and blue, respectively and loop sequence in green. Original shRNA sequence is underlined and mismatched nucleotides are bolded. shRNA targeting *Luciferase* (*Luc*) was used as non-target control, three sequences were identified for efficient *N1* knockdown (N1.1-N1.3) and two sequences were identified for *N2* (N2.1 and N2.2).

Name		Sequence	shRNA source
Luc	Fwd	5'pho- TCGAGAAGGTATATTGCTGTTGACAGTGAGCG**C**TACGCTGAGTACTTCGAAATGTAGTGAAGCCACAGATG TACATTTCGAAGTACTCAGCGTA**A**TGCCTACTGCCTCGG -3'	In-house design
	Rev	5'pho- AATTCCGAGGCAGTAGGCATTACGCTGAGTACTTCGAAATGTACATCTGTGGCTTCACTACATTTCGAAGTA CTCAGCGTAGCGCTCACTGTCAACAGCAATATACCTTC -3'	
N1.1	Fwd	5'pho- TCGAGAAGGTATATTGCTGTTGACAGTGAGCG**A**GGGGCTAACAAAGATATGCAGTAGTGAAGCCACAGATG TACTGCATATCTTTGTTAGCCCC**G**TGCCTACTGCCTCGG -3'	[10]
	Rev	5'pho- AATTCCGAGGCAGTAGGCACGGGGCTAACAAAGATATGCAGTACATCTGTGGCTTCACTACTGCATATCTTT GTTAGCCCCTCGCTCACTGTCAACAGCAATATACCTTC -3'	
N1.2	Fwd	5'pho- TCGAGAAGGTATATTGCTGTTGACAGTGAGCG**A**CAGGTGCAGCCACAAAACTTATAGTGAAGCCACAGATG TATAAGTTTTGTGGCTGCACCTG**C**TGCCTACTGCCTCGG -3'	Dharmacon™ pGIPZ
	Rev	5'pho- AATTCCGAGGCAGTAGGCAGCAGGTGCAGCCACAAAACTTATACATCTGTGGCTTCACTATAAGTTTTGTG GCTGCACCTGTCGCTCACTGTCAACAGCAATATACCTTC -3'	
N1.3	Fwd	5'pho- TCGAGAAGGTATATTGCTGTTGACAGTGAGCG**C**CCGGGACATCACGGATCATATTAGTGAAGCCACAGATG TAATATGATCCGTGATGTCCCGG**T**TGCCTACTGCCTCGG -3'	MISSION® shRNA Library
	Rev	5'pho- AATTCCGAGGCAGTAGGCAACCGGGACATCACGGATCATATTACATCTGTGGCTTCACTAATATGATCCGT GATGTCCCGGGCGCTCACTGTCAACAGCAATATACCTTC -3'	
N2.1	Fwd	5'pho- TCGAGAAGGTATATTGCTGTTGACAGTGAGCG**C**CCACATCCTCTCCAATGATTATAGTGAAGCCACAGATGT ATAATCATTGGAGAGGATGTGG**T**TGCCTACTGCCTCGG -3'	Dharmacon™ pGIPZ
	Rev	5'pho- AATTCCGAGGCAGTAGGCAACCACATCCTCTCCAATGATTATACATCTGTGGCTTCACTATAATCATTGGAG AGGATGTGGGCGCTCACTGTCAACAGCAATATACCTTC -3'	
N2.2	Fwd	5'pho- TCGAGAAGGTATATTGCTGTTGACAGTGAGCG**C**GCAGAGGACTCTTCTGCTAACTAGTGAAGCCACAGATG TAGTTAGCAGAAGAGTCCTCTGC**A**TGCCTACTGCCTCGG -3'	[11]
	Rev	5'pho- AATTCCGAGGCAGTAGGCATGCAGAGGACTCTTCTGCTAACTACATCTGTGGCTTCACTAGTTAGCAGAAG AGTCCTCTGCGCGCTCACTGTCAACAGCAATATACCTTC -3'	

Table II.6 – Forward (fwd) and reverse (rev) shRNA oligos for cloning in the CS-H1-shRNA-EG vector. Sense and anti-sense sequences identified in red and blue, respectively, and loop sequence in green.

Name		Sequence	shRNA source
Luc	Fwd	5'pho- GATCCCCACGCTGAGTACTTCGAAATGTTTCAAGAGAACATTTCGAAGTACTCAGCGTTTTTTGGAAAT-3'	In-house design
	Rev	5'pho- CTAGATTTCCAAAAAACGCTGAGTACTTCGAAATGTTCTCTTGAAACATTTCGAAGTACTCAGCGTGGG-3'	
N1.2	Fwd	5'pho- GATCCCCAGGTGCAGCCACAAAACTTACTTCAAGAGAGTAAGTTTTGTGGCTGCACCTTTTTTGGAAAT-3'	Dharmacon™ pGIPZ
	Rev	5'pho- CTAGATTTCCAAAAAAGGTGCAGCCACAAAACTTACTCTCTTGAAGTAAGTTTTGTGGCTGCACCTGGG-3'	
N1.4	Fwd	5'pho- GATCCCCAGCATGTGTAACATCAACATCTTCAAGAGAGATGTTGATGTTACACATGCTTTTTTGGAAAT-3'	[11]
	Rev	5'pho- CTAGATTTCCAAAAAAGCATGTGTAACATCAACATCTCTCTTGAAGATGTTGATGTTACACATGCTGGG-3'	
N2.1	Fwd	5'pho- GATCCCCACCACATCCTCTCCAATGATTTTCAAGAGAAATCATTGGAGAGGATGTGGTTTTTTGGAAAT-3'	Dharmacon™ pGIPZ
	Rev	5'pho- CTAGATTTCCAAAAAACCACATCCTCTCCAATGATTTCTCTTGAAAATCATTGGAGAGGATGTGGTGGG-3'	
N2.2	Fwd	5'pho- GATCCCCGCAGAGGACTCTTCTGCTAACTTCAAGAGAGTTAGCAGAAGAGTCCTCTGCTTTTTTGGAAAT-3'	[11]
	Rev	5'pho- CTAGATTTCCAAAAAGCAGAGGACTCTTCTGCTAACTCTCTTGAAGTTAGCAGAAGAGTCCTCTGCGGG-3'	

APPENDIX II – ANTIBODIES

Table II.7 – List of primary antibodies used for Western blotting.

Antibody	Clone	Reference/ Company	Dilution
Notch1	D1E11	#3608S Cell Signaling Technology (Leiden, The Netherlands)	1:1000
Cleaved Notch1	D3B8	#4147S Cell Signaling Technology	1:500
Notch2	D76A6	#5732S Cell Signaling Technology	1:1000
Cleaved Notch2 (Ala1734)	Polyclonal	#PA5-37433 Thermo Fisher Scientific	1:300
Notch4	L5C5	#2423S Cell Signaling Technology	1:1000
Notch4	Polyclonal	#sc-5594 (discontinued) Santa Cruz Biotechnology (Dallas, TX, USA)	1:1000
β-Actin	AC-15	#A5441 (Merck)	1:10000

Table II.8 – List of primary antibodies used for IHC and ICC.

Antibody	Clone	Reference/ Company	Dilution
Dll4	Polyclonal	#NB600-892 Novus Biologicals (Abingdon, UK)	1:100 (10 µg/mL)
Jag1	N-17	#sc-34473 (discontinued) Santa Cruz Biotechnology	1:100 (2 µg/mL)
Dll1	Polyclonal	#ab84620 Abcam Plc (Cambridge, UK)	1:100 (5 µg/mL)
Dll1	Polyclonal	#NBP2-27088 Novus Biologicals	1:50 (10 µg/mL)
CD31	JC70A	#M0823 Agilent Technologies	1:100 (10 µg/mL)
Vimentin	V9	#sc-6260 Santa Cruz Biotechnology	1:100 (2 µg/mL)
CK8	Polyclonal	#ab14053 Abcam	1:100 (10 µg/mL)
Cleaved Notch1 (Val1744)	Polyclonal	#2421 (discontinued) Cell Signaling Technology	1:200 (0.15 µg/mL)
Cleaved Notch2 (Asp1733)	Polyclonal	#ab52302 (discontinued) Abcam	1:200 (5 µg/mL)

Table II.9 – List of secondary antibodies used in this work.

Antibody	Conjugation	Reference/ Company	Dilution		
			WB	IHC	ICC
Goat anti-rabbit	HRP	Agilent Technologies	1:5000	1:100	-
Goat anti-mouse	HRP	Agilent Technologies	1:5000	-	-
Donkey anti-goat	HRP	Santa Cruz Biotechnology	-	1:100	-
Goat anti-chicken	Alexa Fluor 546	#A-11040 Thermo Fisher Scientific	-	1:400	-
Goat anti-mouse	Alexa Fluor 546	#A-11030 Thermo Fisher Scientific	-	1:400	-
Goat anti-rabbit	Alexa Fluor 488	#A-11006 Thermo Fisher Scientific	-	1:400	1:400
Donkey anti-goat	Alexa Fluor 488	#A-11055 Thermo Fisher Scientific	-	1:400	-
Donkey anti-mouse	Alexa Fluor 546	#A-21203 Thermo Fisher Scientific	-	1:400	-

Table II.10 – List of antibodies used for flow cytometry.

Antibody	Fluorochrome	Clone	Final dilution	Company
CD10	APC	CB-CALLA	1:10	Thermo Fisher Scientific
CD11c	PE	B-ly6	1:10	BD Biosciences
CD11c	APC	MJ4-27G12	1:10	Miltenyi Biotec (Bergisch Gladbach, Germany)
CD14	PE-Cy7	61D3	1:10	Thermo Fisher Scientific
CD19	APCe780	HIB19	1:10	Thermo Fisher Scientific
CD19	eFluor 450	SJ25C1	1:10	Thermo Fisher Scientific
CD33	APC	P67.6	1:10	BD Biosciences
CD33	BV711	WM53	1:10	BD Biosciences
CD34	APC	581	1:10	BD Biosciences
CD34	PerCP	8G12	1:10	BD Biosciences
CD38	APC-eFluor 780	HIT2	1:10	Thermo Fisher Scientific
CD38	PE-Cy7	HB7	1:10	Thermo Fisher Scientific
CD45RA	PE-Cy7	HI100	1:10	Thermo Fisher Scientific
CD45RA	APC Fire 750	HI100	1:10	Biolegend (San Diego, CA, EUA)
CD56	BV605	5.1H11	1:10	Biolegend
CD90	BV605	5E10	1:10	BD Biosciences
CD90	PE	5E10	1:10	Thermo Fisher Scientific
CD135	BV711	4G8	1:10	BD Biosciences
CD271	AF647	C40-1457	1:10	BD Biosciences
Cleaved Notch1 (Val1744)	-	Polyclonal	1:200	Cell Signaling Technology (#2421 discontinued)
Cleaved Notch2 (Asp1733)	-	Polyclonal	1:200	Abcam Plc (#ab52302 discontinued)
Ki67	FITC	B56	1:5	BD Biosciences
Lineage	eFluor 450	RPA-2.10, OKT3, 61D3, CB16, HIB19, TULY56, HIR2	1:10	Thermo Fisher Scientific
Mouse IgG1 κ isotype control	PE	MOPC-21	1:10	BD Biosciences
Mouse IgG1 κ isotype control	FITC	MOPC-21	1:10	BD Biosciences
Mouse IgG2a κ isotype control	PE	G155-178	1:10	BD Biosciences
Notch1	PE	MHN1-519	1:20	BD Biosciences
Notch2	PE	MHN2-25	1:20	BD Biosciences
Notch4	PE	MHN4-2	1:20	BD Biosciences
Notch4 (for intracellular staining)	-	Polyclonal	1:625	Santa Cruz Biotechnology (#sc-5594 discontinued)

APPENDIX III – qPCR PRIMERS

Table II.11 – List of qPCR primers used in this work.

Cell Cycle Regulators	**Forward**	**Reverse**
CCNA2	5'-CGCTGGCGGTACTGAAGTC-3'	5'-AAGGAGGAACGGTGACATGC-3'
CCNB2	5'-ACACCAAAGTTCCAGTTCAACC-3'	5'-TCAATGTCCTCGATTTTGCAG-3'
CCND1	5'-GAACAAACAGATCATCCGCAAAC-3'	5'-GCGGTAGTAGGACAGGAAGTTG-3'
CCND2	5'-CTACCTTCCGCAGTGCTCCTA-3	5'-CCAAGAAACGGTCCAGGTAA-3'
CCND3	5'-TGATTGCACATGATTTCCTGG-3'	5'-CGGGTACATGGCAAAGGTATAAT-3'
CCNE1	5'-ATCAGCACTTTCTTGAGCAACA-3'	5'-TTGTGCCAAGTAAAAGGTCTCC-3'
CDK2	5'-TGGTGTGGCCAGGAGTTACTT-3'	5'- CCGCTTGTTAGGGTCGTAGTG-3'
CDK4	5'-CAGATGGCACTTACACCCGT-3'	5'-CAGCCCAATCAGGTCAAAGA-3'
CDK6	5'-AGTTTCCAGATGGCTCTAACCT-3'	5'-TTCTACGAAACATTTCTGCAAAT-3'
CDKN1A	5'-CCTGTCACTGTCTTGTACCCTTG-3'	5'-AGAAGATCAGCCGGCGTTT-3'
CDKN1B	5'-TAATTGGGGCTCCGGCTAACT-3'	5'-TTGCAGGTCGCTTCCTTATTC-3'
CDKN1C	5'-TCTGATCTCCGATTTCTTCGC-3'	5'-TGCTGCTACATGAACGGTCC-3'
CDKN2C	5'-GGGGGGACCTAGAGCAACTTACT-3'	5'-CAGCAAAGTCTGTAAAGTGTCCA-3'
HSPC Differentiation		
CEBPA	5'-TTGTGCCTTGGAAATGCAAA -3'	5'-TTAGGTTCCAAGCCCCAAGTC -3'
GATA1	5'-AGGCCTACAGACACTCCCCA-3'	5'-TGCCTTTTCCATCCAGATCTT-3'
MPO	5'-CTGCTGCCCTTTGACAACCT-3'	5'-CCGAAGTAAGAGGGTGTGCAT-3'
SPI1	5'-CACAGCGAGTTCGAGAGCTT-3'	5'-GATGGGTACTGGAGGCACAT-3'
Housekeeping		
GAPDH	5'-GGGAAGGTGAAGGTCGGAGT-3'	5'-GGGTCATTGATGGCAACAATA-3'

APPENDIX IV – SOLUTIONS

Annealing buffer

100 mM Potassium acetate

30 mM HEPES pH7.4

2 mM Magnesium acetate

Dissolved in milli-Q® water

Stored at -20°C

Blocking solution

5% (w/v) skimmed milk powder

0.05% (v/v) Tween®20

Dissolved in TBS

Stored at 4°C for 1 week

Laemmli buffer 6×

375 mM Tris-hydrochloride pH 6.8

12% SDS

60% Glycerol

0.06% Bromophenol blue

0.6 M Dithiothreitol (DTT)

Dissolved in milli-Q® water

Stored at -20°C

TAE 25×

1 M Tris-base

25 mM EDTA

0.5 M Glacial Acetic Acid

Dissolved in milli-Q® water

Adjusted to pH 8.6

Stored at RT

TBS 20×

1 M Tris-base

3 M NaCl

Dissolved in milli-Q® H_2O

Adjusted to pH 7.6

Stored at RT

II.7. REFERENCES

1. Fellmann C, Hoffmann T, Sridhar V, Hopfgartner B, Muhar M, Roth M et al. An optimized microRNA backbone for effective single-copy RNAi. Cell reports. 2013;5(6):1704-13.

2. Schneider CA, Rasband WS, Eliceiri KW. NIH Image to ImageJ: 25 years of image analysis. Nature Methods. 2012;9:671.

3. Livak KJ, Schmittgen TD. Analysis of relative gene expression data using real-time quantitative PCR and the 2(-Delta Delta C(T)) Method. Methods. 2001;25(4):402-8.

4. Schmittgen TD, Zakrajsek BA, Mills AG, Gorn V, Singer MJ, Reed MW. Quantitative reverse transcription-polymerase chain reaction to study mRNA decay: comparison of endpoint and real-time methods. Anal Biochem. 2000;285(2):194-204.

5. Winer J, Jung CK, Shackel I, Williams PM. Development and validation of real-time quantitative reverse transcriptase-polymerase chain reaction for monitoring gene expression in cardiac myocytes in vitro. Anal Biochem. 1999;270(1):41-9.

6. Pear WS, Nolan GP, Scott ML, Baltimore D. Production of high-titer helper-free retroviruses by transient transfection. Proceedings of the National Academy of Sciences. 1993;90(18):8392.

7. Meerbrey KL, Hu G, Kessler JD, Roarty K, Li MZ, Fang JE et al. The pINDUCER lentiviral toolkit for inducible RNA interference in vitro and in vivo. Proc Natl Acad Sci U S A. 2011;108(9):3665-70.

8. Certo MT, Ryu BY, Annis JE, Garibov M, Jarjour J, Rawlings DJ et al. Tracking genome engineering outcome at individual DNA breakpoints. Nat Methods. 2011;8(8):671-6.

9. Szulc J, Wiznerowicz M, Sauvain MO, Trono D, Aebischer P. A versatile tool for conditional gene expression and knockdown. Nat Methods. 2006;3(2):109-16.

10. Zhu MS, Xu LB, Zeng H, Shi XD, Wu WR, Liu C. Association of Notch1 with vasculogenic mimicry in human hepatocellular carcinoma cell lines. Int J Clin Exp Pathol. 2014;7(9):5782-91.

11. Delaney C, Varnum-Finney B, Aoyama K, Brashem-Stein C, Bernstein ID. Dose-dependent effects of the Notch ligand Delta1 on ex vivo differentiation and in vivo marrow repopulating ability of cord blood cells. Blood. 2005;106(8):2693-9.

CHAPTER III

NOTCH RECEPTOR-LIGAND INTERACTIONS IN HUMAN HAEMATOPOIETIC STEM AND PROGENITOR CELLS

III.1. INTRODUCTION

Many studies have now established that different Notch receptors and ligands have differential effects in distinct haematopoietic microenvironments and differentiation stages. For instance, although multiple Notch receptors such as N1, N2, and N3 as well as ligands Jag1, Jag2, Dll1, and Dll4 are expressed on thymocytes and/or thymic epithelium, T cell commitment and maturation appears to be mediated exclusively via N1-Dll4 interaction [1]. This is consistent with the finding that conditional inactivation of N2 does not affect T cell development but is instead necessary for marginal zone B cell specification [2]. Furthermore, Dll1 was proved to be essential for the generation of these cells, indicating that N2-Dll1 interaction is essential to specify this subclass of splenic B cells [3].

As previously described, a few studies have tried to understand the role of different Notch receptor-ligand interactions in human HSPC regulation *in vitro* (sections **I.2.2.3** and **I.3.2**). However, all these studies have focused not only on the effect of either one or two Notch ligands but also the presentation of Notch ligands, culture media and the input HSPC population have all been widely variable. For instance, presentation of Notch ligands is either carried out through co-culture with BM endothelial cells that naturally express Jag1 and Jag2, but not Dll1 and Dll4 [4-6], BM stromal cell lines (S17 and OP9) overexpressing Dll4, Dll1 or Jag1 [7-13] or through immobilised Dll1 [14-17].

Therefore, there is still a lack of more comprehensive studies that compare the effects of different ligands under the same *in vitro* conditions and explore the molecular mechanisms triggered by these interactions. This chapter aims to distinguish the effects of the different Notch ligands on CB HSPCs *in vitro* through a side-by-side comparison. This allows to evaluate their effect in HSPCs *ex* vivo maintenance, the respective activated mechanisms and the preferential Notch receptor activation to help better understand the roles of different Notch receptor-ligand interactions and preferential pairings.

Specific Notch receptor activation can be technically challenging to analyse since the usual tools to assay Notch signalling activation focus on canonical Notch target genes,

like the expression of *HES1* [18]. Also, to verify if a specific Notch receptor is being activated one must make sure that the ab is specific for the cleaved form of that receptor. To this end, the ab specificity must be verified by WB. Furthermore, to corroborate flow cytometry data, it is good practice to verify the receptors expression by WB. Thus, given that there was no established protocol in the lab for Notch receptors detection by WB, another aim of this chapter was to optimise these protocols and validate the detection of activated Notch receptors (sections **III.2.1** and **III.2.2**).

III.2. RESULTS

III.2.1. OPTIMISATION OF WESTERN BLOT FOR DETECTION OF NOTCH RECEPTORS IN LOW PROTEIN SAMPLES

The first aim of this study was to establish WB protocols that would allow to identify the different protein forms of each Notch receptor (N1, N2 and N4) in total protein extract. The expression of the N3 receptor was not assessed, as it was previously shown that this receptor is absent on human HSPC [19]. Notch receptors expressing (positive) cell lines were used and decreasing quantities of total protein extracts were tested to assess the minimum amount that is required to detect Notch proteins by the respective abs, as this will be crucial for detection in low protein extracts from HSPC lysates.

Notch abs against the Notch receptor C-terminus should be able to detect the main forms of these receptors: the Notch immature full length (NFL), the Notch transmembrane form (NTM) that corresponds to the mature receptor after S1 cleavage and the Notch cleaved forms NEXT and NICD generated after S2 and S3 cleavage respectively (**Figure I.2**). Of note, due to the SDS-PAGE reducing conditions the calcium noncovalent bond of the transmembrane receptor is disrupted and therefore an antibody against the C-terminus of a Notch receptor will only detect the transmembrane subunit of the receptor [20]. There are also commercially available abs that can supposedly detect specifically the activated forms of N1 and N2. These abs recognise and bind to the N-terminus domain of NICD that is only accessible for the antibody binding when the receptor is cleaved and exposed.

Table III.1 shows the predicted protein sizes for the different forms of each Notch receptor based on the predicted cleavage sites of each individual Notch receptor [20-26]. While for N1 receptor the precise cleavage sites have been identified for S1 [22], S2 [23] and S3 [21], for N2 receptor only S1 and S2 sites have been confirmed [25, 26]. On the other hand, N2 S3 site and all N4 cleavage sites have only been predicted based on consensus sequences amongst the receptors [24, 27], and therefore the expected sizes for the resultant forms of these cleavages must be regarded as prediction only.

Table III.1 – Predicted protein sizes of the different forms of Notch receptors 1, 2 and 4 and predicted cleavage sites.

Notch Receptor	Pred. Protein Sizes (KDa)				Pred. Cleavage Sites
	NFL	NTM	NEXT	NICD	
Notch1 (2555 a.a)	280	98	92	88	S1 – R1665 S2 – V1722 S3 – V1754
Notch2 (2471 a.a)	270	95	89	85	S1 – R1608 S2 – V1666 S3 – V1697
Notch4 (2003 a.a)	220	74	63	59	S1 – R1330 S2 – V1432 S3 – V1467

Cell lines and primary cells that are positive and negative for the expression of each Notch receptor were previously screened in the lab for the extracellular Notch expression by flow cytometry (data not shown). Based on these results, Notch receptor expressing cell lines were used for Notch receptors detection by WB such as, the haematopoietic cell lines Molt4, Raji and Jurkat for N1, N2 and N4, respectively. Furthermore, a high concentration EDTA treatment (described in section **II.1.3.1**) was also applied to these cells before protein extraction, which has been shown to promote Notch receptor S2 cleavage thus, increasing the NEXT and NICD forms [28].

As illustrated in **Figure III.1A**, the ab against the C-terminus of N1 clearly detected all forms of the N1 receptor in Molt4, a well-known T-ALL cell line with high N1 expression. Thus, N1 was detected even when loading only 5 µg of Molt4 total protein extract, whereas no expression was detected in the primary AML sample, which is in accordance with previous studies demonstrating that Notch signalling is silenced in the majority of primary AML samples [29, 30]. Furthermore, this immunoblot clearly shows a reduction of the band correspondent to the N1TM form (~100 KDa) resultant from EDTA-promoted S2 cleavage, whereas the cleaved N1 receptor increased in expression upon EDTA treatment. Of note, when using an ab against the C-terminus it is difficult to distinguish or surely affirm if the bands bellow the NTM correspond to the NEXT or NICD forms. Also, the N1ICD can appear as a double band corresponding to posttranslational modifications as previously reported [21].

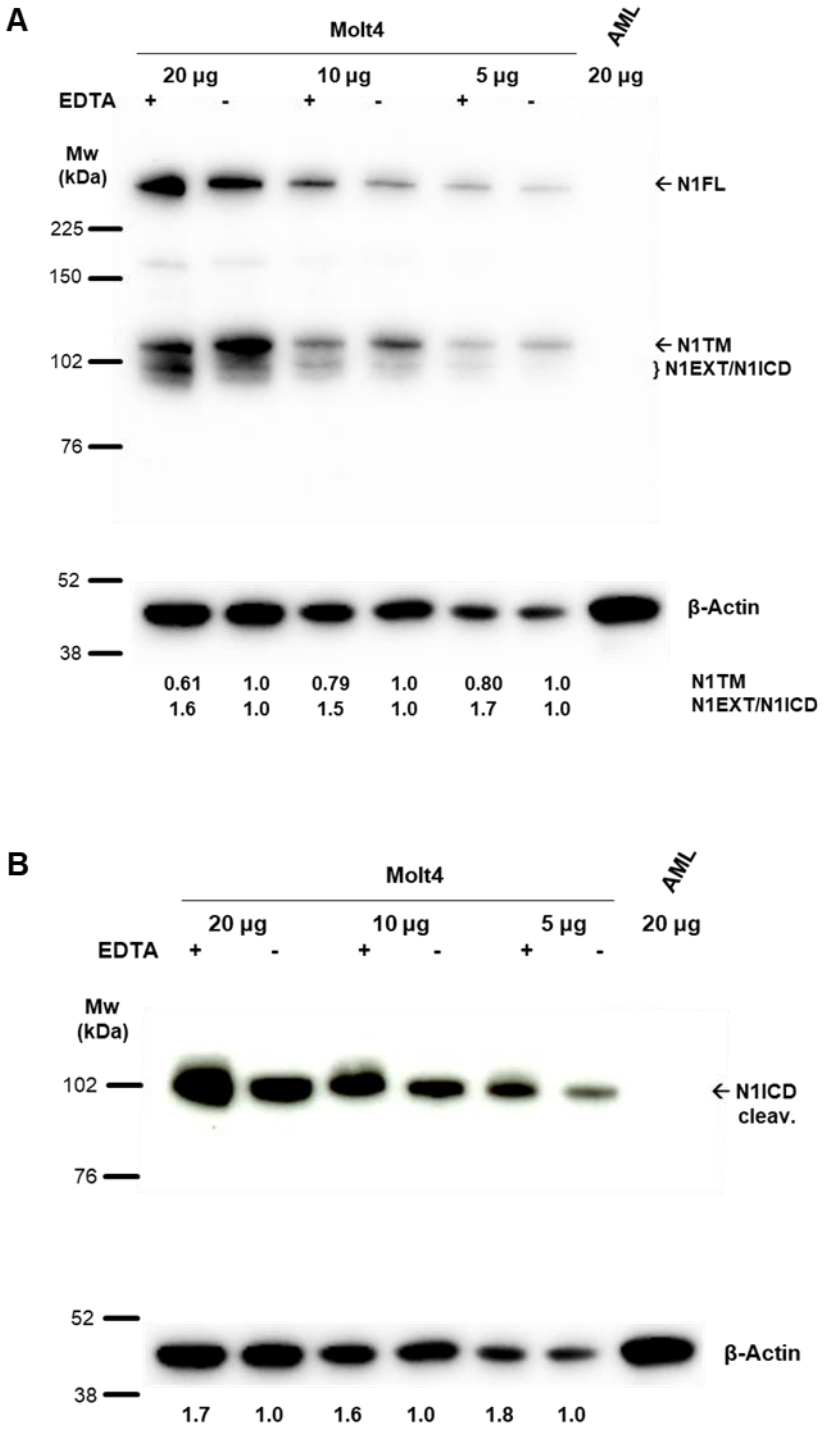

Figure III.1 – Representative immunoblots probing for Notch1 (N1) in lysates in different cells. N1 expressing cells (Molt4) were either treated (+) or not (-) with EDTA for 15 min at 37°C followed by 45 min in fresh medium prior to protein extraction. Samples were probed with ab against the C-terminus of N1 (**A**) and with ab against the N-terminus of cleaved/activated N1 (**B**). Protein bands of N1TM and N1ICD were quantified and normalised to β-actin. The values shown are the fold change relative to the untreated samples (β-Actin normalised). A primary AML sample was used as negative control for Notch1 expression.

Nevertheless, for the detection of N1ICD specifically, the immunoblot in **Figure III.1B** shows that using the anti-N-terminus of N1ICD ab only one band (<100 KDa) was detected, which accordingly showed increased signal upon EDTA treatment. No expression was detected in the primary AML sample which demonstrates the specificity of this antibody

The anti-N2 ab against the C-terminus of N2 was able to detect the three receptor forms in Raji cells, although only in the samples treated with EDTA the cleaved form was visible (**Figure III.2A**). While this ab was able to detect N2 with 10 µg of protein extract, the ab against the cleaved N2ICD was only efficient in detecting the cleaved form when at least 20 µg of protein were loaded (**Figure III.2B**). As observed above, EDTA treatment induced a reduction in the TM form of N2 with a concomitant increase in the cleaved form which was detected with both abs, with the expected protein size of <100 KDa. N2 expression was not detected in the primary AML sample thus, demonstrating the specificity of these antibodies.

For N4 receptor, no reliable antibody to detect specifically the activated/cleaved form of N4ICD was found. Using one ab against the C-terminus of N4 the expected N4TM band of ~70 KDa in size was detected (**Figure III.3A**) in the N4 expressing Jurkat cell line. As expected, low N4TM expression was detected in the N4 negative/low expressing HeLa cells. However, this monoclonal antibody was not able to detect the N4ICD even in samples treated with EDTA. In addition, it was also difficult to detect the N4FL that was expected using this monoclonal antibody. Instead, a different anti-N4 ab was able to efficiently detect the N4ICD form (**Figure III.3B**), showing a band above 40 KDa with increased signal in samples treated with EDTA, even with a minimum of 3 µg of protein extract. For unknown reasons, this ab was not able to detect the NFL and NTM forms of N4 in Jurkat cell lysates as was expected to do. Please refer to **Table II.7** (chapter II) for detailed information on the antibodies and concentrations used in this study.

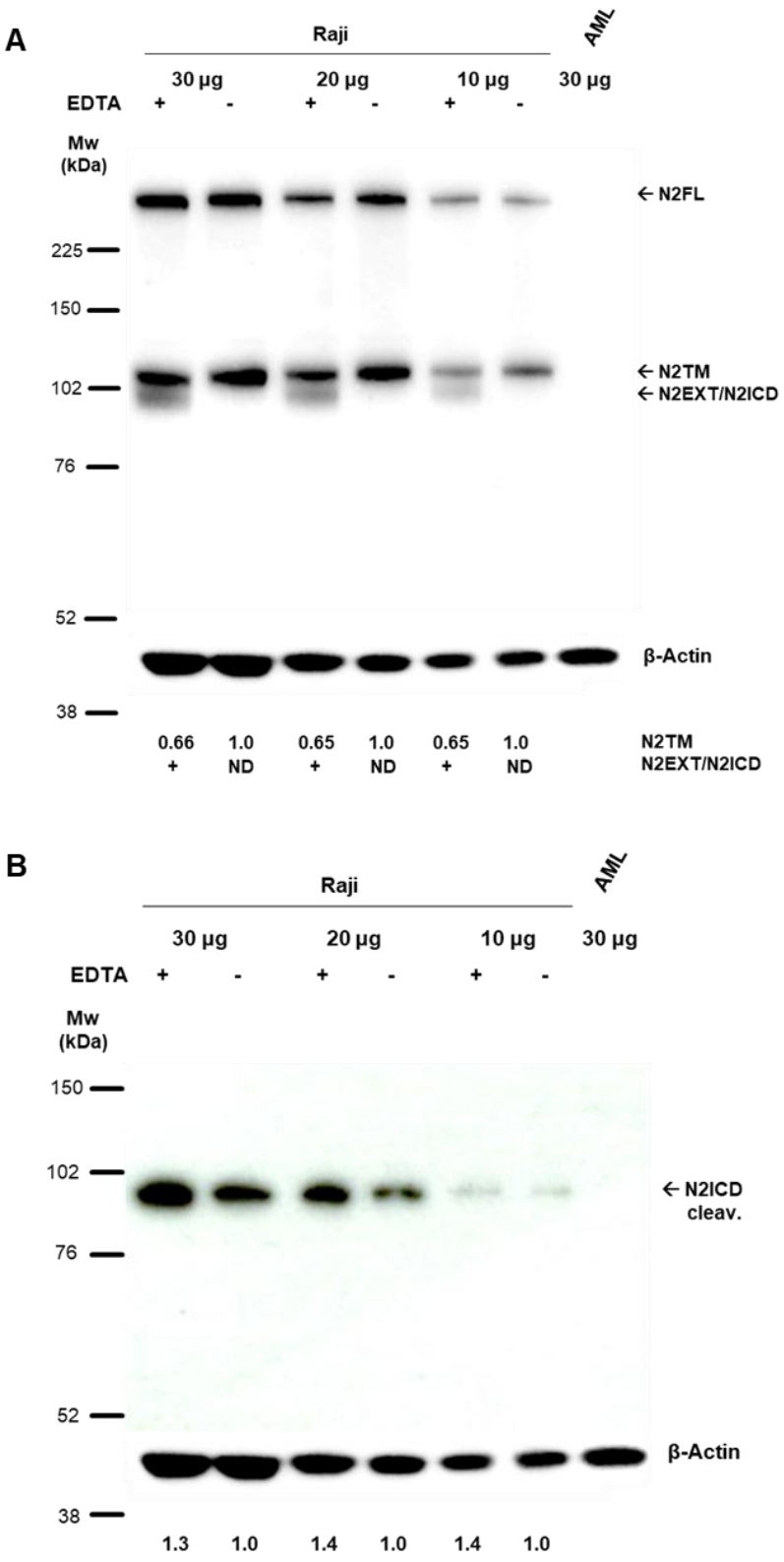

Figure III.2 – Representative immunoblots probing for Notch2 (N2) in lysates from different cells. N2 expressing cells (Raji) were either treated (+) or not (-) with EDTA for 15 min at 37°C followed by 45 min in fresh medium prior to protein extraction. Samples were probed with ab against the C-terminus of N2 (**A**) and with ab against the N-terminus of cleaved/activated N2 (B). Protein bands of N2TM and N2ICD were quantified and normalised to β-actin. The values shown are the fold change relative to the untreated (β-Actin normalised) samples. A primary AML sample was used as negative control for Notch2 expression.

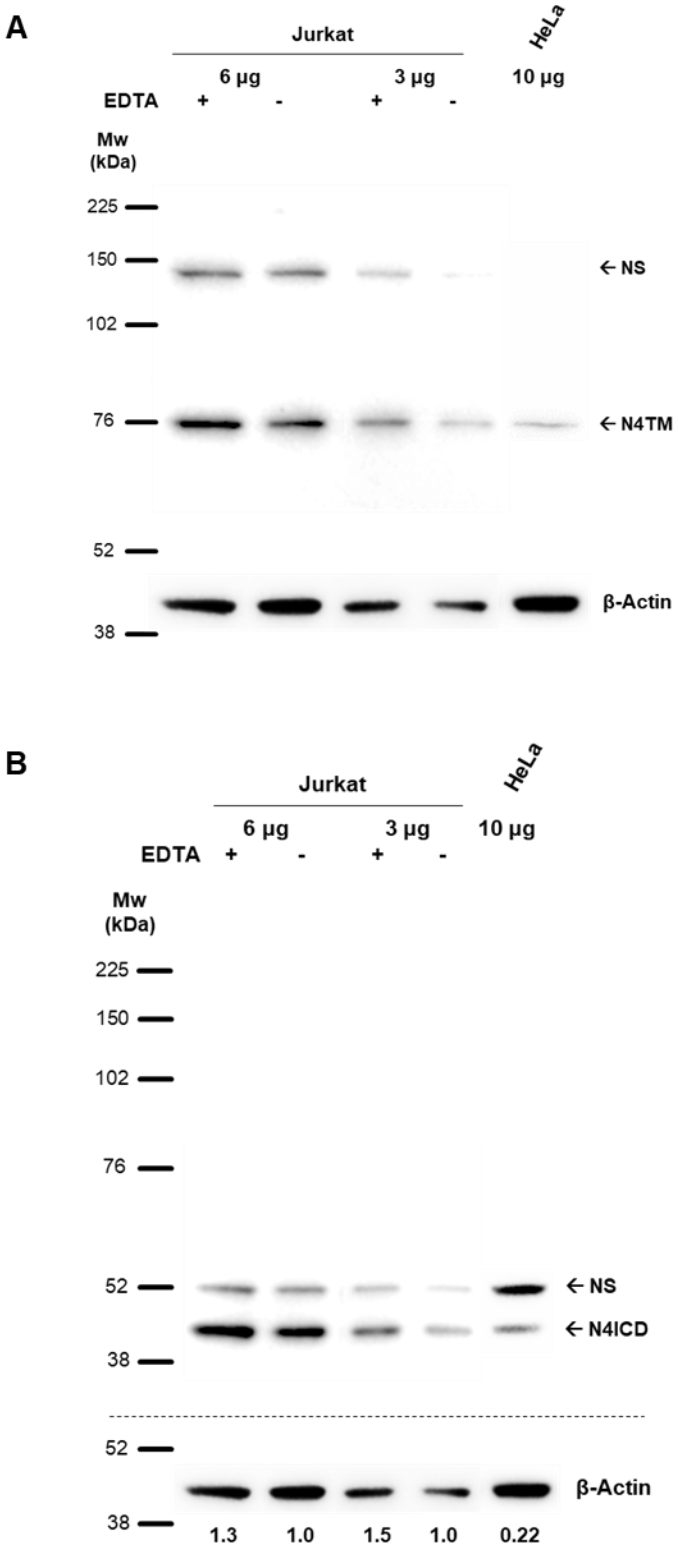

Figure III.3 – Representative immunoblots probing for Notch4 (N4) in lysates from different cell lines. N4 expressing cells (Jurkat) were either treated (+) or not (-) with EDTA for 15 min at 37°C followed by 45 min in fresh medium prior to protein extraction. Samples were probed with two different antibodies against the C-terminus of N4. (**A**) The monoclonal ab (L5C5) detects the N4TM domain while the polyclonal ab (H-225) detects the N4ICD (**B**). Protein bands of N4ICD were quantified and normalised to β-actin to confirm N4 activation in EDTA-treated samples and low N4 activation in HeLa cells. Ratio of N4ICD expression in HeLa cells is relative to sample of Jurkat with 6 µg without EDTA.

Of note, some variability of Notch receptors protein level was observed between different cell lines in the immunoblots (data not shown) therefore, higher amounts of total protein may be necessary for HSPCs if these cells have a lower receptor expression. Nevertheless, a minimum of 10 µg of total protein extract appears to be sufficient for detection with all the abs tested with the exception of the anti-N2ICD ab which may require at least 20 µg of protein extract.

III.2.2. Detection of Intracellular/Activated Notch Receptors by Flow Cytometry

It was also necessary to search for abs able to detect each activated Notch receptor that would allow to quantify the activation of each receptor by FCM, which is a more convenient and less time consuming method. Furthermore, these abs would be used to detect receptor activation in different HSPCs populations all in one assay/analysis by combining with cell surface antigens staining.

As above, the specificity of each anti-cleaved Notch receptor ab was previously validated by WB which demonstrated that only the cleaved form of the respective protein was detected. As such, different cell lines and primary cells for Notch activation were used to validate the detection of expression of the different NICDs by FCM, ICC and WB (**Figure III.4**). The Notch negative/low expressing cells used were primary AML, Saos2 and HeLa cells for N1ICD, N2ICD and N4 respectively. Also, the y-secretase inhibitor Compound E (compE) was added to Saos2 and HeLa cells to further decrease the Notch activation in these cell lines.

The anti-N1ICD ab previously validated by WB (**Figure III.1B**) was then used to detect the expression of N1ICD in Molt4 cells by FCM, which was successful. The data shows that a near 2-fold higher MFI (mean fluorescence intensity) was obtained as compared to the no primary ab control condition. As expected, in primary AML cells the staining achieved with the anti-N1ICD ab showed no difference as compared to the no primary ab control condition (**Figure III.4Ai**). These results were also corroborated by the ICC staining (**Figure III.4Aii**) and further validated by WB (**Figure III.4Aiii**). Altogether, these results support that this anti-N1ICD ab can be used in FCM analysis.

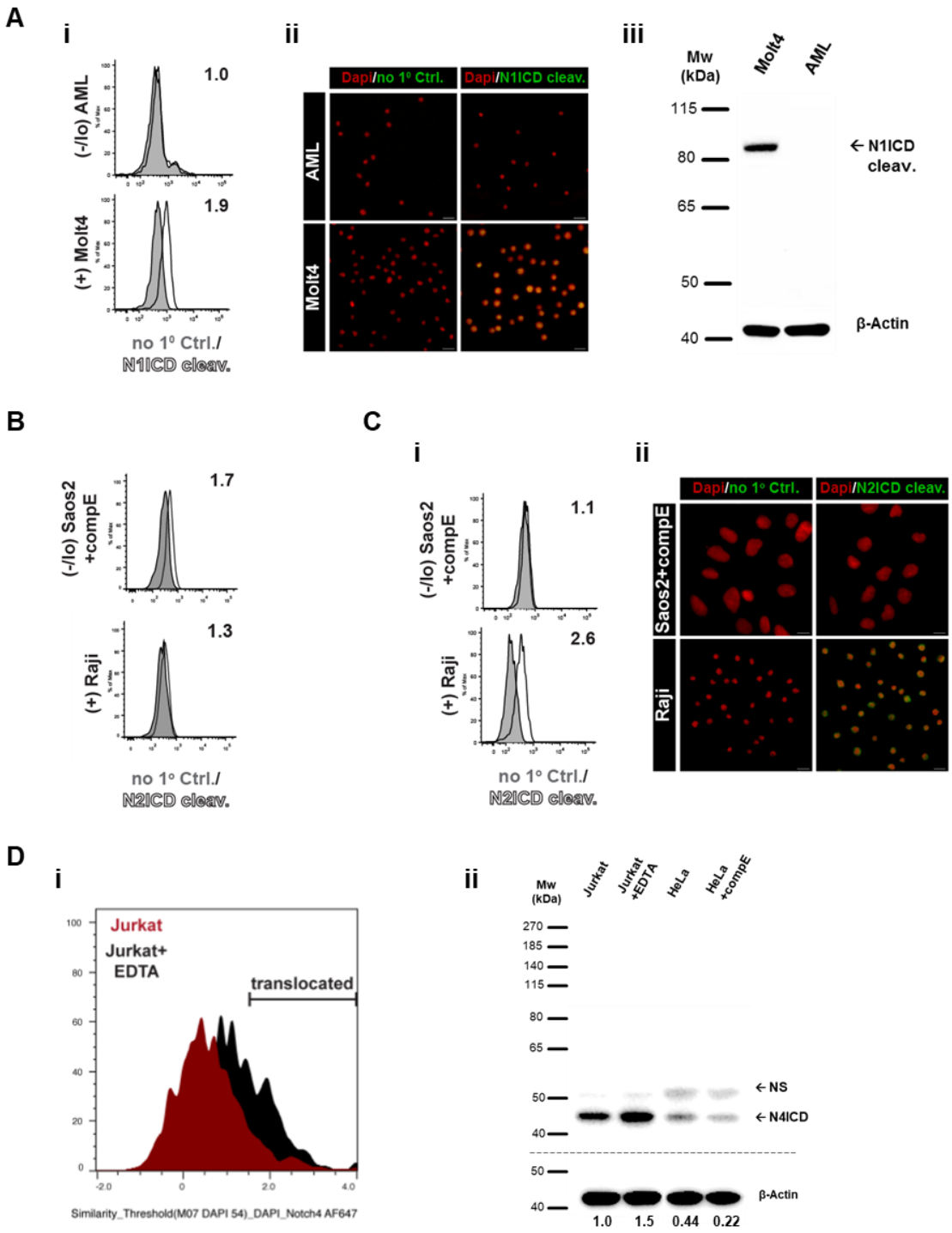

Figure III.4 – Detection of the cleaved forms of Notch receptors using FCM, ICC and WB performed with the indicated Notch expressing cells. (A) Representative FCM histograms **(i)**, immunofluorescence pictures **(ii)** and immunoblot **(iii)** of Molt4 and AML cells/cell lysates probed with ab against the N-terminus of cleaved N1. **(B)** Representative FCM histograms of Saos2 cells (treated with compE) and Raji cells probed with the polyclonal ab PA5-37433 against the N-terminus of cleaved N2. **(C)** Representative FCM histograms **(i)** and immunofluorescence pictures **(ii)** of Raji and Saos-2 (treated with compE) cells probed with the polyclonal ab ab52302 against the N-terminus of cleaved N2. **(Di)** ImageStream histograms showing the colocalisation of DAPI and the ab against C-terminus of N4 stains in Jurkat cells with and without EDTA treatment. **(Dii)** Immunoblot from Jurkat (with and without EDTA) and HeLa (with and without compE treatment) cell lysates probed with ab against C-terminus of N4; Fold change relative to untreated Jurkat (β-Actin normalised). The values in FCM histograms indicate the MFI ratio between the respective staining and no primary ab control. Scale bars: 5 µm.

To detect the expression of the cleaved form of N2 by FCM, unfortunately the ab previously validated by WB (**Figure III.2B**) was not able to detect the difference in N2ICD expression between the N2 expressing and non-expressing cells used (**Figure III.4B**). Therefore, a different ab (ab52302) was used instead. The data showed that when detecting N2ICD in Raji cells a 2.6-fold increase in MFI was achieved between the anti-N2ICD and the no primary antibody staining condition, while in Saos2 cells treated with compE no difference in MFI was observed between the two staining conditions (**Figure III.4Ci**). These results were further supported by the ICC stainings (**Figure III.4Cii**). Unfortunately, this ab has been discontinued and it was not possible to validate it by WB. Of note, another commercially available ab for cleaved N2 (07-1234) was tested by WB with different concentrations and with different ab production lots, from which no specificity was found. This was because the observed bands were smaller than expected (<80 kDa) and showed no differences between the different N2 expressing cell lines and EDTA treatment (data not shown). In summary, these results support that the anti-N2ICD PA5-37433 ab can be used to detect specifically N2ICD in WB, while the ab52302 is suitable for FCM studies.

Regarding N4ICD, because the ab previously validated (**Figure III.3B**) could efficiently detect the N4ICD form but it is not entirely specific to it, the activation of N4 must be quantified by ImageStream flow cytometry which allows to analyse the amount of N4ICD translocated into the nucleus upon N4 activation/cleavage by analysing its colocalisation with DAPI. Using this method, an increase in N4ICD expression in the nucleus was observed when the cells were treated with EDTA (**Figure III.4Di**). In agreement, immunoblotting experiments with this ab also showed an increase in the detection of N4ICD when Jurkat cells were treated with EDTA, whereas the expression of N4ICD detected in HeLa cells lysate was further decreased when these cells were treated with compE (**Figure III.4Dii**). In conclusion, due to the lack of a specific anti-N4ICD ab available, N4 translocation studies either using this method or others such as WB using nuclear extracts is required to properly detect the N4ICD form in cells.

III.2.3. NOTCH RECEPTORS EXPRESSION AND ACTIVATION IN UCB HSPCS AND HSCS

The expression of the different Notch receptors and their respective levels of activation in human HSPCs have not been properly investigated. Almost all reports refer to Notch receptors expression based on mRNA quantification which may not correlate to the protein level. Only recently, Anjos-Afonso *et al.* quantified the expression of extracellular Notch receptors on different CB HSPCs populations by FCM [19].

In order to first assess the importance of each Notch receptor for HSPCs and HSCs, the expression of extracellular Notch receptors and intracellular NICDs were quantified by FCM in these populations. **Figure III.5** shows the gating strategy used to identify HSPCs ($CD34^+CD38^-$) and phenotypically defined HSCs ($CD34^+CD38^-CD45RA^-CD90^+$).

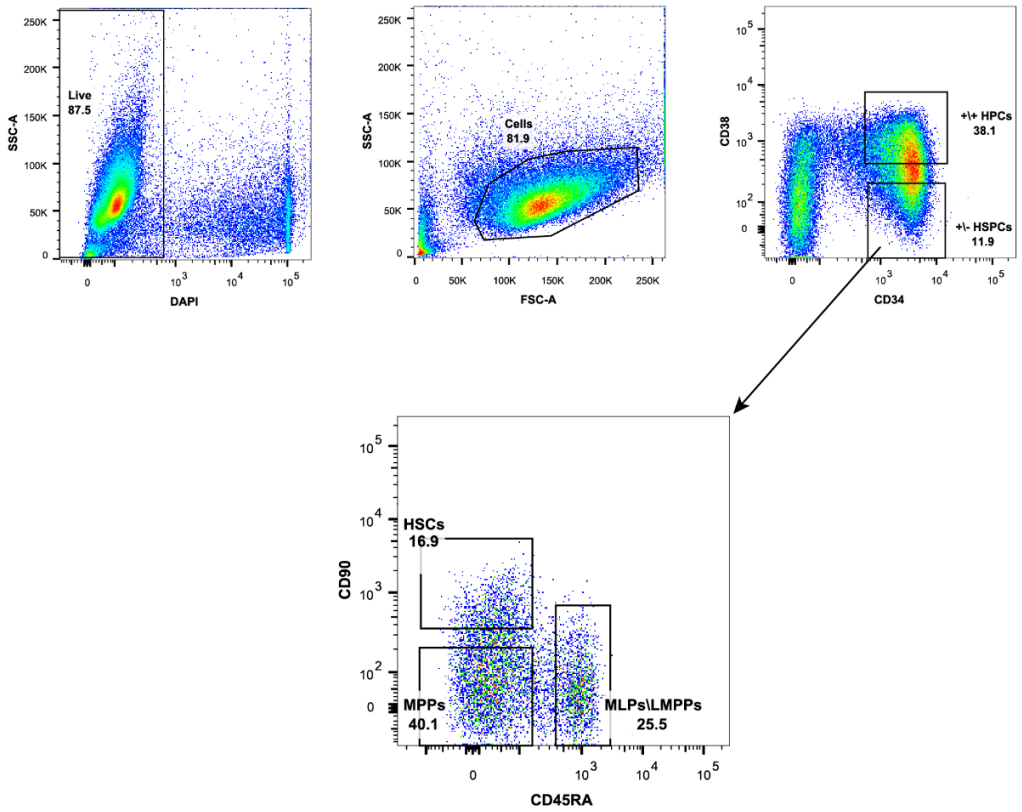

Figure III.5 – Gating strategy of different UCB haematopoietic populations. In the $CD34^+$ compartment HSPC population is distinguished from the more committed progenitors population (HPC) by the lack of CD38 expression. Within the $CD34^+CD38^-$ compartment, HSCs and less committed progenitors populations (MPP and MLP/LMPP) can be identified based on CD90 and CD45RA expression.

The expression of extracellular Notch receptors was then quantified on HSPC and HSC populations (**Figure III.6**). Please refer to **Table II.10** for details on the human Notch receptors antibodies and concentrations used in this study. All abs were previously titrated and validated using different cell lines to detect the presence or lack of expression of the different Notch receptors. In addition to this, the Chinese hamster ovary cell line (CHO) was also used to further validate the specificity of the antibodies employed (**Figure III.6A**). When comparing to the respective Notch receptor expressing cell line, N1 and N2 were found to be highly expressed on HSCs. On the other hand, extracellular N4 was not detected on HSPCs and HSCs although N4 expression was clearly detected on Jurkat cells. Importantly, the expression of extracellular Notch receptors on HSCs did not differ from the overall HSPCs population (**Figure III.6B**).

Then, using the validated abs for detecting N1ICD and N2ICD by FCM (**Figure III.7A**), and N4 nuclear translocation by ImageStream (**Figure III.7B**), the activation of the respective Notch receptor was determined in the HSC and HSPC populations (**Figure III.7C**, work previously performed by António Soure). In accordance with the pattern of extracellular expression, activation of N1 and N2 was more significant than N4. Indeed, only less than 9% of cells were found to have nuclear N4 expression. Furthermore, the data shown suggest that HSCs have higher activation of N1 and N2 in particular as compared to HSPCs. These data also infer that the levels of extracellular expression may not correlate to the degree of receptor activation, since HSCs levels of N1 and N2 extracellular expression are similar to HSPCs, but HSCs have increased activation of these receptors.

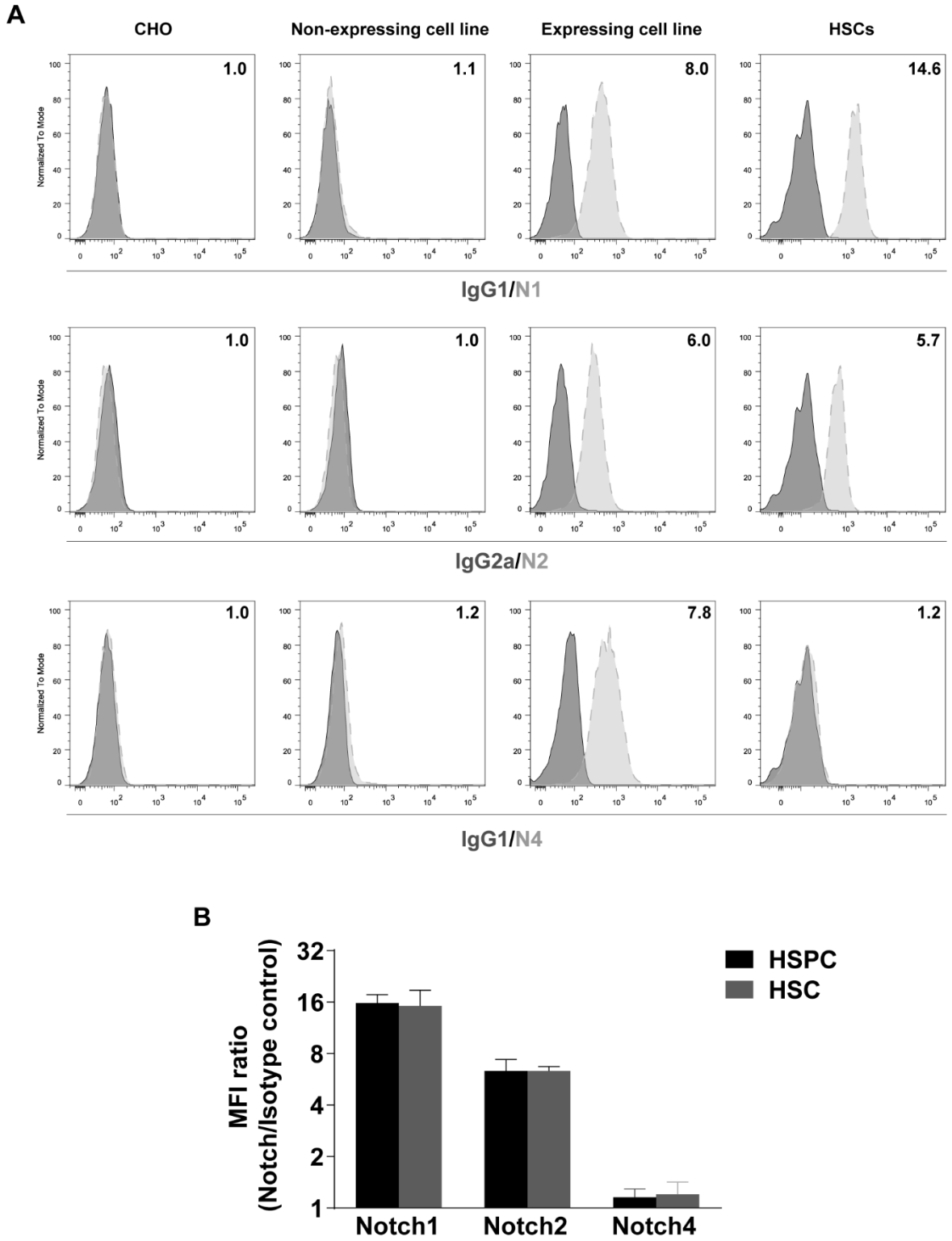

Figure III.6 – Expression of extracellular Notch receptors on UCB HSPC and HSC populations. (**A**) Representative histograms of each Notch receptor (light grey) and respective isotype control (dark grey) stainings on the indicated Notch receptor non-expressing cell lines (CHO cells for all; U266 for N1 and K562 for N2 and N4) and Notch receptor expressing cell lines (Jurkat for N1 and N4 and Raji for N2) and HSC as the testing population. The values in the histograms indicate the MFI ratio between the Notch staining and respective isotype control. (**B**) Quantification of Notch receptors expression (MFI ratios) in the indicated haematopoietic populations (n=3). Error bars shown represent S.D.

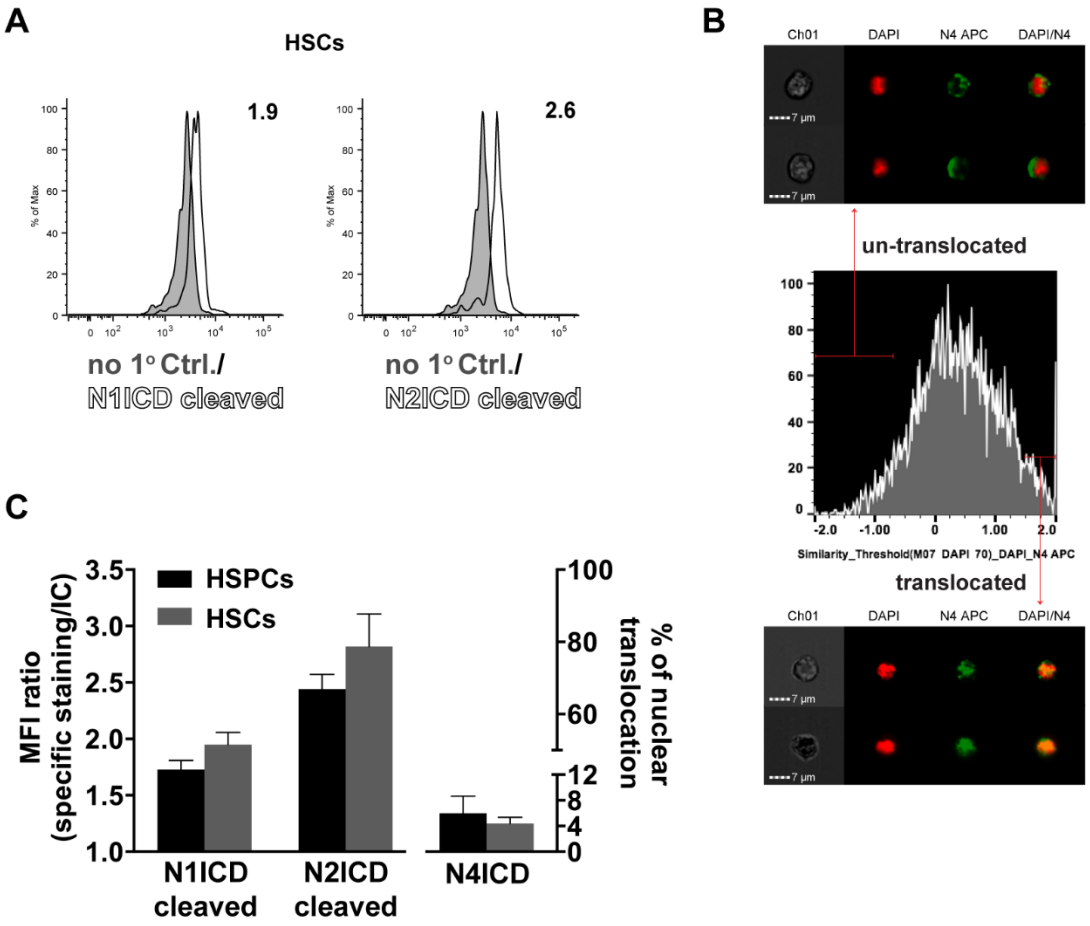

Figure III.7 – Notch receptors activation in HSPC and HSC populations. (**A**) Representative histograms of N1ICD and N2ICD stainings (white) compared to no primary ab control staining (grey) in HSC population. (**B**) Representative analysis of ImageStream data showing N4ICD nuclear translocation through colocalisation with DAPI staining. (**C**) N1ICD and N2ICD expression quantified by MFI ratio (NICD/control) and N4ICD quantified by the % of nuclear translocation (n=4). Error bars shown represent S.D.

III.2.4. NOTCH LIGANDS EXPRESSION IN HUMAN PLACENTA

To corroborate that CB HSPCs are likely to be exposed to Notch signals in their natural environment, the expression of Notch ligands Dll1, Dll4 and Jag1 was evaluated by IHC on tissue sections of human placental bed.

The human term placenta is comprised by highly vascularised foetal-derived chorionic plate and villi, the latter being in direct contact with the maternal blood that circulate in the intervillous space [31]. It was previously demonstrated that $CD34^+CD45^+$ haematopoietic cells can be found within placental villi stroma throughout gestation and that high percentages of $CD34^+CD38^-$ cells and SRCs can be isolated from collagenase treated vessels, suggesting the idea of an haematopoietic niche in the placenta villi [32].

Immunostaining of Notch ligands in sections of the chorionic villi revealed expression of Jag1 and in particular high levels of Dll4 (**Figure III.8**), whereas Dll1 expression was poorly detected (**Figure III.9**). While Dll4 expression was mainly detected on endothelial cells ($CD31^+$ cells) and syncytiotrophoblasts (**Figure III.8A**), Jag1 expression was found on endothelial, smooth muscle and stromal cells (**Figure III.8B**). On the other hand, Dll1 expression was found to be very scattered in the placenta and importantly at very low levels when compared to the expression observed on bladder urothelial cells [33] used as positive staining control. In fact, two polyclonal antibodies against Dll1 were tested to validate this observation (ab84620 and NBP2-27088 shown in **Figure III.9**) and only the ab ab84620 was able to detect scattered Dll1 expression in the placenta villi. Furthermore, Dll1 expression was only observed in a few areas of the tissue and appears to be exclusive to endothelial cells (represented in the first two images of both DAB and immunofluorescence stainings). However, in most of the placenta tissue no signal was detected. Of note, Dll1 expression was not detected in the same areas of the placenta tissue when using the ab NBP2-27088, although this antibody was able to clearly detect Dll1 on the urothelial cells. These observations suggest that Dll1 has a very low expression in the placenta haematopoietic niche unlike Dll4 and Jag1.

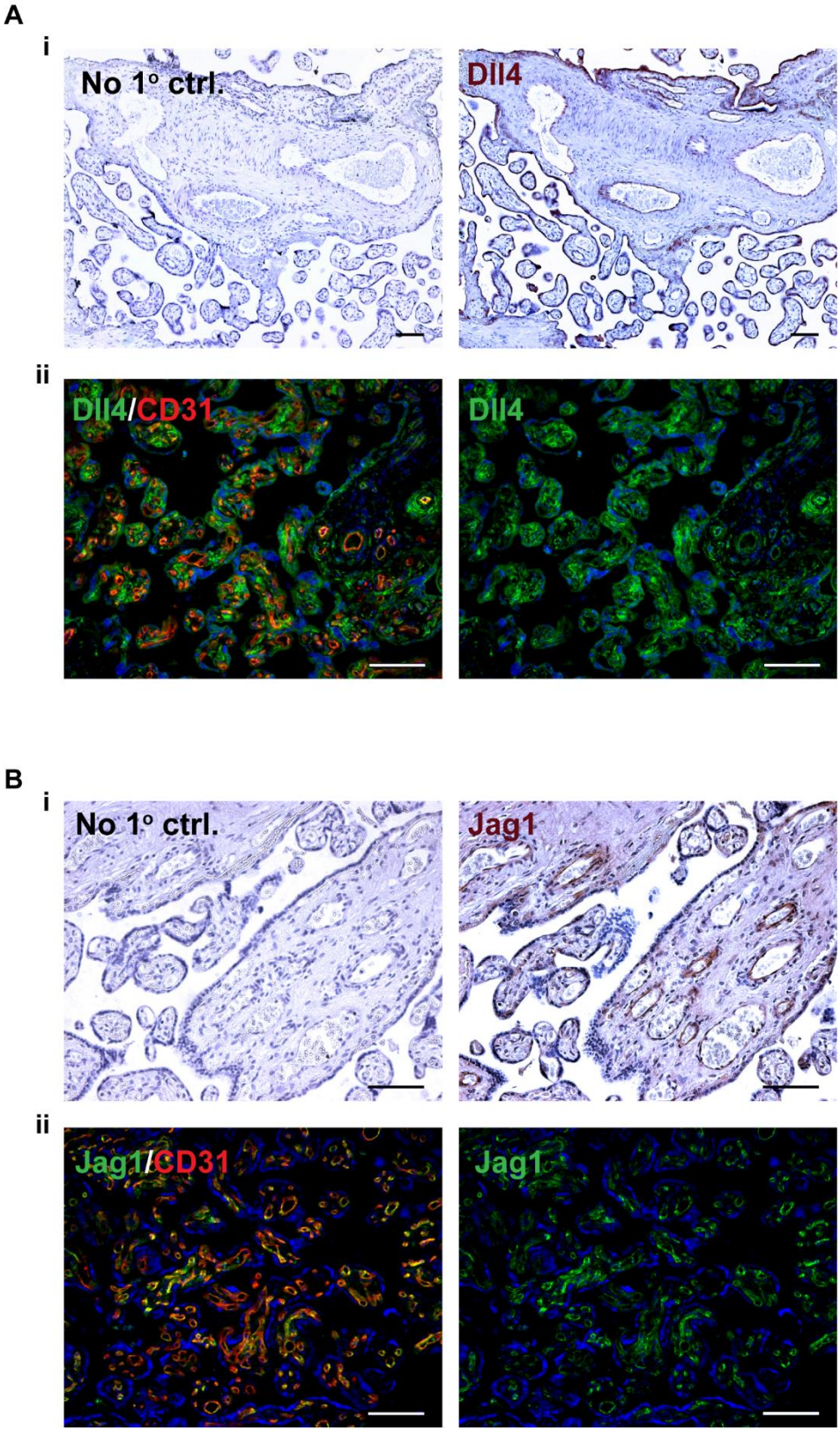

Figure III.8 – Immunohistochemistry staining of Dll4 (A) and Jag1 (B) on paraffin sections of human placental bed. (i) Representative image of Red AP staining without primary ab as negative control and Dll4 or Jag1 staining on the respective serial sections. **(ii)** Double-fluorescent immunostaining of Dll4 or Jag and CD31 counterstained with DAPI. Scale bars represent 100 µm.

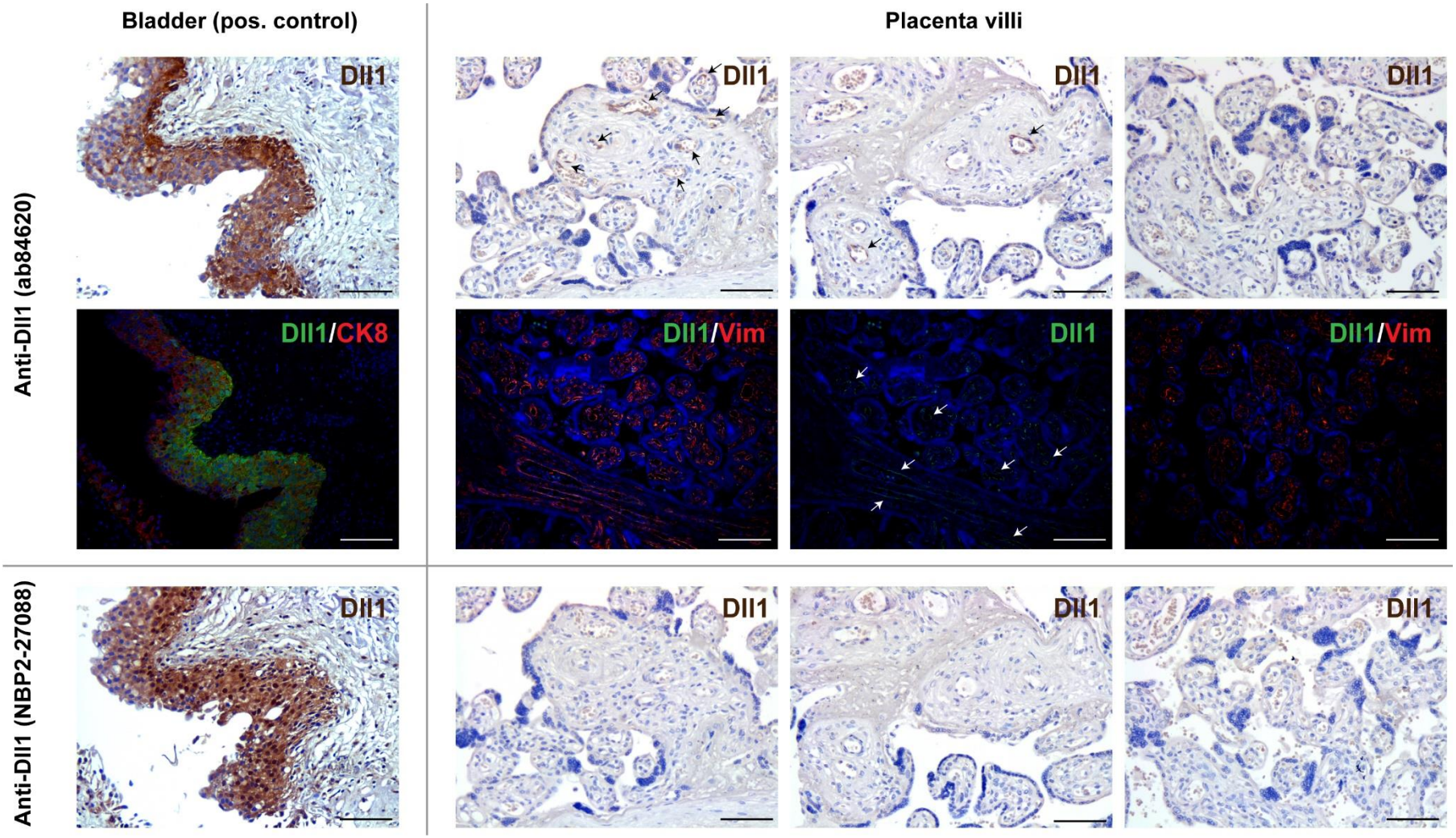

Figure III.9 – Immunohistochemistry staining of Dll1 on paraffin sections of human placental bed with two different anti-Dll1 abs. Human bladder tissue was used as positive control for Dll1 staining**.** For the ab ab84620 the first row of images shows representative DAB stainings with black arrows indicating Dll1 expression in placenta sections. Second row of images shows double-fluorescent immunostaining of Dll1 and CK8 or Vimentin (Vim) on bladder or placenta tissue, respectively. Tissues were counterstained with DAPI. For the ab NBP2-27088 representative DAB staining images show that Dll1 could not be detected in placenta sections. Scale bars represent 100 µm.

III.2.5. EFFECTS OF NOTCH LIGANDS INTERACTIONS WITH HSPCS *IN VITRO*

The observed results suggest that Notch signalling activation in freshly isolated HSPCs from CB could be mostly mediated by N1 and N2 interactions with Dll4 and/or Jag1 *in vivo.* To investigate the role of each Notch ligand on the regulation of CB HSPCs, an *in vitro* model with a stromal feeder layer was used to expose HSPCs to the Notch ligands. As depicted in **Figure III.10**, HSPCs were cultured on the stromal cell line S17, which is able to maintain HSPCs survival but promoting their differentiation [34]. S17 cells do not have significant expression of Notch ligands and therefore S17 overexpressing different ligands have been used before to assess their effect on haematopoietic cells [10, 19]. Hence, in this study $CD34^{+}CD38^{-}$ HSPCs were cultured either on parental S17 cells or on S17 cells engineered to overexpress either Dll1 or Dll4 or Jag1.

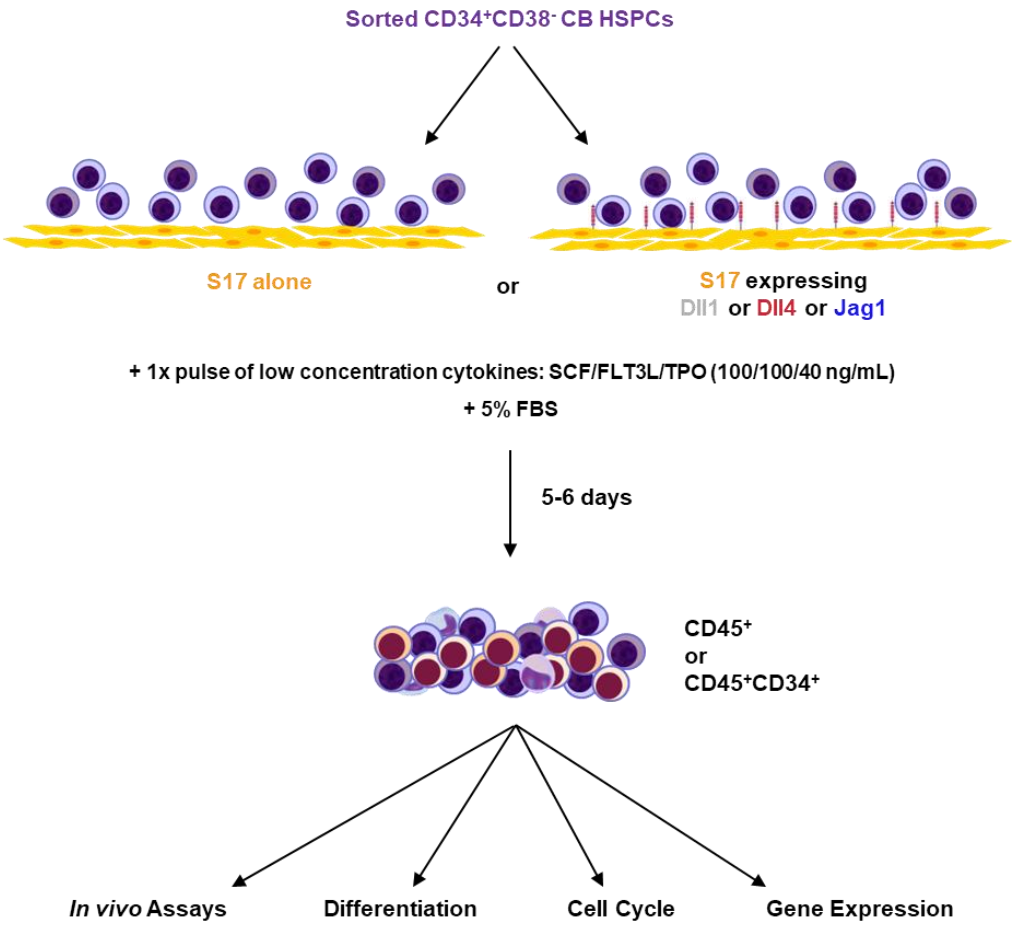

Figure III.10 – Schematic representation of the experimental work to identify the roles of Notch ligands Dll1, Dll4 and Jag1 in human HSPCs regulation.

Of note, as described in section **II.5.3**, these cultures were maintained in medium with low concentration of cytokines and presence of serum which is known to promote differentiation of HSPCs [35]. All cells were collected after 5-6 days of co-culture and the total haematopoietic cells ($CD45^+$) or the HSPC population ($CD45^+CD34^+$) were analysed for cell cycle, phenotype, gene expression, engraftment ability and SRC content.

Cell cycle analysis was performed by FCM in $CD45^+CD34^+$ HSPCs using Ki67 and DAPI staining as described in section **II.3.3**. From all the Notch ligands Jag1 promoted greater effect in blocking HSPCs cell cycle progression (**Figure III.11A, B**), which resulted not only in a significantly lower proportion of dividing (G2-M) and S phase cells (~46% and 37% less, respectively) but also ~7-fold more quiescent cells (G0) when compared to cells from S17 co-cultures. Dll4 stimulated a weaker effect which induced a significantly fewer S phase cells (34% less) and an average 4.5-fold increase in the proportion of quiescent cells albeit not statistically significant. Co-culturing with S17-Dll1 cells, on the other hand, did not promote any differences in HSPCs' cell cycle status compared to HSPCs cocultured with S17 cells.

Accordingly, many cell cycle regulators expression was significantly altered in HSPCs derived from S17-Jag1 cocultures compared to HSPCs from S17 co-cultures (**Figure III.11C**). In particular, cell cycle inhibitor cyclin-dependent kinase inhibitor 1c (*CDKN1C*, also known as *P57*), a regulator of G0/G1 transition, showed significantly greater expression (~3.6-fold), as well as *CDKN1A* (also known as *P21*), a regulator of G1 progression (~1.8-fold). Furthermore, several cyclins (*CCND1*, *CCND3*, *CCNE1*) and cyclin dependent kinase 6 (*CDK6*) required for G1 progression and G1/S transition were significantly less expressed, as well as cyclins *CCNA2* and *CCNB2* that are required for G2/M transition. Interactions with Dll4 also promoted lower levels of *CCND1* expression (~4-fold) but in contrast, a significant 2-fold lower expression in *CDKN1A* was observed, which might justify the non-significant increase in the proportion of G0 cells when compared to HSPCs that were co-cultured with S17-Jag1 cells. As expected, HSPCs derived from S17-Dll1 cocultures did not show any differences in cell cycle regulators expression compared to HSPCs from S17 co-cultures.

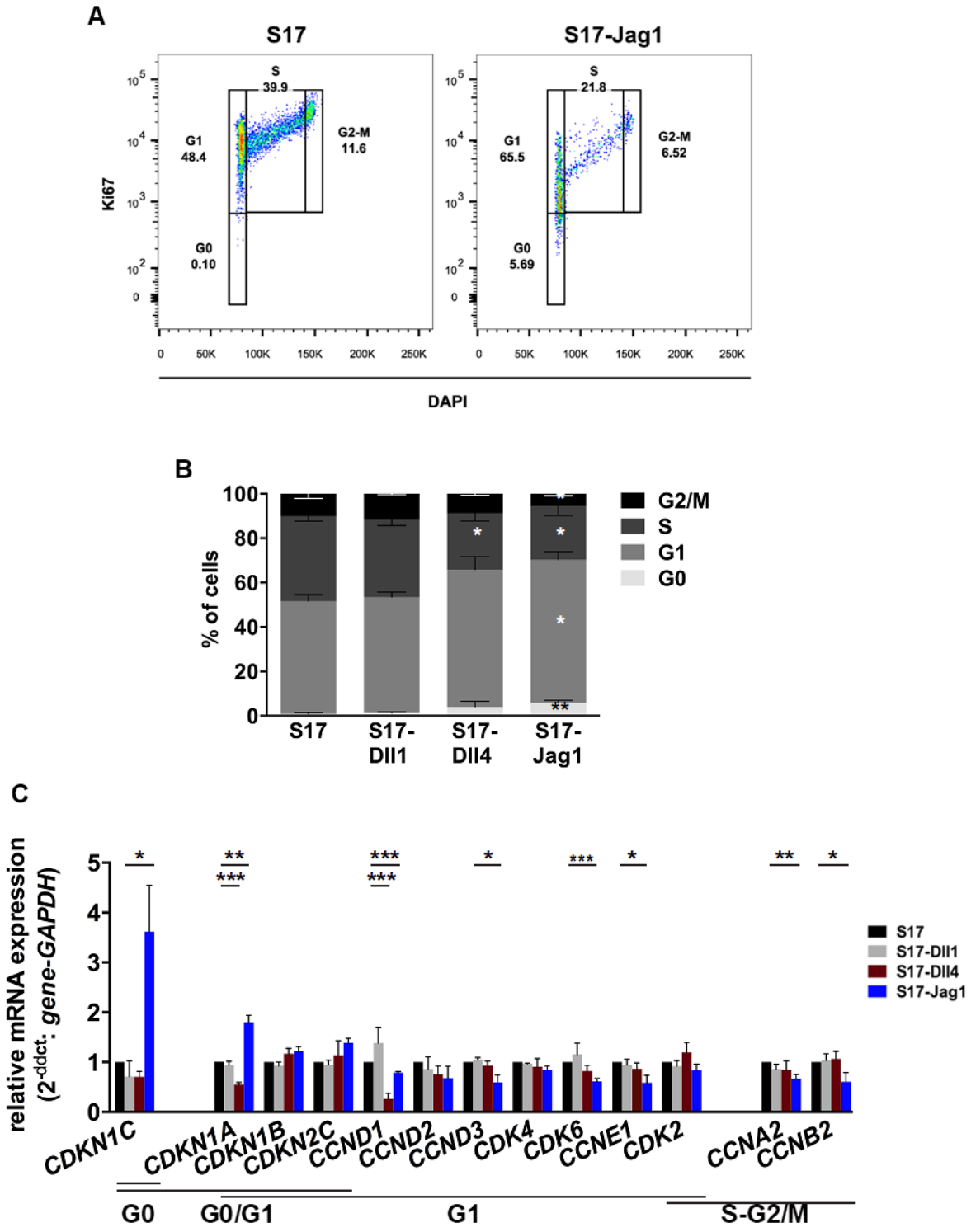

Figure III.11 – Cell cycle analysis of CD34⁺ HSPCs isolated after 5-6 days in coculture with S17 alone or S17 overexpressing the indicated Notch ligand. (A) Representative flow cytometry analysis of cell cycle status in HSPCs derived from S17 alone and S17-Jag1 cocultures. **(B)** Cell cycle status of HSPCs from the different S17 cocultures (n=3). **(C)** Relative gene expression of different cell cycle regulators in HSPCs derived from the different S17 cocultures determined by qRT-PCR. Gene expression values from HSPCs derived from S17 cocultures were used as reference (n=3). Error bars shown represent S.D.; *p≤0.03, **p≤0.003, ***p≤0.0003.

Regarding the effect of the different Notch ligands on HSPCs differentiation, immunophenotypic analysis performed on the output haematopoietic populations revealed a significant 10% higher proportion of $CD34^+$ HSPCs in S17-Dll4 cocultures compared to S17 cocultures (**Figure III.12A, B**). Moreover, this population had around 70% less committed progenitors ($CD45RA^+$), suggesting a blocking in differentiation in the presence of Dll4. In S17-Jag1 cocultures it was observed around 7% more $CD34^+$ HSPCs than with S17 cells, although not statistically significant, and also there was no significant differences in the percentage of $CD45RA^+$ progenitors. Similarly, no immunophenotypic differences were observed between HSPCs derived from S17-Dll1 and S17 co-cultures (**Figure III.12B**).

The expression of various differentiation markers/regulators (**Figure III.12C**) was then determined and it was observed that in the presence of Dll4, cultured HSPCs showed a significantly lower expression of myeloid marker *MPO* (myeloperoxidase) and transcription factor *CEBPA* (positive regulator of MPO transcription) compared to HSPCs isolated from S17 co-cultures (4-fold and 10-fold, respectively). Comparable lower levels of *MPO* expression was observed in cells isolated from S17-Jag1 co-cultures, although not associated to low *CEBPA* expression. In fact, there was a contrasting increased expression in myeloid transcription factor *GATA1* (~2.7-fold), known to be upregulated in megakaryocytic–erythroid cells. Nevertheless, the expression of another myeloid regulator *SPI1* (also known as *PU.1*) was also found at significant lower levels (~20% less) in cells exposed to Dll4 or Jag1 as compared to cells from S17 co-cultures. HSPCs derived from S17-Dll1 co-cultures showed similar expression levels of *SPI1* and *CEBPA* compared to HSPCs isolated from S17 cocultures, though a significantly higher expression of *MPO* (~1.7-fold) and lower expression of *GATA1* (~1.4-fold) was observed.

Collectively, these data suggest that Jag1 and Dll4 have distinct roles in HSPCs regulation *in vitro.* While interactions with Jag1 appear to act mainly by blocking cell cycle progression, binding with Dll4 appears to block differentiation more effectively. This was reflected on alterations in gene expression patterns of different cell cycle and differentiation regulators, more outstandingly in the upregulation of cell cycle inhibitors *CDKN1C* and *CDKN1A* when exposed to Jag1 and downregulation of the myeloid regulator *CEBPA* by Dll4 interactions.

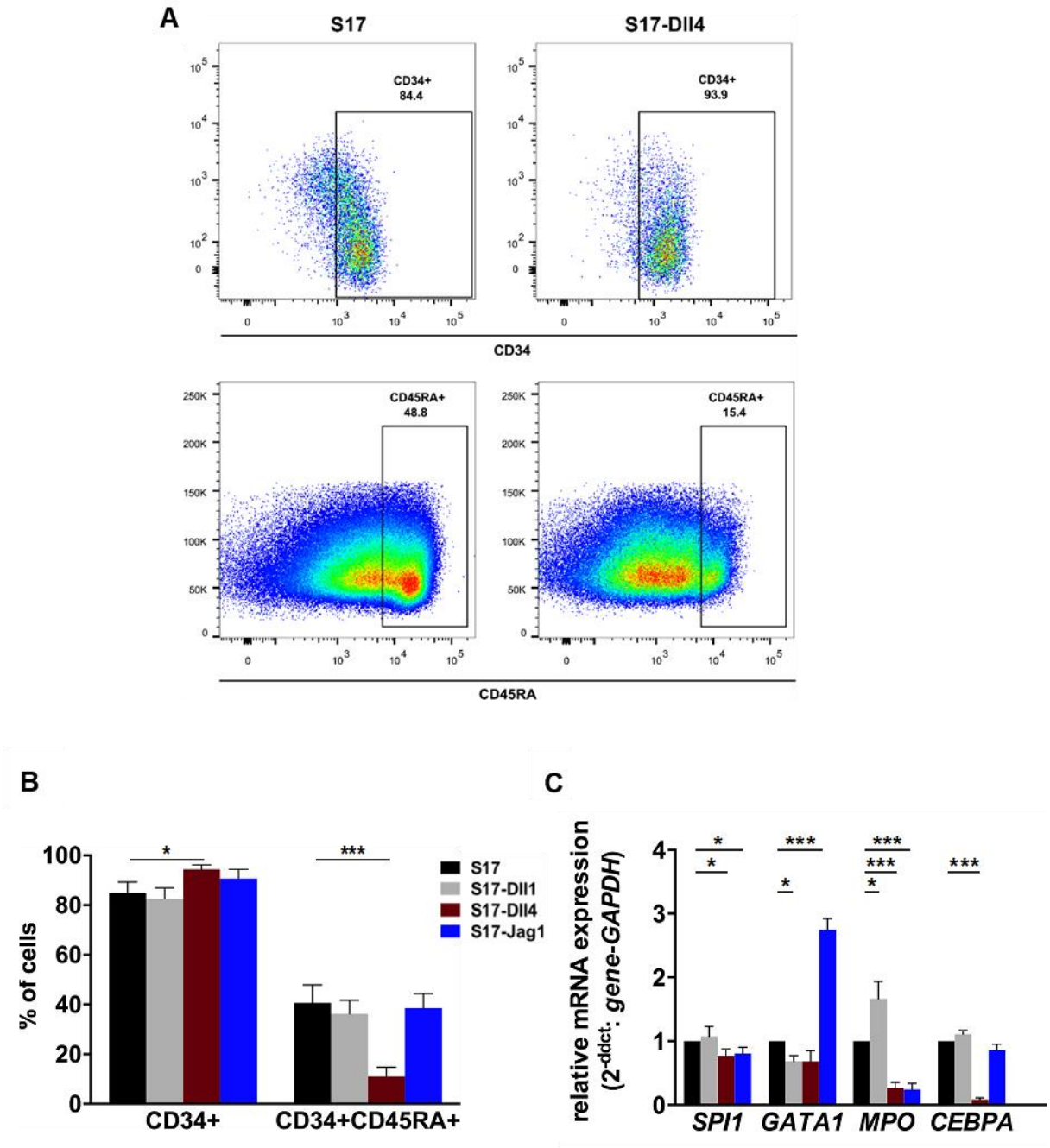

Figure III.12 – Analysis of HSPC differentiation after 5-6 days of coculture with S17 cells or with S17 cells overexpressing the indicated ligand. (A) Representative flow cytometry analysis of CD34 and CD45RA expression on cells derived from S17 and S17-Dll4 cocultures. **(B)** Proportion of $CD34^+$ and $CD34^+CD45RA^+$ populations in the total haematopoietic cells derived from the different S17 cocultures (n=5). **(C)** Relative gene expression of differentiation markers/regulators in HSPCs derived from the different S17 cocultures. Gene expression values from HSPCs derived from S17 cocultures were used as reference (n=3). Error bars shown represent S.D.; *p≤0.03, **p≤0.003, ***p≤0.0003.

Since no measurable effects were observed on the regulation of cell cycle or differentiation in HSPCs co-cultured with Dll1 on these experimental conditions and no significant expression of this ligand was detected on the placenta tissue (cord blood HSPCs natural environment) , the potential effects of Dll1 on HSPCs were not further investigated.

To assess the effect of Dll4 and Jag1 in the *ex vivo* maintenance of repopulating HSCs, the total haematopoietic cells derived from S17, S17-Jag1 and S17-Dll4 cocultures were transplanted into NOD/SCID/β2m$^{-/-}$ mice, as well as the initial number of non-cultured CB HSPCs, and human engraftment was quantified 12 weeks post-transplantation (**Figure III.13A**; due to the restricted accessibility rules of the animal facility, both animal adoptive transfer and schedule-1 sacrifice procedures were performed by Dr. Fernando dos Anjos Afonso). As expected, the output population isolated from S17 cocultures showed lower engraftment capacity than noncultured CD34^{+}CD38^{-} HSPC population, given that these stromal cells do not support the stem cell pool. In comparison, when HSPCs were cultured in the presence of Dll4 or Jag1, the engraftment capacity of these output populations was significantly higher, producing similar levels of engraftment as the initial HSPC population.

To quantify the content of HSCs in each coculture condition, limiting dilution analysis of human engraftment 12-weeks post-transplantation was performed as described in section **II.5.6**. As indicated in **Figure III.13B**, the SRC content was much greater in the populations derived from S17-Dll4 and S17-Jag1 cocultures (1 in 2124 and 1 in 2005 cells respectively) when compared to the population derived from S17 cocultures (1 in 23330 cells). Even so, these SRC frequencies were much lower than the SRC content found in the non-cultured HSPC population, which is around 1 in 710 cells (previously determined in the lab). However, considering the total cell fold expansion that was achieved in these cocultures (**Figure III.13C**), the actual SRC frequency from cultured cells that were isolated from S17-Jag1 cocultures was just maintained (~0.95-fold) whereas there was an actual ~1.8-fold increase in SRC frequency in cells isolated from S17-Dll4 cocultures.

These data suggest that both Notch ligands Jag1 and Dll4 have a considerable role in maintaining the stem cell pool *ex vivo*. Indeed, interactions with Jag1 appear to be able to counteract the medium proliferative effects by reducing cycling of HSPCs. On

the other hand, interactions with Dll4 are not only able to maintain but also expand the SRC pool.

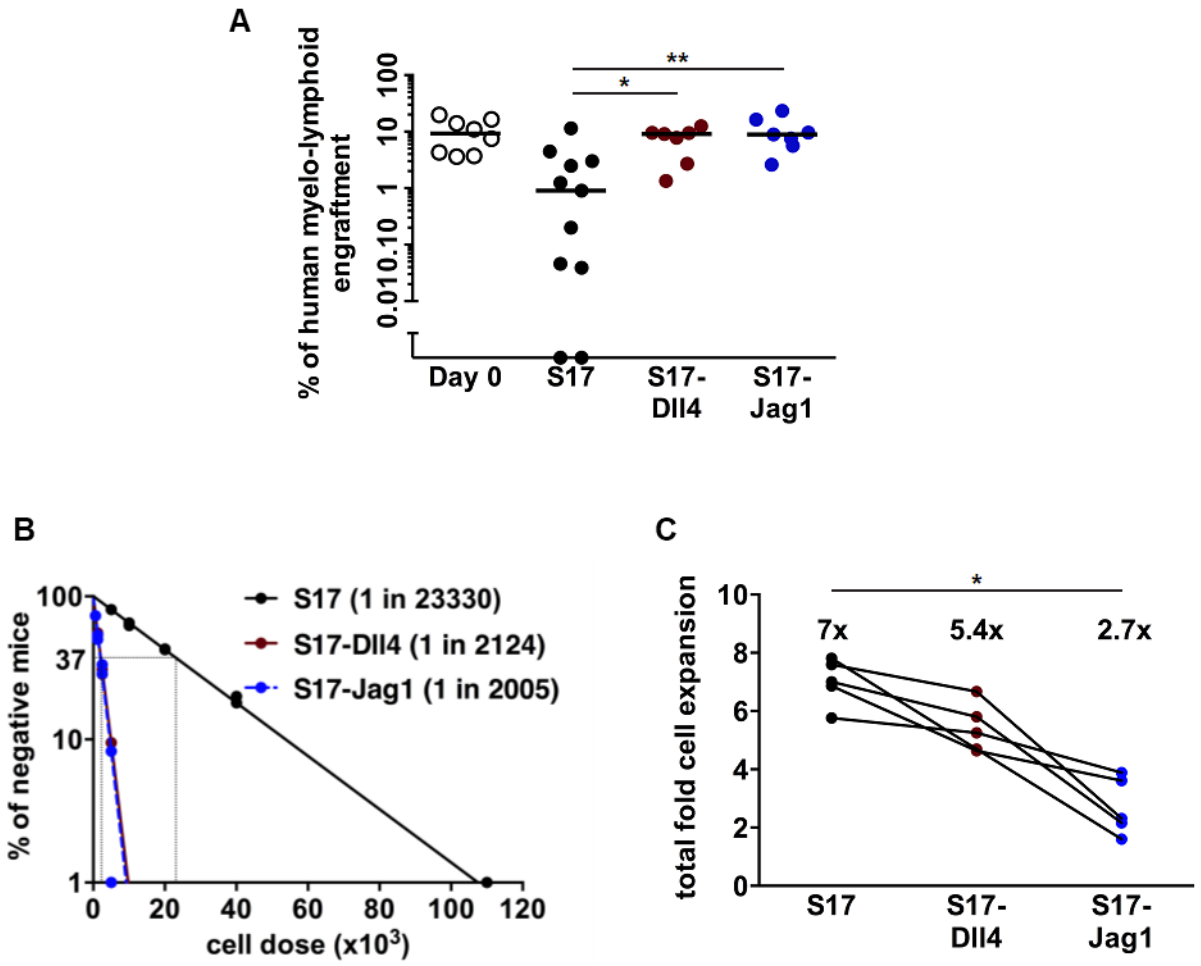

Figure III.13 – *In vivo* repopulation capacity of total haematopoietic cells derived from 5-6 days of culture on S17 cells or S17 cells overexpressing the indicated ligand. (A) Total human engraftment in NOD/SCID/β2m$^{-/-}$ recipients 12-week post-transplantation either with 5000 CD34^{+}CD38^{-} cells (Day0) or the total haematopoietic cells (CD45^{+}) generated from 5000 CD34^{+}CD38^{-} cells in the different S17 cocultures. **(B)** Limiting dilution analysis determined at 12-weeks post-transplantation to determine SRC frequencies in cells derived from the different cocultures. **(C)** Fold expansion of the total haematopoietic cells in the different S17 cocultures. Median bars are shown; *p≤0.03, **p≤0.003.

III.3. DISCUSSION

Arising from the discovery of a fly with a tiny notch on the tip of its wings, Notch signalling has sparked the interest of numerous scientists and clinicians in diverse fields over the last century. In the past 30 years, molecular cloning of the Notch signalling components associated to cell biology, biochemical, bioinformatics and structural studies have uncovered much of the molecular mechanism of this pathway and its involvement in diverse biological processes and numerous human diseases. Notch signalling regulatory networks are context-dependent and are still being unravelled by expanding the list of regulatory factors and downstream target gene networks thus, allowing to further our understanding of Notch signalling molecular mechanisms *in vivo*.

To properly assess these regulatory networks and distinguish the roles of the different Notch receptors in each context, it is imperative to identify consensus tools that will allow to specifically and efficiently target each Notch receptor at the protein level.

Currently, the literature is still lacking studies that distinguish the role of the different receptors activation. In fact, although the ab for detection of N1ICD is well defined and has been widely used in many studies, abs for exclusive detection of N2ICD or N4ICD are still not being extensively used in the literature due to their uncertain specificity. In particular for N2, before finding a trustworthy specific ab for N2ICD detection, several commercial abs for cleaved N2 were tested in this study that did not show specificity. As for N4, the detection of N4ICD was possible through a C-terminus ab that appears to be more specific for the cleaved form and that can be used in ImageStream studies through colocalisation with the nucleus.

Characterisation of the extracellular Notch receptors expression on HSPCs is scarce in the literature, with most studies demonstrating expression of Notch receptors in cells based on gene expression data [36, 11, 5]. Effects on Notch receptors upon exposure to a given ligand have also been evaluated based on upregulation of Notch receptors gene expression [11] or extracellular protein expression [13], which does not always correlate to the activation of the receptor and therefore can not entirely be used to

interpret Notch-ligand preferential interaction. In fact, the quantification of Notch receptors activation in HSPCs has yet to be published and studies analysing different Notch receptor-ligand interactions have resorted to engineered cell lines to measure Notch activation [37, 38].

In this study, the effect of the different Notch ligands on $CD34^{+}CD38^{-}$ HSPCs was assessed based on a short-term interaction (5-6 days) with culture medium intended to promote differentiation. This short-term exposure was probably not ideal to assess the effect of Dll1 ligand, given that no discernible differences were observed on the output of HSPC population in the presence of this ligand, as verified in previous reports. In fact, HSPCs expansion protocol using immobilised Dll1 requires 17-21 days of culture [16] and looking carefully into a more detailed report [17] it can be seen that differences on primitive cells expansion is only visible upon 12 days of culture. Mechanistically, this effect was due to decrease in membrane-bound IL-6 receptor expression which reduces the responsiveness of the cells to IL-6 signalling. This in turn, reduces myeloid differentiation and thus, promotes a more supportive environment for HSPCs expansion. Therefore, the increased numbers of HSPCs observed later in these cultures resulted from an effect in myeloid progenitors to cytokine response and not from a direct effect in the HSC population. Moreover, as demonstrated, Dll1 seems to be very low expressed in the placenta niche, having been mostly identified in splenic and thymic haematopoietic niches [3], which could also justify why there is no immediate effect on CB HSPCs. Based on these observations and since no effects were obtained with Dll1 under our experimental conditions *in vitro*, it was decided to discontinue the studies with this ligand.

Regarding Jag1, some studies have analysed the role of this ligand on human HSPCs *in vitro* [13, 39], while others showed evidences of its importance for mice HSCs *in vivo* [5, 12]. When cocultured with OP9 stromal cell line, which naturally expresses Jag1, $CD34^{+}CD38^{-}$ HSPCs showed decreased total proliferation when compared with a feeder layer not expressing Jag1. In addition, co-culture with $CD146^{+}$ perivascular cells that highly express Jag1, supported the long-term maintenance of myelolymphoid HSPCs able to engraft primary and secondary mice without addition of exogeneous cytokines [39]. These observations are in accordance with results from this study showing that Jag1 supported maintenance of SRCs while inhibiting total proliferation. Further studies have shown that expression of Jag1 *in vivo* is essential for the

maintenance of the HSC pool [5, 12], demonstrating in particular that when co-cultured with OP9-Jag1, LT-HSCs showed reduced cell cycling with a significant increase in the proportion of G0 cells and reduction of total cell proliferation compared to OP9 control cells [12]. Although performed with mice HSCs, these observations seem to be in line with the results from the present study, suggesting an important role for Jag1 in regulating quiescence of human HSPCs *in vitro*.

Work on the role of Dll4 in HSPCs regulation has suggested as well its importance in maintaining HSCs while inhibiting its proliferation *in vitro*, resulting in similar levels of engraftment as non-expanded HSPCs [8]. Indeed, more noteworthy, a study by Benveniste *et al.* showed that when purified human HSCs ($CD135^{+}CD45RA^{-}CD133^{+}Rho^{low}CD90^{+}$) where co-cultured with OP9-Dll4, the frequencies of $CD34^{+}$ cells attained were much higher than in co-culture with OP9 cells alone after 16 days [40]. Furthermore, after 7 days only, a 2-fold increase in phenotypically defined HSCs was observed in the presence of Dll4, associated to a significant lower proportion of $CD45RA^{+}$ cells. These observations clearly support the presented results indicating a major role for Dll4 in delaying differentiation of HSCs, allowing some expansion. However, there is still no detailed study on the molecular mechanism behind these effects on human HSPCs. Downregulation of D-cyclins (D1, D2 and D3) in the presence of Dll4 has also been observed in a study with mice HSPCs (LSK) [9], suggesting also the ability of Dll4 in maintaining cells out of cycle, as was observed in this study, although at lower levels than in the presence of Jag1.

III.4. REFERENCES

1. Besseyrias V, Fiorini E, Strobl LJ, Zimber-Strobl U, Dumortier A, Koch U et al. Hierarchy of Notch-Delta interactions promoting T cell lineage commitment and maturation. J Exp Med. 2007;204(2):331-43.

2. Saito T, Chiba S, Ichikawa M, Kunisato A, Asai T, Shimizu K et al. Notch2 is preferentially expressed in mature B cells and indispensable for marginal zone B lineage development. Immunity. 2003;18(5):675-85.

3. Hozumi K, Negishi N, Suzuki D, Abe N, Sotomaru Y, Tamaoki N et al. Delta-like 1 is necessary for the generation of marginal zone B cells but not T cells in vivo. Nat Immunol. 2004;5(6):638-44.

4. Fernandez L, Rodriguez S, Huang H, Chora A, Fernandes J, Mumaw C et al. Tumor necrosis factor-alpha and endothelial cells modulate Notch signaling in the bone marrow microenvironment during inflammation. Exp Hematol. 2008;36(5):545-58.

5. Poulos MG, Guo P, Kofler NM, Pinho S, Gutkin MC, Tikhonova A et al. Endothelial Jagged-1 is necessary for homeostatic and regenerative hematopoiesis. Cell reports. 2013;4(5):1022-34.

6. Guo P, Poulos MG, Palikuqi B, Badwe CR, Lis R, Kunar B et al. Endothelial jagged-2 sustains hematopoietic stem and progenitor reconstitution after myelosuppression. J Clin Invest. 2017;127(12):4242-56.

7. Lahmar M, Catelain C, Poirault S, Dorsch M, Villeval JL, Vainchenker W et al. Distinct effects of the soluble versus membrane-bound forms of the notch ligand delta-4 on human CD34+CD38low cell expansion and differentiation. Stem cells. 2008;26(3):621-9.

8. Lauret E, Catelain C, Titeux M, Poirault S, Dando JS, Dorsch M et al. Membrane-bound delta-4 notch ligand reduces the proliferative activity of primitive human hematopoietic CD34+CD38low cells while maintaining their LTC-IC potential. Leukemia. 2004;18(4):788-97.

9. Catelain C, Michelet F, Hattabi A, Poirault-Chassac S, Kortulewski T, Tronik-Le Roux D et al. The Notch Delta-4 ligand helps to maintain the quiescence and the short-term reconstitutive potential of haematopoietic progenitor cells through activation of a key gene network. Stem cell research. 2014;13(3 Pt A):431-41.

10. Jaleco AC, Neves H, Hooijberg E, Gameiro P, Clode N, Haury M et al. Differential effects of Notch ligands Delta-1 and Jagged-1 in human lymphoid differentiation. J Exp Med. 2001;194(7):991-1002.

11. Neves H, Weerkamp F, Gomes AC, Naber BAE, Gameiro P, Becker JD et al. Effects of Delta1 and Jagged1 on Early Human Hematopoiesis: Correlation with Expression of Notch Signaling-Related Genes in CD34+ Cells. Stem cells. 2006;24(5):1328-37.

12. Bowers M, Zhang B, Ho Y, Agarwal P, Chen CC, Bhatia R. Osteoblast ablation reduces normal long-term hematopoietic stem cell self-renewal but accelerates leukemia development. Blood. 2015;125(17):2678-88.

13. Fernandez-Sanchez V, Pelayo R, Flores-Guzman P, Flores-Figueroa E, Villanueva-Toledo J, Garrido E et al. In vitro effects of stromal cells expressing different levels of Jagged-1 and Delta-1 on the growth of primitive and intermediate CD34(+) cell subsets from human cord blood. Blood cells, molecules & diseases. 2011;47(4):205-13.

14. Ohishi K, Varnum-Finney B, Bernstein ID. Delta-1 enhances marrow and thymus repopulating ability of human CD34(+)CD38(-) cord blood cells. J Clin Invest. 2002;110(8):1165-74.

15. Delaney C, Varnum-Finney B, Aoyama K, Brashem-Stein C, Bernstein ID. Dose-dependent effects of the Notch ligand Delta1 on ex vivo differentiation and in vivo marrow repopulating ability of cord blood cells. Blood. 2005;106(8):2693-9.

16. Delaney C, Heimfeld S, Brashem-Stein C, Voorhies H, Manger RL, Bernstein ID. Notch-mediated expansion of human cord blood progenitor cells capable of rapid myeloid reconstitution. Nature medicine. 2010;16(2):232-6.

17. Csaszar E, Wang W, Usenko T, Qiao W, Delaney C, Bernstein ID et al. Blood stem cell fate regulation by Delta-1-mediated rewiring of IL-6 paracrine signaling. Blood. 2014;123(5):650-8.

18. Varnum-Finney B, Wu L, Yu M, Brashem-Stein C, Staats S, Flowers D et al. Immobilization of Notch ligand, Delta-1, is required for induction of notch signaling. J Cell Sci. 2000;113 Pt 23:4313-8.

19. Anjos-Afonso F, Currie E, Palmer HG, Foster KE, Taussig DC, Bonnet D. CD34(-) cells at the apex of the human hematopoietic stem cell hierarchy have distinctive cellular and molecular signatures. Cell Stem Cell. 2013;13(2):161-74.

20. Blaumueller CM, Qi H, Zagouras P, Artavanis-Tsakonas S. Intracellular cleavage of Notch leads to a heterodimeric receptor on the plasma membrane. Cell. 1997;90(2):281-91.

21. Schroeter EH, Kisslinger JA, Kopan R. Notch-1 signalling requires ligand-induced proteolytic release of intracellular domain. Nature. 1998;393(6683):382-6.

22. Logeat F, Bessia C, Brou C, LeBail O, Jarriault S, Seidah NG et al. The Notch1 receptor is cleaved constitutively by a furin-like convertase. Proc Natl Acad Sci U S A. 1998;95(14):8108-12.

23. Mumm JS, Schroeter EH, Saxena MT, Griesemer A, Tian X, Pan DJ et al. A ligand-induced extracellular cleavage regulates gamma-secretase-like proteolytic activation of Notch1. Molecular cell. 2000;5(2):197-206.

24. Saxena MT, Schroeter EH, Mumm JS, Kopan R. Murine notch homologs (N1-4) undergo presenilin-dependent proteolysis. J Biol Chem. 2001;276(43):40268-73.

25. Gordon WR, Vardar-Ulu D, Histen G, Sanchez-Irizarry C, Aster JC, Blacklow SC. Structural basis for autoinhibition of Notch. Nat Struct Mol Biol. 2007;14(4):295-300.

26. Gordon WR, Vardar-Ulu D, L'Heureux S, Ashworth T, Malecki MJ, Sanchez-Irizarry C et al. Effects of S1 cleavage on the structure, surface export, and signaling activity of human Notch1 and Notch2. PLoS One. 2009;4(8):e6613.

27. van Tetering G, Vooijs M. Proteolytic cleavage of Notch: "HIT and RUN". Curr Mol Med. 2011;11(4):255-69.

28. Rand MD, Grimm LM, Artavanis-Tsakonas S, Patriub V, Blacklow SC, Sklar J et al. Calcium depletion dissociates and activates heterodimeric notch receptors. Mol Cell Biol. 2000;20(5):1825-35.

29. Lobry C, Ntziachristos P, Ndiaye-Lobry D, Oh P, Cimmino L, Zhu N et al. Notch pathway activation targets AML-initiating cell homeostasis and differentiation. J Exp Med. 2013;210(2):301-19.

30. Takam Kamga P, Bassi G, Cassaro A, Midolo M, Di Trapani M, Gatti A et al. Notch signalling drives bone marrow stromal cell-mediated chemoresistance in acute myeloid leukemia. Oncotarget. 2016;7(16):21713-27.

31. Malassine A, Frendo JL, Evain-Brion D. A comparison of placental development and endocrine functions between the human and mouse model. Human reproduction update. 2003;9(6):531-9.

32. Robin C, Bollerot K, Mendes S, Haak E, Crisan M, Cerisoli F et al. Human placenta is a potent hematopoietic niche containing hematopoietic stem and progenitor cells throughout development. Cell Stem Cell. 2009;5(4):385-95.

33. Greife A, Jankowiak S, Steinbring J, Nikpour P, Niegisch G, Hoffmann MJ et al. Canonical Notch signalling is inactive in urothelial carcinoma. BMC Cancer. 2014;14:628.

34. Collins LS, Dorshkind K. A stromal cell line from myeloid long-term bone marrow cultures can support myelopoiesis and B lymphopoiesis. Journal of immunology. 1987;138(4):1082-7.

35. Migliaccio G, Migliaccio AR, Adamson JW. In vitro differentiation of human granulocyte/macrophage and erythroid progenitors: comparative analysis of the influence of recombinant human erythropoietin, G-CSF, GM-CSF, and IL-3 in serum-supplemented and serum- deprived cultures. Blood. 1988;72(1):248.

36. Karanu FN, Yuefei L, Gallacher L, Sakano S, Bhatia M. Differential response of primitive human CD34− and CD34+ hematopoietic cells to the Notch ligand Jagged-1. Leukemia. 2003;17(7):1366-74.

37. Van de Walle I, De Smet G, Gärtner M, De Smedt M, Waegemans E, Vandekerckhove B et al. Jagged2 acts as a Delta-like Notch ligand during early hematopoietic cell fate decisions. Blood. 2011;117(17):4449-59.

38. Nandagopal N, Santat LA, LeBon L, Sprinzak D, Bronner ME, Elowitz MB. Dynamic Ligand Discrimination in the Notch Signaling Pathway. Cell. 2018;172(4):869-80.e19.

39. Corselli M, Chin CJ, Parekh C, Sahaghian A, Wang W, Ge S et al. Perivascular support of human hematopoietic stem/progenitor cells. Blood. 2013;121(15):2891-901.

40. Benveniste P, Serra P, Dervovic D, Herer E, Knowles G, Mohtashami M et al. Notch signals are required for in vitro but not in vivo maintenance of human hematopoietic stem cells and delay the appearance of multipotent progenitors. Blood. 2014;123(8):1167-77.

CHAPTER IV

ROLES OF NOTCH RECEPTORS IN HUMAN HAEMATOPOIETIC STEM AND PROGENITOR CELLS

IV.1. INTRODUCTION

Based on the current literature introduced before, it is consensual that the role of Notch signalling and particularly the specific functions of each Notch receptor in human HSPC regulation *in vitro* and *in vivo* are still unclear [1]. As demonstrated in the previous chapter, HSPCs express high levels of extracellular N1 and N2, whereas N4 could not be detected. Thus, in order to comprehensively investigate which are the functions of N1 and N2 in HSPCs, tools were developed and optimised for the efficient silencing of these receptors in HSPCs and subsequent functional analysis.

RNA interference (RNAi) is a natural process through which expression of a gene can be knocked down with high specificity and selectivity, making it one of the most powerful tools to explore gene function in mammalian cells. Silencing of a gene of interest can be achieved by RNAi-based tools which act through a posttranscriptional gene silencing process, using a double-stranded RNA that targets the homologous messenger RNA (mRNA) for degradation thereby, reducing the expression of the gene product. In this work, knockdown of Notch receptors was achieved by using synthetic short hairpin RNA (shRNA) systems. These are stem-loop RNA structures consisting of two complementary 19–22 bp RNA sequences connected by a short loop of 4–11 nt similar to the hairpin found in naturally occurring mircroRNAs (miRNAs) [2]. shRNAs can be delivered to the cell by plasmid vectors encoding shRNAs transcribed by RNA polymerase III (Pol III) or modified Pol II promoters and are able of stable DNA integration for long-term expression. Following transcription, the shRNA sequence is exported to the cytosol where it is recognised by an endogenous enzyme Dicer, which processes the shRNA into short interfering RNA (siRNA) duplexes that bind to the target mRNA followed by incorporation into the RISC (RNA-induced silencing complex) for degradation [2]. In a more recent approach vectors have been designed to allow the expression of shRNA embedded in the context of an endogenous miRNA. This strategy is used to overcome saturation of endogenous miRNA pathways and to increase accuracy of Dicer processing by using natural substrates in miRNA biogenesis pathways. These structures can trigger potent knockdown that have been

demonstrated for a number of miRNA backbones, including miRNA30 (miR30shRNA), with less off-target effects [3, 4].

In order to deliver the genetic material into cells, lentiviral vectors are efficient vehicles that are able to integrate shRNAs into the genome of both dividing and non-dividing cells, which makes them highly attractive for HSPCs transduction [5, 6].

Temporally and spatially controlled shRNA expression can be achieved by using inducible systems like the tetracycline-dependent transcriptional regulatory system [7], which has been extensively used with proven efficacy *in vitro* and *in vivo* [8, 9]. The tetracycline-inducible systems can be tTA (tetracycline responsive transactivator)-dependent (Tet-Off) or rtTA (reverse tetracycline responsive transactivator)-dependent (Tet-On). The latter version allows transcription activation in the presence of physiologically relevant doses of tetracycline, or its analogue doxycycline (dox), and is often preferred to the Tet-Off system for *in vivo* applications because maintenance of the off state does not require chronic drug administration. In the Tet-On system, baseline transcription can be kept to background levels when using an optimised rtTA [10]. In the presence of dox the transactivator changes its conformation allowing it to bind to the tetracycline operator sequence (TetO), which regulates binding of polymerase to the promoter hence, activating transcription of the transgene.

Thus, one of the aims of this chapter was to develop a constitutive and an inducible vector for the efficient expression of miR30shRNA in human HSPCs and to identify shRNA sequences that promote efficient silencing of each individual Notch receptor.

Upon efficient knockdown of N1 and N2 receptors in HSPCs, the respective effects in self-renewal and differentiation potential were evaluated *in vitro* and *in vivo* through LTC-IC and long-term xenotransplantation assays, which allow to assess the HSC population.

IV.2. RESULTS

IV.2.1. CONSTRUCTION OF miR30shRNA LENTIVIRAL VECTORS

In order to study the potential functions of each Notch receptor in HSPCs, a constitutive and an inducible lentiviral vector were developed with the aim to achieve an efficient expression of miR30shRNA in these cells.

A GFP sequence was cloned in-frame to the primiR30-shRNA sequence (generally designated miR30shRNA) to allow quantification of the shRNA expression levels in terms of efficiency (expressing cells) and intensity. The GFP reporter is also particularly useful in the inducible vector to monitor expression upon induction. Furthermore, the miR30shRNA sequence was cloned inside an EF1α intron, that allows to be spliced out from the transcript and follow processing, stabilising the reporter gene to be translated.

The rationale for constructing these new vectors was because most commercially available tetracycline inducible vectors that drive shRNAs either use a Pol III promoter (H1 or U6) or cytomegalovirus (CMV) promoter (Pol II), with the latter being known to be silenced in human haematopoietic cells overtime [11]. Although the former option is known to work efficiently in human haematopoietic cells, Pol III promoters are unable to drive the expression of long-transcripts and therefore their usage is limited if envisaged to have a reporter in-frame that allows monitoring the shRNA expression. In addition, most available inducible systems require the use of two plasmids that highly reduces the transduction efficiencies in human HSPCs.

IV.2.1.1. CONSTITUTIVE miR30shRNA LENTIVIRAL VECTOR

A constitutive vector (pLV.EF1α-miR30shRNA-GFP) was developed for expression of miR30shRNA and an in-frame GFP reporter under the EF1α promoter, as depicted in **Figure IV.1**.

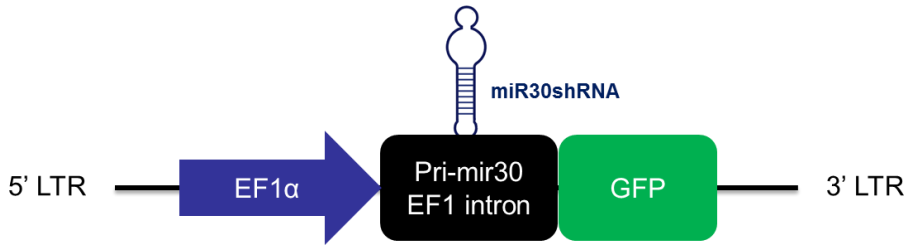

Figure IV.1 – Schematic representation of the developed lentivector for constitutive expression of shRNA designated pLV.EF1α-miR30shRNA-GFP. This vector contains a GFP reporter that allows monitoring the level of the shRNA expression in the transduced cells.

This vector allowed very good transduction efficiencies in several cell lines transduced at MOI 10 (over 95% in HEK293T, Jurkat and K562), showing strong GFP MFI (see following section).

Due to the strong nature of the EF1α promoter, this vector was used to assess the knockdown efficiencies of different miR30shRNA sequences against Notch receptors in order to select the more efficient ones (section **IV.2.2**).

IV.2.1.2. INDUCIBLE TET-ON MIR30SHRNA LENTIVIRAL VECTOR

An inducible vector was developed to allow efficient shRNA expression in HSPCs at specific time points *in vitro* and *in vivo* which could help elucidate the roles of the different Notch receptors on HSPC fate.

Upon transduction and integration this vector should allow to induce the knockdown of a chosen Notch receptor through the RNAi pathway in the presence of doxycycline. Therefore, the aim was to construct a vector as depicted in **Figure IV.2** in which the shRNA expression can be monitored by a gene reporter (GFP) under the same promoter and with the control of tetracycline response elements (TRE). Thus, a state-of-the-art synthetic Pol II promoter (SyntP) was used to meet these requirements [12].

The other component required for a Tet-On system is the regulatory protein rtTA3 (reverse tetracycline-controlled transactivator; 3rd generation [13]) that binds the TetO sequence and activates transcription in the presence of Dox. Thus, this vector was designed to comprise the gene for rtTA3 under a constitutive promoter (SFFV; spleen focus-forming virus) and it is linked to the gene reporter mCherry by a T2A peptide

that allows translation of the two separate proteins (rtTA3 and mCherry) from the single bicistronic mRNA. The mCherry expression will allow identifying and eventually sorting the transduced cells.

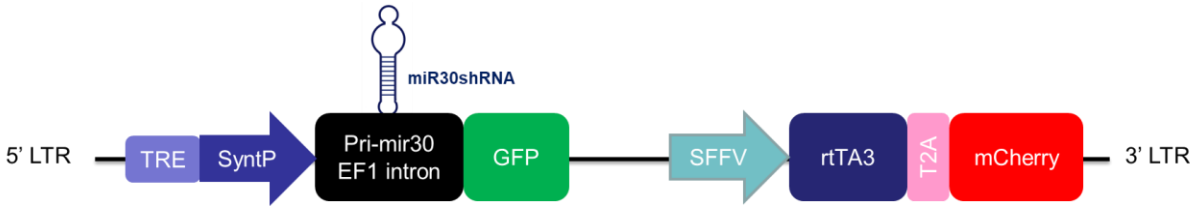

Figure IV.2 – Schematic representation of the developed Tet-On system lentivector for inducible expression of shRNA designated pLV.TetSyntP-miR30shRNA-GFP. TRE, Tetracycline responsive sequence; rtTA3, 3rd generation tetracycline-dependent transactivator; T2A, self-cleaving peptide; GFP, Green fluorescent protein; mCherry, monomeric red fluorescent protein.

In the first line of testing, the shRNA against the non-mammalian target luciferase (sh*Luc*) was cloned into the inducible and the constitutive vectors, which were tested in parallel to compare GFP expression and intensity. Upon transduction and induction with Dox cells were analysed for mCherry and GFP expressions by FCM. As can be seen in **Figure IV.3A,** HEK293T cells transduced at MOI 10 with the inducible pLV.TetSyntP-miR30shRNA-GFP showed good transduction efficiency (around 80% mCherry$^+$ cells) and a very efficient induction with close to 90% of the mCherry$^+$ cells expressing GFP upon addition of Dox (1 µg/mL) and virtually no GFP leakiness in the absence of Dox (**Figure IV.3A** and **B**). Cells transduced with the constitutive pLV.EF1α-miR30shRNA-GFP had near 100% GFP expression (**Figure IV.3B**) and a mean fluorescence intensity (MFI) of 8200, whereas the inducible vector had a mean GFP intensity of 4200 upon induction (**Figure IV.3C**). This difference was expected given the stronger nature of the EF1α promoter, but nevertheless, the inducible vector showed a GFP intensity in the same order of magnitude, which might result in similar knockdown efficiencies as the constitutive vector. Of note, higher concentrations of Dox where tested for induction but all produced very similar levels of GFP expression and intensity (data not shown).

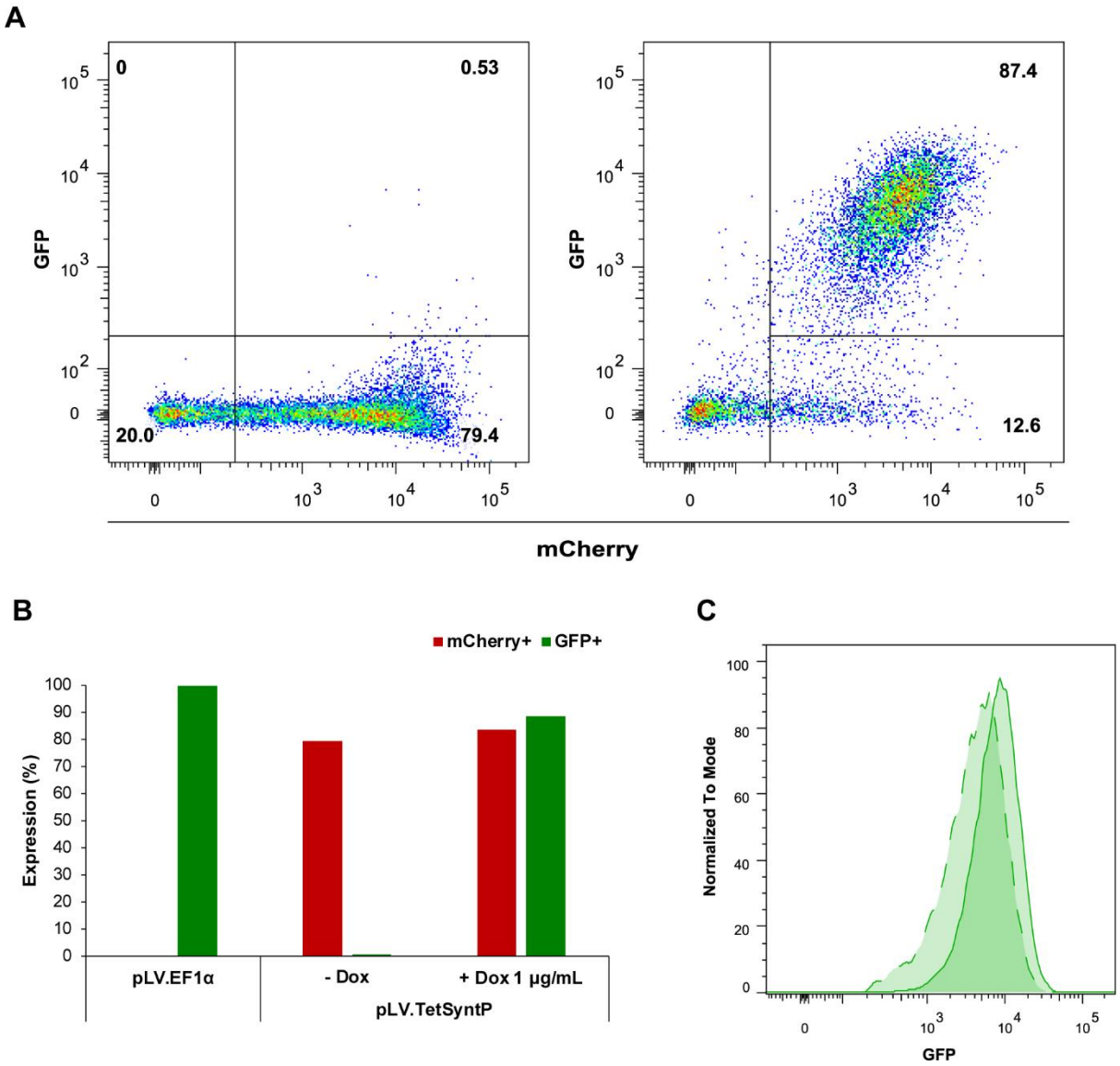

Figure IV.3 – HEK293T cells transduced with the constitutive pLV.EF1α-miR30shRNA-GFP and the inducible pLV.TetSyntP-miR30shRNA-GFP lentivectors. (A) FCM dotplots of cells transduced with the inducible vector in the absence and presence of doxycycline. **(B)** GFP and mCherry expression of cells transduced with constitutive and inducible vector. **(C)** GFP histograms of cells transduced with constitutive (full line) and inducible (dashed line) vectors. Representative experiment is shown.

Thus, at this stage it was demonstrated that the developed inducible lentivector was capable of good transduction and induction efficiencies without leakiness, that could be used to efficiently drive miR30shRNA expression and most importantly to monitor the level of induction through GFP expression. However, to fully achieve a highly functional system there was a need for further development and validation studies which are presented and thoroughly discussed in the next chapter.

IV.2.2. NOTCH RECEPTORS KNOCKDOWN THROUGH A CONSTITUTIVE MIR30SHRNA LENTIVIRAL VECTOR

Following construction of the constitutive vector, selection of specific shRNA sequences targeting each Notch receptor was performed in cell lines, given previous knowledge that usually strong knockdowns in cell lines that highly express the target protein correlate to good knockdowns in HSPCs.

IV.2.2.1. VALIDATION IN CELL LINES

In order to determine the shRNAs with the most efficient knockdown level several shRNA sequences for each Notch receptor were tested in the respective Notch receptor expressing human cell lines using the constitutive vector. Some shRNA sequences were selected from commercially available source such as GE Dharmacon (pGIPZ lentiviral vectors), that were designed taking in consideration for efficient processing from a miR30 backbone, or Sigma (MISSION® shRNA Library). The sequence selection was based on less complementarity to other potential targets and with higher mean knockdown levels (when validated by the respective company). Other sequences were selected from previously published work, where the shRNAs were demonstrated to induce good knockdown of the receptor [14, 15].

As described in section **II.2.1.3**, to clone the shRNA sequences, custom made forward and reverse oligos were annealed and ligated into an intermediate vector (pECFP) where the miR30 sequence was first sub-cloned. The final miR30shRNA sequence was then cut and cloned into the developed constitutive vector.

Silencing of Notch receptors was evaluated six to nine days after transduction at the protein level by FCM of the extracellular receptor and/or by WB of whole cell lysates. In cases where transduction efficiencies where below 95%, GFP positive cells were sorted and cultured for an additional three days before protein extraction.

For N1 receptor, K562 cell line was used to validate the knockdown of ten shRNA sequences. Three sequences yielded good and consistent knockdowns being the sh*N1.1* the most efficient sequence with an 82±5.8% knockdown of N1 receptor quantified by FCM (**Figure IV.4A** and **B**) and 88±7.9% knockdown of the N1TM protein

quantified by WB (**Figure IV.4C** and **D**). Sequences sh*N1.2* and sh*N1.3* had milder effects, with respective knockdowns of 61±1.5% and 55±7.4% quantified by FCM and 75±2.2% and 78±14% quantified by WB. As explained above, WB also allows to detect the immature NFL protein, which also showed good silencing levels (**Figure IV.4C** and **D**) however, the knockdown of the NTM form is the most crucial parameter as it dictates the quantity of functional receptor available on the cell surface for its binding to ligands.

For N2 receptor, HEK293T cell line was used to test the knockdown efficiency of six shRNAs. From these sequences, two produced very efficient knockdowns, although sequence sh*N2.1* was consistently better, with an average knockdown of 88±3.4% of the extracellular receptor quantified by FCM and 96±4.3% of the TM form quantified by WB (**Figure IV.5**). With a higher variation, the sequence sh*N2.2* produced knockdowns of 81±16% and 60±13%, quantified by FCM and WB respectively.

These results show that very efficient knockdowns of the large size N1 and N2 proteins are achievable in cell lines through constitutive miR30shRNA expression. Thus, at least two shRNA sequences were identified for the efficient knockdown of N1 and N2, which were subsequently tested in HSPCs.

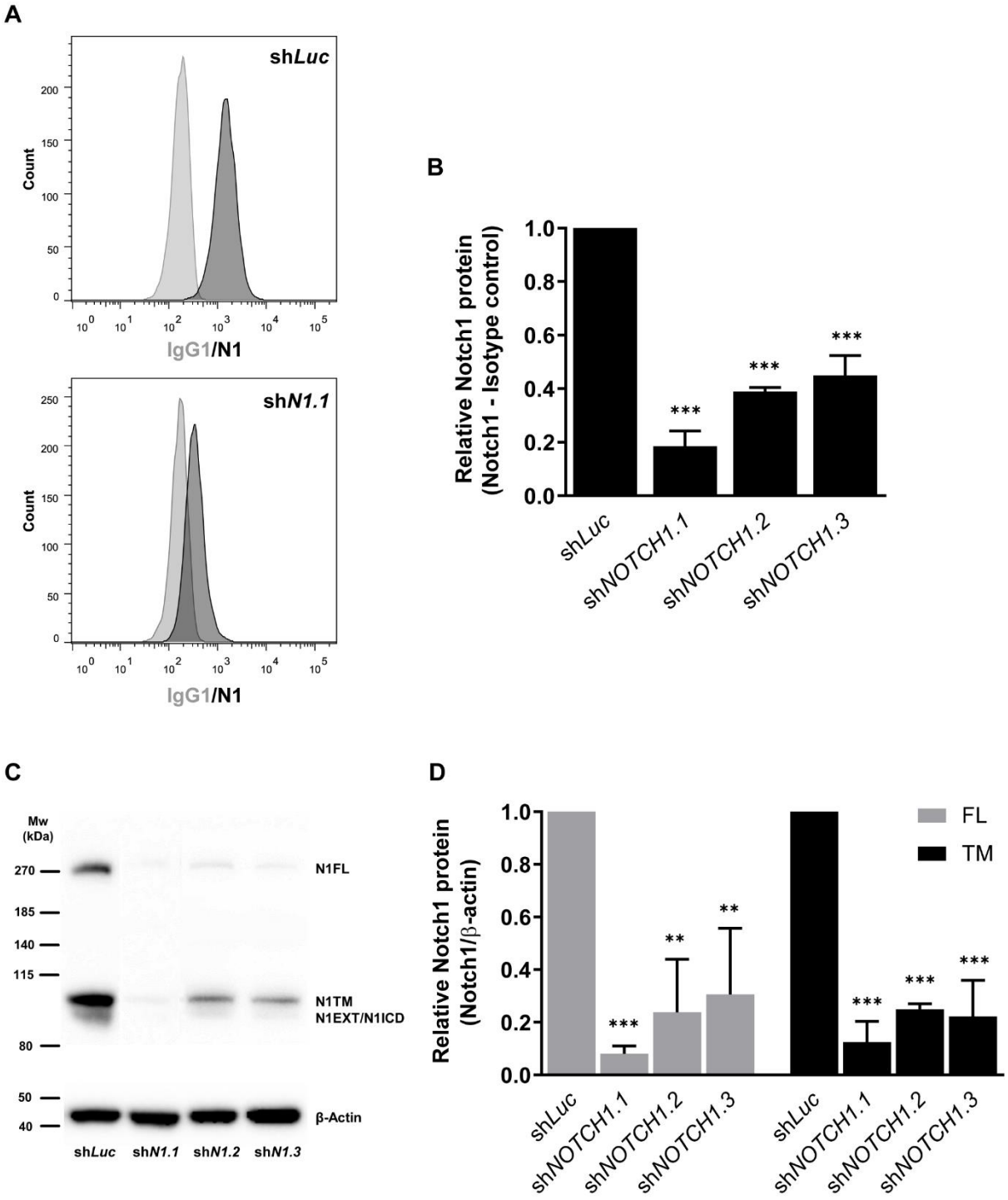

Figure IV.4 – Knockdown of *NOTCH1* (*N1*) receptor in K562 cell line transduced with the constitutive pLV.EF1α-miR30shRNA-GFP lentivector. (A) Representative FCM histogram showing extracellular N1 receptor expression six days after transduction with non-target control sh*Luc* and shRNA targeting *N1* (isotype control shown in light grey). **(B)** Relative N1 receptor levels quantified by FCM on cells transduced with *N1* shRNAs relative to sh*Luc* (n=3). **(C)** Representative immunoblot against N1 receptor in K562 whole cell lysates harvested 9 days after transduction with *N1* shRNAs and shLuc. **(D)** Relative N1 receptor levels quantified by WB of *N1* shRNA transduced cells relative to sh*Luc* transduced cells (n=3). Error bars shown represent S.D.; **p≤0.003, ***p≤0.0003.

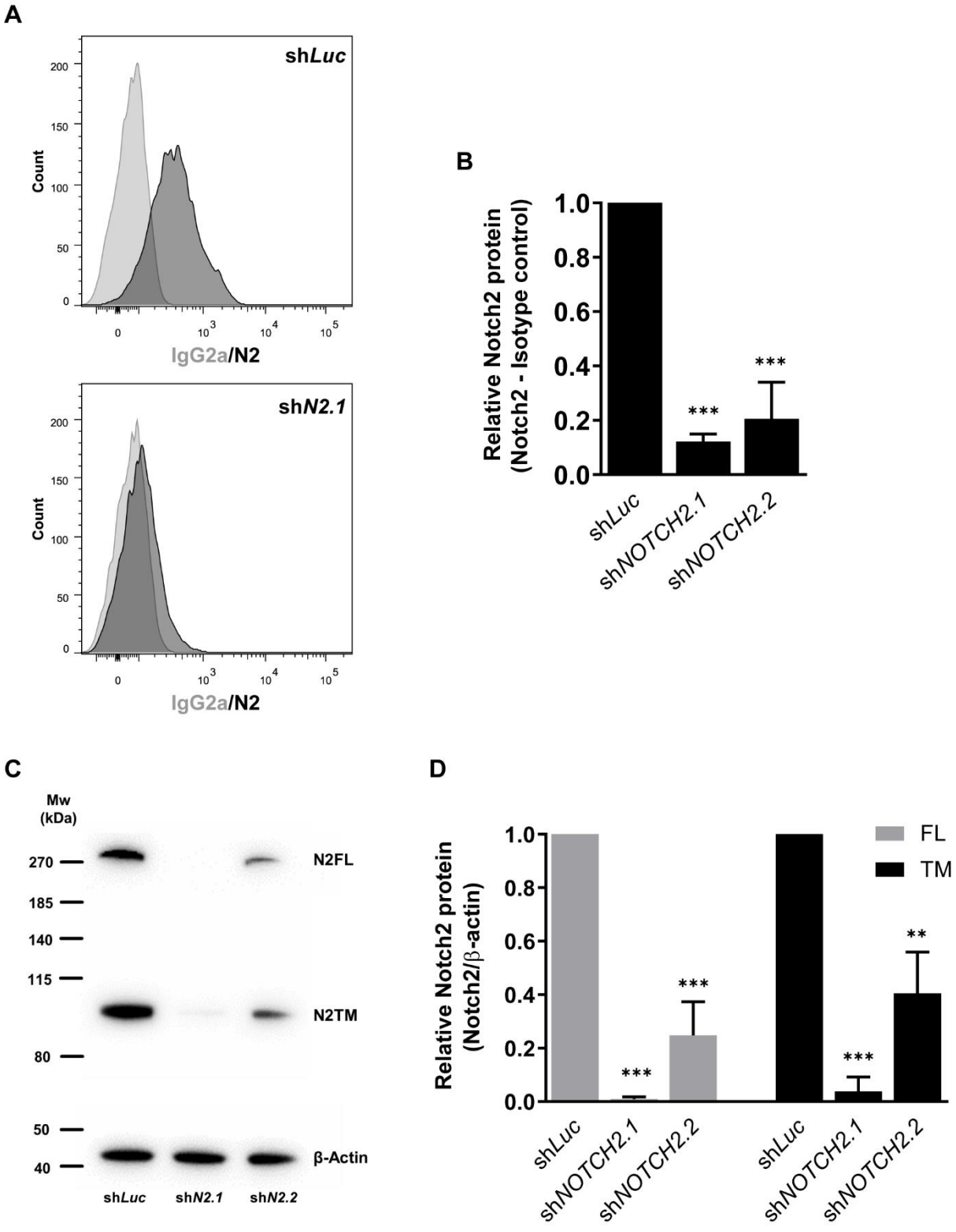

Figure IV.5 – Knockdown of *NOTCH2* (*N2*) receptor in HEK293T cell line transduced with constitutive pLV.EF1α-miR30shRNA-GFP lentivector. (A) Representative FCM histogram showing extracellular N2 receptor expression six days after transduction with non-target control sh*Luc* and shRNA targeting *N2* (isotype control shown in light grey). **(B)** Relative N2 receptor levels quantified by FCM on cells transduced with *N2* shRNAs relative to shLuc (n=3). **(C)** Representative immunoblot against N2 receptor on HEK293T whole cell lysates harvested 9 days after transduction with *N2* shRNAs and shLuc. **(D)** Relative N2 levels quantified by WB of *N2* shRNA transduced cells relative to sh*Luc* transduced cells (n=3). Error bars shown represent S.D.; **p≤0.003, ***p≤0.0003.

IV.2.2.2. VALIDATION IN HSPCS

The control vector shLuc and knockdown vectors sh*N1.1*, sh*N1.2*, sh*N2.1* and sh*N2.2* were then evaluated in CD34^{+}CD38^{-} HSPCs. Briefly, CB CD34^{+}CD38^{-} HSPCs were sorted and transduced with MOI 50 as described in section **II.5.4**. Four days post-transduction, HSPCs transduced with each vector were analysed for GFP expression compared to untransduced HSPCs and GFP-positive cells were collected by FACS.

Surprisingly, transduced HSPCs expressed different intensity levels of GFP, with a smaller frequency of cells expressing high GFP intensity (GFP^{high}), and a larger proportion expressing low GFP intensity (GFP^{low}) without a clear distinction from the negative cells and this was observed for all five vectors. A representative dotplot compared to untransduced HSPCs is presented in **Figure IV.6A**.

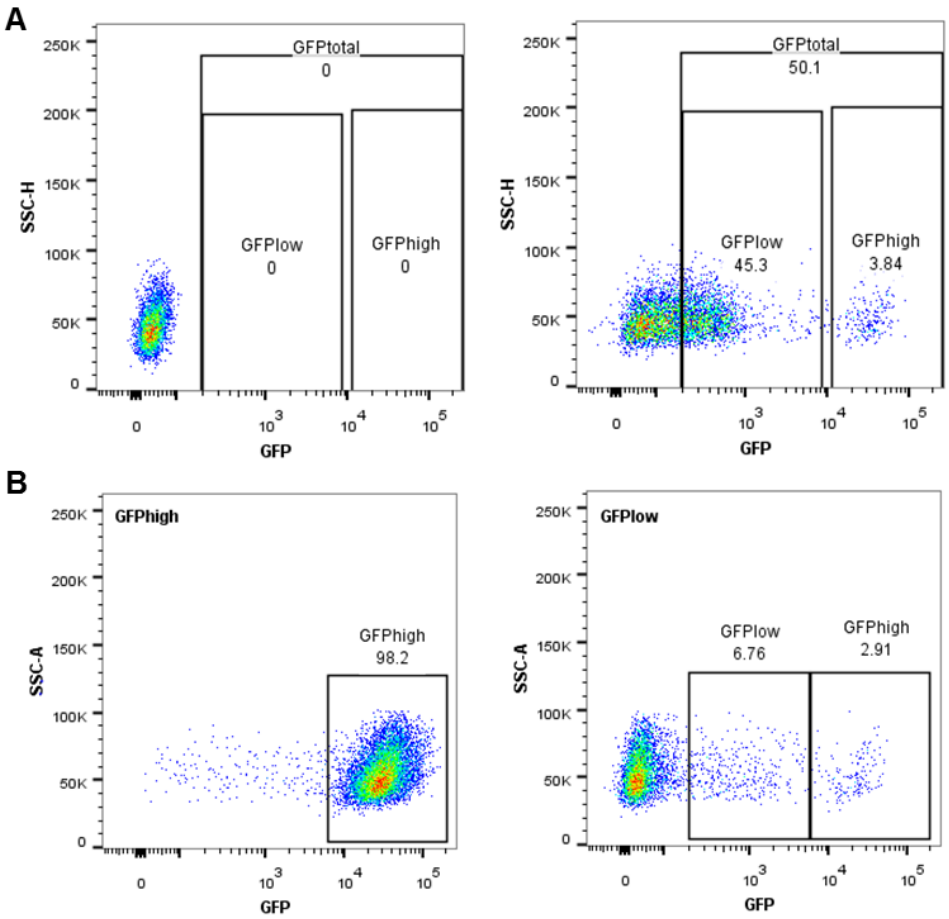

Figure IV.6 – Representative dotplot of GFP expression of CB HSPCs (CD34^{+}CD38^{-}) transduced with a constitutive pLV.EF1α-miR30shRNA-GFP lentivector. (A) GFP levels were analysed four days after transduction compared to untransduced HSPCs and populations GFP^{low} and GFP^{high} were collected separately by FACS. **(B)** GFP levels of GFP^{high} and GFP^{low} populations were analysed after 7 days in culture.

Both GFP^{low} and GFP^{high} cells were sorted separately, as depicted by the gates in **Figure IV.6A**, and cultured *in vitro* for seven days, as described in section **II.5.4**, after which GFP expression was analysed again. As can be seen in **Figure IV.6B**, after culture, virtually all (>98%) GFP^{high} HSPCs maintained the GFP expression, whereas most of (>90%) the GFP^{low} cells lost the GFP expression. This indicated that, unlike the GFP^{high} cells, the sorted GFP^{low} population was only transiently transfected and could not be considered. GFP^{high} HSPCs were cultured for 10 days to obtain sufficient numbers for N1 and N2 detection by WB as shown in **Figure IV.7A** and **B**, respectively. According to these results, the selected shRNAs produced knockdown levels near 80% or higher for both N1TM and N2TM compared to control (**Figure IV.7C**).

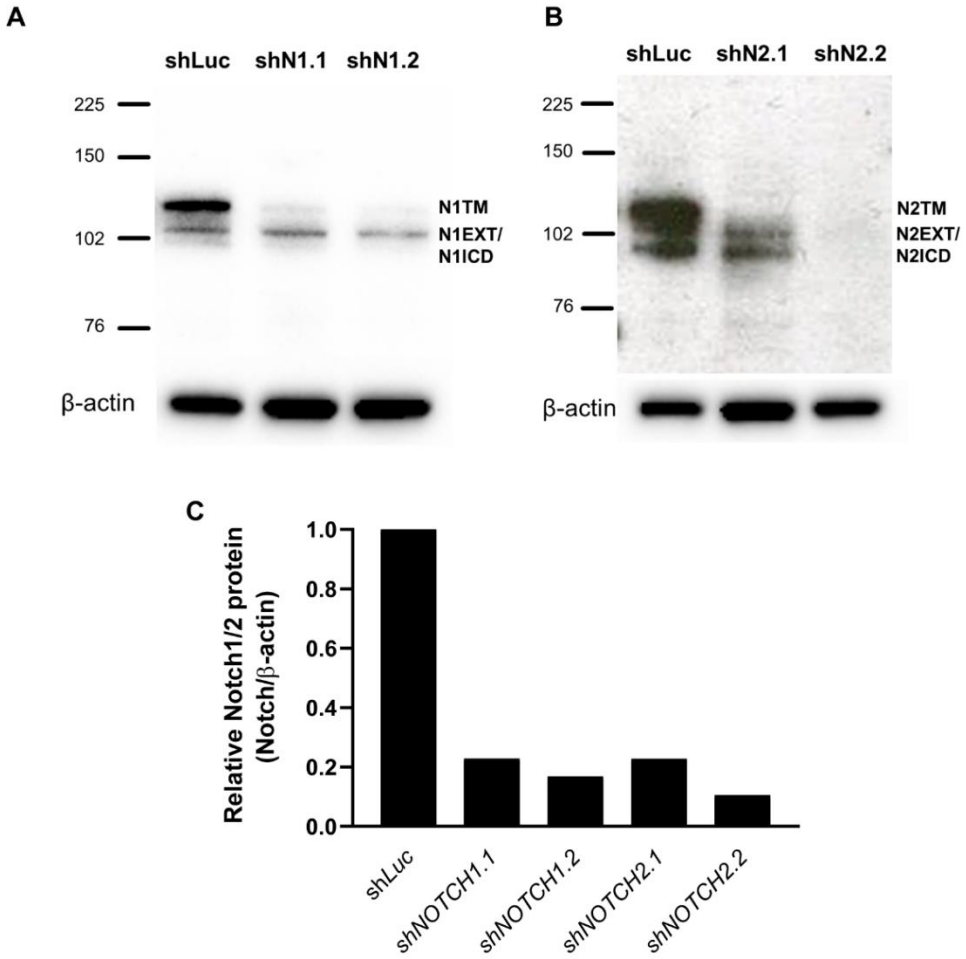

Figure IV.7 – Knockdown of *NOTCH1* and *NOTCH2* receptors in HSPCs transduced with constitutive pLV.EF1α-miR30shRNA-GFP lentivector. Immunoblots against N1 **(A)** and N2 **(B)** receptor protein in HSPCs whole cell lysates harvested 14 days after transduction with *N1* or *N2* shRNAs and shLuc. **(C)** Relative transmembrane N1 and N2 levels quantified from WB of *N1* and *N2* shRNA transduced cells relative to sh*Luc* transduced cells and normalised to the respective β-actin levels (n=1).

However, this experiment was repeated two additional times with different lentivirus batches and the observed transduction efficiencies (percentage of GFP^{high} cells) were still drastically low, varying between 4% to 15%. From previous knowledge, HSPCs transduced with a commercial shRNA lentivector at MOI 40-50 should result in at least 30-40% transduction efficiency.

Unfortunately, these low transduction efficiencies invalidate the feasibility of the developed miR30shRNA vector in HSPCs studies. Besides the inconvenient low cell number after sorting, this unusual low efficiency may result in the transduction of a specific HSPC subpopulation, which can influence the outcome of the studies. It is possible that this impairment is related to the viral vector elements present in the backbone of the developed vector or to the miR30 backbone that for some reason is incompatible with these cells.

Due to time constrains and the complexity of this subject that was out of scope of this study, it was decided to move forward with the silencing studies using a commercially available lentiviral vector, described in the following section, which was known to transduce well HSPCs.

IV.2.3. NOTCH RECEPTORS KNOCKDOWN THROUGH A CONSTITUTIVE H1-SHRNA LENTIVECTOR

As previously mentioned, most commercially available vectors that drive shRNAs use a Pol III promoter (H1 or U6), that are known to work efficiently in human haematopoietic cells. However, Pol III promoters are unable to drive the expression of long-transcripts and therefore do not allow the expression of an in-frame reporter for monitoring the shRNA expression, as in the developed vector. Thus, an additional constitutive promoter (Pol II) must be present in these vectors to drive the expression of the reporter, which means that in these cases the reporter signal represents only the transduced cells and not the strength of the shRNA expression.

IV.2.3.1. CONSTITUTIVE H1-SHRNA LENTIVIRAL VECTOR

The commercial lentivector used henceforward for the HSPCs silencing studies was the CS-H1-shRNA-EG from Riken which contains an H1 promoter to drive the expression of the shRNA and an EF1α promoter to drive the expression of the GFP reporter, as illustrated in **Figure IV.8**.

Cloning of the shRNA sequences in this vector was performed through Gateway® recombination cloning, as described in section **II.2.1.4**.

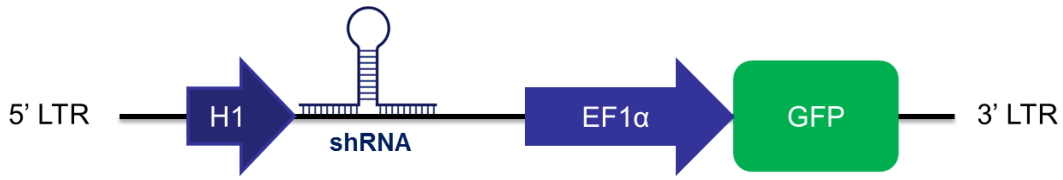

Figure IV.8 – Schematic representation of the commercial lentivector for constitutive expression of shRNA designated CS-H1-shRNA-EG. In this vector the shRNA is expressed through a H1 promoter, while an EF1α promoter drives the GFP reporter that allows monitoring of transduced cells.

IV.2.3.2. VALIDATION IN CELL LINES

Initially, the shRNA sequences previously validated with the miR30shRNA vector were tested with the CS-H1-shRNA-EG vector (termed H1-shRNA henceforward), with some sequences being slightly modified so that it contains an A or G in the beginning of the sequence (as required by Pol III promoters).

shRNA sequences against N1 and N2 receptors, sh*N1.1*-1.2 and sh*N2.1*-2.2, were tested in K562 and HEK293T cell lines respectively, as previously described. However, sequence sh*N1.1* failed to produce efficient knockdowns (data not shown) as observed in the miR30shRNA context, and therefore two more shRNA sequences were tested for N1 (sh*N1.3* and sh*N1.4*).

For N1 receptor knockdown in K562 cells (**Figure IV.9**), sh*N1.2* and sh*N1.4* proved to be the more efficient with consistent knockdowns of around 99% determined by FCM (**Figure IV.9A** and **B**) and accordingly, knockdowns of 99%±0.4% and 93%%±1.2% of N1TM fragment was determined by WB for sh*N1.2* and sh*N1.4* respectively (**Figure IV.9C** and **D**).

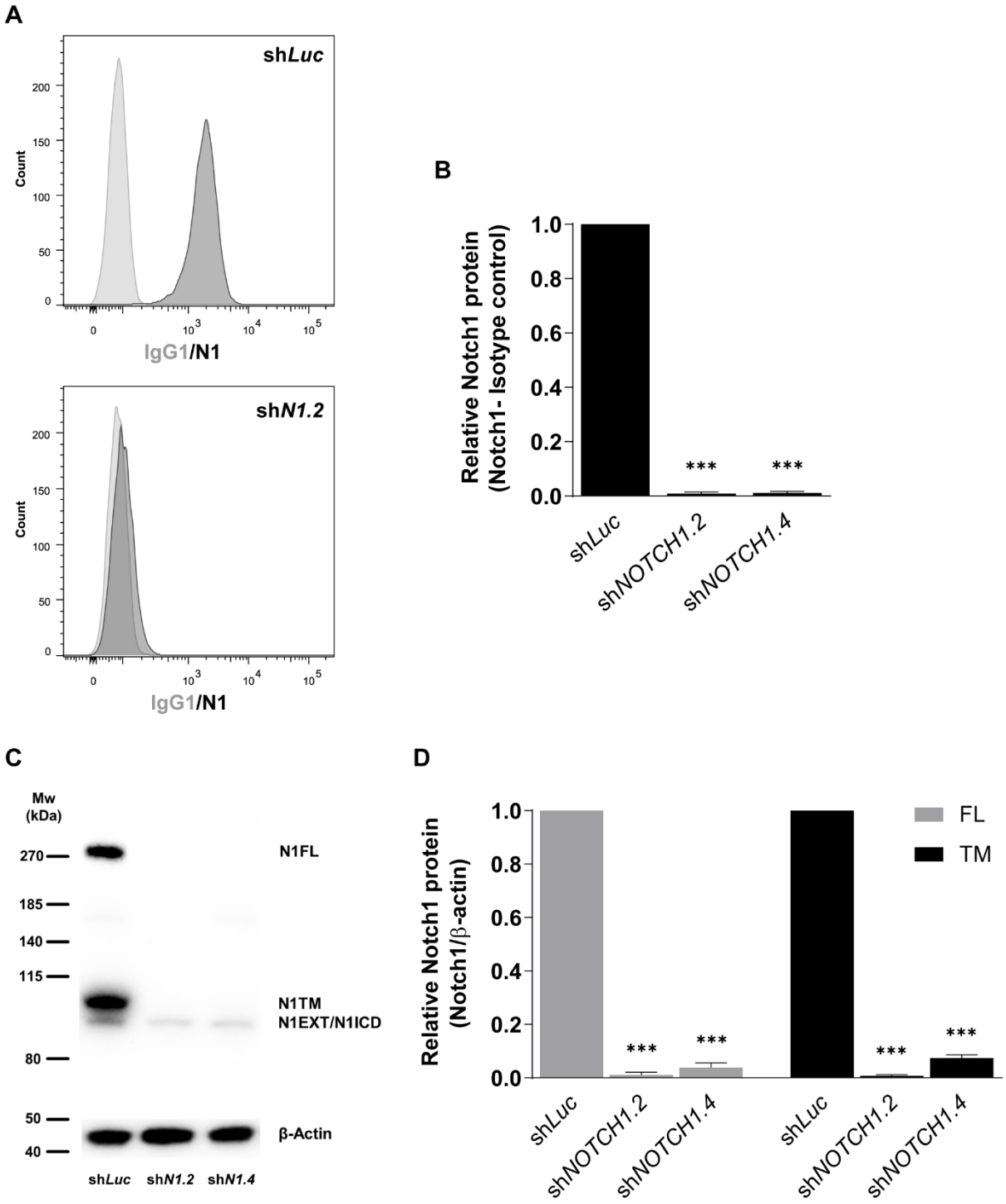

Figure IV.9 – Knockdown of *NOTCH1* (*N1*) receptor in K562 cell line transduced with H1-shRNA lentivector. (A) Representative FCM histogram showing extracellular N1 receptor expression six days after transduction with non-target control sh*Luc* and shRNA targeting *N1* (isotype control shown in light grey). **(B)** Relative N1 receptor levels quantified by FCM on cells transduced with *N1* shRNAs relative to sh*Luc* (n=3). **(C)** Representative immunoblot against N1 receptor in K562 whole cell lysates harvested 9 days after transduction with *N1* shRNAs and shLuc. (D) Relative N1 receptor levels quantified from WB of *N1* shRNA transduced cells relative to sh*Luc* transduced cells (n=3). Error bars shown represent S.D.; ***p≤0.0003.

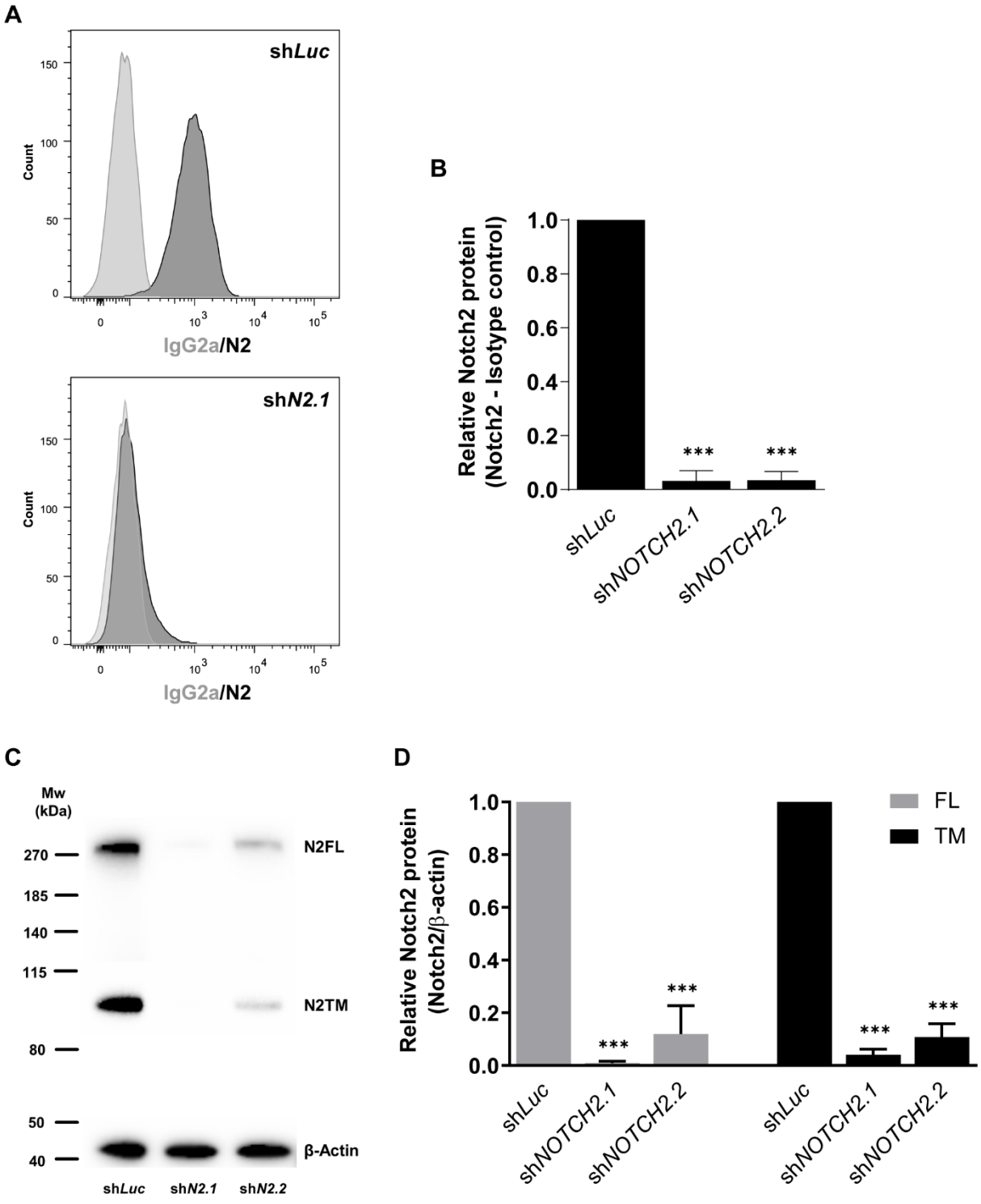

Figure IV.10 – Knockdown of *NOTCH2* (*N2*) receptor in HEK293T cell line transduced with H1-shRNA lentivector. (A) Representative FCM histogram showing extracellular N2 receptor expression six days after transduction with non-target control sh*Luc* and shRNA targeting *N2* receptor (isotype control shown in light grey). **(B)** Relative N2 receptor levels quantified by FCM on cells transduced with *N2* shRNAs relative to shLuc (n=4). **(C)** Representative immunoblot against N2 receptor in HEK293T whole cell lysates harvested 9 days after transduction with *N2* shRNAs and shLuc. **(D)** Relative N2 levels quantified from WB of *N2* shRNA transduced cells relative to sh*Luc* transduced cells (n=4). Error bars shown represent S.D.; ***p≤0.0003.

For the N2 knockdown in HEK293T cells, sh*N2.1* and sh*N2.2* showed similar knockdown efficiencies quantified by FCM around 97%±3.0% (**Figure IV.10 A** and **B**). WB analysis revealed slightly higher knockdown efficiencies for sh*N2.1* (**Figure IV.10C** and **D**), with TM protein knockdowns of 96%±2.1% and 89%±5.1% for sh*N2.1* and sh*N2.2*, respectively. Thus, in comparison to the developed miR30 vector, the H1-shRNA system allowed even higher knockdown efficiencies of Notch receptors in cell lines.

IV.2.4. NOTCH RECEPTORS KNOCKDOWN IN CD34⁺CD38⁻ HSPCS

As mentioned above, lentiviral mediated gene silencing in HSPCs was achieved by transducing CD34⁺CD38⁻ HSPCs with MOI 40-50, after which GFP⁺ cells were collected by FACS four days post-transduction. Illustrated in **Figure IV.11** is the experimental work that was performed to assess the effects of Notch receptors knockdown in the output of the haematopoietic populations *in vitro* (LTC-IC) and *in vivo* (NSG xenotransplant).

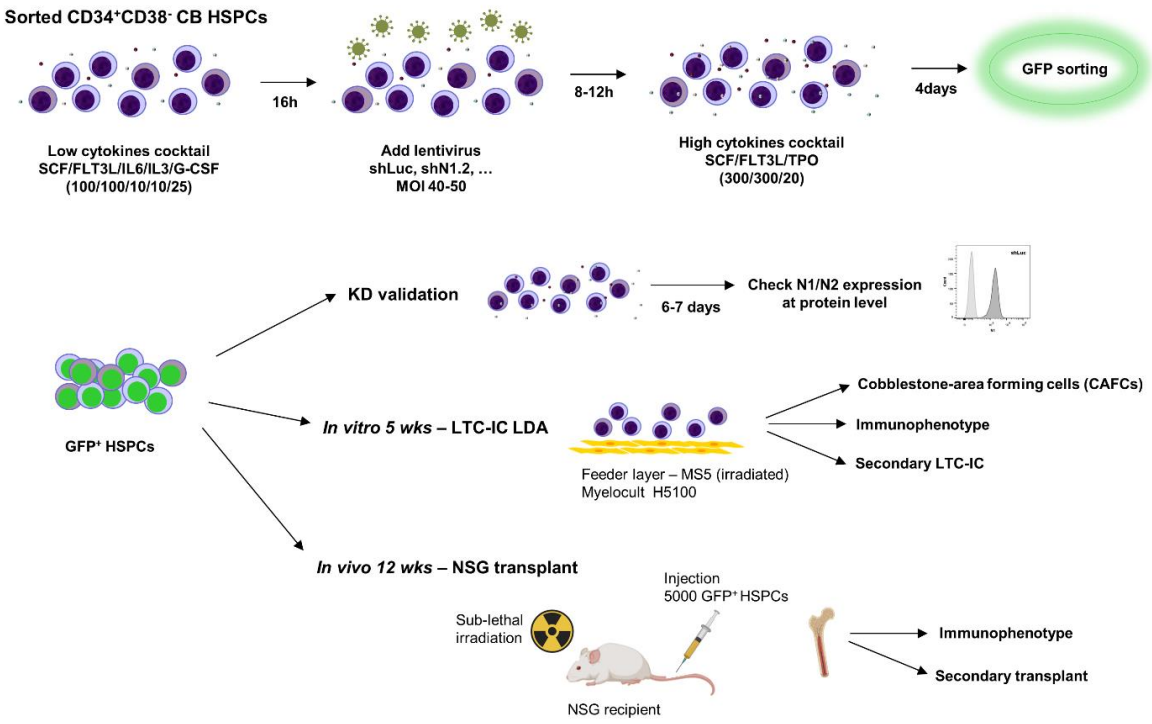

Figure IV.11 – Schematic representation of the experimental work to identify the roles of N1 and N2 receptors in human HSPCs *in vitro* and *in vivo*.

As can be seen in **Figure IV.12A**, transduction effieciencies using the H1-shRNA vector were aroud 30-40% for the different shRNA sequences. These effencies were as expected for HSPCs and GFP$^+$ cells were then plated in suspension cultures for 7 days, as described in section **II.5.4** to assess levels of knockdown by FCM.

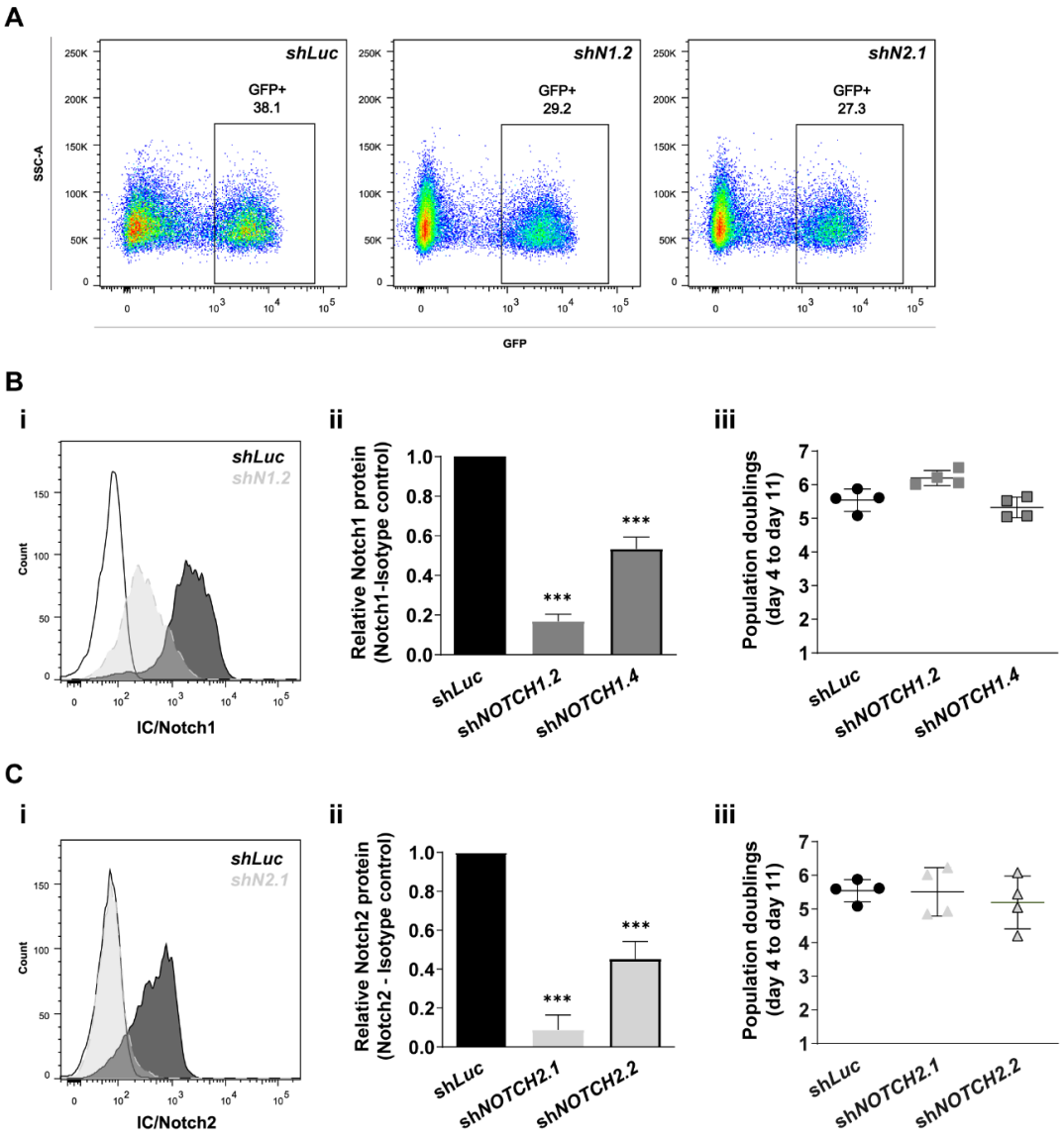

Figure IV.12 – Transduction, knockdown efficiencies and cell growth of CB CD34$^+$CD38$^-$ HSPCs transduced with H1-shRNA lentivectors for knockdown of *NOTCH1* (*N1*) and *NOTCH2* (*N2*) receptors. (A) GFP levels in HSPCs analysed four days after transduction. **(B, C) - (i)** Representative FCM histograms showing extracellular N1 or N2 receptor expression 6-7 days after transduction with sh*Luc* (black) and shRNA targeting *N1* or *N2* (grey dashed line, isotype control shown in empty black line). **(ii)** Relative N1 or N2 levels quantified by FCM on cells transduced with *N1* or *N2* shRNAs relative to shLuc (n=4). **(iii)** Population doublings of HSPCs transduced with the different shRNAs were quantified after 7 days of culture from the day when GFP$^+$ HSPCs were sorted (day4). Error bars shown represent S.D.; ***p≤0.0003.

In general, knockdown effiecies in HSPCs were good for all shRNAs: for N1 receptor, sh*N1.2* resulted in very good knockdowns (83±3.6%), whereas sh*N1.4* induced reasonable knockdowns of 47±5.9% (**Figure IV.12Bi, ii**); similarly, for N2 receptor, sh*N2.1* produced very high knockdowns of 91±7.7%, while sh*N2.2* showed more modest knockdowns of 55±8.9% (**Figure IV.12Ci, ii**). Cell numbers of HSPCs transduced with these shRNAs were determined after 7 days of culture to assess any shRNA toxic effect. As shown in **Figure IV.12Biii** and **Figure IV.12Ciii,** at this early stage no effect in cell growth was detected for all N1 and N2 shRNAs tested.

Therefore, using the H1-shRNA lentiviral system it was demonstrated a robust and efficient shRNA-mediated silencing of N1 and N2 receptors in CB HSPCs without apparent toxic effects.

IV.2.5. EFFECTS OF NOTCH RECEPTORS SILENCING IN HSPCS – *IN VITRO*

The long-term culture assay (LTC-IC) was used as first line of study to assess any effects of Notch receptors silencing in HSPCs. As previously mentioned, these long-term cultures allow to measure the frequency of HSCs or immature progenitors content in a population maintained *in vitro* (section **I.1.2.1**).

For this assay, GFP^+ HSPCs were plated onto MS5 feeder layers at different cell doses as described in section **II.5.5**. After 4 weeks, the number of CAFCs was determined and at week 5 all cells were collected from the wells for immunophenotypic characterisation by FCM described in sections **II.5.5.1**.

Notch receptors silencing on GFP^+CD34^+ LTC cells was also determined by FCM as shown in **Figure IV.13A** and **B** for N1 and N2, respectively. Similar to the suspension cultures, for N1 receptor, knockdowns were 74%±7.0% and 52%±5.0% with sh*N1.2* and sh*N1.4*, respectively, while N2 knockdowns were 88%±2.8% and 46%±10% with sh*N2.1* and sh*N2.2*, respectively. This shows that knockdown levels of Notch receptors were maintained after long-term assays which is essential when studying the self-renewal potential of HSCs.

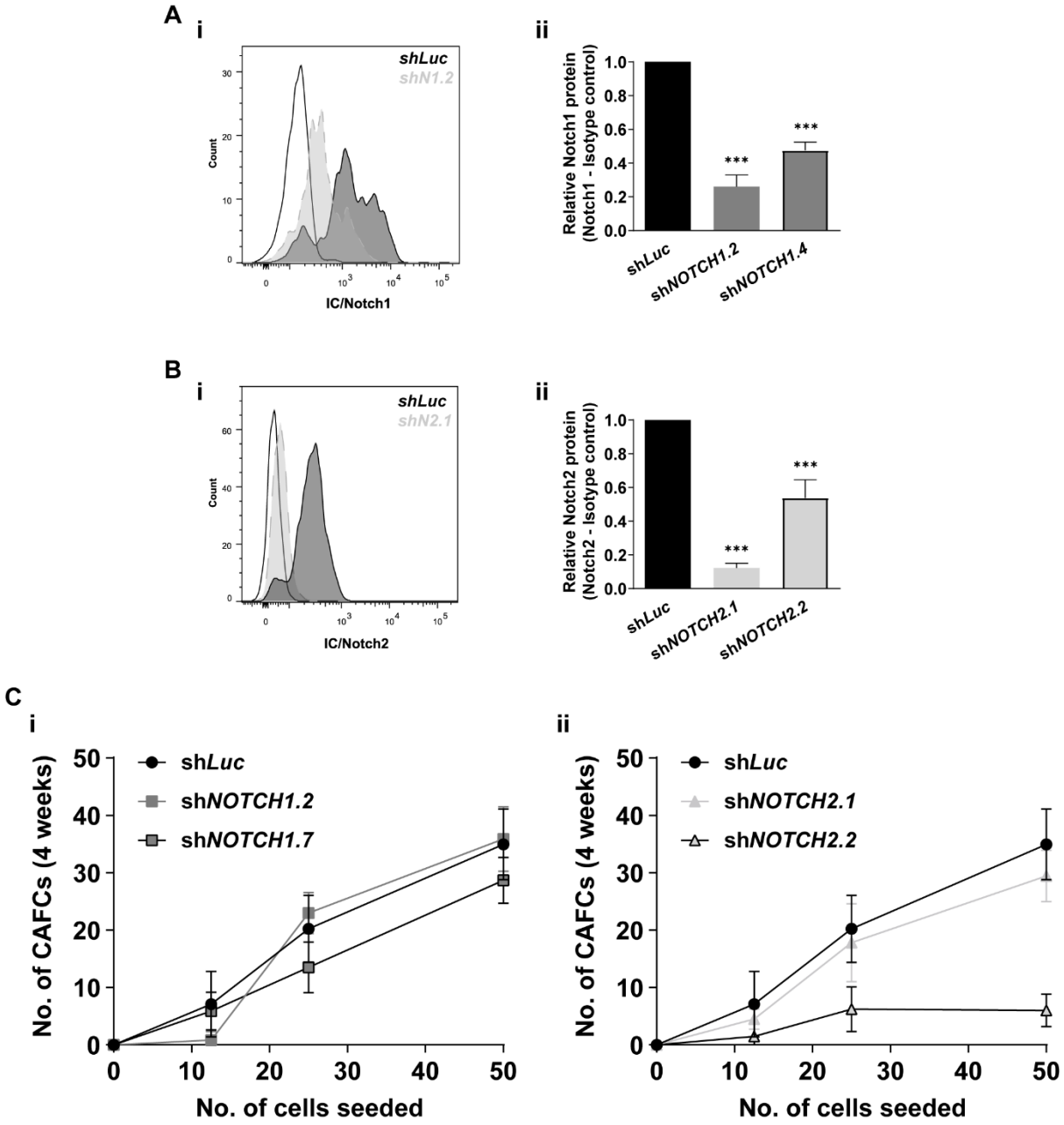

Figure IV.13 – Knockdown efficiencies of *NOTCH1* (*N1*) and *NOTCH2* (*N2*) receptors and colony forming capacity in cells derived from LTC-IC assay of CD34$^+$CD38$^-$ HSPCs transduced with sh*Luc* and shRNA targeting *N1* or *N2*. (A, B) – (i) Representative FCM histograms showing extracellular N1 or N2 receptor expression on LTC derived CD34$^+$ cells expressing sh*Luc* (black) and shRNA targeting *N1* or *N2* (grey dashed line, isotype control shown in empty black line). **(ii)** Relative N1 or N2 levels quantified by FCM on these cells relative to shLuc control (n=3-4). **(C)** Number of cobblestone-area forming cells (CAFCs) generated from the indicated cell doses of CD34$^+$CD38$^-$ transduced with sh*Luc* and shRNA targeting *N1* **(ii)** and *N2* **(ii)** (n=3)**.** Error bars shown represent S.D.; ***p≤0.0003.

When looking at the number of CAFCs resulting from HSPCs transduced with the different shRNAs, no significant differences were observed for *N1* **(Figure IV.13Ci)** or *N2* **(Figure IV.13Cii)** silencing, with the exception of cells transduced with sh*N2.2*, which showed much lower CAFC numbers. Given that no significant reduction of the number of CAFCs was observed with the sh*N2.1* sequence which should have a stronger effect due to the higher knockdown efficiency, it was considered that this reduction in the sh*N2.2* condition could be due to toxic effects of this shRNA.

Indeed, the frequency of GFP^+ cells, which represents the total haematopoietic population present in the total collected cells (**Figure IV.14A**), showed no major differences for N1 and N2 receptors knockdowns as compared to control sh*Luc*, again with the exception of sh*N2.2*. The latter is in accordance with the CAFC quantification and therefore this shRNA was not considered for further analysis.

As the LTC-IC assay measures the presence of primitive haematopoietic cells and the functional output of this assay (CAFC) correlates with the presence of $CD34^+CD38^-$ HSPCs, FCM analysis of the LTC output cells was performed with the aim to shed some light on the affected subpopulations.

Upon N2 knockdown, a significant 3-fold decrease in the frequency of HSCs ($CD45RA^-$ $CD90^+$) associated to an increase in the MLP/LMPP subpopulation ($CD45RA^+CD90^-$) was observed (**Figure IV.14Bi, ii**). On the other hand, silencing of N1 receptor did not show significant differences in HSPCs subpopulations.

Additionally, differentiated cell populations were analysed within the $CD34^-$ population (**Figure IV.14C**) however, no differences in the frequencies of myeloid or lymphoid cells were observed for any Notch receptor knockdown in this assay.

Nevertheless, the effects observed in long-term *in vitro* studies have to be corroborated by *in vivo* xenotransplantation studies to be able to assess the effects in “true” HSCs that are maintained *in vivo* for a longer period of time.

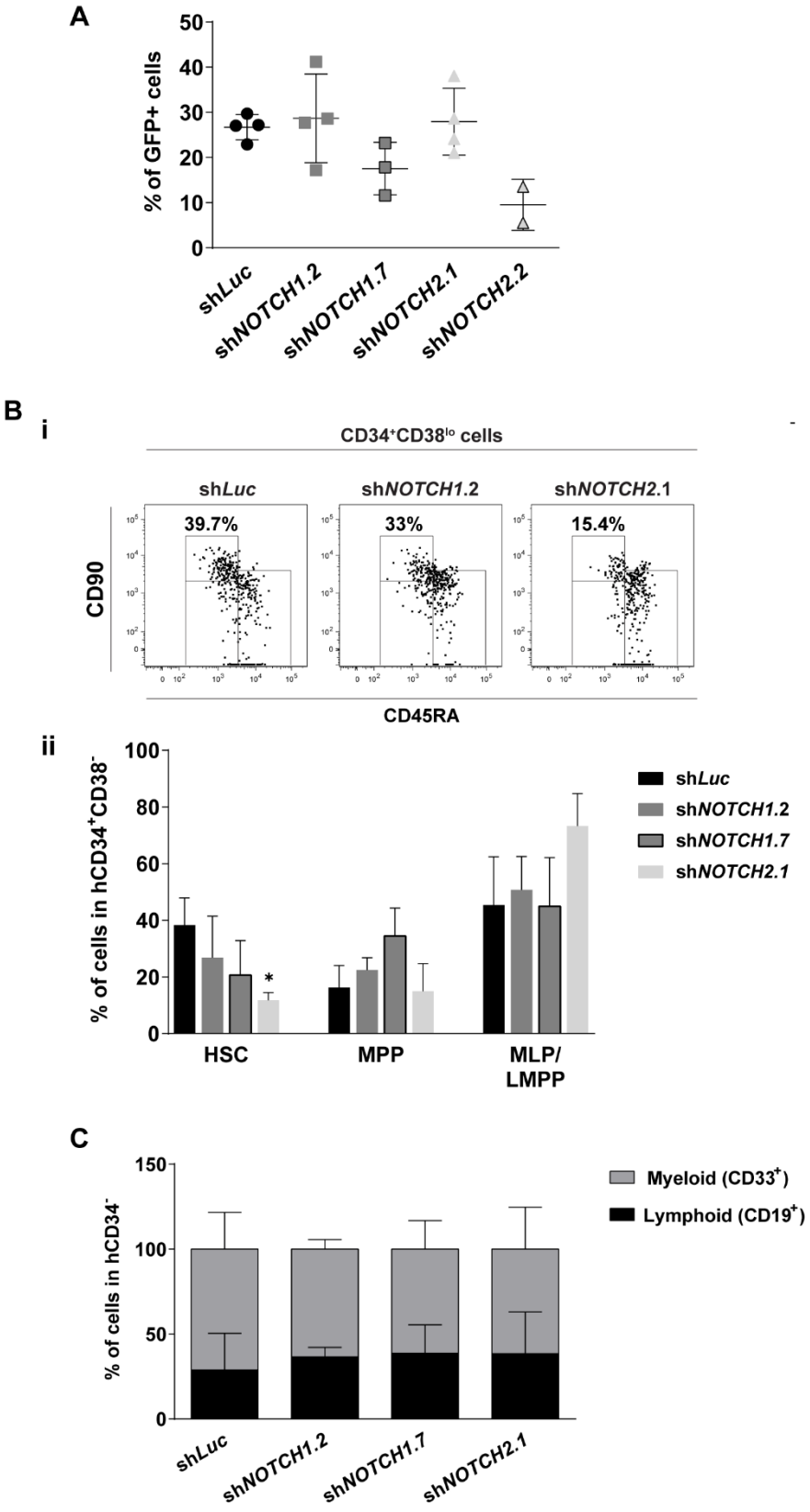

Figure IV.14 – Frequencies of haematopoietic populations generated in the LTC-IC assay with CD34$^+$CD38$^-$ HSPCs transduced with sh*Luc* and shRNA targeting *NOTCH1* (*N1*) or *NOTCH2* (*N2*). **(A)** Frequency of haematopietic cells (GFP$^+$) in the total cells collected from the LTC assay. **(B) – (i)** Example of FCM dotplot showing gating of the different HSPC subpopulations and their respective quantification (**ii**). **(C)** Frequency distribution of myeloid and lymphoid (B-cells) differentiated cells. Error bars shown represent S.D.; number of samples as shown in (A); *p≤0.03.

IV.2.6. EFFECTS OF NOTCH RECEPTORS SILENCING IN HSPCS – *IN VIVO*

The xenotransplant assay is currently the gold standard assay to evaluate the effects on long-term self-renewal and multipotential of HSPCs. For the *in vivo* study, only the most potent shRNAs for each Notch receptor (sh*N1.2* and shN2.1) were considered. NSG mice were transplanted as described in section **II.5.6.1** with GFP$^+$ HSPCs and after 12 weeks BM cells were collected, as described in section **II.5.6.2,** and analysed by FCM to assess the frequencies of the different human haematopoietic subpopulations.

In accordance with the observations from the LTC-IC assay, where no differences in total human GFP$^+$ cells were observed compared to sh*Luc* control thus, the total human engraftment in NSG mice, quantified by the frequencies of human myeloid cells and B cells in all live cells, (**Figure IV.15A**), was not affected by either N1 or N2 receptor knockdown (**Figure IV.15B**).

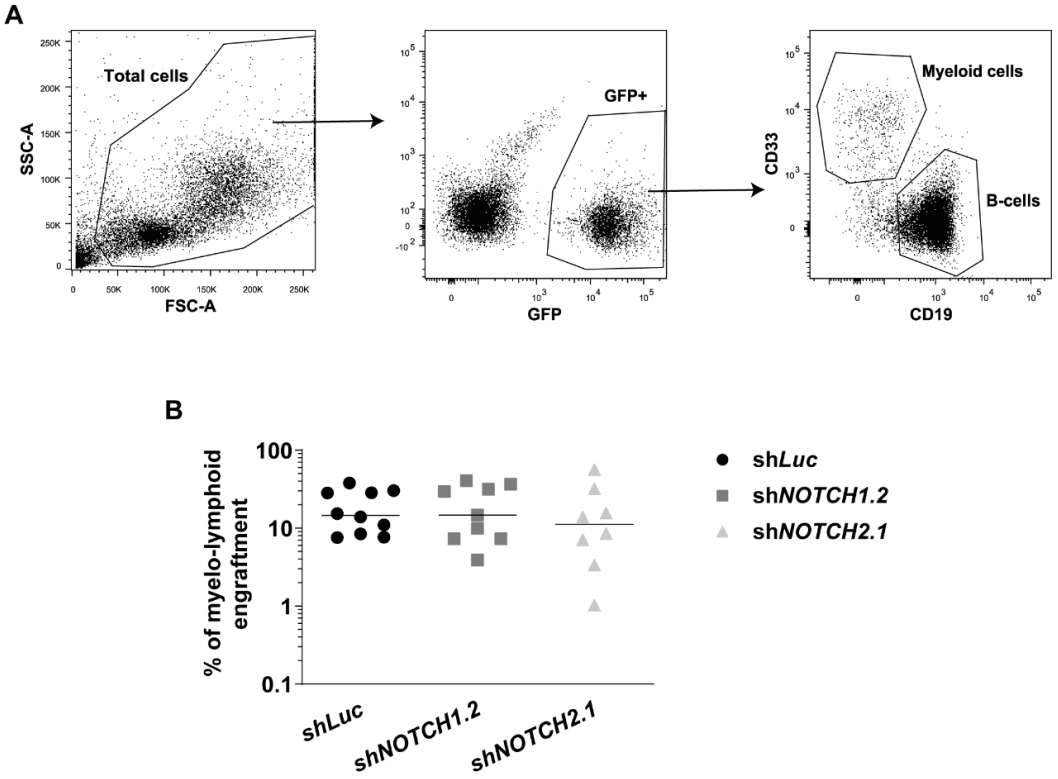

Figure IV.15 – Total human cells engraftment in the BM of NSG mice 12 weeks after transplantation of CD34$^+$CD38$^-$ HSPCs transduced with sh*Luc* and shRNA targeting *NOTCH1* or *NOTCH2.* (A) Gating strategy to quantify total human cells engraftment. **(B)** Quantification of myeloid and B cells frequency in total BM cells. Each dot represents a mouse and median bars are shown.

Moreover, when analysing HSPC and HPC subpopulations (**Figure IV.16A**), it was equally verified that N2 receptor knockdown promoted a significant 9.5-fold decrease in the frequency of the HSC subpopulation (**Figure IV.16B**). Although no significant differences were observed in primitive progenitors or committed progenitors subpopulations (**Figure IV.16B, C**), a decreasing tendency was also noted in the MPP and CMP subpopulations.

For N1 receptor knockdown, no significant differences were verified for any HSPC or HPC subpopulation (**Figure IV.16B** and **C**), although a 4.3-fold increase was noticed in the frequency of LMPPs.

When looking into differentiated cells (**Figure IV.17A**), unlike previously observed in the LTC-IC assay, a significant increase in myeloid differentiation was observed in N1 knockdown, associated to a 1.7-fold reduction in B cells production, whereas no effect was promoted by N2 knockdown (**Figure IV.17B**).

Collectively, these data show that, although not enough to affect total engraftment at 12 weeks post-transplant, the results obtained support that N2 receptor has an important role in maintaining HSC self-renewal potential. On the other hand, N1 seems to have a role in the regulation of more committed progenitors, which is verified by an increase in total LMPPs, albeit not significant, that might had translated to an increase in myeloid differentiation and decrease in B cells output.

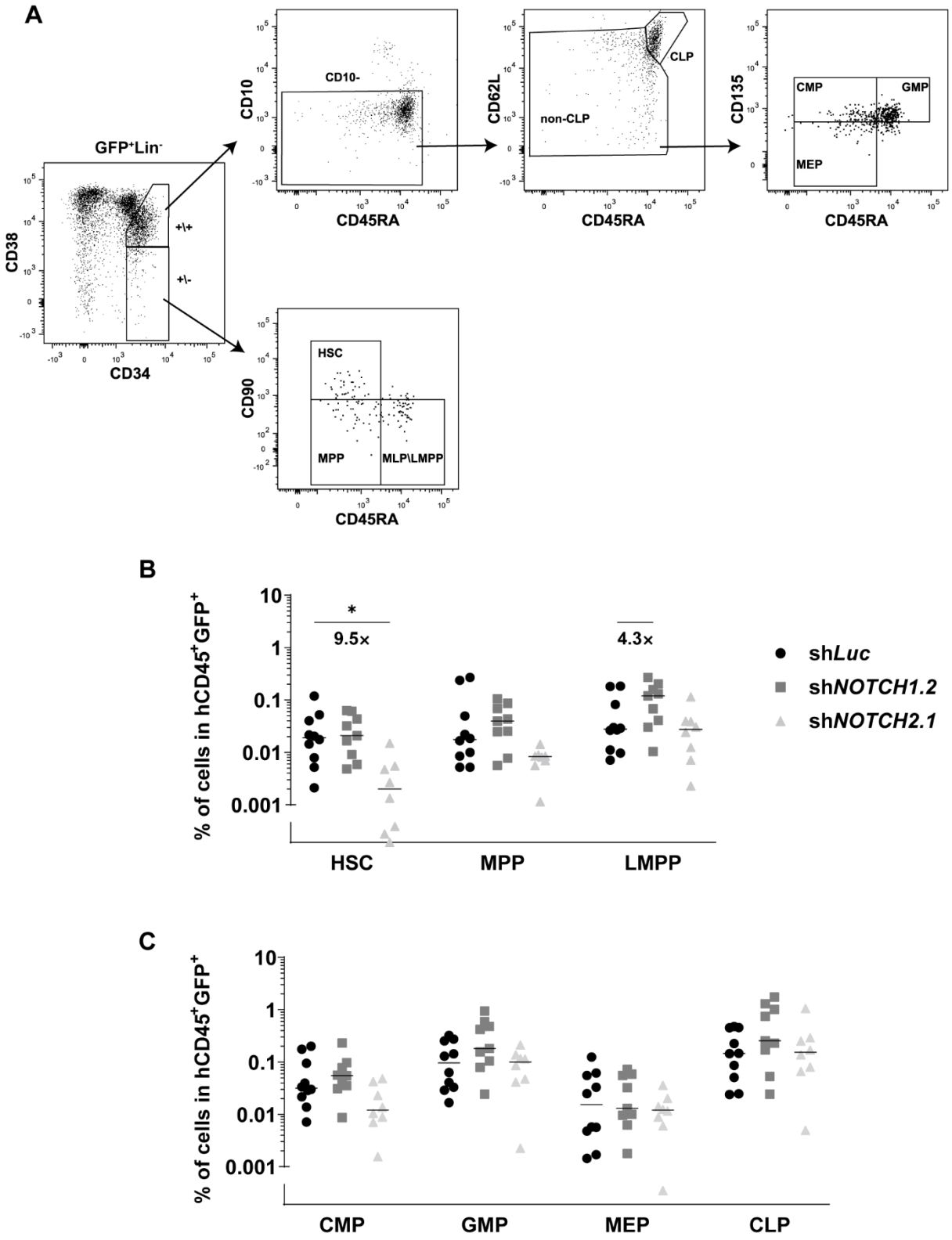

Figure IV.16 – Human haematopoietic stem and progenitor populations in the BM cells of NSG mice 12 weeks after transplantation of CD34$^+$CD38$^-$ HSPCs transduced with sh*Luc* and shRNA targeting *NOTCH1* or *NOTCH2.* (A) Gating strategy to quantify haematopoietic stem and progenitor populations. Quantification of stem and primitive progenitors **(B)** and commited progenitors **(C)** frequencies in total human GFP$^+$ haematopoietic cells. Each dot represents a mouse and median bars are shown. *p≤0.03, **p≤0.003.

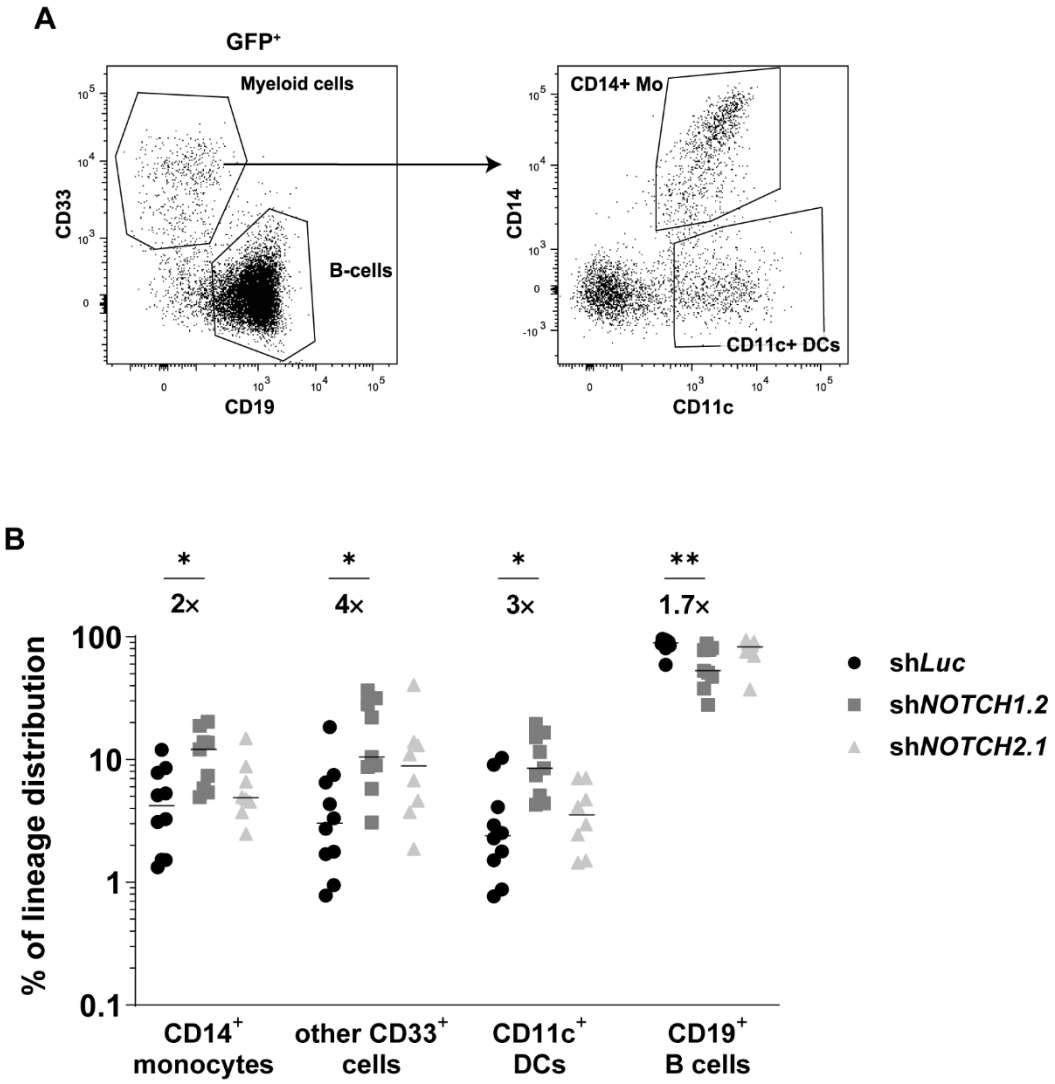

Figure IV.17 – Human haematopoietic differentiation in the BM cells of NSG mice 12 weeks after transplantation of CD34^{+}CD38^{-} HSPCs transduced with sh*Luc* and shRNA targeting *NOTCH1* or *NOTCH2.* (A) Gating strategy to quantify B-cells and CD33^{+} myeloid cells, in particular, monocytes and denditric cells (DCs). **(B)** Quantification of differentiated cells frequencies in total huamn GFP^{+} haematopoietic cells. Each dot represents a mouse and median bars are shown. *p≤0.03, **p≤0.003.

IV.3. DISCUSSION

The current literature suggests that Notch signalling might have a more prominent role in human HSCs than what has been described in the mouse system. However, there is a need for more studies on human HSCs with more stringent and well-described methods to disrupt Notch signalling. Also, to the best of the author knowledge, no studies have been described on the role of individual Notch receptors in human HSCs.

To properly assess regulatory networks and distinguish the roles of the different Notch receptors, it is imperative to identify consensus tools that will allow to specifically and efficiently target each Notch receptor without off-target or toxic effects. Indeed, efficient knockdowns of Notch receptors through RNAi are not well characterised in the literature, with many studies using expensive not defined commercially available siRNAs pools to achieve potent knockdowns. In this work it was identified at least two shRNA and miR30shRNA sequences that produced strong silencing of N1 and N2 receptors and that can hopefully be used by the Notch community in other biological systems.

The initial development of a state-of-the-art inducible system for shRNA-mediated gene silencing was also presented in this chapter. However, although the main goal of developing a new all-in-one inducible vector was to achieve a strong and efficient knockdown in human HSPCs in an inducible manner, this was not attainable given that when testing the constitutive version of this vector it failed to allow efficient transduction efficiencies in HSPCs. Unfortunately, this is a dismissible factor when studying HSPCs since not only represents a higher cost in reagents but also a much higher requirement of initial cord blood mononuclear cells making it pragmatically unfeasible. Also, when dealing with low transduction efficiency in a mixed population like the $CD34^{+}CD38^{-}$ HSPCs there is the concern of selecting a specific subpopulation more prone to transduction which can skew the results of the knockdown effects. Therefore, due to time constrains, it was decided to pursue the silencing studies using a commercially available less sophisticated constitutive vector for shRNA expression

that nonetheless, allowed high and robust knockdowns of N1 and N2 with at least two shRNA sequences.

In fact, despite being commonly advertised that mir30shRNAs promote more potent knockdowns than conventional shRNA, this was not observed in this work, where it was clear that for most sequences the latter produced stronger knockdowns. However, this was not true for all sequences, in particular for sh*N1.1* that showed a poorer knockdown in K562 cells (around 50%, data not shown) compared to the miR30 version. These conflicting results seem to be sequence-specific, although it has been shown that shRNAs are generally more potent than artificial miR-based shRNAs in mediating gene silencing independent of target sequence and experimental setting, since shRNAs are expressed at considerably higher levels [16]. Nevertheless, miR-based shRNA systems offer several technical advantages that will be discussed in the next chapter. Furthermore, miR30 backbone has recently been optimised in order to promote more potent knockdowns [17], which will be explored in the next chapter.

Once it was achieved a robust system for the efficient silencing of N1 and N2 receptors in CB HSPCs, LTC-IC assays were performed as first line of study on HSPCs self-renewal and differentiation. Identification of primitive cells in this assay can be made through direct quantification of CAFCs in the feeder layer. In this work, silencing of N1 or N2 receptor did not promote any measurable alteration in the number of primary CAFCs. However, looking into the phenotypic characterisation of the output population from shN2.1 expressing-HSPCs, it was observed that within the HSPC compartment there is a significant decrease in the HSC subpopulation associated to an increase in LMPPs.

In fact, in the only study in the literature assessing the role of Notch signalling in purified human HSCs [18], the authors verified that in the presence of Dll4 ligand, canonical Notch inhibition (through overexpression of dnMAML) promoted accelerated progression of HSCs to $CD45RA^{int}$ and $CD45RA^{hi}$ stages (LMPPs). As seen in the previous chapter, exposure of HSPCs to Dll4 *in vitro*, leads to expansion with reduced $CD45RA^{+}$ progenitors (**Figure III.12B**). Moreover, the authors also showed that Notch inhibition completely blocked cellular expansion of $CD45RA^{-}$ subpopulations promoted by Dll4 ligand resulting in a decrease of HSC subpopulation, which is in line with the results from this study.

The *in vivo* xenotransplantation assay gave definitive proof that N2 has an important role in the regulation of human HSCs since its frequency was significantly reduced in mice transplanted with shN2.1 expressing-HSPCs. This result is the first indication that Notch signalling through N2 receptor is important for maintenance of human HSCs self-renewal capacity. However, this effect was not strong enough to decrease HSCs repopulation capacity at the 12-week time-point, since lymphomyeloid reconstitution was not significantly affected. This is in line with the *in vitro* results, where no decrease in total GFP^+ cells was observed in LTC-IC output population. Therefore, evaluation of secondary transplants is essential to verify the effect on long-term reconstituting HSCs. Additionally, secondary LTC-ICs should also be performed to verify the extent of HSCs self-renewal reduction *in vitro*.

Somewhat in accordance with these results, *in vivo* studies with mouse HSPCs demonstrated a prominent role of N2 receptor and not N1 in self-renewal and repopulation capacity under regenerative conditions [19]. Moreover, activation of N2 receptor was associated to regulation of HSPC cell cycle during regeneration, suggesting that N2 receptor is involved in maintaining HSPC quiescence [20, 21].

Regarding N1 receptor, in line with what was reported for the mouse system, it seems that N1 receptor is not essential for the regulation of HSCs self-renewal and differentiation, at least for the experimental settings used. It seems however, that this receptor is important for the regulation of differentiation *in vivo*, since decrease in N1 expression promoted myeloid over lymphoid differentiation. However, it is difficult to understand at what progenitor stage N1 receptor might have a regulatory effect in cell fate decision, since no significant changes were observed in the more committed progenitor subpopulations analysed. Only the primitive LMPPs appeared to show increased frequency, although not significant, which can suggest a block in lymphoid differentiation at this stage.

Similar to this observation, mice with pan-haematopoietic deletion of *Pofut*, which disables the receptors capacity to bind to Delta-like ligands, showed increased numbers of myeloid cells and reduced lymphocytes, which were rescued by overexpression of N1ICD in Pofut-deficient cells [22]. Moreover, a subsequent work demonstrated that mice transplanted with Nicastrin (γ-secretase component)-deficient HSCs developed myeloproliferative disease with an expanded HSPC compartment

associated to a de-repressed myeloid program, which is thought to be carried out by Hes1-mediated inhibition of *Cepba* and *Spi1* expression [23].

IV.4. REFERENCES

1. Lampreia FP, Carmelo JG, Anjos-Afonso F. Notch Signaling in the Regulation of Hematopoietic Stem Cell. Current stem cell reports. 2017;3(3):202-9.

2. Moore CB, Guthrie EH, Huang MT, Taxman DJ. Short hairpin RNA (shRNA): design, delivery, and assessment of gene knockdown. Methods Mol Biol. 2010;629:141-58.

3. Zeng Y, Cullen BR. Sequence requirements for micro RNA processing and function in human cells. RNA. 2003;9(1):112-23.

4. Zeng Y, Wagner EJ, Cullen BR. Both natural and designed micro RNAs can inhibit the expression of cognate mRNAs when expressed in human cells. Mol Cell. 2002;9(6):1327-33.

5. Woods NB, Fahlman C, Mikkola H, Hamaguchi I, Olsson K, Zufferey R et al. Lentiviral gene transfer into primary and secondary NOD/SCID repopulating cells. Blood. 2000;96(12):3725-33.

6. Ali N, Karlsson C, Aspling M, Hu G, Hacohen N, Scadden DT et al. Forward RNAi screens in primary human hematopoietic stem/progenitor cells. Blood. 2009;113(16):3690-5.

7. Gossen M, Bujard H. Tight control of gene expression in mammalian cells by tetracycline-responsive promoters. Proc Natl Acad Sci U S A. 1992;89(12):5547-51.

8. Lewandoski M. Conditional control of gene expression in the mouse. Nat Rev Genet. 2001;2(10):743-55.

9. Freundlieb S, Schirra-Muller C, Bujard H. A tetracycline controlled activation/repression system with increased potential for gene transfer into mammalian cells. J Gene Med. 1999;1(1):4-12.

10. Urlinger S, Baron U, Thellmann M, Hasan MT, Bujard H, Hillen W. Exploring the sequence space for tetracycline-dependent transcriptional activators: novel mutations yield expanded range and sensitivity. Proc Natl Acad Sci U S A. 2000;97(14):7963-8.

11. Ramezani A, Hawley TS, Hawley RG. Lentiviral vectors for enhanced gene expression in human hematopoietic cells. Mol Ther. 2000;2(5):458-69.

12. Loew R, Heinz N, Hampf M, Bujard H, Gossen M. Improved Tet-responsive promoters with minimized background expression. BMC Biotechnol. 2010;10:81.

13. Das AT, Zhou X, Vink M, Klaver B, Verhoef K, Marzio G et al. Viral evolution as a tool to improve the tetracycline-regulated gene expression system. J Biol Chem. 2004;279(18):18776-82.

14. Zhu MS, Xu LB, Zeng H, Shi XD, Wu WR, Liu C. Association of Notch1 with vasculogenic mimicry in human hepatocellular carcinoma cell lines. Int J Clin Exp Pathol. 2014;7(9):5782-91.

15. Delaney C, Varnum-Finney B, Aoyama K, Brashem-Stein C, Bernstein ID. Dose-dependent effects of the Notch ligand Delta1 on ex vivo differentiation and in vivo marrow repopulating ability of cord blood cells. Blood. 2005;106(8):2693-9.

16. Boudreau RL, Monteys AM, Davidson BL. Minimizing variables among hairpin-based RNAi vectors reveals the potency of shRNAs. RNA. 2008;14(9):1834-44.

17. Fellmann C, Hoffmann T, Sridhar V, Hopfgartner B, Muhar M, Roth M et al. An optimized microRNA backbone for effective single-copy RNAi. Cell reports. 2013;5(6):1704-13.

18. Benveniste P, Serra P, Dervovic D, Herer E, Knowles G, Mohtashami M et al. Notch signals are required for in vitro but not in vivo maintenance of human hematopoietic stem cells and delay the appearance of multipotent progenitors. Blood. 2014;123(8):1167-77.

19. Varnum-Finney B, Halasz LM, Sun M, Gridley T, Radtke F, Bernstein ID. Notch2 governs the rate of generation of mouse long- and short-term repopulating stem cells. J Clin Invest. 2011;121(3):1207-16.

20. Guo P, Poulos MG, Palikuqi B, Badwe CR, Lis R, Kunar B et al. Endothelial jagged-2 sustains hematopoietic stem and progenitor reconstitution after myelosuppression. J Clin Invest. 2017;127(12):4242-56.

21. Wang W, Yu S, Myers J, Wang Y, Xin WW, Albakri M et al. Notch2 blockade enhances hematopoietic stem cell mobilization and homing. Haematologica. 2017;102(10):1785-95.

22. Yao D, Huang Y, Huang X, Wang W, Yan Q, Wei L et al. Protein O-fucosyltransferase 1 (Pofut1) regulates lymphoid and myeloid homeostasis through modulation of Notch receptor ligand interactions. Blood. 2011;117(21):5652-62.

23. Klinakis A, Lobry C, Abdel-Wahab O, Oh P, Haeno H, Buonamici S et al. A novel tumour-suppressor function for the Notch pathway in myeloid leukaemia. Nature. 2011;473(7346):230-3.

CHAPTER V

DEVELOPMENT OF STATE-OF-THE-ART LENTIVECTORS FOR INDUCIBLE GENE SILENCING AND OVEREXPRESSION

V.1. INTRODUCTION

As introduced in the previous chapter, the advent of gene silencing through the RNAi pathway has significantly impacted the field of biological research as a powerful tool for functional genomics, allowing to easily explore gene function in mammalian cells with great specificity.

RNAi-mediated knockdown or post-transcriptional gene silencing of the gene of interest can be achieved either by transient expression of synthetic short interfering RNAs (siRNAs) or stable expression of shRNAs [1, 2]. Viral delivery of synthetic shRNAs in gene expression cassettes has allowed stable and heritable gene silencing. In particular, lentiviral vectors are capable of infecting a wide variety of dividing and non-dividing cells, integrating stably into the host genome allowing long term expression of the transgene (reviewed in [3]).

As briefly mentioned, the initial and still widely used shRNA expression systems rely on RNA Pol III promoters such as the H1 or U6 promoter which direct high levels of shRNA expression mediating highly potent gene silencing. However, these promoters cannot be used for cell specific expression since they are constitutively expressed in all cell types. In addition, exceedingly high levels of shRNA can elicit off-target silencing and non-specific effects such as interferon response and cellular toxicity [4-6]. Thus, a second generation of RNAi-systems implemented the expression of shRNA embedded into endogenous miRNA backbones (miRshRNA) which, as previously explained, are processed through the complete RNAi biogenesis pathway, limiting its build-up but still eliciting potent knockdowns [7, 8]. In particular, human miRNA30 has been extensively used in these systems [9-12] since processing of the larger pre-miRNA transcript to its functional miRNA has been well characterised *in vitro* and *in vivo* (reviewed in [13]). Furthermore, expression of miRshRNAs is driven by Pol II promoters which, besides enabling tissue-specific expression, allow transcription of a reporter gene linked to the miRshRNA in a polycistronic sequence to monitor cells with effective shRNA expression [8, 12]. This further enables to isolate clonal populations

with stronger reporter expression which correlates to higher shRNA copies and consequently more potent gene silencing.

Inducible miRshRNA systems have also been developed and optimised in the last decade [12, 11] which offer many advantages over the constitutive systems, particularly for the study of essential genes. Since constitutively expressed shRNAs targeting essential genes promote a toxic effect in the transduced cells, controlling the timing and levels of shRNA expression is valuable for many experimental settings. Moreover, the ability to regulate shRNA expression makes it possible to investigate time- and dose-dependent effects which can be completely reversed. Also, inducible systems allow for strict isogenic controls within an experiment, since the ability to control expression of the gene of interest in a population of cells can minimise experimental variations due to clonal heterogeneity.

As previously introduced, rtTA-dependent inducible systems (Tet-on) allow transcription activation in the presence of doxycycline. Several efforts have been made towards optimisation of the rtTA protein in order to improve dynamic range, by reducing residual DNA binding in the non-induced state and enhancing dox sensitivity and transcriptional activity in the induced state [14-16]. The rtTA3 protein used in the present inducible vectors has been developed to meet these criteria [15] and has been used as well in recent inducible systems [12, 11]. Other approaches have focused on the manipulation of the tetracycline responsive elements (TRE) and downstream promoter (usually a minimal CMV promoter) to minimise background expression while maintaining high levels of induced expression [17, 18]. In this regard, a synthetic inducible promoter (commercialised by Takara Bio Inc. as PTRE3G) was modified for optimal performance, lacking binding sites for endogenous mammalian transcription factors thus, being virtually silent in the absence of induction [17].

However, many inducible shRNA systems still require delivery of two vectors to introduce the transactivator protein and the inducible promoter controlling the transgene expression. These two-vector systems are unfeasible for difficult to transduce cells and usually involve a time-consuming multi-step clone selection process precluding studies in cell types with limited lifespan in culture.

Moreover, another key problem associated to inducible vectors is the heterogeneity in transgene expression levels among cells due to different integration sites [19] or the variable inducibility due to different rtTA expression levels.

To circumvent these issues all-in-one dual colour inducible systems like the pINDUCER lentiviral system [11] and the retroviral TRMPVIR [12] have been developed, which coupled fluorescent reporters to both the inducible shRNA expression and the constitutive rtTA expression. These systems broaden the applicability of inducible shRNA vectors and allow the identification not only of transduced cells but more specifically, cells that express the functional shRNA construct upon induction thus, enabling isolation of cells with higher rtTA expression and shRNA inducibility. However, these systems still present some limitations like intrinsic leakiness and unstable reporter expression that will be discussed below.

In this chapter, long-term *in vitro* validation was performed to assure the stability and functionality of the developed state-of-the art inducible lentivectors which initial design was introduced in the previous chapter. Modifications to this initial Tet-on miR30shRNA lentivector were required as will be described in this chapter. Furthermore, the development and validation of analogous inducible systems for overexpression of a protein of interest is also described.

V.2. RESULTS

V.2.1. INDUCIBLE TET-ON MIR30SHRNA LENTIVECTORS – LONG-TERM VALIDATION IN VITRO

When developing new lentiviral vectors, it is important to assess the stability and toxicity of the new constructs during cell culture that are essential to validate long-term transgene expression. This is particularly important to confirm the usefulness of the lentivector for stem cell assays that can take up to several weeks in culture.

After developing the inducible Tet-On miR30shRNA vector described in the previous chapter (section **IV.2.1.2**) long-term cultures were performed to assess the stability of integrated vector in cell lines (monitored by mCherry expression) as well as levels of inducibility (GFP expression) and gene knockdown throughout time.

V.2.1.1. TET-ON MIR30SHRNA LENTIVECTOR WITH SFFV PROMOTER

The originally developed lentivector pLV.TetSyntP-miR30shRNA-GFP, now renamed as pLV.TetSyntP-miR30shRNA-GFP-SFFV-rtTA3-mCherry (SyntPshmiR-SFFV; refer to **Figure IV.2**), was transduced in HEK293T cells with an MOI of 10, followed by sorting of $mCherry^+$ cells which were monitored throughout culture. Surprisingly, it was observed that mCherry expression decreased steadily at high rate throughout time in culture and only 30% of the population was still positive after 3 weeks, as demonstrated in **Figure V.1**.

To verify if this effect was not exclusive to HEK293T cells, the K562 cell line was also transduced with this lentivector and monitored in long-term cultures. As can be seen in **Figure V.2**, although the loss of mCherry expression was not as steep as observed in HEK293T, after 3 weeks only around half of the population was still positive for mCherry expression. In addition, during cell culture it was observed that cell growth was slower when a higher proportion of $mCherry^+$ cells was present, which returned to normal as mCherry expression decreased (data not shown).

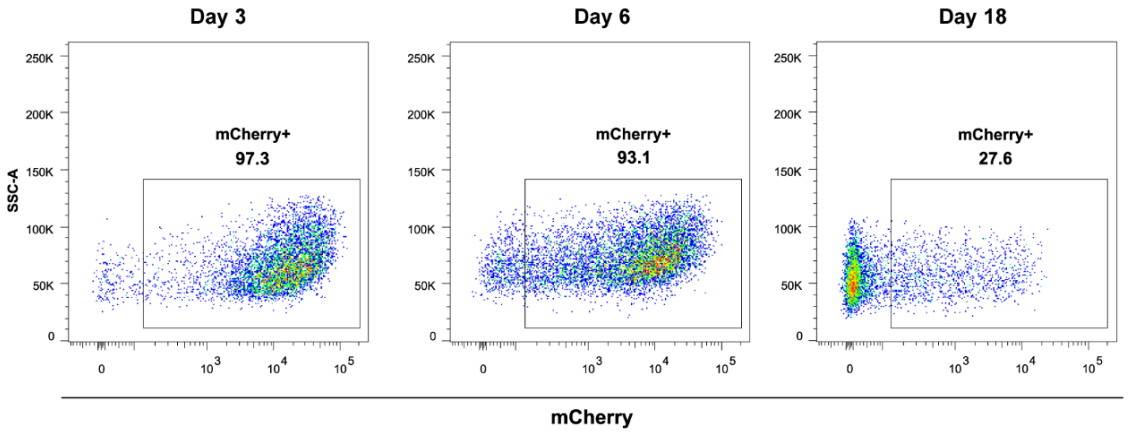

Figure V.1 – Lost of mCherry expression in HEK293T cells transduced with the inducible SyntPshmiR-SFFV. Representative FCM dotplots showing the percentage of mCherry$^+$ cells at different time points in culture (n=2).

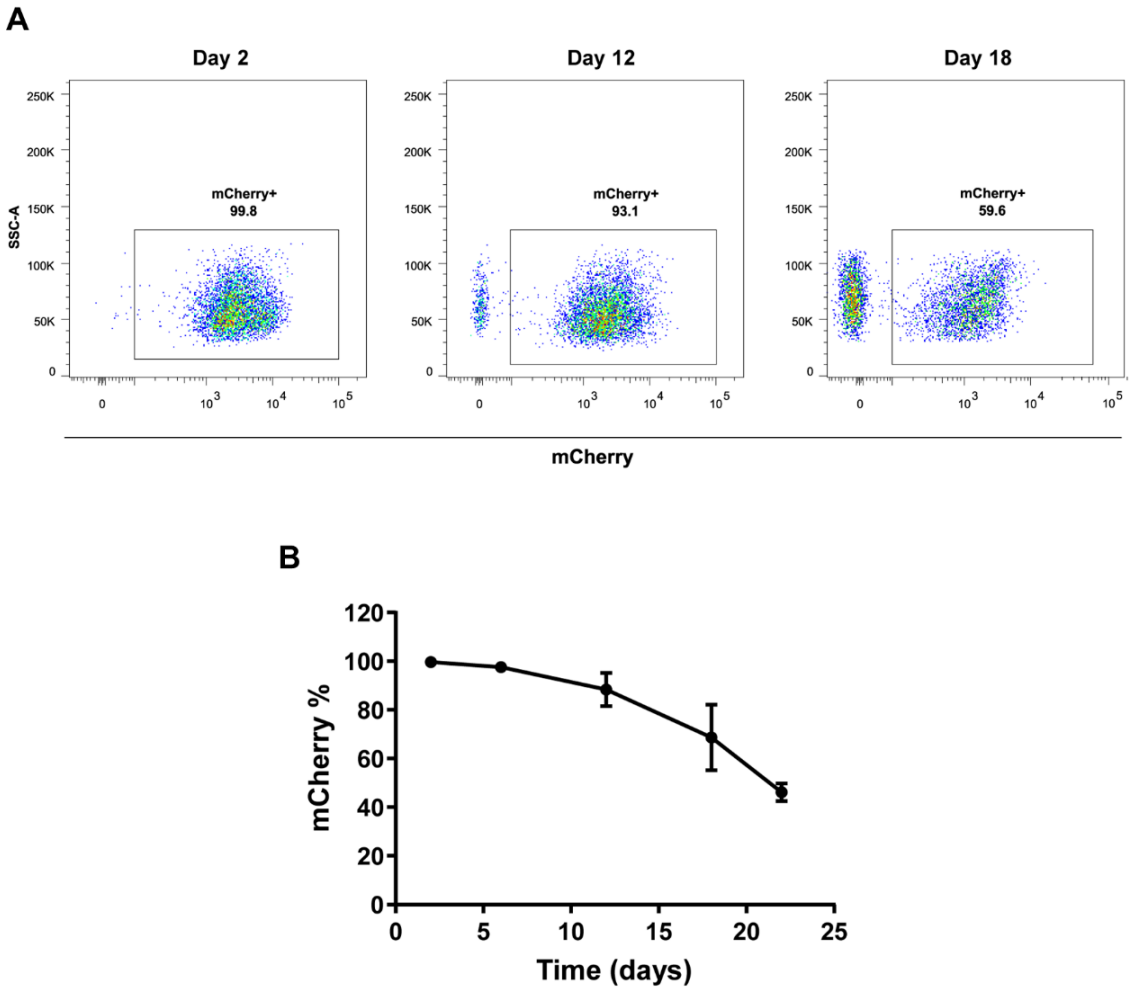

Figure V.2 – Loss of mCherry expression in K562 cells transduced with the inducible SyntPshmiR-SFFV. (A) Representative FCM dotplots showing the percentage of mCherry$^+$ cells at different time points in culture. **(B)** Percentage of mCherry$^+$ cells throughout time in culture (n=3). Error bars shown represent S.D.

After some investigation where different lentivectors were tested it was realised that the underlying problem was associated to the strong expression of the rtTA3 transactivator driven by the SFFV promoter. The high levels of transactivator obtained driven by the SFFV promoter in cell lines appeared to interfere with the expression cassette that led to the shutdown of the promoter over time. Note that this inducible lentivector was initially conceived to be used in human HSPCs in which stable long-term expression of transgenes driven by the SFFV promoter has been observed *in vivo* [20, 21]. However, more recent studies have demonstrated that unlike human promoters, virally derived promoters like SFFV and CMV promoters are highly prone to epigenetic silencing by extensive CpG methylation [22-24].

In light of this drawback, two alternative Tet-on lentivectors were developed where the ubiquitous human PGK (phosphoglycerate kinase) and human UBC (ubiquitin C) promoters drive the constitutive expression of rtTA3 given the weaker nature of these promoters.

V.2.1.2. TET-ON MIR30SHRNA LENTIVECTORS WITH HUMAN PGK AND UBC PROMOTERS

The new inducible lentivectors using the PGK or UBC constitutive promoter in the Tet-on mirR30shRNA system, termed pLV.TetSyntP-miR30shRNA-GFP-PGK-rtTA3-mCherry (SyntPshmiR-PGK) and pLV.TetSyntP-miR30shRNA-GFP-UBC-rtTA3-mCherry (SyntPshmiR-UBC), respectively, are depicted in **Figure V.3**. Details on the construction of these vectors can be found in section **II.2.1.5.**

Stability, inducibility and functional validations of these vectors were all performed in K562 cells using shRNA for non-target control sh*Luc* and shRNA targeting *Notch1* (sh*N1.1* previously validated with the constitutive vector [section **IV.3.2.1**] now referred as sh*N1*) to assess N1 receptor knockdown in all conditions in the presence or absence of dox. K562 cells were transduced with an MOI of 5 and subsequently sorted for mCherry^{+} cells. As shown above, the stability and efficacy of these vectors were monitored in long-term cultures. Dox at a concentration of 0.5 µg/mL was added in parallel cultures every 48 hours. In contrast to what was observed with the SyntPshmiR-SFFV vector, cells transduced with SyntPshmiR-PGK (**Figure V.4Ai**) or

SyntPshmiR-UBC (**Figure V.4Aii**) did not show a significant decrease in mCherry expression throughout time in culture, attaining levels above 95% after 18 days in culture (**Figure V.4B**). Furthermore, as can be seen in the representative dotplots in **Figure V.4A**, the inducibility of mCherry^{+} cells upon dox induction was close to 100% and steady throughout time (**Figure V.4C**), whilst in the absence of dox no GFP leakiness was observed. These features were observed for both inducible vectors independently of the shRNA expressed (sh*Luc* or sh*N1*). Thus, it was demonstrated that the new Tet-On lentivectors allowed stable vector integration showing great inducibility associated to a tight control of the miR30shRNA expression.

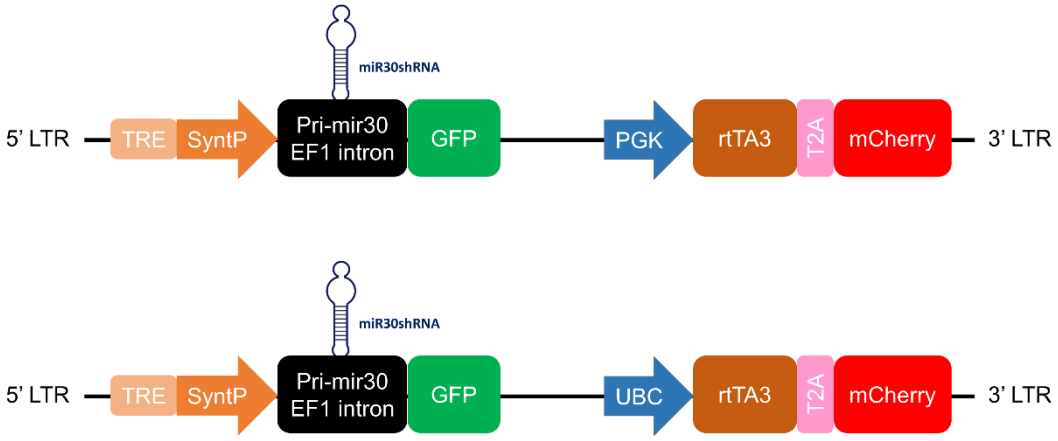

Figure V.3 – Schematic representation of the new Tet-On miR30shRNA lentivectors designated pLV.TetSyntP-miR30shRNA-GFP-PGK-rtTA3-mCherry (top) and pLV.TetSyntP-miR30shRNA-GFP-UBC-rtTA3-mCherry (bottom).

The functionality of these Tet-On miR30shRNA lentivectors was assessed based on the levels of N1 receptor quantified by FCM on sh*Luc* and sh*N1* transduced cells in the presence of doxycycline relatively to N1 receptor levels in the absence of dox (**Figure V.5**). As demonstrated in the representative FCM dotplots in **Figure V.5A**, in the absence of dox, there was no significant differences in N1 receptor expression between cells transduced with sh*Luc* and sh*N1* in SyntPshmiR-PGK (**Figure V.5Ai**) or SyntPshmiR-UBC (**Figure V.5Aii**). Upon dox induction, it can be seen that with both inducible vectors there was a significant decrease in N1 receptor expression in cells transduced with sh*N1*, whereas N1 receptor expression in cells transduced with sh*Luc* remained mostly unaltered as expected (**Figure V.5B**).

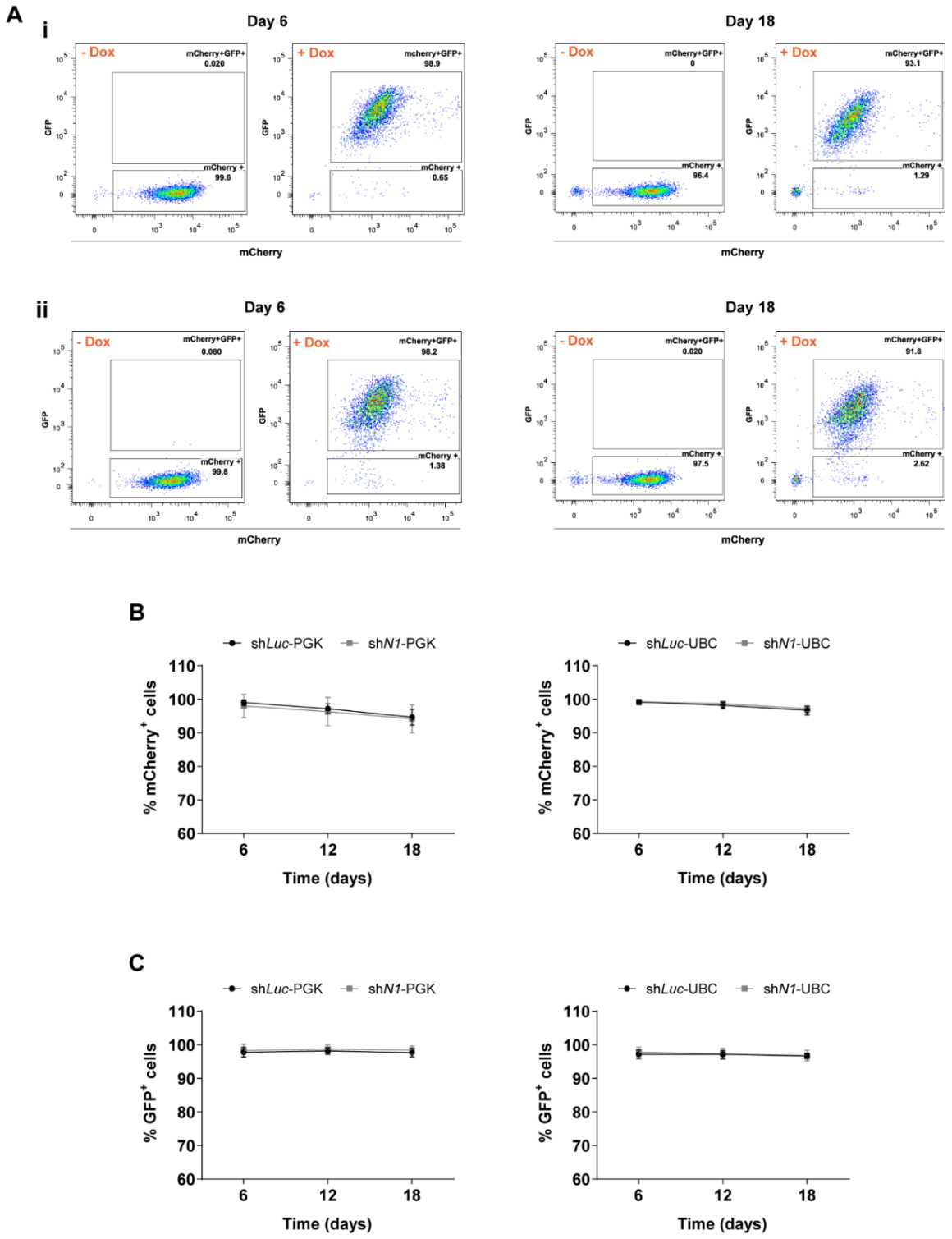

Figure V.4 – Stability and inducibility validation of SyntPshmiR-PGK and SyntPshmiR-UBC lentivectors in K562 transduced with non-target control sh*Luc* and sh*RNA* targeting *NOTCH1* (sh*N1*). (A) Representative FCM dotplots of K562 cells transduced with SyntPshmiR-PGK **(i)** and SyntPshmiR-UBC **(ii)** showing the percentage of mCherry$^+$ and GFP$^+$ cells in the absence and presence of doxycycline (dox) after 6 and 18 days of culture. **(B)** Percentage of mCherry$^+$ cells throughout time in culture (n=3). **(C)** Percentage of GFP$^+$ cells throughout time in culture in the presence of dox (n=3). Error bars shown represent S.D.

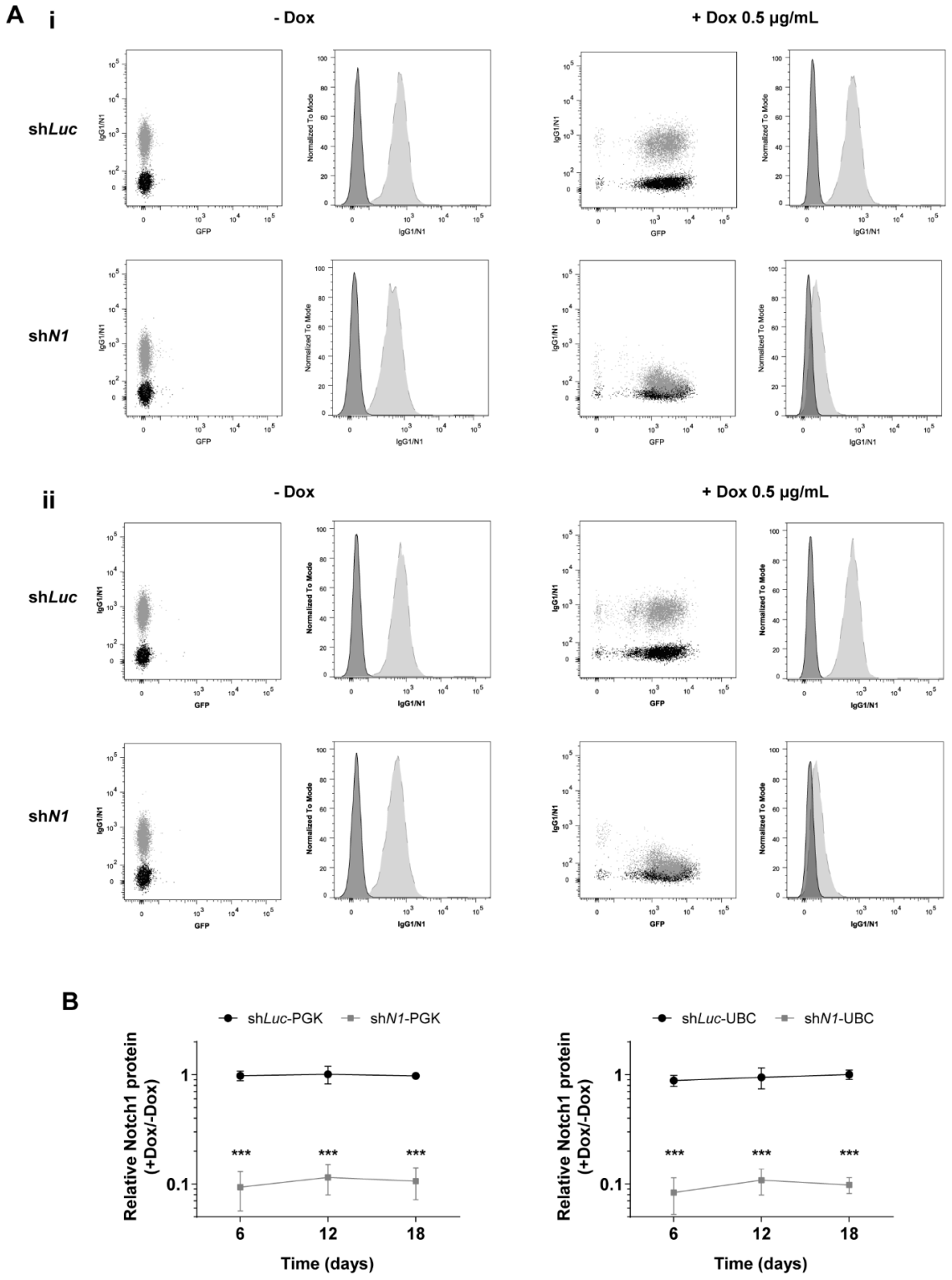

Figure V.5– Functional validation of SyntPshmiR-PGK and SyntPshmiR-UBC lentivectors in K562 transduced with non-target control sh*Luc* and sh*RNA* targeting *N1* (sh*N1*). (A) Representative FCM dotplots and histograms of K562 cells transduced with SyntPshmiR-PGK **(i)** and SyntPshmiR-UBC **(ii)** showing extracellular N1 receptor expression (light grey) and isotype control (black) after 18 days of culture in the absence or presence of doxycycline (dox). GFP expression is also shown in the FCM dotplots. **(B)** Relative N1 receptor levels quantified by FCM on transduced cells in the presence of dox relative to N1 receptor levels in the absence of dox (n=3). Error bars shown represent S.D.; ***p≤0.0003.

Furthermore, in cells transduced with sh*N1* it was noticed that cells with stronger GFP expression (higher MFI) presented lower N1 receptor expression, demonstrating that the levels of GFP reporter in these inducible systems are associated with the degree of miRshRNA expression. As shown in **Figure V.5B**, N1 receptor knockdown efficiencies achieved upon dox induction were consistently around 90% with both lentivectors and remained constant overtime in culture. Thus, it was confirmed that the new Tet-On miR30shRNA lentivectors allowed stable and robust gene silecing in long-term cultures.

To verify the versatility of the developed Tet-On lentivectors, these were also validated in an acute myeloid leukemia cell line OCI-AML3 (**Figure V.6**). Compared to K562 cells, OCI-AML3 cells were less permissive to lentiviral infection thus, providing a stronger proof of the lentivectors efficacy. As described above, cells were transduced with an MOI of 5 and subsequently sorted for mCherry$^+$ cells that were maintained in culture for 18 days, adding dox at a concentration of 0.5 µg/mL to the induced cultures every 48 hours.

As previously observed in K562 cells, transduction with either one of the inducible vectors was stable in OCI-AML3 cells, with more than 95% of the cell population showing mCherry expression after 18 days of culture (**Figure V.6A, B**). In terms of inducibility, the SyntPshmiR-UBC lentivector was more efficient in this cell line, considering that GFP$^+$ cells in the presence of dox were consistently around 95%, whereas cells transduced with the SyntPshmiR-PGK showed more variable inducibility ranging from 75 to 95% of GFP$^+$ cells (**Figure V.6C**). Nevertheless, as can be seen it the representative dotplots (**Figure V.6A**), in the absence of dox no GFP leakiness was observed in cells transduced with any of the lentivectors.

Regarding functionality, although cells transduced with SyntPshmiR-PGK showed more varible inducibility, average N1 receptor knockdown efficiencies were quite consistent and similar to the ones obtained in cells transduced with SyntPshmiR-UBC (**Figure V.6D**). N1 receptor knockdown efficiencies were still highly significant, showing around 75% knockdown with both lentivectors and stable overtime in culture.

In summuary, it was validated the stability of the new developed Tet-on miR30shRNA lentivectors in a less permissive cell line, also demonstrating robust and stable long-term gene silencing.

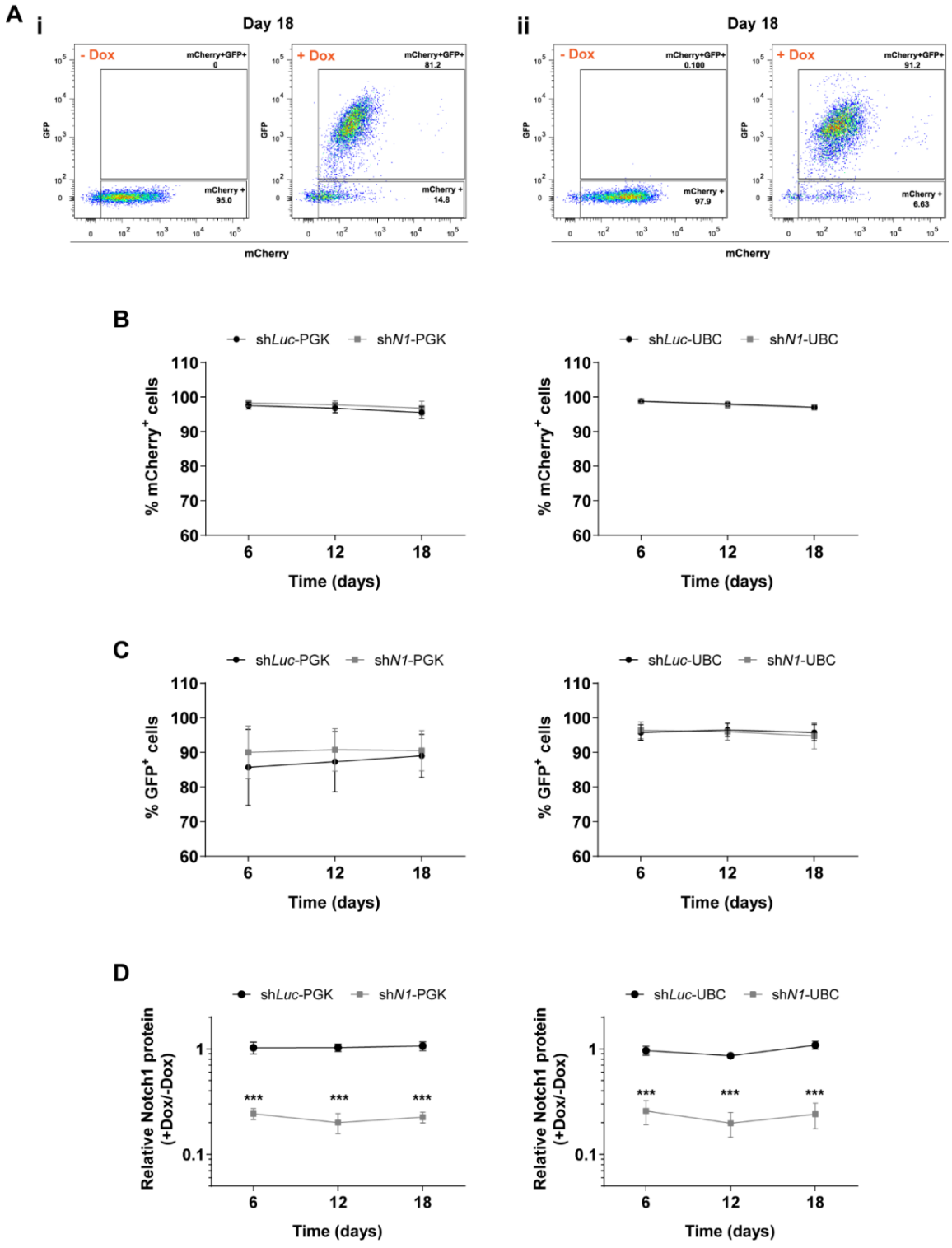

Figure V.6 – Validation of SyntPshmiR-PGK and SyntPshmiR-UBC lentivectors in OCI-AML3 transduced cells. (A) Representative FCM dotplots of OCI-AML3 cells transduced with SyntPshmiR-PGK **(i)** and and SyntPshmiR-UBC **(ii)** showing the percentage of mCherry$^+$ and GFP$^+$ cells in the absence and presence of dox after 18 days of culture. **(B)** Percentage of mCherry$^+$ cells throughout time in culture (n=3). **(C)** Percentage of GFP$^+$ cells throughout time in culture in the presence of dox (n=3). **(D)** Relative N1 receptor levels quantified by FCM on transduced cells in the presence of dox relative to N1 receptor levels in the absence of dox (n=3). Error bars shown represent S.D.; ***p≤0.0003.

V.2.2. VALIDATION OF OPTIMISED MIR30 BACKBONE FOR IMPROVED KNOCKDOWN EFFICIENCY

As verified in the previous chapter, despite allowing several technical advantages, mir30shRNAs often produces less potent knockdowns than conventional shRNAs. Therefore, using a systematic approach, the miR30 backbone has been recently modified to allow optimal miRshRNA processing, increasing mature shRNA levels and knockdown efficiency [25]. This new optimised backbone has been termed “miR-E” by the authors and can be easily attained from existing miR30 sequences. In this work it was demonstrated that even established potent miR30shRNAs can be enhanced by conversion to the miRE design without causing any toxicity.

Thus, in order to further improve the efficacy of the inducible Tet-On miR30shRNA vector, the miRE backbone was also validated in this work. Please refer to section **II.2.1.6** for details on the cloning process used to convert existing miR30shRNA sequences to miREshRNA.

V.2.2.1. COMPARISON OF MIR30 AND MIRE SHRNAS KNOCKDOWN EFFICIENCIES – CONSTITUTIVE LENTIVECTOR

The potency of miRE shRNAs was initially assessed using the constitutive lentivector previously developed for miR30shRNA expression (pLV.EF1α-miR30shRNA-GFP, section **IV.2.1.1**). OCI-AML3 cell line was used to compare knockdown efficiencies of previously validated miR30shRNAs (sh*N1.1* and sh*N1.2*, section **IV.2.2**) since, as seen before, this cell line is less permissive to infection and knockdown than K562 cells. OCI-AML3 were transduced at MOI 10 with either miR30 or miRE shRNA-expressing vectors and knockdown efficiencies were compared side-by-side (**Figure V.7**). Transduction efficiencies for these cells were around 75-90% which allowed to have an internal negative control, as can be observed in the FCM dotplots in **Figure V.7A.** As expected, FCM analysis revealed that expression of miREshRNAs consistently produced significantly higher knockdown levels compared to miR30shRNAs (**Figure V.7B**), particularly for the less potent sh*N1.2*, showing an increase from 65±2.6% to 87±2.1%, while sh*N1.1* resulted in an increase from 71±7.4% to 83±2.7%.

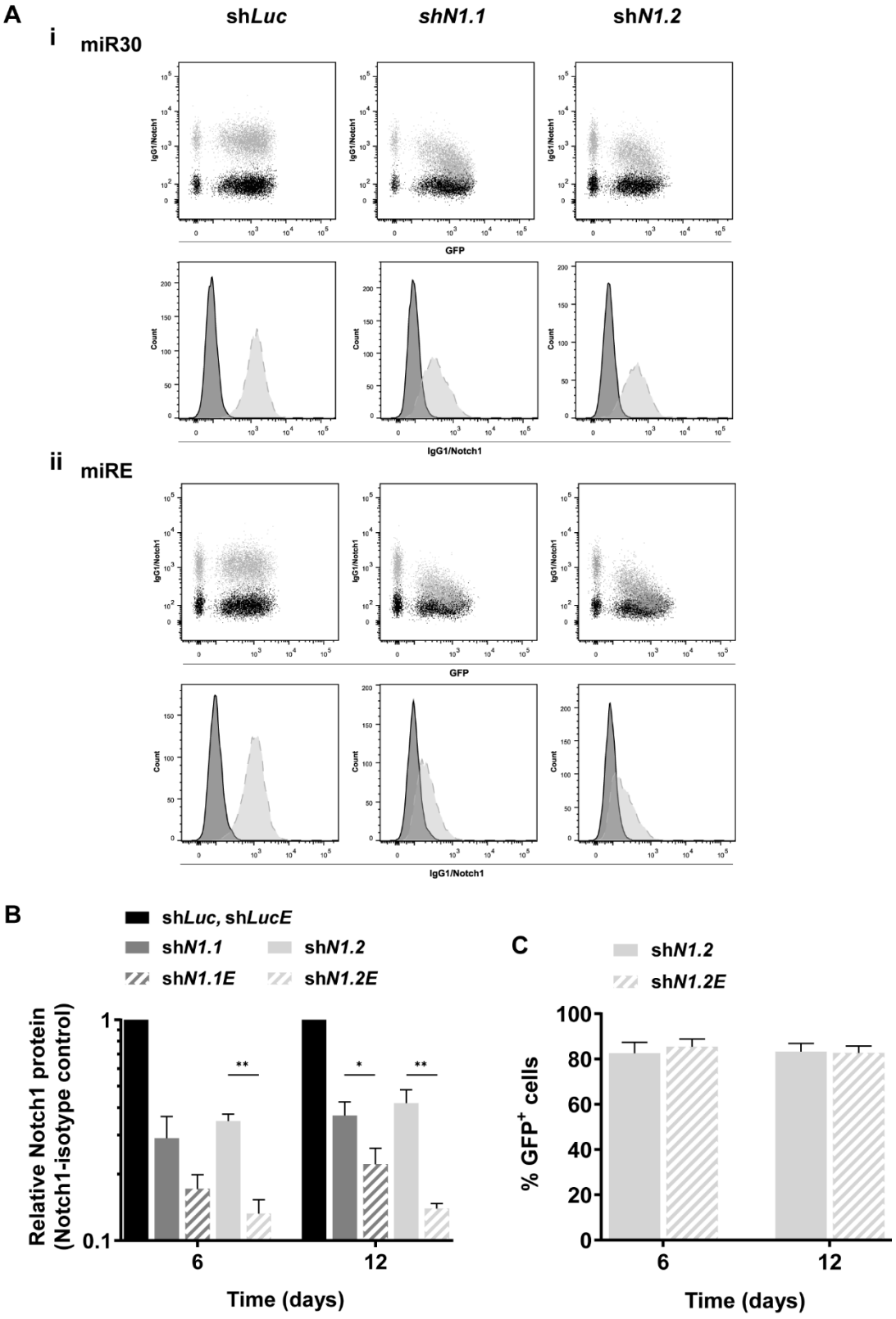

Figure V.7 – Knockdown of *NOTCH1* (*N1*) receptor in OCI-AML3 cell line transduced with the constitutive lentivector pLV.EF1α-miRshRNA-GFP expressing miR30 or miRE shRNAs. (A) Representative FCM dotplots of extracellular N1 receptor expression in function of GFP expression and respective histograms six days after transduction with non-target control sh*Luc* and shRNAs targeting *N1* in miR30 **(i)** or miRE **(ii)** backbones (isotype control shown in black). **(B)** Relative N1 receptor levels quantified by FCM on cells transduced with *N1* shRNAs relative to sh*Luc* (n=3). **(C)** GFP levels overtime in cells transduced with miR30 or miRE sh*N1.2*. Error bars shown represent S.D.; *p≤0.03, **p≤0.003.

Looking to the FACS dotplots, it can be appreciated that the levels of GFP expression were not affected by the mirE backbone (**Figure V.7C)**, meaning that the resulting improved knockdown potency does not reduce the GFP mRNA processing (unlike previously reported [25]) and that reporter expression can accurately correlate to shRNA expression and efficacy.

V.2.2.2. TET-ON MIRESHRNA LENTIVECTOR

Following the confirmation of mirEshRNA enhanced knockdown potency, its inducible expression was evaluated in the SyntPshmiR-UBC lentivector (**Figure V.8**).

Inducibility and knockdown efficiencies in OCI-AML3 cells were verified after 6 days in the presence of dox and the same two N1 shRNAs were tested, where sh*N1.1* corresponds to the shN1 previously evaluated in the miR30 Tet-On lentivectors.

As can be seen in the dotplots in **Figure V.8A**, miRE lentivectors showed great inducibility, with GFP expression varying from 85 to 95%, similarly to the mirE vectors (**Figure V.6C**). Also, likewise, in the absence of dox, GFP expression was virtually silent.

Regarding knockdown efficiencies, as verified with the constitutive vector, sh*N1.2*E showed greater potency with a 94±0.6% knockdown efficiency (**Figure V.8B)**. sh*N1.1*E produced knockdown levels of 86±3%, which represents a significant increase of around 10% from sh*N1.1* in the same conditions shown before.

Moreover, as observed in the constitutive vector, the doplots in **Figure V.8Bi** clearly show that the intensity of GFP expression seen upon induction correlated well with the strength of the silencing level.

In summary, mirEshRNAs proved to be highly efficient, allowing improvements up to 20% in knockdown levels generated by miR30shRNAs. Importantly, the miRE backbone was successfully integrated in the developed Tet-on lentivectors maintaing the strong knockdown potencies seen in the consitutive lentivector.

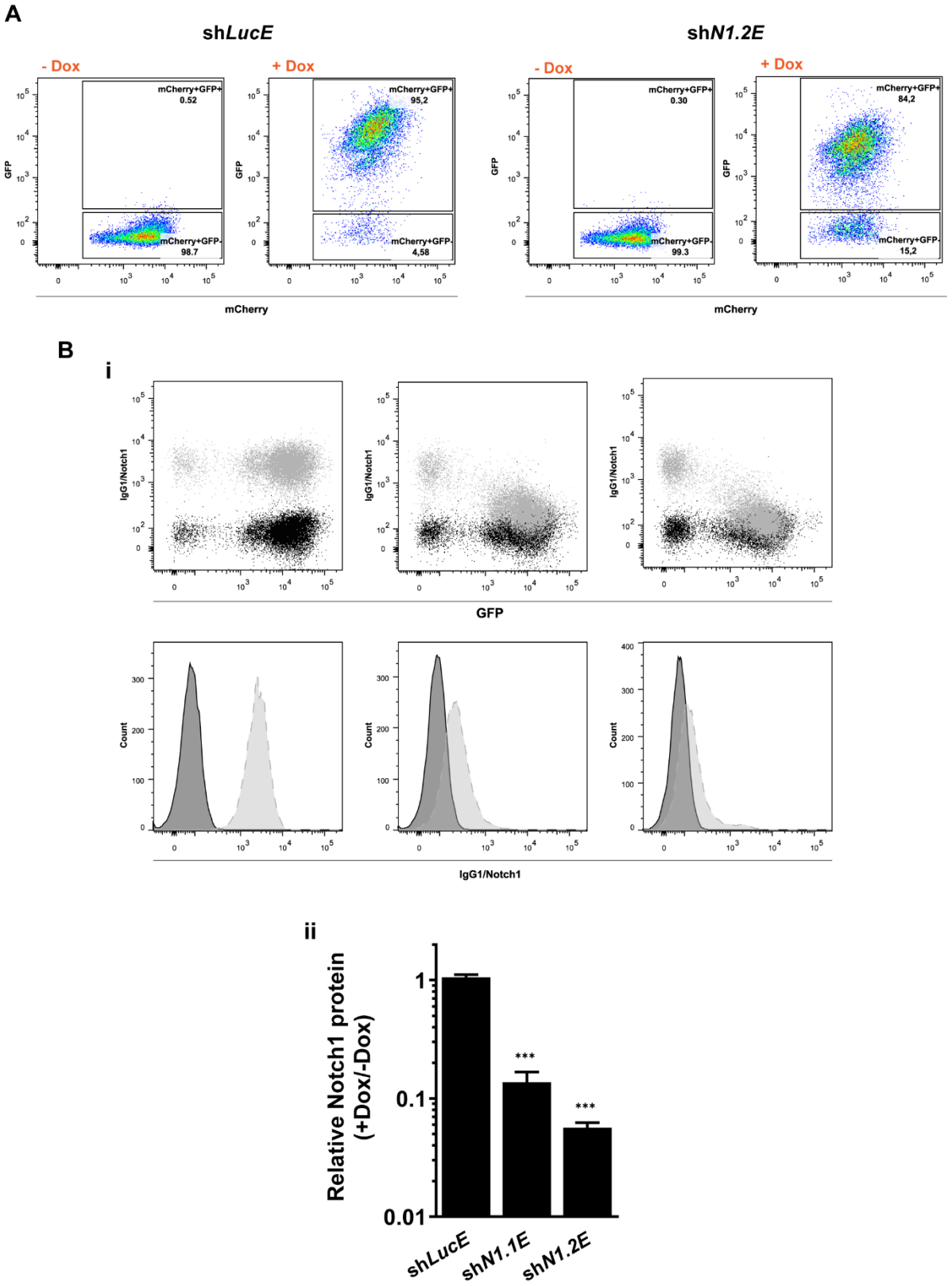

Figure V.8 – Inducible expression of miR30shRNAs using SyntPshmiR-UBC lentivectors in OCI-AML3 cells. (A) Representative FCM dotplots showing mCherry and GFP expression in the absence and presence of dox for 6 days of culture after transduction with non-target control sh*Luc* and shRNA targeting *N1*. **(B) – (i)** Representative FCM dotplots of extracellular N1 receptor expression in function of GFP expression and respective histograms (isotype control shown in black). **(ii)** Relative N1 receptor levels quantified by FCM on transduced cells in the presence of dox relative to N1 receptor levels in the absence of dox (n=3). Error bars shown represent S.D.; ***p≤0.0003.

V.2.3. INDUCIBLE TET-ON OVEREXPRESSION LENTIVECTORS – LONG-TERM VALIDATION *IN VITRO*

Given the promising results obtained with this state-of-the-art inducible system, new lentivectors were designed to allow inducible expression of a transgene of interest. As illustrated in **Figure V.9**, the inducible portion of these vectors still contains the state-of-the-art TRE and synthetic promoter, only now followed by a multiple cloning site (MCS) linked to the GFP reporter by the self-cleaving peptide P2A, which much like T2A, allows separation of both proteins after translation of the single bicistronic mRNA. For the constitutive rtTA3 expression, a lentivector with the stronger human EF1α promoter (referred as SyntP[gene]-EF1) was also tested in parallel with lentivectors with the human PGK (SyntP[gene]-PGK) and UBC (SyntP[gene]-UBC) promoters previously validated in the miR30shRNA system. Please refer to section **II.2.1.7** for details on the construction of theses vectors.

In this study, all lentivectors were cloned to overexpress either GFP alone (without the MCS and P2A) or the firefly luciferase (LUC). Like previously described, these lentivectors were firstly validated in the K562 cell line by transducing cells with an MOI of 5 and subsequently sorting for mCherry^{+} cells which were maintained in culture for 18 days. Dox at a concentration of 0.5 µg/mL was added in parallel to cultures every 48 hours.

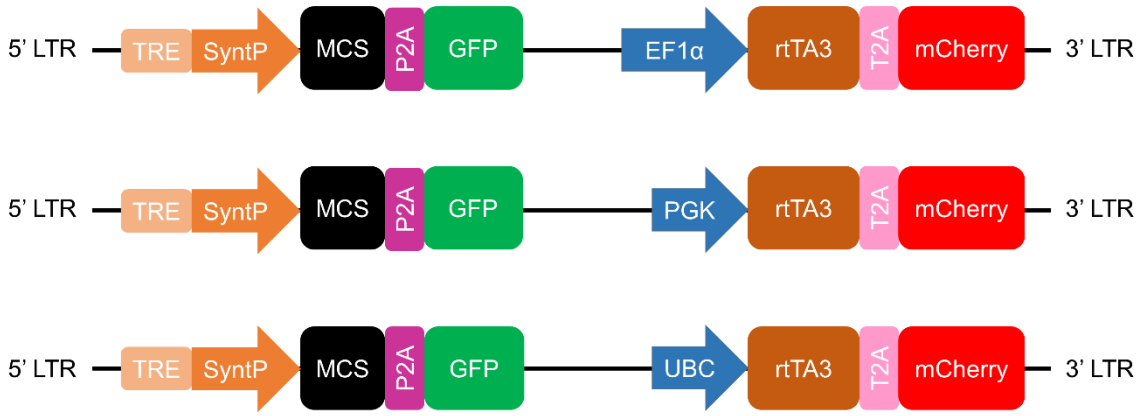

Figure V.9 – Schematic representation of the developed Tet-On overexpression lentivectors designated pLV.TetSyntP-MCS-GFP-EF1 (top), pLV.TetSyntP-MCS-GFP-PGK (middle) and pLV.TetSyntP-MCS-GFP-UBC (bottom).

Although the EF1α promoter is known to be a strong human promoter it was observed that cells transduced with this lentivector were able to maintain mCherry expression in long-term cultures (top panel of **Figure V.10**), unlike what was observed with the strong viral SFFV promoter. However, for unknown reasons, in cultures with dox a considerable reduction in GFP$^+$ cells and in total mCherry$^+$ cells were observed throughout time in culture (bottom panel of **Figure V.10**). Indeed, after a few days in the presence of dox, cell cultures showed a substantial decrease in cell growth and viability that was not restored to normal as observed in cultures with the SyntPshmiR-SFFV lentivector. Therefore, based on these observations, the SyntP[gene]-EF1 overexpression lentivector was not further considered.

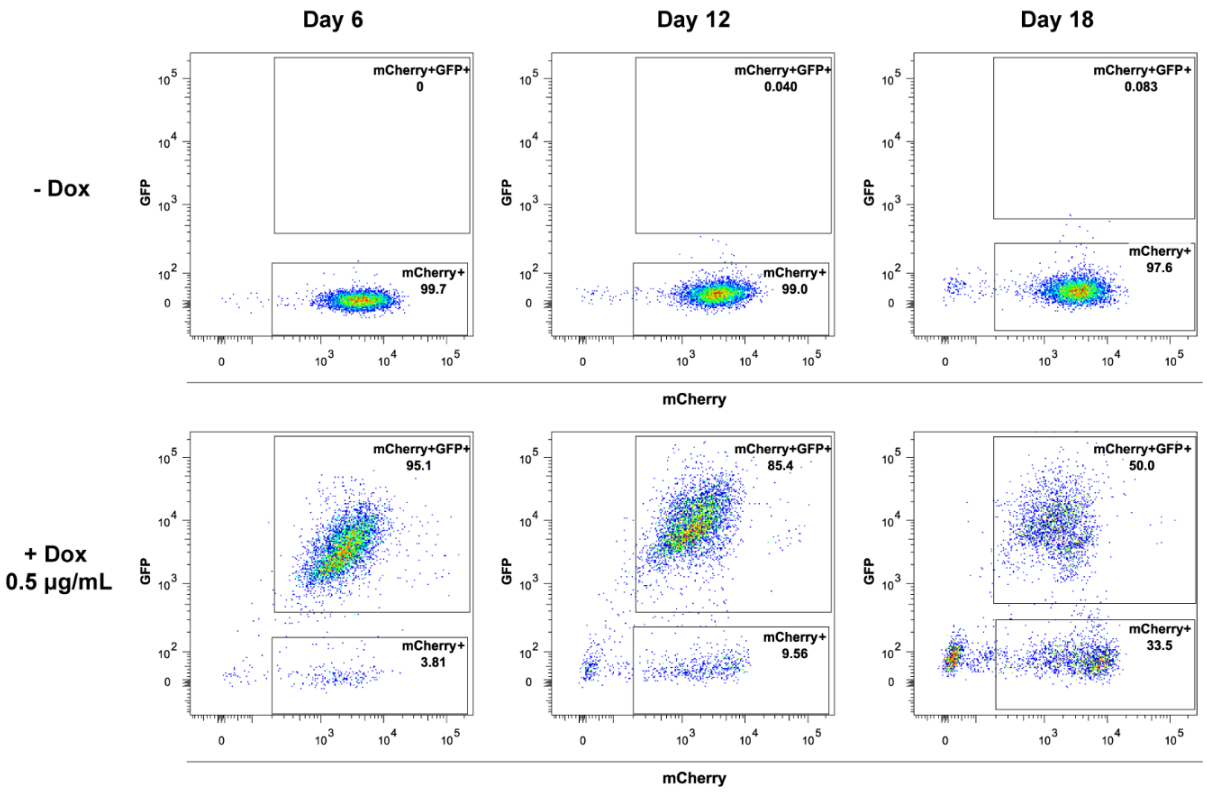

Figure V.10 – Lost of inducibility of the Tet-On overexpression lentivector pLV.TetSyntP-GFP-EF1 in K562 cells in the presence of doxycycline. Representative FCM dotplots of K562 cells transduced with pLV.TetSyntP-GFP-EF1 showing the percentage of mCherry$^+$ and GFP$^+$ cells in the absence and presence of dox throughout time in culture (n=2).

On the other hand, for lentivectors with PGK and UBC constitutive promoters (**Figure V.11Ai** and **ii,** respectively), K562 cells transduced with either GFP or LUC overexpression lentivectors demonstrated great stability and inducibility throughout all time in culture (**Figure V.11B** and **C**, respectively). As can be observed, the proportion of mCherry$^+$ cells remained close to 100% after 18 days of culture and no significant GFP leakiness was observed in absence of dox, whilst great inducibility was observed with virtually 100% of GFP$^+$ cells in the presence of dox. Additionally, luciferase quantification was performed through a luminescence assay as a functional analysis to evaluate overexpression of the transgene upon induction (**Figure V.11D**). This assay was performed using lysates from cells transduced with LUC overexpression lentivectors (SyntPLUC-PGK or SyntPLUC-UBC) that were cultured in the absence or presence of dox. As expected, the quantified luciferase activity was very high in samples from induced cells, whereas samples from non-induced cells showed low basal levels of luciferase activity. Hence, significantly high fold inductions were obtained with both lentivectors upon dox induction, with averages around 8800-fold in cells transduced with SyntPLUC-PGK and 4300-fold in cells transduced with SyntPLUC-UBC.

As detailed before, validation of the Tet-on overexpression lentivectors was performed with the OCI-AML3 cell line (**Figure V.12**). As can be observed in the representative FCM dotplots, either cells transduced with SyntPGFP/LUC-PGK (**Figure V.12Ai)** or with SyntPGFP/LUC-UBC (**Figure V.12Aii)** were able to maintain mCherry expression, with near 100% mCherry$^+$ cells after 18 days of culture (**Figure V.12B).** Regarding inducibility, as previously observed with the Tet-on shmiR vectors, cells transduced with the PGK lentivector showed lower inducibility, although only for overexpression of LUC (**Figure V.12C**), obtaining around 80% of GFP$^+$ cells compared to cells transduced with the UBC lentivector which showed around 90% of GFP$^+$ cells. In fact, is denoted in the FCM dotplots that the GFP intensity is higher in cells overexpressing GFP alone (also observed in K562 cells) attaining virtually 100% of GFP$^+$ cells with both lentivectors. Importantly, no significant GFP leakiness was observed in the absence of dox in all conditions. Consistent with the lower GFP levels observed for these cells when compared to K562 cells, the luminescence assay with lysates from OCI-AML3 cells overexpressing LUC showed lower fold inductions but

still significant of around 880-fold and 960-fold in cells transduced with SyntPLUC-PGK and SyntPLUC-UBC, respectively.

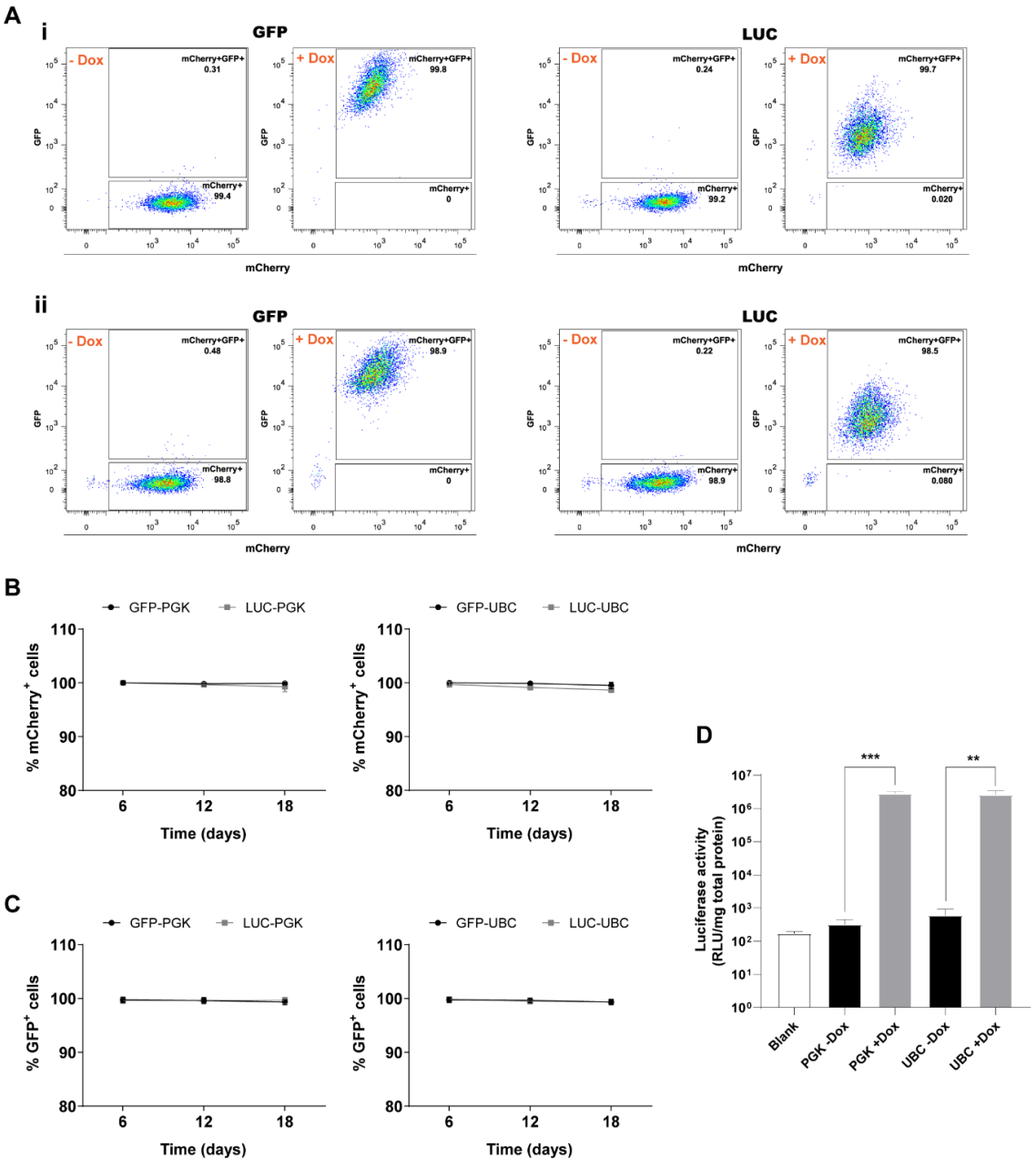

Figure V.11 – Validation of pLV.TetSyntP-GFP/LUC-PGK and pLV.TetSyntP-GFP/LUC-UBC lentivectors in K562 transduced cells. (A) Representative FCM dotplots of K562 cells transduced with pLV.TetSyntP-GFP/LUC-PGK **(i)** and pLV.TetSyntP-GFP/LUC-UBC **(ii)** showing the percentage of mCherry$^+$ and GFP$^+$ cells in the absence and presence of dox after 18 days of culture. **(B)** Average percentage of mCherry$^+$ cells throughout time in culture (n=3). **(C)** Average percentage of GFP$^+$ cells throughout time in culture in the presence of dox (n=3). **(D)** Relative luciferase units (RLU) normalised to total protein of cells transduced with LUC overexpression vectors and cultured in the absence (black bars) or presence (grey bars) of dox; luminometer background is also shown (white bar) (n=3). Error bars shown represent S.D.; ***p≤0.0003, **p≤0.003.

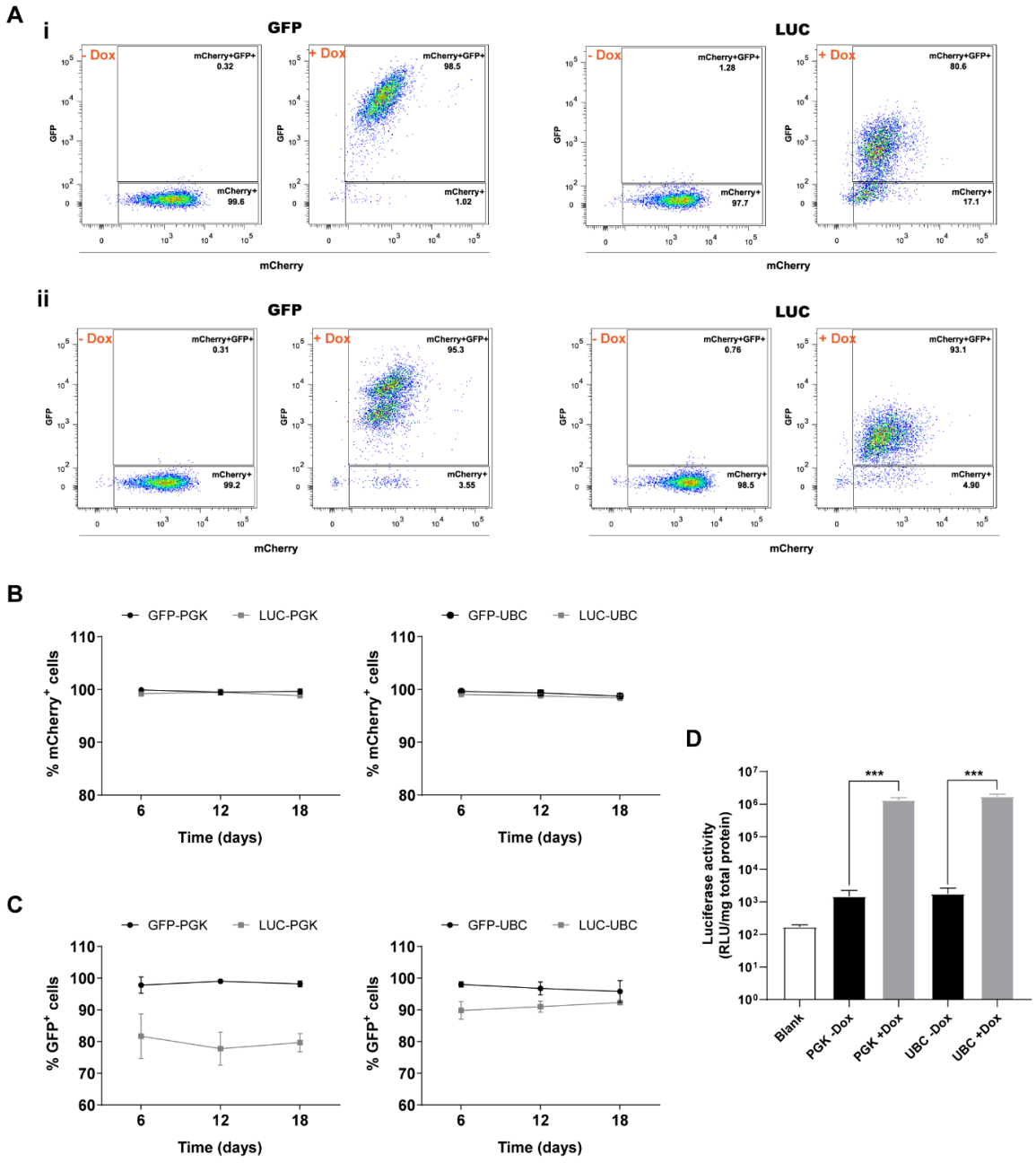

Figure V.12 – Validation of pLV.TetSyntP-GFP/LUC-PGK and pLV.TetSyntP-GFP/LUC-UBC lentivectors in OCI-AML3 transduced cells. (A) Representative FCM dotplots of OCI-AML3 cells transduced with pLV.TetSyntP-GFP/LUC-PGK **(i)** and pLV.TetSyntP-GFP/LUC-UBC **(ii)** showing the percentage of mCherry$^+$ and GFP$^+$ cells in the absence and presence of dox after 18 days of culture. **(B)** Percentage of mCherry$^+$ cells throughout time in culture (n=3). **(C)** Percentage of GFP$^+$ cells throughout time in culture in the presence of dox (n=3). **(D)** Relative luciferase units (RLU) normalised to total protein of cells transduced with LUC overexpression vectors and cultured in the absence (black bars) or presence (grey bars) of dox; luminometer background is also shown (white bar) (n=3). Error bars shown represent S.D.; ***p≤0.0003.

Altogether these results evidence that two efficient state-of-the-art inducible lentivectors for transgene overexpression have been developed in this work. Both versions demonstrate stable genomic integration, strong inducibility and negligible leakiness which allow potent fold inductions of the protein of interest. Of note, selection of the constitutive promoter that drive the transactivator expression might offer some advantage depending on the target cells.

V.3. DISCUSSION

Gene function studies and genetic screens in mammalian systems have been revolutionised by the potential of RNAi-based systems for gene knockdown. However, unlike conventional gene deletion, these RNAi-based loss of function studies require strong and stable shRNA expression throughout time. Thus, as previously introduced, many efforts have been made to overcome initial technical challenges of this technology and further optimisations continue to improve their efficiency and applicability.

Based on the limitations from existing systems, this chapter focused on the development and long-term validation of inducible miR30shRNA expression systems in all-in-one dual colour lentiviral vectors comprising state-of-the-art elements for inducible expression.

As demonstrated, long-term validation of the initial construct with constitutive rtTA3 expression under the SFFV promoter showed a poor performance, with abrupt loss of the constitutive reporter starting after 1 week in culture. This instability was associated to the high levels of rtTA protein derived from the strong SFFV promoter. In fact, the use of a transactivator technology (tTA for Tet-Off or rtTA for Tet-On systems) can be frowned upon due to the presence of the activating domain of the herpes virus simplex viral protein 16 (VP-16) linked to the TetR repressor. The presence of this transactivating domain can make these proteins toxic due to the sequestration of transcription factors required for cell growth (squelching) [26]. Therefore, it seems that when selecting a promoter for the rtTA expression, the strength of this promoter in the target cells should be taken in consideration.

In line with this hypothesis, new Tet-on miR30shRNA constructs where rtTA3 is constitutively expressed by weaker promoters (PGK and UBC promoter) showed great long-term stability *in vitro*. Moreover, these optimised all-in-one dual colour inducible vectors demonstrated almost undetectable leakiness and great inducibility associated to robust gene silencing consistent overtime.

The developed vectors stand out in several aspects from previously published dual colour, all-in-one systems like pINDUCER [11] or TRMPVIR [12] or more recent optimisations [27]. Firstly, by featuring an upgraded inducible promoter containing an optimised TRE and modified minimal CMV promoter (SyntP) shown to be virtually silent in the absence of induction [17]. This new Tet-regulated promoter contains mutations that reduce background expression by 5–20 fold compared to the previous version (TRE2 or Ptight) used in the pInducer and TRMPVIR systems.

Additionally, unlike the other dual colour systems, in which the reporter is expressed in frame with the miR30shRNA and the transcripts are then separated during miR processing, in the developed system the miR30shRNA is integrated in the EF1α intron upstream the GFP reporter. This is known to lead to a more stable expression of both genes given that the splicing event allows separation of the transcripts to undergo each processing pathway required for the generation of miR versus mRNA and, therefore avoiding competition and maximising the efficiency of both processes [28]. Thus, the developed inducible system allows a more stable miR30shRNA expression associated to a thigh and efficient inducibility that can be reliably monitored through stable GFP expression.

Moreover, it was confirmed that the newly optimised miRE backbone [25] was able to significantly improve the potency of miR30shRNAs. According to the authors, miRE contains a conserved sequence from endogenous human miR30, found by systematic testing that resulted in increased knockdown levels due to enhanced pri-miRNA processing. However, this resulted in significantly lower reporter levels compared to miR30shRNAs expression, since a larger fraction of the transcripts were recognised and processed as pri-miRNAs reducing availability for reporter protein expression. As highlighted before, by integrating miRshRNA in the EF1α intron, this issue is no longer observed, and therefore, when expressed in the developed vectors, miREshRNA increased knockdown potency was not associated to lower reporter expression. Additionally, the authors report that for the same reasons, packaging of miRE containing retroviruses yielded significantly lower virus titers, which was also circumvented using the EF1α intron expression system.

In light of the exceptional performance of the Tet-on miRshRNA lentivectors, these were adapted for inducible protein overexpression, which can be valuable for gain-of-

function studies. Once again, a construct containing a strong constitutive promoter (human EF1α) did not perform well, although in this case only upon induction. Nevertheless, inducible lentivectors with the constitutive PGK and UBC promoters demonstrated genome integration perfectly stable overtime with great and constant levels of inducibility.

Two cell lines were used to validate the developed inducible systems. Comparing to K562 cells, the OCI-AML3 cell line demonstrated lower knockdown efficiency and protein fold-induction. As previously mentioned, one of the major advantages of a dual colour inducible system, is the ability to select clones (when possible) with optimal levels of fold-induction, *i.e.*, highest signal-to-noise ratio upon dox induction. In viral vector systems, an unfavourable proviral integration site can actually prevent shRNA expression through promoter interference, epigenetic silencing or other inhibitory effects [29, 30]. As could be observed by FCM, higher levels of the GFP reporter were associated to more potent knockdowns and the same should be true for protein overexpression. Therefore, in cells that were more difficult to transduce, a variable inducibility was observed, whereas in a cell population where transduction was more efficient, inducibility was stronger and more stable.

Nonetheless, N1 receptor knockdown efficiencies over 90% and close to 1×10^4-fold induction in luciferase activity were obtained in K562 cells transduced with the miR30shRNA and overexpression systems, respectively. Moreover, knockdown efficiencies over 90% were obtained in OCI-AML3 cells with the miREshRNA system. In fact, the knockdown efficiency obtained with the miR30 and miRE inducible vectors were identical to the ones obtained with analogous constitutive vectors with the same shRNA sequences, further confirming the functionality of this inducible all-in-one lentivector. Regarding transgene overexpression, according to the information provided in the Takara Bio website, previously published all-in-one vector designs typically showed only 50- to 100-fold induced luciferase activity, even in selected clones, whereas in their all-in-one vector design (with the same inducible promoter used in the present systems) HeLa clones with up to 1×10^4-fold induction can be found, similar to what was observed in this work.

V.4. REFERENCES

1. Brummelkamp TR, Bernards R, Agami R. A system for stable expression of short interfering RNAs in mammalian cells. Science. 2002;296(5567):550-3.

2. Paddison PJ, Caudy AA, Hannon GJ. Stable suppression of gene expression by RNAi in mammalian cells. Proc Natl Acad Sci U S A. 2002;99(3):1443-8.

3. Singer O, Verma IM. Applications of lentiviral vectors for shRNA delivery and transgenesis. Curr Gene Ther. 2008;8(6):483-8.

4. Jackson AL, Bartz SR, Schelter J, Kobayashi SV, Burchard J, Mao M et al. Expression profiling reveals off-target gene regulation by RNAi. Nat Biotechnol. 2003;21(6):635-7.

5. Bridge AJ, Pebernard S, Ducraux A, Nicoulaz AL, Iggo R. Induction of an interferon response by RNAi vectors in mammalian cells. Nat Genet. 2003;34(3):263-4.

6. Grimm D, Streetz KL, Jopling CL, Storm TA, Pandey K, Davis CR et al. Fatality in mice due to oversaturation of cellular microRNA/short hairpin RNA pathways. Nature. 2006;441(7092):537-41.

7. Zhou H, Xia XG, Xu Z. An RNA polymerase II construct synthesizes short-hairpin RNA with a quantitative indicator and mediates highly efficient RNAi. Nucleic Acids Res. 2005;33(6):e62.

8. Stegmeier F, Hu G, Rickles RJ, Hannon GJ, Elledge SJ. A lentiviral microRNA-based system for single-copy polymerase II-regulated RNA interference in mammalian cells. Proceedings of the National Academy of Sciences of the United States of America. 2005;102(37):13212.

9. Silva JM, Li MZ, Chang K, Ge W, Golding MC, Rickles RJ et al. Second-generation shRNA libraries covering the mouse and human genomes. Nature Genetics. 2005;37(11):1281-8.

10. Shin K-J, Wall EA, Zavzavadjian JR, Santat LA, Liu J, Hwang J-I et al. A single lentiviral vector platform for microRNA-based conditional RNA interference and coordinated transgene expression. Proceedings of the National Academy of Sciences. 2006;103(37):13759.

11. Meerbrey KL, Hu G, Kessler JD, Roarty K, Li MZ, Fang JE et al. The pINDUCER lentiviral toolkit for inducible RNA interference in vitro and in vivo. Proc Natl Acad Sci U S A. 2011;108(9):3665-70.

12. Zuber J, McJunkin K, Fellmann C, Dow LE, Taylor MJ, Hannon GJ et al. Toolkit for evaluating genes required for proliferation and survival using tetracycline-regulated RNAi. Nat Biotechnol. 2011;29(1):79-83.

13. Cullen BR. Transcription and processing of human microRNA precursors. Mol Cell. 2004;16(6):861-5.

14. Urlinger S, Baron U, Thellmann M, Hasan MT, Bujard H, Hillen W. Exploring the sequence space for tetracycline-dependent transcriptional activators: novel mutations yield expanded range and sensitivity. Proc Natl Acad Sci U S A. 2000;97(14):7963-8.

15. Das AT, Zhou X, Vink M, Klaver B, Verhoef K, Marzio G et al. Viral evolution as a tool to improve the tetracycline-regulated gene expression system. J Biol Chem. 2004;279(18):18776-82.

16. Zhou X, Vink M, Klaver B, Berkhout B, Das AT. Optimization of the Tet-On system for regulated gene expression through viral evolution. Gene Therapy. 2006;13(19):1382-90.

17. Loew R, Heinz N, Hampf M, Bujard H, Gossen M. Improved Tet-responsive promoters with minimized background expression. BMC Biotechnol. 2010;10:81.

18. Agha-Mohammadi S, O'Malley M, Etemad A, Wang Z, Xiao X, Lotze MT. Second-generation tetracycline-regulatable promoter: repositioned tet operator elements optimize transactivator synergy while shorter minimal promoter offers tight basal leakiness. The Journal of Gene Medicine. 2004;6(7):817-28.

19. Levis R, Hazelrigg T, Rubin GM. Effects of genomic position on the expression of transduced copies of the white gene of Drosophila. Science. 1985;229(4713):558.

20. Demaison C, Parsley K, Brouns G, Scherr M, Battmer K, Kinnon C et al. High-level transduction and gene expression in hematopoietic repopulating cells using a human immunodeficiency [correction of imunodeficiency] virus type 1-based lentiviral vector containing an internal spleen focus forming virus promoter. Human gene therapy. 2002;13(7):803-13.

21. Yam PY, Li S, Wu J, Hu J, Zaia JA, Yee JK. Design of HIV vectors for efficient gene delivery into human hematopoietic cells. Molecular therapy : the journal of the American Society of Gene Therapy. 2002;5(4):479-84.

22. Herbst F, Ball CR, Tuorto F, Nowrouzi A, Wang W, Zavidij O et al. Extensive methylation of promoter sequences silences lentiviral transgene expression during stem cell differentiation in vivo. Molecular therapy : the journal of the American Society of Gene Therapy. 2012;20(5):1014-21.

23. Stein S, Ott MG, Schultze-Strasser S, Jauch A, Burwinkel B, Kinner A et al. Genomic instability and myelodysplasia with monosomy 7 consequent to EVI1 activation after gene therapy for chronic granulomatous disease. Nature medicine. 2010;16(2):198-204.

24. Zhang F, Frost AR, Blundell MP, Bales O, Antoniou MN, Thrasher AJ. A Ubiquitous Chromatin Opening Element (UCOE) Confers Resistance to DNA Methylation–mediated Silencing of Lentiviral Vectors. Molecular Therapy. 2010;18(9):1640-9.

25. Fellmann C, Hoffmann T, Sridhar V, Hopfgartner B, Muhar M, Roth M et al. An optimized microRNA backbone for effective single-copy RNAi. Cell reports. 2013;5(6):1704-13.

26. Benabdellah K, Muñoz P, Cobo M, Gutierrez-Guerrero A, Sánchez-Hernández S, Garcia-Perez A et al. Lent-On-Plus Lentiviral vectors for conditional expression in human stem cells. Scientific Reports. 2016;6:37289.

27. Adams FF, Heckl D, Hoffmann T, Talbot SR, Kloos A, Thol F et al. An optimized lentiviral vector system for conditional RNAi and efficient cloning of microRNA embedded short hairpin RNA libraries. Biomaterials. 2017;139:102-15.

28. Amendola M, Passerini L, Pucci F, Gentner B, Bacchetta R, Naldini L. Regulated and multiple miRNA and siRNA delivery into primary cells by a lentiviral platform. Mol Ther. 2009;17(6):1039-52.

29. Pikaart MJ, Recillas-Targa F, Felsenfeld G. Loss of transcriptional activity of a transgene is accompanied by DNA methylation and histone deacetylation and is prevented by insulators. Genes Dev. 1998;12(18):2852-62.

30. Ellis J, Hotta A, Rastegar M. Retrovirus Silencing by an Epigenetic TRIM. Cell. 2007;131(1):13-4.

CHAPTER VI

CONCLUSIONS AND FUTURE DIRECTIONS

VI.1. GENERAL CONCLUSIONS

VI.1.1. OPTIMISED PROTOCOLS AND TOOLS TO ASSAY NOTCH SIGNALLING IN HUMAN HSPCS

The functional roles of specific Notch receptors in human primary cells are still technically challenging to identify, mostly because the usual tools to assay Notch signalling activation focus on canonical Notch target genes which are not entirely specific to this pathway and do not allow to distinguish the activated receptor. Therefore, to definitely assess the roles of Notch receptors it was essential to identify tools that allow to specifically and efficiently target each Notch receptor.

In this work it was established WB protocols that allow to efficiently detect N1, N2 and N4 receptors, in particular the activated forms of these receptors, that have not been clearly described in the literature for N2 and N4 receptors. While for N1 and N2 receptors, specific antibodies for the cleaved forms were found, detection of N4ICD was achieved by a C-terminus ab with higher specificity for the cleaved form.

Unfortunately, the antibodies that allowed the characterisation of N1 and N2 activation by FCM in HSPCs have been discontinued and the ones validated for WB were ineffective for intracellular staining, excluding their application for multicolour FCM analysis.

Regarding extracellular Notch receptors expression on HSPCs, although it has been previously described in the literature [1], new FCM antibodies have been validated demonstrating high N1 and N2 receptors expression on HSPCs and HSCs and negligible N4 receptor expression.

Furthermore, efficient and specific silencing of N1 and N2 receptors through RNAi was achieved in this work. It is currently difficult to find in the literature information on shRNA target sequences that undoubtedly allow efficient silencing of Notch receptors, specially at the protein level. Here, at least two shRNA and miR30shRNA sequences

that allow potent knockdowns of N1 and N2 receptors in cell lines were identified based on a thorough validation at the protein level.

In HSPCs, knockdowns over 80% were successfully attained for N1 and N2 receptors with one of the validated shRNAs for each receptor using a H1-shRNA lentiviral system.

VI.1.2. EFFECTS OF NOTCH LIGANDS IN HUMAN HSPCS REGULATION *IN VITRO*

It is still largely unknown which Notch ligand/receptor pairing is preferentially used by HSPCs or if the different receptor-ligand interactions trigger different responses. Given the lack of comprehensive studies on the effects of different Notch ligands in human HSPCs, a side-by-side comparison was performed in an attempt to understand the roles of Dll1, Dll4 and Jag1 ligands in HSPCs regulation *in vitro*. This study was based on a short-term exposure under differentiation promoting conditions to assess the effect in HSPCs maintenance *ex vivo*.

No discernible effects were observed in the presence of Dll1 ligand, probably due to the short-term nature of the study, since expansion promoting effects described in the literature [2] were only visible upon 12 days of culture due to a block in myeloid progenitors differentiation [3]. This, together with the observations that, unlike Dll4 and Jag1, Dll1 ligand appears to have low expression in the human placenta niche, suggests that Dll1 ligand does not have a relevant role in the regulation of CB HSPCs.

On the other hand, the effects of Jag1 and Dll4 ligands revealed distinct roles in HSPCs regulation *in vitro.* Jag1 ligand promoted greater effect in blocking HSPCs cell cycle progression, resulting in significantly fewer dividing cells and ~7-fold more quiescent cells, associated to a significant decrease in total cell expansion. This effect was correlated to a significant upregulation of cell cycle inhibitors *CDKN1C* and *CDKN1A*. Dll4 ligand promoted a blocking in HSPCs differentiation, resulting in a population with around 70% less committed progenitors ($CD45RA^{+}$), without significantly affecting total cell expansion. This effect was associated to a significant downregulation of myeloid regulator *CEBPA*.

Moreover, the HSC content, estimated based on limiting dilution analysis of human engraftment in immunodeficient mice, was maintained in the presence of Jag1 ligand and almost doubled in the presence of Dll4, in contrast with a 5-fold decrease observed in the control without the presence of any ligand.

Therefore, Notch ligands Jag1 and Dll4 seem to have a considerable role in HSPCs regulation, promoting the maintenance of the stem cell pool *ex vivo*, by limiting entry in cell cycle and differentiation.

Importantly, it should be highlighted that Dll4 alone was able to promote expansion of HSCs with repopulation capacity under differentiation promoting conditions and therefore, Dll4 could be a promising candidate to explore in CB HSPCs expansion protocols.

VI.1.3. Role of Notch Receptors in Human HSPCs Regulation

To this day, the understanding of the functional role of Notch signalling in HSPCs remains unclear and controversial. While several loss of function studies in mice models have led to the proposal that Notch signalling is not required for HSPCs regulation in steady-state haematopoiesis [4-8], many others have shown that appropriate Notch signalling is required in the BM microenvironment, mostly for environmental cues but also some cell-autonomous mechanisms [9-14]. Moreover, few studies have properly assessed the effect of Notch signalling disruption in human HSPCs. The only report using purified human HSCs claims that, similar to the mice system, no effect was observed in the repopulation capacity [15], although this conclusion can be open to interpretation as previously discussed.

This uncertainty underlies the need for having more stringent and well-described methods to disrupt Notch signalling in human HSPCs, in particular, to explore the roles of N1 and N2 receptors, which are expressed and activated in HSPCs and HSCs. Therefore, in this work it was achieved a robust system for efficient silencing of N1 and N2 receptors in human HSPCs to definitively identify the importance of these receptors for HSPCs regulation *in vitro* and *in vivo*.

In vitro assays demonstrated that, although silencing of N1 or N2 receptor did affect the total number of primitive cells (CAFCs) after long-term culture, phenotypic characterisation of this population showed a significant reduction in HSCs with an increase in LMPPs when N2 was silenced, whereas N1 knockdown did not show significant differences. More importantly, *in vivo* repopulation with N2-knockdown HSPCs confirmed this result, showing a significantly lower HSCs frequency. On the other hand, repopulation with N1-knockdown HSPCs had increased myeloid differentiation and less lymphoid. It was also observed a non-significant increase in LMPPs, which can suggest a block in lymphoid differentiation at this stage.

These results prove for the first time that Notch signalling, specifically through N2 receptor, has an important role in the regulation of human HSCs self-renewal capacity. Although the effect was not strong enough to decrease repopulation capacity at the 12-week time-point, evaluation of secondary transplants will allow to verify the effect on long-term reconstituting HSCs. N1 receptor appears to have an important role at the multipotent progenitor stage, where the fine-tuning of the pathway regulates the lymphoid *versus* myeloid cell fate decisions.

VI.1.4. State-of-the-art Lentivectors for Inducible Gene Silencing and Overexpression

In an attempt to develop a sophisticated system to efficiently knockdown genes in an inducible manner, state-of-the-art lentiviral vectors were developed to allow robust gene silencing upon induction.

In this work, optimised all-in-one Tet-on dual colour vectors were developed by integrating the best features available in the literature: an improved TRE and promoter shown to be virtually silent in the absence of induction [16], a miR30shRNA integrated in the EF1α intron upstream the GFP reporter which leads to more stable expression of both genes [17] and finally the newly optimised miRE backbone [18] which significantly improves the potency of miR30shRNAs to the same level as standard shRNAs.

In summary, the developed lentiviral vectors allowed a tight inducibility that led to potent knockdowns which were stable overtime *in vitro* and virtually silent in the

absence of induction. Moreover, the intensity of the GFP expression seen upon induction was correlated with the knockdown level which allows to select cells based on the desired level of gene silencing.

Given the exceptional performance of the Tet-on miRshRNA lentivectors, these were also adapted for inducible protein overexpression, demonstrating as well a tight regulation and great fold induction stable overtime *in vitro*, allowing high levels of the protein of interest.

Additionally, different constitutive promoters that drive the transactivator expression were evaluated in these vectors and might be worth to select based on the target cells.

VI.2. FUTURE WORK

Once established platforms that allow to distinguish individual Notch receptors activation and efficiently knockdown Notch receptors, future work can focus on identifying preferential ligand-receptor pairings and the roles of different Notch receptor-ligand interactions.

Although, ideally, to work with human HSPCs, detection of Notch receptors activation should be quantifiable by FCM, to allow analysis in different subpopulations and detection in limited numbers of cells. As mentioned, previously established antibodies for N1ICD and N2ICD detection by FCM were discontinued and several commercially available antibodies have been tested without success. Thus, it would be of great value to the field to identify new NICD abs that allow FCM application.

Nevertheless, further assessment on the effects of Notch ligands in HSPCs regulation can focus on identifying the Notch receptor preferentially activated by each ligand *in vitro* and confirm if this receptor is responsible for the observed effects by knocking down the receptor in HSPCs before exposure to the ligand.

Furthermore, given that exposure to Dll4, even under differentiation conditions, was able to promote expansion of repopulating HSCs, it would be interesting to explore its effect as an immobilised ligand in combination with cytokines cocktails and other molecules that promote stemness and expansion.

On the role of Notch receptors, evaluation of secondary LTC-ICs and secondary xenotransplants is currently undergoing to further verify the effect on HSCs self-renewal *in vitro* and on long-term reconstituting HSCs, respectively.

Moreover, it is also currently undergoing, work for the assessment of molecular mechanisms triggered by the activation of N1 and N2 receptors in HSPCs. To activate each Notch receptor, specific agonistic antibodies were validated, allowing great levels of activation of each receptor specifically. RNA-seq will be performed to HSPCs samples with activation of each Notch receptor or both, to evaluate alterations in gene expression of cell cycle and differentiation regulators, as well as HSC “fingerprint”

genes [1], which will hopefully allow to correlate with the observations from HSPCs exposed do Jag1 and Dll4 and define the molecular mechanisms triggered by these interactions.

Finally, to complete the work on the development of optimised lentivectors for inducible gene silencing or overexpression, the functionality of these vectors will be evaluated *in vivo* by transplanting transduced OCI-AML3 cells, which are able to engraft NSG mice. N1 receptor knockdown or Luciferase overexpression will be monitored while mice are on doxycycline diet. Furthermore, in collaboration with a pancreatic cancer group, overexpression vectors are currently being tested in epithelial cell lines and mouse pancreas organoids, that will allow to further validate the applicability of the developed vectors in different settings.

VI.3. REFERENCES

1. Anjos-Afonso F, Currie E, Palmer HG, Foster KE, Taussig DC, Bonnet D. CD34(-) cells at the apex of the human hematopoietic stem cell hierarchy have distinctive cellular and molecular signatures. Cell Stem Cell. 2013;13(2):161-74.

2. Delaney C, Heimfeld S, Brashem-Stein C, Voorhies H, Manger RL, Bernstein ID. Notch-mediated expansion of human cord blood progenitor cells capable of rapid myeloid reconstitution. Nature medicine. 2010;16(2):232-6.

3. Csaszar E, Wang W, Usenko T, Qiao W, Delaney C, Bernstein ID et al. Blood stem cell fate regulation by Delta-1-mediated rewiring of IL-6 paracrine signaling. Blood. 2014;123(5):650-8.

4. Mancini SJ, Mantei N, Dumortier A, Suter U, MacDonald HR, Radtke F. Jagged1-dependent Notch signaling is dispensable for hematopoietic stem cell self-renewal and differentiation. Blood. 2005;105(6):2340-2.

5. Varnum-Finney B, Halasz LM, Sun M, Gridley T, Radtke F, Bernstein ID. Notch2 governs the rate of generation of mouse long- and short-term repopulating stem cells. J Clin Invest. 2011;121(3):1207-16.

6. Guo P, Poulos MG, Palikuqi B, Badwe CR, Lis R, Kunar B et al. Endothelial jagged-2 sustains hematopoietic stem and progenitor reconstitution after myelosuppression. J Clin Invest. 2017;127(12):4242-56.

7. Wang W, Yu S, Myers J, Wang Y, Xin WW, Albakri M et al. Notch2 blockade enhances hematopoietic stem cell mobilization and homing. Haematologica. 2017;102(10):1785-95.

8. Maillard I, Koch U, Dumortier A, Shestova O, Xu L, Sai H et al. Canonical notch signaling is dispensable for the maintenance of adult hematopoietic stem cells. Cell Stem Cell. 2008;2(4):356-66.

9. Zhou L, Li LW, Yan Q, Petryniak B, Man Y, Su C et al. Notch-dependent control of myelopoiesis is regulated by fucosylation. Blood. 2008;112(2):308-19.

10. Yao D, Huang Y, Huang X, Wang W, Yan Q, Wei L et al. Protein O-fucosyltransferase 1 (Pofut1) regulates lymphoid and myeloid homeostasis through modulation of Notch receptor ligand interactions. Blood. 2011;117(21):5652-62.

11. Kim YW, Koo BK, Jeong HW, Yoon MJ, Song R, Shin J et al. Defective Notch activation in microenvironment leads to myeloproliferative disease. Blood. 2008;112(12):4628-38.

12. Yoda M, Kimura T, Tohmonda T, Uchikawa S, Koba T, Takito J et al. Dual functions of cell-autonomous and non-cell-autonomous ADAM10 activity in granulopoiesis. Blood. 2011;118(26):6939-42.

13. Klinakis A, Lobry C, Abdel-Wahab O, Oh P, Haeno H, Buonamici S et al. A novel tumour-suppressor function for the Notch pathway in myeloid leukaemia. Nature. 2011;473(7346):230-3.

14. Wang L, Zhang H, Rodriguez S, Cao L, Parish J, Mumaw C et al. Notch-dependent repression of miR-155 in the bone marrow niche regulates hematopoiesis in an NF-kappaB-dependent manner. Cell Stem Cell. 2014;15(1):51-65.

15. Benveniste P, Serra P, Dervovic D, Herer E, Knowles G, Mohtashami M et al. Notch signals are required for in vitro but not in vivo maintenance of human hematopoietic stem cells and delay the appearance of multipotent progenitors. Blood. 2014;123(8):1167-77.

16. Loew R, Heinz N, Hampf M, Bujard H, Gossen M. Improved Tet-responsive promoters with minimized background expression. BMC Biotechnol. 2010;10:81.

17. Amendola M, Passerini L, Pucci F, Gentner B, Bacchetta R, Naldini L. Regulated and multiple miRNA and siRNA delivery into primary cells by a lentiviral platform. Mol Ther. 2009;17(6):1039-52.

18. Fellmann C, Hoffmann T, Sridhar V, Hopfgartner B, Muhar M, Roth M et al. An optimized microRNA backbone for effective single-copy RNAi. Cell reports. 2013;5(6):1704-13.